



UNIVERSITY OF  
LIVERPOOL

# Modulation of ion channels as cardioprotective targets in ischaemic injury

By

Abrar Ibrahim Alnaimi

Department of Cardiovascular and Metabolic Medicine,  
Institute of Life Course and Medical Sciences, Faculty of Health and Life Sciences, University  
of Liverpool

# Abstract

**Author:** Abrar Alnaimi

**Title:** Modulation of ion channels as cardioprotective targets in ischaemic injury

**Introduction:** In the UK alone there are around 76,000 heart attacks each year with around 48,000 of these being the most serious ST-segment elevation myocardial infarctions. Ischaemia occurs during a coronary blockage when the downstream tissue does not receive effective blood flow; however, ischaemia can persist following reperfusion where small collateral arteries are still impaired, leading to continued ischaemic damage. Despite many years of research, there are still no drugs that could be given to the patient to reduce the spread of ischaemic damage in the myocardium during ischaemia and into reperfusion. The intrinsic cardioprotective pathways within the heart have shown great promise in pre-clinical animal models at reducing infarct size, yet most have failed to translate to clinical efficacy. In most cardioprotective interventions there is a reduction in electrical excitability leading to a reduction in the  $\text{Ca}^{2+}$  accumulation during each systolic interval, so reducing cellular energy consumption to restore  $\text{Ca}^{2+}$  homeostasis. In this study, ion channel modulators will be used to alter outward  $\text{K}^+$  currents, including the ATP-sensitive  $\text{K}^+$  ( $I_{\text{KATP}}$ ) currents and slowly activating  $\text{K}^+$  ( $I_{\text{Ks}}$ ) currents, to directly mimic the changes seen in electrical activity in cardioprotection. It is hypothesised that this will directly impart cardioprotection against ischaemia, bypassing the conventional signalling pathways.

**Methods:** 1) Whole-cell patch clamp electrophysiology to measure currents and action potentials, 2) simulated ischaemia/reperfusion injury to measure contractile function and cell death in an isolated cardiomyocyte model, 3) fluorescence imaging to measure  $\text{Ca}^{2+}$ -handling, and 4) *ex vivo* Langendorff whole heart coronary ligation experiments as a model of myocardial infarction. Selective modulators of  $I_{\text{KATP}}$  and  $I_{\text{Ks}}$  were used to assess the roles of these currents in protection and toxicity.

**Results:** The key finding was that selective potentiation of  $I_{\text{Ks}}$  or  $I_{\text{KATP}}$  imparted a protection to cardiomyocytes. The mechanism for this is suggested to be due to a modulation of  $\text{Ca}^{2+}$  homeostasis and so preservation of ATP. The presence of a newly-identified sarcolemmal cardiac  $K_{\text{ATP}}$  channel, containing a  $K_{\text{ir}}6.1$  pore, was demonstrated. This was potentiated by  $K_{\text{ATP}}$  activators and inhibited by selective  $K_{\text{ATP}}$  blockers. Both  $K_{\text{ATP}}$  ( $K_{\text{ir}}6.1$ ) and  $I_{\text{Ks}}$  currents were demonstrated to have a role in modulating the action potential duration, and the  $\text{Ca}^{2+}$  transients. Finally, potentiation of both  $I_{\text{Ks}}$  and  $K_{\text{ir}}6.1$  activity had a protective effect in a cellular ischaemia/reperfusion assay and in a whole heart *ex vivo* coronary ligation model.  $K_{\text{ir}}6.1$  blockers were shown to have a cardiotoxic effect in these assays, whereas  $I_{\text{Ks}}$  inhibition had limited effects.

**Conclusion:** Pharmacological manipulation of the  $I_{\text{Ks}}$  and  $I_{\text{KATP}}$  currents mimics the effects of known endogenous cardioprotective stimuli on the action potential. Data presented in this thesis suggest that modulation of these ventricular currents could be used clinically as a novel pharmacological cardioprotection against myocardial ischaemia.

## **Dedication**

I would like to dedicate this thesis to my parents. They have inspired me by their dedication to challenge the odds and keep moving forward. Throughout my education and career, they have been there to offer all the support they could possibly offer.

## Acknowledgements

First of all, I would like to show my greatest thanks to Almighty God, for giving me strength, ability, opportunity to study my PhD, and to finish it successfully. Without his blessings and mercy, it would not be possible to start and finish it. I would like to express my thanks to myself to faced difficulties and challenges throughout my PhD journey.

My utmost acknowledgement very rightfully belongs to my primary supervisor, Dr Richard Rainbow, for his support, encouragement, and valuable guidance throughout my PhD journey. I am grateful for this opportunity, for the valuable time that he has always given me, for provoking input during experiments, and for his valuable feedback throughout my thesis writing. I could not have succeeded without his pushing me in the first place. I am highly thankful for him to provide a chance when I requested to change my supervisor after I passed my first-year probation at the University of Leicester and for his support at the time when his group was transferred to the University of Liverpool. I proffer an enormous thank you to Dr Sean Brennan for never-ending advice and encouragement, for his endless support, and for being ever helpful in facilitating the bulk of experiments. I would also like to thank Dr Simona Esposito for helping with my experiments and data analysis. I was glad you have been my office comradery throughout this journey. I would also like to thank my second supervisor, Dr Parveen Sharma, for her contributions and regular asking about my progress.

My heartfelt thanks to all the people who made this journey wonderful. Special thanks to Fada, Avnish, Lauren, and Dr Mohammed for sharing lab tools, our office, unending help, insight, fun times, and friendship. Thanks to all the other students, including Rob and Noorann, who have helped me generate the data for this thesis; I will always be grateful. To all people I have been met at the University of Leicester, particularly Prof. Andre Ng, Prof. David Lambert, Dr Karl Herbert, Dr Lory Francescut, Dr Rishma Chauhan, Dr Emily Allen, and Dr Pott Pongpaopattanakul; I thank you for being great people and for your help throughout the first period of my PhD.

I am also thankful to Prof. Antonio Corno and his wife, Josie Mondani, for giving me highly valuable advice and guidance. You both have been like a second family for me and for my brother during my stay in Leicester. I am especially indebted to you for opening your hearts and your house for us when we needed somewhere to sense a family gathering. To NK, your support during my PhD has been unwavering and your words of encouragement have been brilliant, and not forgotten.

My sincere thanks and appreciation go to my Mum and Dad. I would not have reached this stage of completing my experimental works and writing up my thesis without your prayers, support, encouragement, and unwavering belief in me. I am lucky enough to have parents like you in my life who have always given me all the love and motivation to overcome difficult challenges. I would like to thank my soul, my brother Moath. You have been my strength and my shield, and without you, truly I could not have made it through the difficult time of my

PhD. You have been with me every step on this scholarship journey through the highs and the lows. More than anyone else, you have made me laugh and kept my spirits up. To my one and only sister, Haya, thank you for inspiring me to think outside the box. I will never imagine how emotionally stressed I would be without your support. I also want to thank my little hero, my brother Muhannad, for your continuous support, especially during my last two years of completing my PhD. Without you, I might still be carrying on this journey alone. Many thanks to you, my brothers; Muhammad, Naif, and Ziyad for your inspiration and prayers throughout my study. I hope that I have made all of you proud of me by completing my PhD degree.

I would like to express my thanks to all my friends outside the University for being a part of my journey. To my friend Afnan, you left a memory during my thesis writing. I will not forget the time we spent together during the quarantine period when we were infected with COVID-19. It was grim, but your smile, care, sharing the coffee, and the jokes kept my head above the water. Thank you for all your attempts to make me smile and laugh during that tough time. To my friend Sahar, I enjoyed our regular discussion about how much we were achieving in our write-ups, our issues, and our plans. I will never forget how we tried to fix it together. To my friend Alhanoof, you are someone who has always tried to make me laugh from your sense of humour, even when things have been tough on you. You have been the magic glue that helped hold us together through this journey. You are truly a blessing to me. To my friend Aisha, full of quietness, an example of strength that alone is an inspirational quality—thank you. To my friend Areej, you are a side of support when things have been tough. To my friend Bayan, I appreciate the listening ear you always lent. To my friend Sondous, thank you for always having been with me whenever I needed to talk and be inspired. To Nouf (my partner on the GYM), thanks for being there for me, kept me motivated in the final writing days and for sharing me your Laptop whenever I needed. Special thanks to Liverpool friends; Faten, Wedad, Reem, Amirah, Manal, Shihanah, Eman, Samar, Mai, Tahera, Maria, Hanaa and Maha. I would also like to express my thanks to my friends in Leicester; Amal, Afnan, Maha, Mai, Najawa, Jawaher and Malak.

Lastly, I would like to extend my gratitude to the Saudi government, which funded my study, and to the University of Imam Abdulrahman Bin Faisal for being an integral part of funding the project. I would also like to thank the Department of Cardiovascular and Metabolic Medicine and the University of Liverpool for facilitating my education.

# Table of contents

<b>Chapter 1 Introduction .....</b>	<b>1</b>
<b>1.1 The cardiovascular system.....</b>	<b>1</b>
<b>1.2 Cardiomyocytes.....</b>	<b>2</b>
1.2.1 The structure of the myocardial cell surface .....	2
1.2.2 Cell membrane potentials.....	5
1.2.3 Ion Channels.....	8
1.2.3.1 Voltage-gated ion channels .....	8
1.2.3.2 Twin-pore potassium channels.....	15
1.2.3.3 Inwardly rectifying potassium channels .....	16
1.2.4 Cardiac action potentials .....	17
1.2.4.1 Phases of ventricular cardiac action potentials .....	19
1.2.4.2 Automatic generation of electrical impulses in the heart.....	21
1.2.4.3 The role of the autonomic nervous system in the regulation of cardiac action potentials.....	24
1.2.5 The role of calcium currents in the regulation of cardiac contraction....	25
<b>1.3 ATP sensitive potassium (<math>K_{ATP}</math>) channel .....</b>	<b>31</b>
1.3.1 Molecular structure and the distribution of $K_{ATP}$ channels .....	31
1.3.2 Properties of physiological function of $K_{ATP}$ channels .....	35
1.3.2.1 ATP sensitivity .....	37
1.3.2.2 ADP sensitivity.....	39
1.3.2.3 The physiological role of the $K_{ATP}$ channel in pancreatic $\beta$ -cells.....	40
1.3.2.4 The physiological role of $K_{ATP}$ channel in skeletal muscle cells.....	41
1.3.3 The physiological role of $K_{ATP}$ channel in cardiac muscle .....	42
1.3.4 The pharmacological modulation of $K_{ATP}$ channels.....	44
1.3.4.1 Pharmacological blockers of $K_{ATP}$ channels.....	44
1.3.4.2 Pharmacological openers of $K_{ATP}$ channels .....	45
1.3.5 Mitochondrial $K_{ATP}$ channels .....	46
1.3.5.1 The physiological role of mitochondrial $K_{ATP}$ channels.....	46
1.3.5.2 The molecular composition of mitochondrial $K_{ATP}$ channels.....	48

1.3.5.3 Effects of different pharmacological modulators of mitochondrial K <sub>ATP</sub> channels and their role in cardioprotection .....	49
<i>1.4 Slowly activating delayed rectifier potassium current (I<sub>Ks</sub>).....</i>	<i>51</i>
1.4.1 The KCNQ family .....	51
1.4.1.1 Molecular structure of KCNQ family.....	51
1.4.1.2 Different expression and their physiological roles of KCNQ family....	55
1.4.2 The KCNE family.....	56
1.4.3 The I <sub>Ks</sub> complex in cardiac cells .....	58
1.4.3.1 The Molecular structure of I <sub>Ks</sub> .....	58
1.4.3.2 The physiological role of I <sub>Ks</sub> .....	59
1.4.4 The pharmacological modulation of I <sub>Ks</sub> .....	63
1.4.4.1 Pharmacological blockers of the I <sub>Ks</sub> complex.....	63
1.4.4.2 Pharmacological activators of the I <sub>Ks</sub> complex .....	64
<i>1.5 The modulation of cardiac action potential in disease conditions .....</i>	<i>67</i>
1.5.1 Acute coronary syndrome .....	67
1.5.2 Ischaemic and reperfusion injury .....	68
1.5.2.1 Ischaemic injury .....	68
1.5.2.2 Reperfusion injury.....	69
<i>1.6 Cardioprotection .....</i>	<i>71</i>
1.6.1 Definition .....	71
1.6.2 Ischaemic conditioning .....	71
1.6.2.1 Ischaemic preconditioning .....	71
1.6.2.2 Ischaemic postconditioning .....	73
1.6.2.3 Remote ischaemic conditioning.....	73
1.6.2.4 Cardioprotective drugs .....	74
1.6.3 The mechanisms of cardioprotection .....	76
1.6.3.1 The cyclic guanosine monophosphate/cGMP-dependent protein kinase (cGMP/PKG) pathway.....	77
1.6.3.2 The reperfusion injury salvage kinase (RISK) pathway .....	78
1.6.3.3 The survivor activating factor enhancement (SAFE) pathway.....	78
<i>1.7 Aims and hypotheses .....</i>	<i>80</i>

<b>Chapter 2 General methods .....</b>	<b>83</b>
2.1 <i>Solutions</i> .....	83
2.2 <i>Isolation of cardiomyocytes</i> .....	83
2.3 <i>Patch clamp electrophysiology</i> .....	86
2.3.1 Cell attached patch recording.....	88
2.3.2 Whole cell recording of currents .....	88
2.3.3 Action potential recording .....	89
2.4 <i>Metabolic inhibition and reperfusion (MI/R) model and contractile function measurements</i> .....	90
2.5 <i>Fluorescence imaging</i> .....	91
2.5.1 Calcium measurements .....	92
2.6 <i>Langendorff experimental protocol</i> .....	93
2.7 <i>Statistical analysis</i> .....	96
<b>Chapter 3 The cardioprotective role of <math>I_{KATP}</math> activation .....</b>	<b>97</b>
3.1 <i>Introduction</i> .....	97
3.2 <i>Results</i> .....	100
3.2.1 Identification of a channel with a current with amplitude half of that compared to the $K_{ir}6.2/SUR2A$ cardiac $K_{ATP}$ current.....	100
3.2.2 $I_{KATP}$ activation with pinacidil causes a shortening of the action potential duration.....	104
3.2.3 Activation of $K_{ATP}$ currents by different concentrations of pinacidil treatment in rat ventricular myocytes changes the inward rectifier potassium currents.....	107
3.2.4 Identification of a second $K_{ATP}$ channel in cardiomyocytes by the application of a selective $K_{ir}6.1$ blocker (PNU37883) .....	112
3.2.4.1 PNU37883 prolongs the cardiac action potential.....	112
3.2.4.2 PNU37883 blocks $K_{ir}6.1$ currents in rat ventricular myocytes.....	115
3.2.5 The classical $K_{ATP}$ channel ( $K_{ir}6.2/SUR2A$ ) remains inactive following HMR1098 (selective $K_{ir}6.2$ blocker) treatment in cardiac muscle cells.....	118

3.2.6 Identification of $K_{ir}6.1$ as a component of the $I_{K1}$ in cardiomyocytes using selective blockers of $K_{ir}6.1$ and $K_{ir}2.1$ .....	121
3.2.7 Calcium transients are shortened by $K_{ir}6.1$ activation in rat ventricular myocytes.....	125
3.2.8 Calcium transients are prolonged by $K_{ir}6.1$ inhibition in rat ventricular myocytes.....	128
3.2.9 Potentiation of ventricular $K_{ir}6.1$ channels with pinacidil delays $K_{ir}6.2$ channel openings during metabolic inhibition .....	129
3.2.10 Potentiation of ventricular $K_{ir}6.1$ channels by pre-treatment with pinacidil imparts cardioprotection in isolated rat ventricular myocytes.....	133
3.2.11 PNU37883 is cardiotoxic to cells during metabolic inhibition protocol	137
3.2.12 The presence of 10 $\mu M$ pinacidil reduced infarct size in a whole heart <i>ex vivo</i> coronary ligation model via potentiation of ventricular $K_{ir}6.1$ channels .....	140
3.2.13 Selective inhibition of $K_{ir}6.1$ with PNU37883 increased infarct size in a whole heart <i>ex vivo</i> coronary ligation model .....	141
<i>3.3 Discussion</i> .....	143
3.3.1 Identification of $K_{ir}6.1$ containing channels expressed in sarcolemmal cardiomyocytes and their role in regulation of the cardiac electrophysiology.....	144
3.3.2 The modulation of $K_{ir}6.1$ -containing channels alters calcium influx by limiting the opening time of the L-type calcium channel.....	149
3.3.3 Activation of $K_{ir}6.1$ imparts protection to cardiomyocytes and isolated hearts.....	150
3.3.4 Blockade of $K_{ir}6.1$ causes cardiotoxicity to cardiomyocytes and isolated hearts.....	152
<b>Chapter 4 Characterisation of <math>I_{Ks}</math> in the heart .....</b>	<b>154</b>
4.1 <i>Introduction</i> .....	154
4.2 <i>Results</i> .....	156
4.2.1 ML277 (a selective activator of the $I_{Ks}$ ) shortens the cardiac action potential.....	156

4.2.2 JNJ303 (a selective $I_{Ks}$ blocker) did not prolong cardiac action potentials.....	158
4.2.3 ML277 selectively activates the $I_{Ks}$ in rat cardiomyocytes .....	161
4.2.4 JNJ303 blocks $I_{Ks}$ cardiac currents.....	167
4.2.5 ML277 increases $I_{Ks}$ over the duration of a normal human cardiac action potential.....	172
4.2.6 The activation curve of ML277 in rat cardiomyocytes .....	174
4.2.7 $I_{Ks}$ activation reduced the peak amplitude and duration of the calcium transient.....	177
4.2.8 $I_{Ks}$ inhibition enhanced the peak amplitude and prolonged the calcium transient duration.....	179
4.3 <i>Discussion</i> .....	180
4.3.1 The potentiation of the $I_{Ks}$ channel imparts cardioprotection via direct modulation of the cardiac action potential .....	181
4.3.2 The inhibition of the $I_{Ks}$ channel may cause a cardiotoxic effect via direct modulation of the cardiac action potential .....	183
4.3.3 $I_{Ks}$ channel modulators alter calcium influx by limiting the opening time of the L-type calcium channel....	185
<b>Chapter 5 The cardioprotective role of <math>I_{Ks}</math> potentiation.....</b>	<b>187</b>
5.1 <i>Introduction</i> .....	187
5.2 <i>Results</i> .....	188
5.2.1 Potentiation of $I_{Ks}$ does not delay $Kir6.2$ channel openings during metabolic inhibition.....	188
5.2.2 ML277 imparts cardioprotection from metabolic inhibition and washout protocol in a concentration-dependent manner.....	193
5.2.3 JNJ303 is cardiotoxic to cells during metabolic inhibition and washout protocol.....	197
5.2.4 ML277 protects the whole heart from damage during a whole-heart <i>ex vivo</i> coronary ligation protocol.....	199

5.2.5 JNJ303 increases infarct size in a whole-heart <i>ex vivo</i> coronary ligation model.....	201
5.2.6 ML277 imparts cardioprotection when introduced during the coronary artery block or reperfusion.....	202
<i>5.3 Discussion</i> .....	205
5.3.1 Perfusion with the pharmacological $I_{Ks}$ potentiation imparts cardioprotection to cardiomyocytes and isolated hearts .....	205
5.3.2 Perfusion with the pharmacological $I_{Ks}$ inhibition causes a cardiotoxic effect to cardiomyocytes and isolated hearts .....	208
<b>Chapter 6 General Discussion.....</b>	<b>211</b>
6.1 <i>An overview of the findings</i> .....	211
6.2 <i>Clinical implications and translational aspects</i> .....	215
6.3 <i>Future work</i> .....	217
6.4 <i>Overall conclusion</i> .....	218

## List of Figures

Figure 1.1: Diagram shows the structure of the heart and the cardiac conduction system.....	2
Figure 1.2: Components of the cell membrane.....	3
Figure 1.3: Passive movement of ions across the cell membrane.....	5
Figure 1.4: The general structure of voltage-gated $\text{Na}^+$ , $\text{Ca}^{2+}$ and $\text{K}^+$ channels.....	10
Figure 1.5: Action potential of ventricular myocytes in human and rat.....	18
Figure 1.6: Regional differences in cardiac action potential configurations (AP) and a corresponding electrocardiogram (ECG) showing the waves and time correlation between the AP and the ECG.....	19
Figure 1.7: Phases of the action potential of sinoatrial nodal (SAN) pacemaker, showing the ionic current responsible to generate each phase.....	23
Figure 1.8: Cardiac calcium cycling.....	31
Figure 1.9: The molecular structure of $\text{K}_{\text{ATP}}$ channel.....	32
Figure 1.10: The functional role of $\text{K}_{\text{ATP}}$ channel subunits by control the close and open states in the response to alteration of the intracellular ATP/ADP level.....	37
Figure 1.11: The role of $\text{K}_{\text{ATP}}$ channel in the pancreatic $\beta$ -cell.....	41
Figure 1.12: The role of $\text{K}_{\text{ATP}}$ channel in cardiomyocytes.....	43
Figure 1.13: The mechanical function thought to be involved in the opening of mito $\text{K}_{\text{ATP}}$ channel.....	47
Figure 1.14: Molecular structure of KCNQ $\alpha$ -subunits.....	54
Figure 1.15: The molecular component and the electrophysiological characteristic of KCNQ1 in the absence and presence of KCNE1.....	59
Figure 1.16: The functional role of Kv7 channel in cardiac myocytes.....	62
Figure 1.17: The modulation of ion homeostasis and therefore cardiac action potential during ischaemic and reperfusion injury.....	71
Figure 1.18: The early- and late- phase cardioprotective signalling pathways in ischaemic conditioning.....	79
Figure 2.1: Diagram to demonstrate the Langendorff perfusion mode for enzymatic isolation of ventricular myocytes.....	85

Figure 2.2: Diagram to illustrate the arrangement of instruments that were used for patch clamp recording .....	88
Figure 2.3: The metabolic inhibition and washout protocol was used to simulate ischaemia and reperfusion. ....	91
Figure 2.4: A Langendorff experimental model of ex vivo coronary ligation. ....	95
Figure 3.1: Identification a channel with a current with amplitude half of that compared to the Kir6.2/SUR2A cardiac K <sub>ATP</sub> current on the surface of ventricular myocytes. ....	103
Figure 3.2: pinacidil causes shortening of action potential duration in rat cardiomyocytes.....	107
Figure 3.3: A designed protocol with a voltage clamp mode for whole-cell recording in rat ventricular myocytes.....	108
Figure 3.4: Comparison of whole-cell patch clamp recordings with a voltage clamp mode in the absence and presence of different concentrations of pinacidil treatments, highlighted with a red circle. ....	109
Figure 3.5: Pinacidil at different concentrations changes I <sub>K1</sub> , which leads to maintaining K <sup>+</sup> efflux at the -20 mV voltage step. ....	111
Figure 3.6: A selective blocker of Kir6.1 (PNU) prolongs the duration of cardiac action potential at 90% repolarisation. ....	114
Figure 3.7: PNU reduces potassium currents at different membrane potentials....	116
Figure 3.8: The classical K <sub>ATP</sub> channel (Kir6.2/SUR2A) maintains inactive following a selective pharmacological activator (HMR1098).....	121
Figure 3.9: The Kir6.1 is a component of the I <sub>K1</sub> in cardiomyocytes using selective blockers of Kir6.1 and Kir2.1. ....	125
Figure 3.10: Pinacidil treatment at different concentrations reduced Ca <sup>2+</sup> transients. ....	127
Figure 3.11: PNU treatment increased Ca <sup>2+</sup> transients, which may have a cardiotoxic effect to cardiac muscle cells during metabolic stress. ....	129
Figure 3.12: Potentiation of Kir6.1 led to a delay in the opening of Kir6.2/SUR2A channels and consequently delayed time to ATP depletion. ....	133
Figure 3.13: Pre-treatment with pinacidil imparts cardioprotection in isolated cardiomyocytes.....	136

Figure 3.14: The application of PNU treatment leads to cardiotoxic effects on isolated cardiomyocytes during the metabolic inhibition protocol.....	139
Figure 3.15: Pinacidil imparts cardioprotection by reducing infarct size in the whole heart after coronary ligation via potentiation of ventricular Kir6.1 channels. ....	141
Figure 3.16: PNU treatment causes a cardiotoxic effect via inhibition of Kir6.1 channel, increasing the infarct size in whole-heart preparation. ....	142
Figure 4.1: The representative effect of ML277 on action potential duration (APD) in a rat ventricular myocyte compared to the control condition.....	157
Figure 4.2: ML277 treatment shortened action potential duration (ADP) with no effect on resting membrane potential.....	158
Figure 4.3: The effect of JNJ303 on action potential duration (APD) from a rat ventricular myocyte compared to the control condition. ....	160
Figure 4.4: Representative trace from multi-current protocol used for whole-cell recording from rat ventricular myocytes which was illustrated the currents measured. ....	164
Figure 4.5: Comparison of the whole-cell patch clamp recordings in the absence and present of ML277, highlighted the treatment effect on $I_{Ks}$ .....	165
Figure 4.6: The limited effect of ML277 on the activation of $I_{Ks}$ . ....	166
Figure 4.7: Comparison between single cardiomyocytes under control condition with NT solution and after the administration of JNJ303, using whole-cell patch clamp recordings with a voltage clamp mode.....	168
Figure 4.8: The effect of JNJ303 on the blocking of $I_{Ks}$ . ....	169
Figure 4.9: The possibility of run-down in the currents at equivalent time of drug recordings in the absence of the drug with recordings in the presence of NT solution. ....	171
Figure 4.10: A whole-cell recording was used to examine the effect of ML277 on $I_{Ks}$ over the normal human action potential. ....	174
Figure 4.11: The activation curve of ML277 shows that the activation of the $I_{Ks}$ occurred at resting potentials that were more negative. ....	177
Figure 4.12: ML277 treatment reduced $\text{Ca}^{2+}$ transients.....	178
Figure 4.13: JNJ303 treatment tended to prolong the duration of the $\text{Ca}^{2+}$ transients, which may have detrimental impacts on cardiac muscle.....	180
Figure 5.1: Potentiation of the $I_{Ks}$ does not delay cardiac Kir6.2/SUR2A channel opening following metabolic inhibition. ....	191

Figure 5.2: ML277 did not cause hyperpolarisation of the membrane potential.....	193
Figure 5.3: Pre-treatment with ML277 imparts cardioprotection in isolated cardiomyocytes.....	196
Figure 5.4: Pre-treatment with JNJ303 causes cardiotoxicity in isolated rat ventricular cells. ....	199
Figure 5.5: ML277 imparts cardioprotection by reducing the infarct size in the whole heart after coronary ligation using the Langendorff technique.....	200
Figure 5.6: JNJ303 causes cardiotoxicity by increasing the infarct size in the whole heart after blocking the coronary artery using the Langendorff approach. ....	202
Figure 5.7: ML277 imparts cardioprotection by reducing infarct size in the whole heart when applied during coronary artery ligation or only during reperfusion. ....	204

## List of tables

Table 1.1: Normal ionic concentrations and equilibrium cardiac membrane potentials. ....	5
Table 1.2: The distribution of K <sub>ATP</sub> channels in the body by differing combinations of Kir6.x and SURx subunits. ....	34
Table 1.3: Biophysical properties of different types of K <sub>ATP</sub> channels, including the single-channel conductance in inside-out patches in ~140 mM symmetrical of K <sup>+</sup> concentrations, ATP sensitivity and ADP sensitivity. ....	38
Table 1.4: Pharmacological properties by using a selective openers and blockers of K <sub>ATP</sub> channels in major tissues with different subunit combinations. ....	45
Table 1.5: Kv7 family genes and proteins and their properties expressed as homotetramers.....	55
Table 1.6: Functional implications of the interaction of KCNE1-5 auxiliary subunits with Kv7 channel α-subunits.....	57
Table 1.7: Pharmacological modulators acting on Kv7 channels, including blockers and activators.....	65
Table 1.8: A summary of preclinical and clinical trials for certain potentially cardioprotective drugs aimed at mimicking ischaemic conditioning .....	75

## Abbreviation

0-CaT	Ca <sup>2+</sup> free Tyrode's solution
2 CaT	2 mmol/L Ca <sup>2+</sup> Tyrode's solution
2TMD	Two transmembrane domains
4TMD	Four transmembrane domains
5-HD	5-hydroxy derivative of decanoate
6TMD	six transmembrane domains
ABC	ATP-binding cassette family
AC	Adenylyl cyclase
ACh	Acetylcholine
ACS	Acute coronary syndrome
ANS	Autonomic nervous system
AP	Action potential
APD	Action potential duration
AVN	Atrio-ventricular node
BHF	British Heart Foundation
Ca <sup>2+</sup>	Calcium ion
CABG	Coronary Artery Bypass Graft Bypass Graft study
CAD	Coronary artery disease
CaM	Calmodulin
cAMP	cyclic adenosine monophosphate
Cav	Voltage-gated calcium channel
cGMP	cyclic guanosine monophosphate
CICR	Ca <sup>2+</sup> -induced Ca <sup>2+</sup> release
CK-AUC	Area under the curve of serum creatine kinase
Cl <sup>-</sup> /HCO <sub>3</sub> <sup>-</sup>	Chloride/bicarbonate exchanger
Cx40	Connexin 40 proteins
DAG	Diacylglycerol
DADs	Delayed after depolarizations
DF	Driving force
DNP	2,4-Dinitrophenol

ECC	Excitation-contraction coupling
ECG	Electrocardiograms
EGFR	Epidermal growth factor receptor
$E_{ion}$	Equilibrium potential
$E_K$	Equilibrium membrane potential of potassium
ENC	Extracellular Negative Cluster
eNOS	Endothelial nitric oxide
ER	Endoplasmic reticulum
$E_{rev}$	Reversal membrane potential
ERICCA	The Effect of Remote Ischaemia Conditioning in Coronary Artery
$ER_{K1/2}$	Extracellular signal regulated kinase $\frac{1}{2}$
ESC	European Society of Cardiology
CaMKII	Calcium/calmodulin-dependent protein kinase II
GFG	Glycine-phenylalanine-glycine sequence
GIRK	G protein-coupled $K_{ir}$ channels
GPCR	G-protein coupled receptors
GSK-3 $\beta$	Glycogen synthetase kinase 3 $\beta$
GYG	Glycine-tyrosine-glycine motif
$G\alpha$	G-protein $\alpha$
HCN	Hyperpolarization-activated cyclic-nucleotide gated
HCS	Hydrophobic Constriction Site
I/R injury	Ischaemia and reperfusion injury
$I_{Ca,L}$	L-type $Ca^{2+}$ current
$I_{Ca,T}$	T-type $Ca^{2+}$ current
$I_f$	funny current
$I_{Ks}$	Slowly activating delayed rectifier potassium current
$I_{NaCa}$	Sodium/Calcium exchange current
INC	Intracellular Negative Cluster
$IP_3$	Inositol-1,4,5-trisphosphate
IPC	Ischaemic pre-conditioning
IPostC	Ischaemic post-conditioning
I-V	Current-voltage relationship

JAK	Janus kinase
K <sup>+</sup>	Potassium ion
K <sub>ACh</sub>	ACh-dependent K <sup>+</sup> channels
K <sub>ATP</sub>	ATP-sensitive potassium channel
KCOs	Potassium channel openers
kDa	kilodaltons
K <sub>ir</sub>	Inwardly rectifying family of potassium channels
K <sub>v</sub>	Voltage-gated potassium channel
LTCC	L-type calcium channel
mM	millimolar
MVO	Microvascular obstruction
NA	Noradrenaline
Na <sup>+</sup>	Sodium ion
Nav	Voltage-gated sodium channel
NBF	Nucleotide-binding domains
NBS	Nucleotide binding sites
NCX	Na <sup>+</sup> /Ca <sup>2+</sup> exchanger
NHE	Sodium/hydrogen exchanger
nM	nanomolar
nm	nanometres
NO	Nitric oxide
NSTEMI	non-ST segment elevation myocardial infarction
NT	Normal Tyrode's solution
PCI	Percutaneous coronary intervention
PI3K	Phosphoinositide 3 kinase
PI3K-AKT	Phosphatidylinositol 3- kinase-Protein Kinase B
PIP <sub>2</sub>	phosphatidylinositol bisphosphate
PLC	phosphoinositide-specific phospholipase C
PKA	Protein kinase A
PKC	Protein kinase C
PKC $\epsilon$	Protein kinase C-epsilon
PKG	cGMP-dependent protein kinases

PM	Plasma membrane
PMCA	Plasma membrane Ca <sup>2+</sup> -ATPase
PSNS	Parasympathetic nervous systems
P-pore	Pore-forming loop
PUFA	Polyunsaturated fatty acids
RCT	Randomize control trials
RIC	Remote ischaemic conditioning
RISK	Reperfusion Injury Survival Kinase pathway
RKR	endoplasmic reticulum retention signals
RMP	Resting membrane potential
ROS	Reactive oxygen sepsis
RyR2	Type 2 ryanodine receptors
SAFE	Survivor Activating Factor Enhancement pathway
SAN	Sinoatrial node
SarcoK <sub>ATP</sub>	Sarcolemmal K <sub>ATP</sub> channel
SCD	Sudden cardiac death
SDH	Succinate dehydrogenase
SERCA	Sarco-endoplasmic reticulum Ca <sup>2+</sup> -ATPase
sGC	soluble Guanylyl Cyclase
SGK	the serum- and glucocorticoid-inducible kinase 1
SNS	Sympathetic nervous systems
SR	Sarcoplasmic reticulum
STAT-3	Single transducer and activator of transcription 3
STEMI	ST-segment elevation myocardial infarction
SUR	Sulphonylurea receptor
SVC	Superior vena cava
TASK	two-pore domain acid-sensitive K <sup>+</sup> channel
TdP	Torsades de Pointes
THIK	tandem of pore domains in halothane inhibited K <sup>+</sup> channel
TMD	Trans-membrane domain
TNFR2	TNF receptor 2
TNF $\alpha$	Tumor necrosis factor alpha

TRAAK	TWIK-related arachidonic acid activated K <sup>+</sup> channel
TREK	TWIK-related K <sup>+</sup> channel
TRESK	TWIK-related spinal cord K <sup>+</sup> channel
TWIK	tandem of pore domains in a weak inward rectifier K <sup>+</sup> channel
UA	unstable angina
WHO	World Health Organisation

# Chapter 1 Introduction

In the UK alone there are around 76,000 heart attacks each year with around 48,000 of these being the most serious ST-segment elevation myocardial infarctions (STEMI) (BHF, 2021). Despite many years of research, there are still no approved cardioprotective interventions that could be given to the patient to reduce the spread of ischaemic damage in the myocardium during the ischaemia and into the reperfusion. The intrinsic cardioprotective pathways within the heart have shown great promise in pre-clinical animal models at being able to reduce infarct size, yet most of these have failed to translate to clinical efficacy. In most cardioprotective phenotypes there is a reduction in electrical excitability and so reduction in the calcium accumulation during each systolic interval, so a reduction in cellular energy required to remove that calcium. In this current study, the reduction in the electrical excitability to improve calcium overload was investigated by modulation of repolarizing outward currents of potassium ions through various types of ion channels located on the myocardial surface. This is achieved by using ion channel modulators to directly influence the changes seen in electrical activity as a mechanism for directly imparting cardioprotection pharmacologically, by-passing the conventional signalling pathways.

## 1.1 The cardiovascular system

The cardiovascular system comprises the heart and a network of blood vessels (Levick, 2013) (Figure 1.1). The main function of the cardiovascular system is to transport blood containing oxygen and essential nutrients and remove waste products, such as carbon dioxide and other metabolites.

The heart is a muscular organ that is comprised of four chambers; the right atrium which receives deoxygenated blood from the superior and inferior vena cava; right ventricle which then pumps the deoxygenated blood into the pulmonary arteries; left atrium which receives oxygenated blood from the lungs via the pulmonary veins and left ventricle which then pumps the oxygenated blood into the rest of the body via the aorta. The blood flow in the heart is maintained in one direction via the presence of valves. The middle layer of the heart walls is known as the myocardium formed from cardiomyocytes which are responsible for the

contractile function of the cardiac pump. The aetiology of most cardiovascular diseases, such as contractile dysfunction and areas of cell death leading to dysfunction, involve this layer of cardiac muscle cells (Tran et al., 2021).

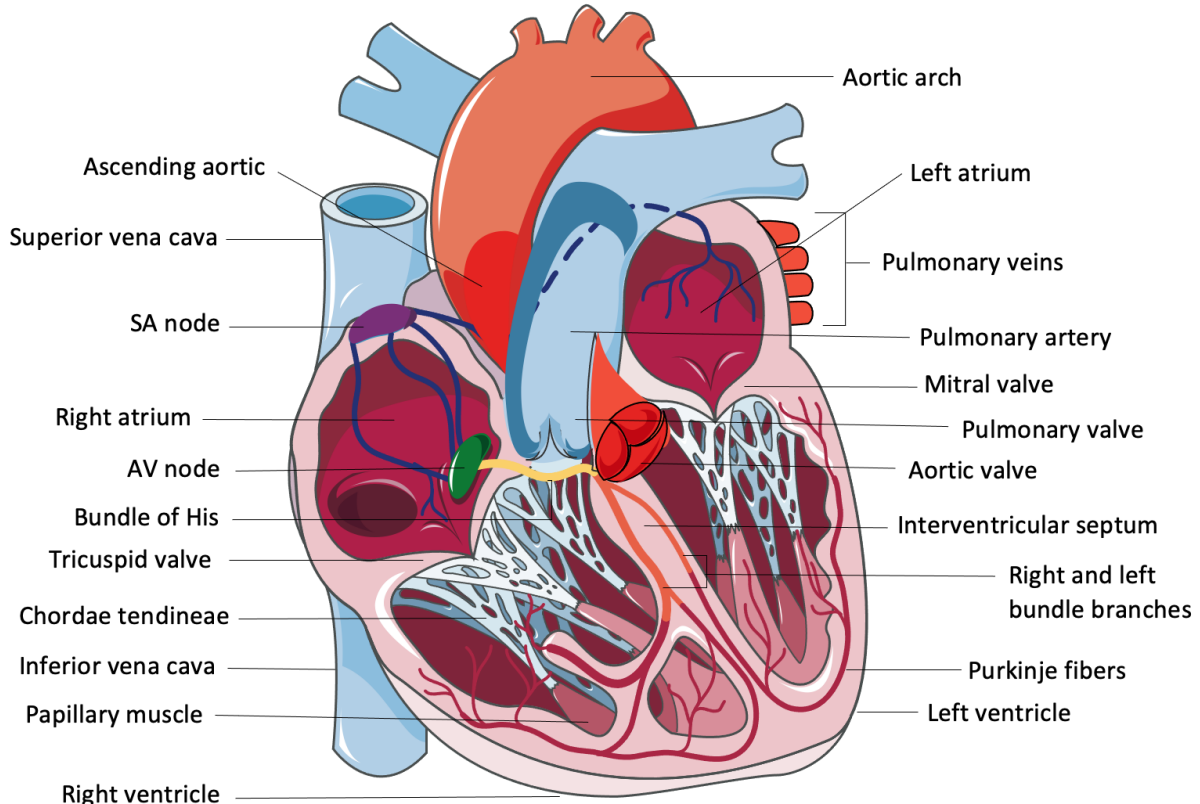


**Figure 1.1:** Diagram shows the structure of the heart and the cardiac conduction system.

(Amended from (Herring and Paterson, 2018; Levick, 2013)

## 1.2 Cardiomyocytes

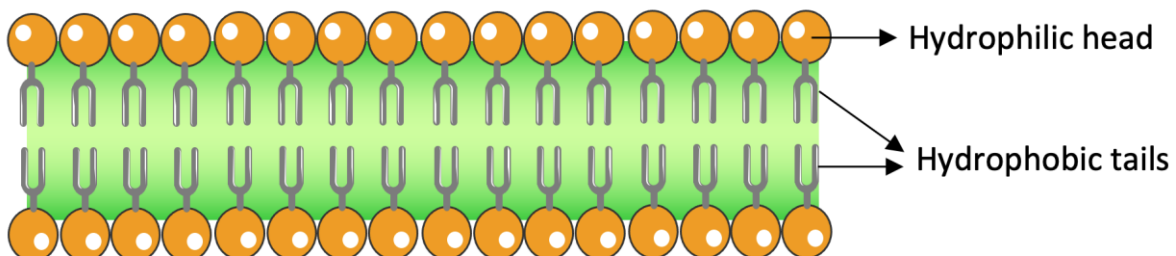
### 1.2.1 The structure of the myocardial cell surface

The heart is composed of specialised muscle cells, most of which are cardiomyocytes (Burton et al., 2014). Each cardiomyocyte is highly compartmentalised by the cell membrane which invaginates to form the transverse tubule (T-tubule) network, and the intracellular components. The plasma membrane of a cell is comprised of a phospholipid bilayer; each lipid layer with hydrophilic heads facing outwards and two hydrophobic tails located between these head groups forming a hydrophobic core in the membrane (Figure 1.2). This membrane

is a semipermeable layer which has the ability to allow the passing of small non-charged molecules (such as  $\text{CO}_2$ ,  $\text{O}_2$ ) and lipid-soluble molecules (such as steroids), in order to maintain the integrated function of internal metabolic processes (Subczynski et al., 1989; Gutknecht et al., 1977; Giorgi and Stein, 1981).

In addition to the phospholipid bilayer, the plasma membrane contains two additional primary components; glycolipids and cholesterol (Cooper et al., 2007). The glycolipids are considered as a minor component of the plasma membrane ( $\sim 2\%$ ), whereas cholesterol is considered as a major membrane constituent of cells. Cholesterol plays an important role in the membrane structure, particularly on the basic fluidity of the membrane. Cholesterol inserts into a bilayer of phospholipids with its polar hydroxyl group close to head groups and plays an important role in regulation of membrane fluidity across a range of temperatures. At high temperatures, cholesterol makes the membrane less fluid by reducing the motility of phospholipid fatty acid chains to restrict permeability to small molecules. However, at low temperatures, cholesterol maintains membrane fluidity by interfering with interactions between fatty acid chains to prevent membrane from clumping together in solid forms and so prevents freeze-fracture of the membrane.

### Outside of the cell



### Inside of the cell

Figure 1.2: Components of the cell membrane.

*The membrane is comprised of a bilayer of phospholipids; each lipid layer with hydrophilic heads facing outwards and two hydrophobic tails located between these head groups.*

The cell membrane is a selectively permeable barrier between the intracellular and extracellular environments. Whilst gasses, water and lipid soluble substances may diffuse

across the membrane, ions and polar molecules require a route to facilitate their diffusion using specialised transport mechanisms (Figure 1.3). These are usually integral proteins that span the membrane. There are 3 main classes of membrane transport protein; 1) ion channels, 2) carrier proteins, and 3) pumps. Ion channels provide a regulated pathway for diffusion of ions down their concentration and electrical gradient. This process is dependent on there being an ionic or electrical gradient across the membrane. Carriers are also a form of facilitated diffusion, allowing a pathway for movement across the membrane and can be grouped into 3 types, 1) Uniports, where the movement of a molecule occurs in one direction, 2) symports, where the coupled movement of two or more molecules occurs in the same direction, and antiports, where molecules move in different directions. The final group of transport proteins are the membrane pumps. These use the energy, for example from the hydrolysis of ATP, electron transfer, or photon-coupling (e.g. chloroplasts in plants), to move ions across the membrane, generally against their concentration gradient (Maeda, 2022). The Na-K-ATPase and plasma membrane calcium ATPase (PMCA) are examples of ATP-dependent pumps that moves ions against their concentration gradients. This primary active transport sets up the ionic concentration gradients that allow ion channels to function as a diffusion pathway. The potential energy stored in the sodium gradient can be utilised in the movement of molecules that are not lipid soluble into the cell through carriers. An example of a symport that uses this is the sodium glucose co-transporter SGLUT1 (Gorboulev et al., 2012). This co-transporter utilises the potential energy of the  $\text{Na}^+$  gradient to drive the uptake of glucose into the cell. This is an example of secondary active transport (Maeda, 2022). This same secondary active transport is extremely important in cardiomyocytes in the recovery of resting  $\text{Ca}^{2+}$  levels during diastole, where the sodium-calcium exchanger (NCX) uses the energy of the  $\text{Na}^+$  gradient to remove a  $\text{Ca}^{2+}$  ion, against the concentration gradient, for 3  $\text{Na}^+$  ions moving into the cell. This antiport activity is a key part of the regulation of  $\text{Ca}^{2+}$  homeostasis.

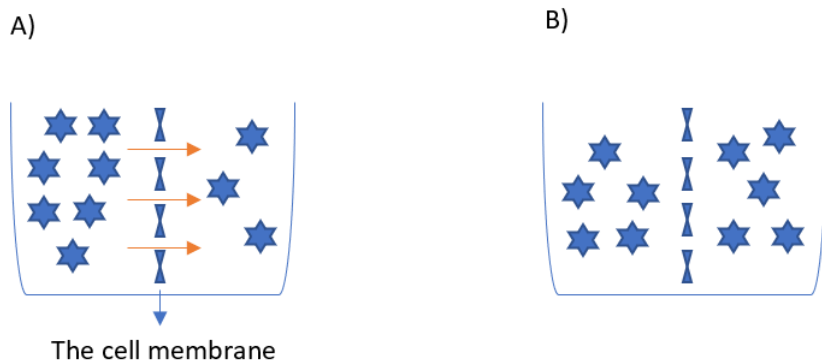


Figure 1.3: Passive movement of ions across the cell membrane.

A, At different concentration gradients, ions move from higher to lower concentration. B, At the equilibrium of concentrations of ions, there is no net movement across the cell membrane. (Diagram adapted from (Aidley and Stanfield, 1996))

### 1.2.2 Cell membrane potentials

The membrane potential of a cell depends on two primary factors, 1) the concentration differences of the ions across the cell membrane in the intra- and extracellular environments (Table 1.1) (Herring and Paterson, 2018) and 2) the relative permeability of the membrane to those ions, determined primarily by ion channel activity. Cardiac cells express three main types of selective cation channels,  $\text{Na}^+$ ,  $\text{K}^+$ , and  $\text{Ca}^{2+}$ -selective channels. There are also chloride ( $\text{Cl}^-$ ) channels in human heart which contribute to the resting membrane potential, where perturbations in  $\text{Cl}^-$  concentrations can cause a marked prolongation of the action potential (Hiraoka et al., 1998; Adkins and Curtis, 2015). Furthermore, the chloride/bicarbonate exchanger ( $\text{Cl}^-/\text{HCO}_3^-$ ) is highly expressed in cardiac tissues and may play a role in the maintenance of intracellular pH through myocyte acid loading (Alvarez et al., 2004).

Table 1.1: Normal ionic concentrations and equilibrium cardiac membrane potentials.

Ion	Ionic intracellular concentration (mM)	Ionic extracellular concentration (mM)	Equilibrium membrane potential (mV)
$\text{K}^+$	140	5-6	-95
$\text{Na}^+$	10-12	135-140	+70
$\text{Ca}^{2+}$	0.0001	1.2	+130

In the cardiac cell, K<sup>+</sup> ions play an important role in determining the resting membrane potential (RMP). While the concentration gradient K<sup>+</sup> is 30 times higher inside the cell (140 mM) than outside (5 mM), K<sup>+</sup> diffuses out of the cell down its chemical gradient (concentration difference) (Levick, 2013). Specifically, the inwardly rectifying family of potassium channels is partially in the open state at the more negative resting membrane potentials, creating a resting outward current of K<sup>+</sup> (Hibino et al., 2010). As the K<sup>+</sup> ions diffuse from inside of the cell to the outside, the positively charged K<sup>+</sup> ions leaving the cell reduce the positive charge in the cell, i.e. making the inside of the cell more negative than the outside. This electrostatic gradient (charge difference) drives the movement of K<sup>+</sup> ions to be attracted back inside the cell. As a result, ionic flow is dependent on an electrochemical gradient which is defined as the combined gradient of the concentration difference and the electrical charge difference across the membrane to drive the movement of particular ion. Effectively, the chemical gradient driving K<sup>+</sup> out of the cell and the electrostatic gradient driving K<sup>+</sup> into the cell are equal at the equilibrium potential ( $E_{ion}$ ), in this case, for K<sup>+</sup> ions,  $E_K$ . The opposite situation for Na<sup>+</sup> and Ca<sup>2+</sup>, is that these ions exist to diffuse inside the cell down their chemical gradients. The equilibrium potential of an ion is the voltage at which there is no net movement of that ion across the cell membrane. The value of the equilibrium potential for different ions depends on the temperature and the ionic charge number, which are approximated in Table 1.1. This value can be calculated by the following Nernst equation (Hille, 1978):

$$E = \frac{RT}{zF} \ln \left( \frac{[ion]_o}{[ion]_i} \right)$$

Where R represents the Gas constant (8.314 J K<sup>-1</sup> mol<sup>-1</sup>), T the absolute temperature (in degree of Kelvin), Z the charge number of the ion (e.g. +1 for Na<sup>+</sup> and K<sup>+</sup> ions, whereas +2 for Ca<sup>2+</sup> ions), F the Faraday constant. [ion]<sub>o</sub> and [ion]<sub>i</sub> the concentration of the given ion outside and inside the cell, respectively.

The equilibrium potential of K<sup>+</sup> is the theoretical resting membrane potential if the membrane was solely permeable to K<sup>+</sup> ions alone. However, in reality, membranes are not perfectly selective for a single ion, and there is always leak of other ions. Therefore, the K<sup>+</sup> equilibrium potential ( $E_K$ ) is not identical to the cellular membrane potential. In most cell types  $E_m$  is

depolarised relative to  $E_K$ , the driving force (DF) of  $K^+$  efflux is equal to the difference in voltage between equilibrium potential and the cellular membrane potential (i.e.  $DF = E_{ion} - E_m$ ) which leads to the outward movement of positive charge. This outward current induces hyperpolarisation of the cell. In contrast, if  $E_m$  is negative to  $E_K$ , there is a driving force for  $K^+$  influx, leading to movement of positive charge into the cell. This inward current causes depolarisation of the cell.

To maintain the electrochemical gradient for  $Na^+$  and  $K^+$ , there is ion transporters such as  $Na^+/K^+$  ATPase which play a critical role to reach the electrochemical equilibrium (Maeda, 2022). The  $Na^+/K^+$  ATPase transporter uses the energy from ATP hydrolysis to pump 3  $Na^+$  out of the cell and 2  $K^+$  into the cell, which is against the concentration gradients. Once the active ion transporters has been taken into account, the Goldman, Hodgkin and Katz (GHK) equation (Hodgkin and Katz, 1949) is used to calculate the membrane potential while considering the permeability of all ion moving across the cell membrane:

$$V_m = \frac{RT}{F} \ln \left( \frac{p_K [K^+]_o + p_{Na} [Na^+]_o + p_{Cl^-} [Cl^-]_o}{p_K [K^+]_i + p_{Na} [Na^+]_i + p_{Cl^-} [Cl^-]_o} \right)$$

Where  $V_m$  is the cellular membrane potential, the  $p_K$ ,  $p_{Na}$  and  $p_{Cl^-}$  are the relative membrane permeabilities of  $K^+$ ,  $Na^+$  and  $Cl^-$  ions, respectively.  $[K^+]_o$ ,  $[Na^+]_o$  and  $[Cl^-]_o$  are the extracellular concentrations of the ions.  $[K^+]_i$ ,  $[Na^+]_i$  and  $[Cl^-]_i$  are the intracellular concentrations of the ions.

The relative membrane permeabilities of different ions play an additional important role to determine the membrane potential. For instance, if the membrane has a higher permeability to specific ion than others, the membrane potential becomes more influence by this ion. As described above, a membrane potential of resting ventricular myocytes is near to  $K^+$  equilibrium potential because this cell in the resting state is more permeable to  $K^+$  than others. The current flowing through an open single channel can be calculated by using Ohm's law, which sates as the current ( $i$ ) is proportional to potential difference ( $\Delta V$ ) and electrical conductance ( $g$ ). In other words,  $i = \Delta V \times g$ . When considering a single ion channel,  $DF = E_{ion} - E_m$ . Single channel conductance is defined as the ion current divided by potential difference, i.e.  $g = i / E_{ion} - E_m$ . The conductance of the membrane to a particular ion is proportional to its

permeability to that ion. For example, an increase in the extracellular  $K^+$  concentration can increase the conductance of  $K^+$  through an open channel and therefore can cause hyperpolarisation.

### 1.2.3 Ion Channels

In the heart, prominent ion channels include  $Na^+$ ,  $Ca^{2+}$ , and  $K^+$  channels which play an essential role in cell physiology by mediating cardiac muscle contraction and relaxation (Hille, 1978; Trezise et al., 2009). All ion channels are formed of transmembrane proteins with a central pore which allow the movement of ions between the extracellular and intracellular environments. Ion channels undergo gating into at least two conformational states, including open and close states. The open state is conducting of ions, while the close state is non-conducting.

Ion channels consist of two types; voltage-gated channels and receptor-gated channels (Levick, 2013). The opening and closing state of voltage-gated cation channels are regulated by a change in the membrane potential. For simplicity, depolarisation of the cell membrane evokes a conformational change through the movement of positively charged residues and other parts of the channel structure. This is referred to as a voltage sensor in voltage-dependent ion channels. Receptor-gated channels, in contrast, open and close in response to the chemical energy of ligand. For instance, G-protein-gated  $K^+$  ( $I_{KACH}$ ) channel opens in response to acetylcholine which is released by the stimulation of parasympathetic nerve system (DiFrancesco, 2010).

#### 1.2.3.1 Voltage-gated ion channels

Voltage-dependent ion channels share a common molecular architecture, which consist of  $\alpha$ -subunits (the transmembrane domains) and accessory subunits (such as  $\beta$ ). Together the repeat transmembrane domains form a functional channel with the primary pore-forming subunit which is generally the core of the channel. In particular, voltage-gated  $Na^+$  and  $Ca^{2+}$  channels have a similar structure with at least three distinct subunits. The  $\alpha$  subunit is constructed a single polypeptide with four homologous domains (I, II, III, and IV) (Figure 1.4). Each domain has a similar sequence which consists of six  $\alpha$ -helical transmembrane segments

(S1 to S6) with a substantial intracellular N and C termini that play key roles in channel gating. Additionally, the pore loop is connected to S5 and S6 transmembrane segments via a large loop that forms the lining of the pore and also contains the selectivity motifs that allow the channel to be selective for single ion species. The S1 – S4 transmembrane domains are thought to be the voltage-sensing region, with S4 containing charged amino acids that trigger physical movement in the channel structure on changes in the potential difference across the membrane. This voltage-sensing-induced conformational change is the most “simple” way in which these channels are regulated. On prolonged channel opening, additional mechanisms of reducing the current can be displayed by some voltage-gated channels, termed inactivation. This process of inactivating is often thought to involve the N and C termini, and essentially these provide ion channel inhibition which act by blocking the pore, which known as pore plugging (Ragsdale et al., 1994). For instance, a previous study has suggested that the N-terminus of K<sup>+</sup> channels underlies an inactivation mechanism (Kurata and Fedida, 2006). This is described as the ball and chain mechanisms of inactivation, in which the channel pore is occluded by a sequence of amino acids at the N-terminus of the channel. Therefore, the deletion or enzymatic removal of N-terminus can abolish the inactivation mechanisms of ion channels, leading to the suggestion that an N-type mechanism accounts for blocking a pore of ion channel. This N-type inactivation is thought to be a rapid block, as seen in Na channels. A more prolonged, but ultimately slower, form of inactivating is often referred to as C-type inactivation. This type of inactivation, rather than taking milliseconds to occur, might take up to 100 ms, as is often observed in smooth muscle voltage-gated K<sup>+</sup> channels where depolarisation events may last for long durations. I<sub>Ks</sub> is unusual amongst voltage-gated channels in that it doesn't appear to show a significant inactivation over time.

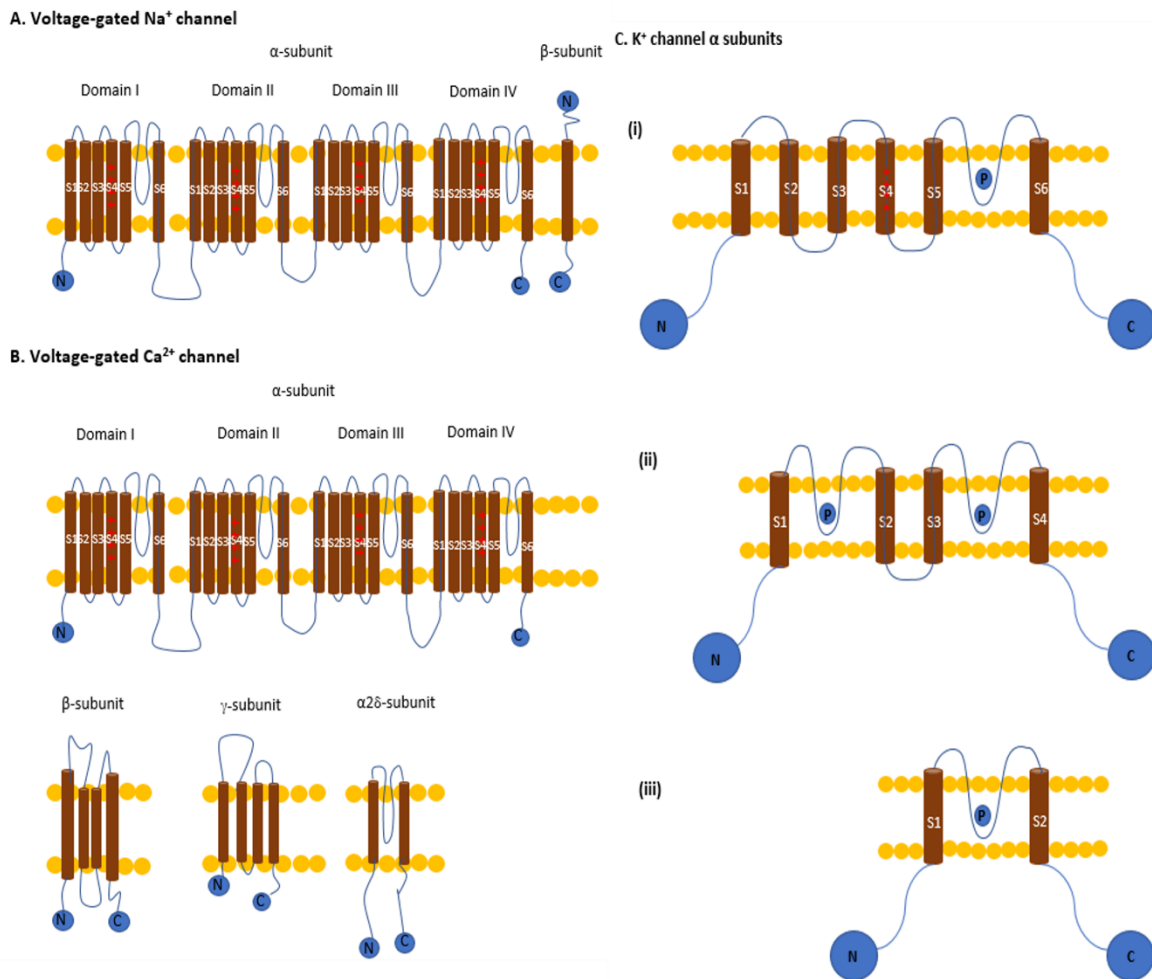


Figure 1.4: The general structure of voltage-gated  $\text{Na}^+$ ,  $\text{Ca}^{2+}$  and  $\text{K}^+$  channels.

**A, The  $\text{Na}^+$  channel  $\alpha$ -subunit consists of a single polypeptide chain with four structurally similar domains (Domains I-IV), with a substantial intracellular N and C termini (as shown in blue colour). Each domain contains six transmembrane segments (S1-S6) (as shown in brown colour). The pore region (P) is located between S5 and S6. The voltage-sensing domain is located primarily in S4 where there are positively charged residues. The  $\text{Na}^+$  channel  $\beta$ -subunit has a single transmembrane segment.**

**B, The  $\text{Ca}^{2+}$  channel  $\alpha$ -subunit has a similar structural basis to  $\text{Na}^+$  channels of a single polypeptide chain with 4 structurally similar domains that coalesce to form the pore. The  $\beta$  and  $\alpha 2\delta$  subunits plays an important role for the  $\text{Ca}^{2+}$  channel  $\alpha$ -subunit, enhancing expression and modulating the voltage-dependence.**

**C, The  $\text{K}^+$  channel is classified into three families based on the structure of  $\alpha$ -subunit.**

**C(i), The voltage-gated  $\text{K}^+$  channel  $\alpha$ -subunit has six transmembrane segments, that are analogous to a single domain in the  $\text{Na}^+$  and  $\text{Ca}^{2+}$  channels, with 4 of these subunits coming together to form a single pore.**

**C(ii), Twin pore loops  $\text{K}^+$  channel  $\alpha$ -subunit consists of four transmembrane segments with two pore loops.**

**C(iii), Inward-rectifying  $\text{K}^+$  channel  $\alpha$ -subunit consists of two transmembrane segments with single pore-forming subunit.**

#### 1.2.3.1.1 Voltage-gated sodium channels

Sodium currents through voltage-gated sodium channel were first identified by Hodgkin and Huxley (Hodgkin and Huxley, 1952). The voltage-gated sodium channels ( $\text{Na}_V$ ) allows the movement of  $\text{Na}^+$  into the intracellular compartment (Hille, 1978). The  $\text{Na}^+$  channel subunits are encoded by several genes, comprises nine members SCN1A-SCN11A ( $\text{Nav1.1-Nav1.9}$ ), in particular SCN5A ( $\text{Nav1.5}$ ) which encodes cardiac sodium channels (Goldin et al., 2000). However, the majority of these channels have a high degree of homology (> 90%) (Goldin, 2002). The subunits of voltage-gated  $\text{Na}^+$  are formed from  $\alpha$ ,  $\beta 1$  and  $\beta 2$ . While the  $\alpha$  subunits form the pore and has a large molecular weight ( $\approx 260$  kDa), the  $\beta$  subunits have a crucial function in regulating the gating processes (Catterall, 2000a; Caterall et al., 2005). In the heart,  $\text{Nav1.5}$  channels consist pore-forming  $\alpha$ -subunits and accessory  $\beta$ -subunits as shown in Figure 1.4A. The  $\alpha$  subunit of  $\text{Na}^+$  and  $\text{Ca}^{2+}$  channels are formed from a single polypeptide chain with a total of 24 transmembrane segments.

The segments S1 to S4 of each group of transmembrane domains play the role of voltage sensor. Particularly, the S4 transmembrane segment is reported as the fundamental voltage sensor which has four positively charged amino acid residues (usually arginine) through the transmembrane domain, and is known as the four helix bundle (Noda et al., 1984). These positive charges are organized in a specific sequence among the gating charge of the voltage sensor and are labelled as R1-R4. Although voltage-gated sodium channels in myocardial cells are closed at resting potentials, the gate of  $\text{Nav1.5}$  opens in response to membrane depolarisation as a result of electrotonic spread from electrically coupled neighbouring cells. Once sufficient  $\text{Na}^+$  channels open, the membrane becomes relatively more permeable to  $\text{Na}^+$  than to  $\text{K}^+$  and the membrane potential depolarises rapidly towards  $E_{\text{Na}}$  in an all-or-nothing fashion, producing the upstroke (phase 0) of the action potential. The critical membrane potential from which action potentials can first be produced as the membrane depolarises is known as the threshold potential. Once activated, this channel is rapidly inactivated within 1-2 milliseconds through blocking the pore gating by the intracellular inactivation particle (Hodgkin and Huxley, 1990; Huang et al., 2017). The level of activation voltage is reached as a response to the generation of electrical impulses by the cardiac pacemaker (Huang et al., 2017). The positive charge of the voltage sensor is exposed to the local change in potential

which causes the movement of the gating charge from the inner surface to the outward direction. In the activated state, the outward movement reflected the helical screw feature of the gating charges (Catterall, 2014). The movement of S4-S5 linker leads to the movement of S5 and S6 segment, and opens the pore allowing  $\text{Na}^+$  ions to pass (Yarov-Yarovoy et al., 2012). The architecture of Nav1.5 pore reveals a wide outer vestibule, a narrow ion selectivity filter, and a large central cavity (Catterall, 2014). Although the overall pore architecture of voltage-gated  $\text{Na}^+$  and  $\text{K}^+$  channels is similar, these channels are varied in the structure of ion selectivity filters and their conductance. The selectivity filter of Nav1.5 channels has a high-field-strength site at its extracellular end, formed by four glutamate residues, which is contained in the P-loop between S5 and S6 (Payandeh et al., 2011). This outer site of Nav1.5 selectivity filter is followed by two ion co-ordination sites formed by backbone carbonyls, which are perfectly designed to conduct  $\text{Na}^+$  as a hydrated ion.

#### 1.2.3.1.2 Voltage-gated calcium channels

In cardiac muscle, the functional roles for  $\text{Ca}^{2+}$  channels are include the generation of cardiac pacemaker automaticity, electrical conduction and ventricular contraction (Huang et al., 2017). In ventricular cardiomyocytes, the voltage-gated  $\text{Ca}^{2+}$  channels are extremely important in maintaining cardiac depolarization by generating the inward movement of  $\text{Ca}^{2+}$  ions. The contractile signals are achieved directly by increasing the intracellular  $\text{Ca}^{2+}$  concentration from L-type  $\text{Ca}^{2+}$  channels and via the  $\text{Ca}^{2+}$ -induced activation of ryanodine receptors in the sarcoplasmic reticulum to mediate the calcium release (Reuter, 1979; Tsien, 1983; Bers, 2002). The intracellular concentration of  $\text{Ca}^{2+}$  ions is generally maintained at low level during diastolic phase, allowing myocardial relaxation. One important mechanism of regulating intracellular  $\text{Ca}^{2+}$  is the sarco/endoplasmic reticulum Ca-ATPase (SERCA) (Eisner et al., 2020). Increasing SERCA activity leads to faster systolic  $\text{Ca}^{2+}$  decay that further diastolic  $[\text{Ca}^{2+}]_i$  will fall before the next beat resulting in lower end-diastolic  $\text{Ca}^{2+}$ . It has been shown that decreasing SERCA activity results in increased diastolic  $\text{Ca}^{2+}$  (Sankaranarayanan et al., 2017; Elliott et al., 2012). Another important mechanism working on maintaining lower  $\text{Ca}^{2+}$  during diastole is the sodium-calcium exchanger (NCX). This transporter actively pumps 1  $\text{Ca}^{2+}$  out of cell in exchange with 3  $\text{Na}^+$ , generating an electric current (Mechmann and Pott, 1986). It is worth noting that NCX works in either direction depending on the ionic gradients and the membrane potential (Barcenas-Ruiz et al., 1987).

Although there are many different types of  $\text{Ca}^{2+}$  channels (e.g N-, Q-, R-, and P-type) in different human cells, L (long lasting and large conductance) and T (transient-opening and small conductance) types are most prominent in the cardiac muscle and play an important role in the controlling of a cardiac function (Hirano et al., 1989). The L-type  $\text{Ca}^{2+}$  channel is considered as the main ventricular type to pass the  $\text{Ca}^{2+}$  ions into the cell and is distributed in all parts of cardiac cells whereas the T-type  $\text{Ca}^{2+}$  channel is expressed in specific regions of the heart such as in cardiac pacemaker, the atrium and Purkinje fibres (Rosati et al., 2007).

Voltage-gated  $\text{Ca}^{2+}$  channels have a structural similarity with the  $\alpha$ -subunit of voltage-gated  $\text{Na}^+$  channels. The  $\alpha$ -subunit of the voltage-gated  $\text{Ca}^{2+}$  channels are modulated by several accessory subunits, including  $\beta$ ,  $\gamma$  and  $\delta$  subunits (Curtis and Catterall, 1984; Takahashi et al., 1987). The  $\alpha 1$  subunit is a large protein with a molecular weight at  $\approx 190$  kDa (Takahashi et al., 1987). The sequence of  $\text{Ca}^{2+}$  channel  $\alpha 1$  subunit is, as with  $\text{Na}^+$  channels, four identical domains, each containing a group of six transmembrane segments with the P loop between S5 and S6 transmembrane segment serve as the pore-forming module (as shown in Figure 1.4B). As in  $\text{Na}^+$  channels, the voltage sensor of  $\text{Ca}^{2+}$  channel is found in the S4 transmembrane segment, while the pore is located between the S5 and S6 segments. The external end of the pore-lining of voltage-gated  $\text{Ca}^{2+}$  channel has a distinctive feature by tapering to a small diameter, providing a high selectivity of  $\text{Ca}^{2+}$  ions (Heinemann et al., 1992). The accessory subunits of voltage-gated  $\text{Ca}^{2+}$  channels give different characteristics to the  $\text{Ca}^{2+}$  current. The presence of  $\beta$  accessory subunit increases the level of  $\text{Ca}^{2+}$  channel expression and the gating function, and has four intracellular membrane segments with a molecular weight at 55 kDa (Ruth et al., 1989; Grant, 2009). The  $\gamma$  subunit has four transmembrane segments with a low protein weight (33 kDa) and has only a minor effect on  $\text{Ca}^{2+}$  gating function (Jay et al., 1990). The 170 kDa  $\alpha 2$  subunit is found at the extracellular level and connected to  $\delta$  subunit throughout the cell membrane by a disulfide-linker ( $\alpha 2\delta$ ) (Gurnett et al., 1996).

Cav1.2 is the principal pore-forming alpha-subunit underlying the L-type  $\text{Ca}^{2+}$  channels in ventricular myocytes. L-type  $\text{Ca}^{2+}$  channels are the main source of excitation–contraction coupling as an influx of calcium occurs through them during membrane depolarization providing long-lasting activity in ventricular myocytes (Hofmann et al., 2014; Zamponi et al.,

2015). In contrast, T-type  $\text{Ca}^{2+}$  channels are a transient (rapid) current which opens when a slight depolarisation occurs. T-type channels are not expressed in ventricular myocytes but are mainly found in atrial or sinusoidal cells of the heart and therefore plays an important role in cardiac pacemaking and electrical impulse conduction (Li et al., 2020; Mangoni et al., 2006). The pore of Cav1.2 channels opens during the depolarisation of the cell membrane to mediate the influx of  $\text{Ca}^{2+}$  through an opening of L-type  $\text{Ca}^{2+}$  channels into the cell. This  $\text{Ca}^{2+}$  influx balances the  $\text{K}^+$  efflux, creating a plateau phase (phase 2) of the action potential. Therefore, the entered  $\text{Ca}^{2+}$  into cells serves an essential role in the regulation of muscle contraction (Cosconati et al., 2007).

#### 1.2.3.1.3 Voltage-gated potassium channels

Cardiac voltage-gated potassium channels ( $\text{K}_v$ ) are proteins spanning the cell membrane which allow the  $\text{K}^+$  ions to move down their electrochemical gradient. This plays a vital role in a cardiac action potential by the outward movement of positive charge driving the membrane potential to a more negative value (Hodgkin and Huxley, 1990). Therefore,  $\text{K}^+$  channels are active during the diastolic period, particularly the inward rectifiers, and stabilise the resting membrane potential of cardiac myocytes. Activation of  $\text{K}^+$  channels can shift the membrane potential towards  $E_K$ , thereby contributing to hyperpolarisation of the resting membrane and reduction in cell excitability (Hille, 1978).  $\text{K}^+$  channels are considered as the most abundant and widely distributed family of ion channels in the human body (Coetzee et al., 1999; Huang et al., 2017). These channels are categorized into three main families, depending on the number of transmembrane domain (TMD) regions within the pore-forming  $\alpha$ -subunits of the  $\text{K}^+$  channels (Figure 1.4C), and include voltage-gated (6TMD), twin pore domain (4TMD) and inwardly rectifying channel (2TMD).

There are various types of  $\text{K}_v$  currents involved in repolarization of action potential; the transient outward  $\text{K}^+$  current ( $I_{\text{to}}$ ), the rapidly activating  $\text{K}^+$  currents ( $I_{\text{Kr}}$ ) and the slowly activating  $\text{K}^+$  currents ( $I_{\text{Ks}}$ ). Voltage-gated  $\text{Na}^+$  and  $\text{Ca}^{2+}$  channels are constructed from a single polypeptide, whereas the  $\text{K}_v$  channels are formed as a tetramer of four individual subunits rather than a single peptide with 4 homologous repeats as seen in  $\text{Na}^+$  and  $\text{Ca}^{2+}$  channels (Tempel et al., 1987; Kamb et al., 1987; Pongs et al., 1988). Each  $\text{K}_v$  subunit includes six transmembrane segments (T1-T6) and intracellular N- and C-terminals (Figure 1.4C(i)). Similar

to  $\text{Na}^+$  and  $\text{Ca}^{2+}$  channels, the voltage sensor of  $\text{K}^+$  channel is in the S4 transmembrane segment which contains of a group of positively charged residues; mainly arginine. The conducting pore of  $\text{K}^+$  channel is between the S5 and S6 transmembrane regions (known as P-region) similar to other voltage-gated ion channels. However, the  $\text{K}^+$  channel conducts the ions in different way compared to  $\text{Na}^+$  channel through the conducting pore. The selectivity filter of  $\text{K}^+$  pore-region is specialized with a narrow diameter because it permits  $\text{K}^+$  ions to pass only in the dehydrated form. Importantly, there are two major key features of  $\text{K}^+$  channels which contribute to the functional role of  $\text{K}^+$  channels (Armstrong, 2003). These include the ion conductance and selectivity, and inactivation properties. In the extracellular field, the  $\text{K}^+$  ions stabilized by binding to water molecules, performing hydrated  $\text{K}^+$  ions ( $\text{K}^+ + \text{H}_2\text{O}$ ). The selectivity filter for potassium channels consist of three residues sequence of glycine – Tyrosine – glycine (GYG) or glycine – phenylalanine – glycine (GFG), which is contained in the P-loop between S5 and S6. This perfectly coordinates the dehydrated  $\text{K}^+$  ion, improving selectivity. This short sequence confers selectivity to  $\text{K}^+$  over all other ions.

#### 1.2.3.2 Twin-pore potassium channels

Twin-pore potassium channels ( $\text{K}_{2\text{P}}$ ) are characterised as having two P-loops in a single  $\alpha$ -subunit of four transmembrane domains (S1 to S4) (Goldstein et al., 2005; Enyedi and Czirják, 2010) (Figure 1.4C(ii)). The functional  $\text{K}^+$  channels are achieved by the co-assembly of only two  $\alpha$ -subunits (Ahern and Kobertz, 2009). These  $\text{K}^+$  channels are known as background or leak current channels due to their lack of a voltage-sensing domain (Coetzee et al., 1999). As a consequence, these channels lack voltage-dependent gating but instead exhibit weak rectification, which plays a role in driving cell membrane toward the negative resting membrane potential to stabilise the cell (Enyedi and Czirják, 2010; Sepúlveda et al., 2015). Fifteen subfamilies have been identified for the  $\text{K}_{2\text{P}}$  family and can be classified into six distinct family groups: TASK (two-pore domain acid-sensitive  $\text{K}^+$  channel), TWIK (tandem of pore domains in a weak inward rectifier  $\text{K}^+$  channel), TREK (TWIK-related  $\text{K}^+$  channel), TRAAK (TWIK-related arachidonic acid-activated  $\text{K}^+$  channel), TRESK (TWIK-related spinal cord  $\text{K}^+$  channel) and THIK (tandem of pore domains in halothane-inhibited  $\text{K}^+$  channel). Importantly, the TASK family includes the TAS<sub>K1</sub> subfamily which is widely distributed in the heart, and its targeting has been recently shown to play an essential role in preventing arrhythmias (Schmidt et al.,

2019). These  $K_{2P}$  channels are controlled by different physiological factors, such as temperature and pH, which alter the open probability of these channels (Plant, 2012).

#### 1.2.3.3 Inwardly rectifying potassium channels

The molecular structure of the inwardly rectifying  $K^+$  channels ( $K_{ir}$ ) is considered less complex than that of other  $K^+$  channels and comprises two transmembrane domains (2TMD) and a single pore-loop (Coetzee et al., 1999; Hibino et al., 2010) (Figure 1.4C(iii)). Functional  $K_{ir}$  channels are produced by the clustering of four  $\alpha$ -subunits of the 2TMD  $K^+$  channel. This group of channels differs from  $Kv$  channels in that they lack the S3-6 segments, responsible for providing voltage-sensing, and so  $K_{ir}$  subunits are thought to be the simplest  $K^+$  channels. Although membrane depolarisation does not trigger the opening of  $K_{ir}$  channels, the passage of ions through this channel is regulated by different mediators, such as intracellular  $Mg^{2+}$  and  $Ca^{2+}$ , extracellular  $Ba^{2+}$ , G proteins and phosphatidylinositol 4,5-bisphosphate (PIP<sub>2</sub>) (Makino et al., 2011; Lopatin et al., 1994; Xie et al., 2007).

This  $K_{ir}$  family is named for its biophysical characteristic of allowing linear ion influx at membrane potential negative to  $E_K$  whilst having limited efflux from the cell at potentials positive to  $E_K$ , so called inward-rectification (Nichols and Lopatin, 1997). As stated, these channels are structurally voltage-independent, however they are blocked by  $Mg^{2+}$  ions and intracellular polyamines, such as spermine, in a voltage-dependent manner giving rise to the rectification properties (Lopatin et al., 1994; Kurata et al., 2008). Movement of  $K^+$  ions in an inward direction is unlikely to ever occur physiologically as the membrane potential of a “real” cell is unlikely to rest more negative than  $E_K$ ,  $\sim -95$  mV (Hille, 1978).

There are seven members in this family, comprising  $K_{ir} 1.x$  to  $K_{ir} 7.x$  (Adelman et al., 2019). They can be subdivided into four groups as follows: classical  $K_{ir}$  channels ( $I_{K1}$ ) ( $K_{ir} 2.x$ ),  $K^+$  transport channels ( $K_{ir} 1.x$ ,  $K_{ir} 4.x$ ,  $K_{ir} 5.x$  and  $K_{ir} 7.x$ ), G protein-coupled  $K_{ir}$  channels (GIRK) ( $K_{ir} 3.x$ ) and adenosine triphosphate (ATP)-sensitive  $K^+$  channels ( $K_{ATP}$ ) ( $K_{ir} 6.x$ ). Additionally, these members can be classified based on their degree of inward rectification into strong ( $K_{ir} 2.x$  and  $K_{ir} 3.x$ ), intermediate ( $K_{ir} 4.x$ ) and weak ( $K_{ir} 1.1$  and  $K_{ir} 6.x$ )  $K_{ir}$  channels.

#### 1.2.4 Cardiac action potentials

The efficient functioning of the heart as a pump is dependent on co-ordinated electrical excitability. This electrical excitation is initiated by depolarisation of the plasma membrane (PM) and is terminated by stabilisation of the membrane potential by repolarisation to shape the cardiac action potential (AP). An AP is the sequence of alterations in the ion gradient through the opening and closing of specific ion channels. Therefore, the shape and duration of Aps vary according to the interplay between different ion channels during various pathophysiological conditions. For instance, heart failure induces a prolongation of cardiac Aps, while acute myocardial ischaemia leads to shortening of APs (Cutler et al., 2007; Rodriguez et al., 2006). However, most cardiac cells have a similar fundamental AP structure, which comprises five phases, as described in the following section (Figure 1.5) (Grant, 2009).

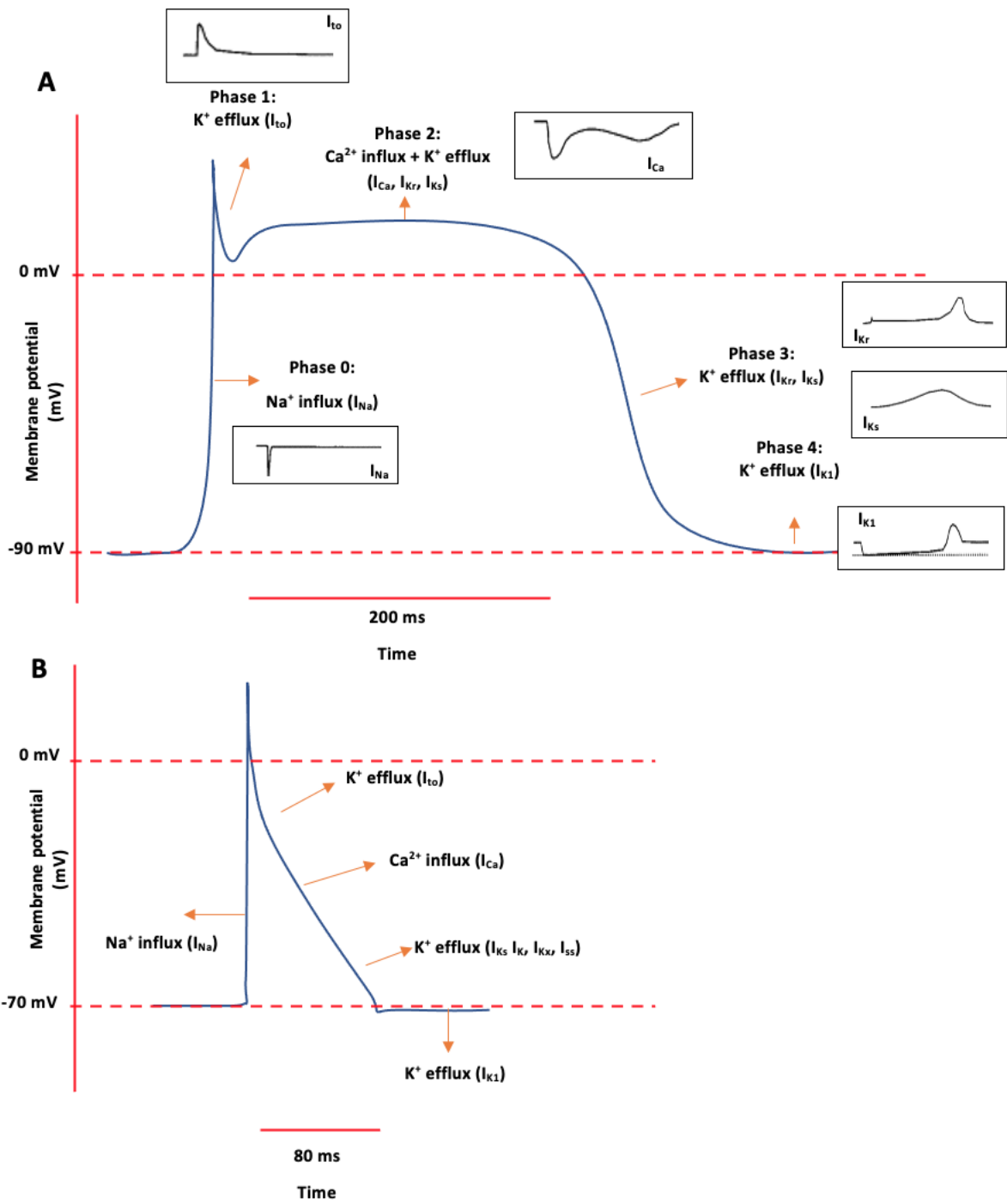
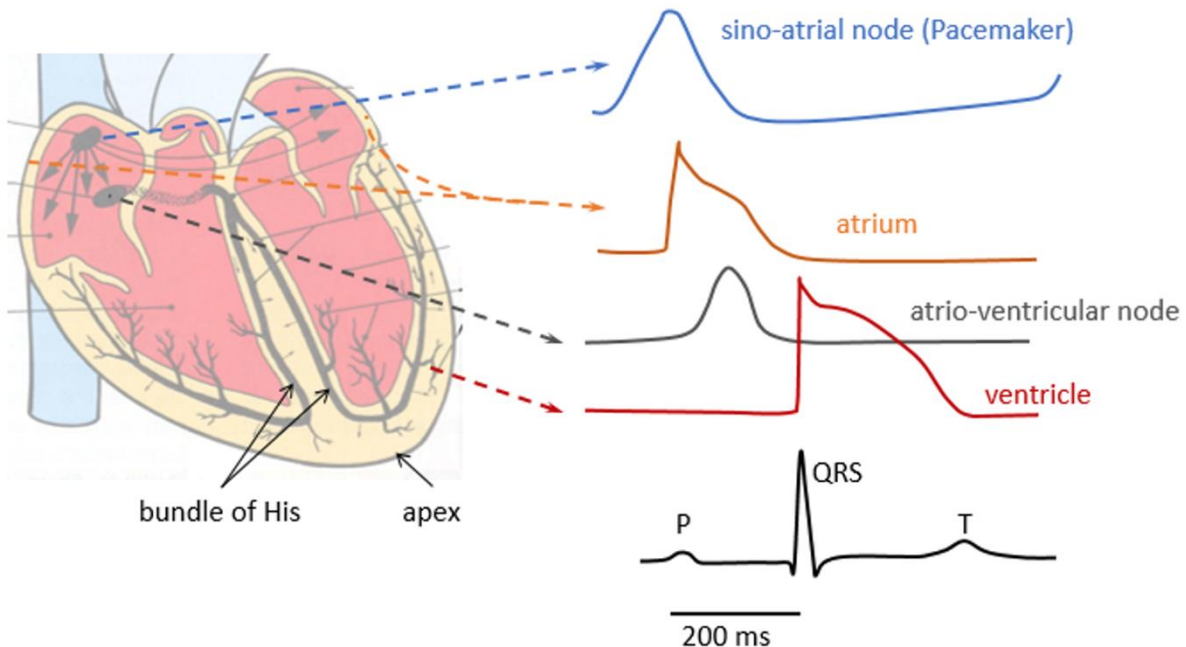


Figure 1.5: Action potential of ventricular myocytes in human and rat.

*A, The main ion currents at different phase of the action potential in human and the principal underlying ionic currents (amended from (James et al., 2007)). B, The main ion currents at different phase of the action potential in rat.*

The Electrocardiogram (ECG) is the average of instantaneous electrical activities of all excitable cells in the heart, which is recorded by electrodes from the body surface. The ECG contains a few characteristic deflections and intervals that can be used clinically to

characterise normo- and pathophysiological conditions (Figure 1.6). The P wave corresponds to atrial depolarisation, the QRS complex ventricular depolarisation, and the T wave shows ventricular repolarization, respectively. Atrial repolarisation occurs during the QRS complex and so is not normally visible.



**Figure 1.6:** Regional differences in cardiac action potential configurations (AP) and a corresponding electrocardiogram (ECG) showing the waves and time correlation between the AP and the ECG.

*Schematic cross section of the heart depicting the corresponding action potential configuration from different regions of the heart indicated by arrows. Sino-atrial node, atrium, atrio-ventricular node and ventricle. A normal electrocardiogram where P and T waves, QRS complex, intervals and segments are shown. Ventricular electrical activity occurs during QT interval, whereas electrical activities of other regions occur during P interval (amended from (Joukar, 2021)).*

#### 1.2.4.1 Phases of ventricular cardiac action potentials

Phase 0 is known as the rapid depolarisation phase which is initiated by electrical stimulation to reach the threshold voltage and activation of voltage-gated  $\text{Na}^+$  ( $\text{Na}_v$ ) channels at approximately -55 mV. This allows the influx of  $\text{Na}^+$  ions into the cell down their electrochemical gradient (Table 1.1). This rapid influx of  $\text{Na}^+$  ions contributes to a sharp increase in the membrane potential to a positive membrane potential towards the  $E_{\text{Na}}$  value as  $\text{Na}^+$  briefly becomes the primary permeating ion (Nerbonne and Kass, 2005; Santana et al., 2010).

Phase 1 is represented by the small downward reflection (notch) in Figure 1.5, which reflects the initial repolarisation phase of the AP. This small repolarisation is achieved by the rapid closure of  $\text{Na}_v$  channels coupled with the activation of the fast-transient outward  $\text{K}^+$  currents. Therefore, the combination of  $\text{K}^+$  efflux and the absence of  $\text{Na}^+$  influx shifts the membrane potential more negative (Tamargo et al., 2004; Liu et al., 1993).

Phase 2 is called the plateau phase, which is maintained by the balanced movements of  $\text{Ca}^{2+}$  influx and  $\text{K}^+$  efflux. Due to the opening of long-lasting  $\text{Ca}_v$  channels, this phase lasts for around 200 ms, at a resting heart rate, to maintain a refractory period that prevents cardiac arrhythmias (Tamargo et al., 2004; Grant, 2009).

Phase 3 is identified as the late and rapid repolarisation phase, which is generated by the activation of the outward delayed rectifier  $\text{K}^+$  channels such as the ultra-rapid delayed rectifier, rapid delayed rectifier ( $I_{\text{Kr}}$ ), and slow delayed rectifier ( $I_{\text{Ks}}$ ) (Nicolas et al., 2008). The  $\text{K}_v$  channels are highly selectively permeable to  $\text{K}^+$  ions meaning that the outward movement of  $\text{K}^+$  ions is 10,000 times more than the inward movement of  $\text{Na}^+$  ions through these channels. Consequently, the membrane potential is driven to more negative potentials as  $\text{K}^+$  is the primary permeant ion. However, the PM is not able to reach  $E_K$  at this stage, as these activated channels are voltage-dependent and do not open at negative membrane potentials.

Phase 4 is the resting membrane phase, which is controlled by the classical inwardly rectifying  $\text{K}^+$  and is termed  $I_{\text{K1}}$ .  $I_{\text{K1}}$  is an outward  $\text{K}^+$  current that contributes to setting of the resting membrane potential. This channel can open at a relatively negative membrane potential and maintains the membrane close to  $E_K$ . The role of this channel is to restore the membrane potential such that once the membrane is highly hyperpolarised, it contributes to an inward  $\text{K}^+$  current that provides slight depolarisation (Hibino et al., 2010).

The diversity in ion currents and channels density leads to variation in type, duration and amplitude of action potentials between species; particularly rat and human ventricular action potentials. In all species, the action potential is initiated by the entry of  $\text{Na}^+$  currents which are passing through the opening of voltage-gated sodium channels (Edwards and Louch,

2017). The rapid upstroke of action potential triggers the opening of voltage-gated calcium channel which allows  $\text{Ca}^{2+}$  influx through this channel and therefore elicits further  $\text{Ca}^{2+}$  released via calcium-induced calcium release mechanism from the sarcoplasmic reticulum (Tamargo et al., 2004; Grant, 2009). In contrast, differences in the  $\text{K}^+$  currents contributing to ventricular repolarisation are the major determinant of species differences in ventricular action potentials (Edwards and Louch, 2017). In human the initial repolarisation due to  $I_{\text{to}}$  (transient outward potassium current) is followed by the plateau of the action potential, and, following the inactivation of calcium current,  $I_{\text{Kr}}$  and  $I_{\text{Ks}}$  (rapidly- and slowly- delayed rectifier potassium current) become dominant (Figure 1.5A). Therefore, the repolarisation phase in human ventricular myocytes relies on  $I_{\text{Kr}}$  and  $I_{\text{Ks}}$  which exhibit slower repolarising currents and responsible for the late repolarisation. In rat, in contrast, ventricular repolarisation relies on  $I_{\text{to}}$  that develop rapidly during action potential and dominates to the early contribution to repolarisation (Figure 1.5B) (Gralinski, 2003).  $I_{\text{Ks}}$  also contributes onto the repolarisation of the rat ventricular AP. Previous studies suggested that there are different components that might contribute to outward current in rat cardiomyocytes, including the inward rectifier current ( $I_{\text{K}}$ ) and the non-inactivating steady-state current ( $I_{\text{ss}}$ ) (Himmel et al., 1999; Choisy et al., 2004). Interestingly, these currents have been shown to exhibit remarkable variability in the shape of action potential. For instance, ventricular action potentials in rat show a shorter duration and a more triangulated morphology than the human ventricular myocytes (Varró et al., 1993). Additionally, the expression of  $I_{\text{K1}}$ , which plays a major role in terminal repolarisation and stabiliser of resting membrane potential, is lower in rat ventricular myocytes compared to human and therefore this contributes to a more negative resting potential of  $\sim -90$  mV in human compared with that rat  $\sim -70$  mV (Santana et al., 2010; Kavak et al., 2008).

#### 1.2.4.2 Automatic generation of electrical impulses in the heart

The contraction of the heart is regulated by the transmission of electrical impulses through the specialised conduction system (Eckert et al., 1988; Silverman et al., 2006). For this to be done efficiently, the conduction system is segmented into three main components to provide coordinated conduction, which comprise the sinoatrial node (SAN), atrioventricular node (AVN) and Purkinje fibres. These parts ensure the uniform spreading of electrical pulses over

the atria and ventricles so that they can effectively pump nutrient- and oxygen-containing blood into the arterial trunks (the aorta and pulmonary arteries).

#### 1.2.4.2.1 Sino-atrial node

The electrical pulse is initiated in the sino-atrial node (SAN), which is known as the cardiac pacemaker and is located in the right atrium (Keith and Flack, 1907; Anderson et al., 2009). This primary pacemaker is distinguished by a unique set of ion channels, leading to SAN APs having features that are different from those of ventricular APs, such as the delayed outward rectifier K<sup>+</sup> current ( $I_K$ ), voltage-dependent activation current (funny current,  $I_f$ ), T-type Ca<sup>2+</sup> current ( $I_{Ca,T}$ ), L-type Ca<sup>2+</sup> current ( $I_{Ca,L}$ ) and Ca<sup>2+</sup> clock current ( $I_{NaCa}$ ) (Monfredi et al., 2010). The AP of the SAN is intrinsic, as the SAN automatically generates electrical impulses, a phenomenon referred to as the pacemaker potential (Figure 1.7) (Bozler, 1943). During the pacemaker potential, the membrane is depolarised with a smaller overshoot to become more positive, resulting in the threshold for activation being reached in phase 4. This phase is controlled by the funny current ( $I_f$ ) which is also known as the inward current carried almost entirely by Na<sup>+</sup> (DiFrancesco, 2010). The hyperpolarisation-activated cyclic-nucleotide gated (HCN) channel is responsible for this  $I_f$  current and is widely expressed in the cardiac pacemaker (Dobrzynski et al., 2007). Once the membrane reaches the threshold level, T-type Ca<sup>2+</sup> channels and LTCCs are activated to initiate the depolarisation phase of SAN AP (referred to as phase 0). Importantly, the APs of the SAN do not have a resting potential phase, unlike ventricular APs, which is due to the lack of  $I_{K1}$ . Repolarization of the sinus node (phase 3) is carried out by the activation of a variety of K<sup>+</sup> currents: transient outward K<sup>+</sup> current ( $I_{to}$ ) and ultra-rapid (possibly), rapid- and slow- delayed rectifier K<sup>+</sup> currents ( $I_{Kur}$ ,  $I_{Kr}$  and  $I_{Ks}$ , respectively) (Dobrzynski et al., 2013).

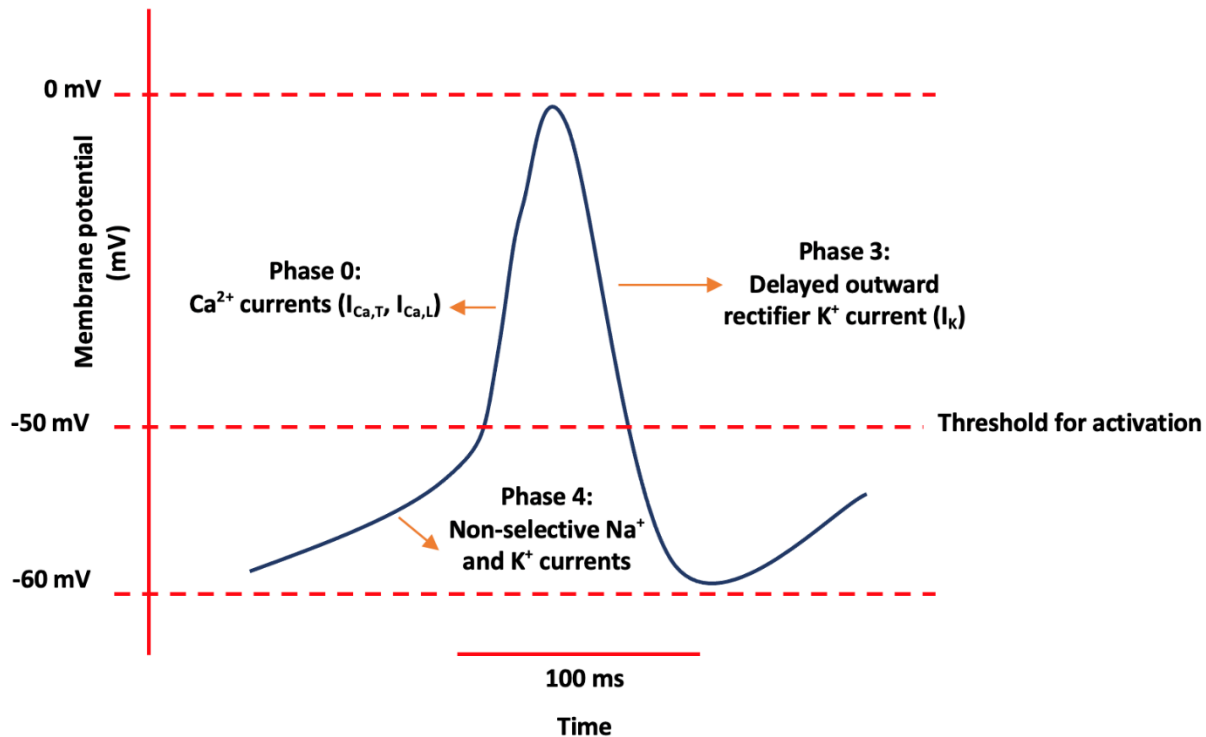


**Figure 1.7:** Phases of the action potential of sinoatrial nodal (SAN) pacemaker, showing the ionic current responsible to generate each phase.

*Phase 4: is the pacemaker potential phase which controlled by the funny current ( $I_f$ ) to reach the threshold level for activation. Phase 0: the depolarization phase which triggers by the activation of different types of voltage-gated channels; T-type  $\text{Ca}^{2+}$  current ( $I_{\text{Ca},T}$ ), L-type  $\text{Ca}^{2+}$  current ( $I_{\text{Ca},L}$ ). phase 3: the repolarization phase which shifts the membrane back to the negative voltage by the opening of delayed outward rectifier  $\text{K}^+$  current ( $I_K$ ). (Adapted from (Dobrzynski et al., 2013)).*

#### 1.2.4.2.2 Atrioventricular node system

Once the sinus impulses have been distributed over the two atrial chambers, these impulses pass through the atrioventricular node (AVN), which is responsible for transporting the electrical pulses from the atria to the ventricles. The most important feature of this conduction system is placed in creating a delay of electrical impulses by up to 0.12 s (Verheule and Kaese, 2013). This delay allows the blood in the atria to fully move into the ventricles before ventricular contraction begins. AVN cells contain channels similar to those of SAN cells, including  $I_K$ ,  $I_f$ ,  $I_{\text{Ca},T}$  and  $I_{\text{Ca},L}$ . However, the action potential duration (APD) of the AVN is longer than that of the SAN because the  $\text{Na}^+$  channels are absent and therefore leads to slow upstroke velocity of the action potential (Greener et al., 2011).

#### 1.2.4.2.3 Purkinje fibres

The electrical signal propagates over the ventricular myocardium via the crucial network of Purkinje fibres. This conduction system specialises in propagating electrical signals at a very rapid velocity due to the extensive expression of connexin (Cx) (Davis et al., 1995; Gourdie and Lo, 1999). Connexins are a large family of highly homologous transmembrane proteins, comprising 20 and 21 different isoforms in mice and humans, respectively (Dobrowolski and Willecke, 2009). Connexin 43 (Cx43) is, by far, the best-known and most ubiquitously expressed isoform, and it is encoded by the GJA1 gene, located, in humans, in chromosome 6 (Fishman et al., 1991). The gene nomenclature for the two other most common human cardiac connexin isoforms, Cx40 and Cx45, are GJA5 and GJC1, respectively (Söhl and Willecke, 2003). Cx43 is the main connexin isoform expressed in the working ventricular myocardium (Rohr, 2004). The rapid pathway also corresponds to the unique structure of these cells, which have fewer myofibrils than the myocardial cells. In addition, the electrical signal can be conducted rapidly due to the high expression of Nav channels which causes a rapid increase in membrane potential in these cells (Nerbonne and Kass, 2005).

#### 1.2.4.3 The role of the autonomic nervous system in the regulation of cardiac action potentials

The major factors modulated by the activation of the autonomic nervous system (ANS) include heart rate (chronotropy), electrical conduction velocity (dromotropy), ventricular contraction (inotropy) and relaxation rate (lusitropy). Importantly, the intrinsic heart rate and the AVN conduction system are controlled by two branches of the extrinsic cardiac ANS: the sympathetic and parasympathetic nervous systems (SNS and PSNS) (Salata and Zipes, 2020). Sympathetic efferent neurones arise in the intermediolateral horn of the spinal cord (Karemaker, 2017). Most sympathetic fibres (>90%) innervate the heart from both sides of the stellate ganglia (cervicothoracic ganglia). Subsequently, the nervous signal travels along sympathetic postganglionic fibres, which are highly concentrated on the right side of the heart and the atrial surface (Deuchars and K. Lall, 2011; Kattar and Flowers, 2020).

Parasympathetic preganglionic neuronal fibres originate from the vagus nerve, arising in the medulla oblongata (Kawashima, 2005). Most parasympathetic preganglionic nerves (~80%) arise from the nucleus ambiguus of the medulla and terminate at the junctional site of the

superior vena cava (SVC) and right atrial surface. The SAN is predominantly influenced by right vagus nerve stimulation, whereas the AVN junction is significantly affected by left vagus nerve stimulation (Ng et al., 2001).

Two major neurotransmitters are released during the activation of the neuronal system: adrenaline, noradrenaline (NA) and acetylcholine (ACh). The activation of the sympathetic system contributes to the release of adrenaline and noradrenaline into the bloodstream, which directly stimulates the adrenergic receptors, including the  $\alpha$  and  $\beta$  receptors, in cardiac cells (Samson et al., 2015; Thomas and Marks, 1978).  $\beta$ -adrenergic receptors are extensively expressed in the heart (~90%), whereas  $\alpha$  receptors are less dominant (~10%) (O'Connell et al., 2014). The targeted activation of  $\beta$ -adrenergic receptors by the binding of NA results in increases in the levels of cyclic adenosine monophosphate which increases protein kinase A (PKA) activity (Alhayek and Preuss, 2020). PKA phosphorylates various protein subunits, such as those of HCN channels ( $I_f$ ) and Cav channels ( $I_{Ca,T}$  and  $I_{Ca,L}$ ). Consequently, this leads to an increased intrinsic heart rate and rapid myocardial contractility.

In opposition to the sympathetic drive, the activation of the parasympathetic system results in the release of ACh, which activates muscarinic and nicotinic receptors (Liu et al., 2012; Zimmermann, 1988). There are several subtypes of muscarinic receptors, including M1 to M5 (Dhein et al., 2001; Liu et al., 2012), of which M2 is considered the most essential for the regulation of cardiovascular function. The stimulation of the vagus nerve leads to reductions in heart rate and cardiac contractility via the activation of ACh-dependent  $K^+$  ( $K_{ACh}$ ) channels in the SAN. The activation of  $K^+$  channels causes the membrane potential to become more negative, which limits its ability to reach the threshold for activation, and therefore slows the heart rate by delaying the functional role of  $I_f$  currents (DiFrancesco, 2010). As a result, the SNS causes a positive chronotropic effect, whereas the PSNS contributes to a negative chronotropic effect.

### 1.2.5 The role of calcium currents in the regulation of cardiac contraction

The surface membrane of cardiomyocyte is invaginated into a set of transverse (T) tubules. The T-tubules possess  $Na^+$  and  $Ca^{2+}$  channels and closely passes the branching tubular

network that forms the sarcoplasmic reticulum (SR) (Hayashi et al., 2009; Pinali et al., 2013). The SR plays an important role in excitation-contraction coupling because it contains a store of calcium. The SR contains two regions that play essential roles in  $\text{Ca}^{2+}$  handling. The first is that the network SR comprises tubes that take up  $\text{Ca}^2$  via  $\text{Ca}^{2+}$ -ATPase pumps. The second is that the junctional SR makes close contact with the T-tubules. Therefore, ryanodine receptors (RyRs) on the surface of SR are very closely located to L-type  $\text{Ca}^{2+}$  channels on the T-tubules, forming the cardiac dyad (dyadic cleft). The close association between L-type  $\text{Ca}^{2+}$  channels and ryanodine receptors at the cardiac dyad ensures the synchronous rise of intracellular  $\text{Ca}^{2+}$  currents during systole (Louch et al., 2004). Previous studies documented that in heart failure, there is a clear change in structure of the cardiac dyad with a reduction in the number of the T-tubules, and therefore a reduction in the synchronicity and the amplitude of  $\text{Ca}^{2+}$  transients (He et al., 2001; Louch et al., 2006; Song et al., 2006).

Excitation-contraction coupling (EC-coupling) is the process converting the electric stimulation (depolarisation of action potential) to mechanical output (contraction) (Santulli et al., 2017; Fabiato and Fabiato, 1975).  $\text{Ca}^{2+}$  plays an essential role in this process as a critical mediator. During excitation, the membrane potential becomes depolarised thereby causing an opening of L-type  $\text{Ca}^{2+}$  channels (Figure 1.8A).  $\text{Ca}^{2+}$  flows via the L-type  $\text{Ca}^{2+}$  channels into a dyadic cleft to initiate cardiac contraction. The movement of  $\text{Ca}^{2+}$  occurs from the extracellular environment, where concentrations are high ( $\sim 1.2 \text{ mM}$ ), into the intracellular environment, where concentrations are low ( $100 \text{ nM}$ ) (Levick, 2013).  $\text{Ca}^{2+}$  ions can reversibly bind to proteins (such as albumin) and form complexes with anions such as citrate and bicarbonate to form complexed calcium (Del Valle et al., 2011). About 90% of the protein-bound calcium is linked to albumin which is not diffusible across the cell membrane. Thus, the extracellular  $\text{Ca}^{2+}$  concentration available for free diffusion is lower than the total extracellular  $\text{Ca}^{2+}$  content which is only about 10 to 15%. Following action potential upstroke, L-type  $\text{Ca}^{2+}$  channels activate rapidly; therefore, the  $\text{Ca}^{2+}$  current has already reached 40% of its peak during phase 1. The current peaks at 2–7 ms, then continues to flow at a very slow declining rate, because L-type  $\text{Ca}^{2+}$  channels inactivate slowly. The  $\text{Ca}^{2+}$  influx signal through L-type  $\text{Ca}^{2+}$  channels is known as a “ $\text{Ca}^{2+}$  sparklet” (Wang et al., 2001). Whereas  $\text{Ca}^{2+}$  sparklets increase intracellular concentration from  $100 \text{ nM}$  to  $\sim 10 \mu\text{M}$ ,  $\text{Ca}^{2+}$  ions are not enough to cause contraction. The trigger  $\text{Ca}^{2+}$  from a single L-type channel is thought to activate a cluster

of 6–20 release channels. Consequently, there is a near-synchronous firing of thousands of  $\text{Ca}^{2+}$  ions released ( $\sim 10\ 000$  per cell), which releases a substantial fraction of the SR store, typically  $\sim 50\%$ . This raises the sarcoplasmic  $\text{Ca}^{2+}$  concentration roughly 10-fold over  $\sim 50$  ms. This process is called  $\text{Ca}^{2+}$ -induced  $\text{Ca}^{2+}$  release (CICR) (Fabiato and Fabiato, 1978; Fabiato, 1985). The mobilization of  $\text{Ca}^{2+}$  from a cluster of release channels on the SR produces a localised elementary  $\text{Ca}^{2+}$  release signal known as a “ $\text{Ca}^{2+}$  spark” (Cheng and Lederer, 2008). Releases of  $\text{Ca}^{2+}$  through CICR from the SR release channels can increase the systolic  $\text{Ca}^{2+}$  concentration up to  $\sim 1\ \mu\text{M}$  transiently (Cheng and Lederer, 2008). The time course of L-type  $\text{Ca}^{2+}$  currents during an action potential has been recorded by applying voltage-clamp pulses consisting of digitised action potentials using a technique called action potential clamp (Doerr et al., 1990). The time course during action potential of global intracellular  $\text{Ca}^{2+}$  concentration ( $\sim 200$  ms) was much slower when compared to the time course of the  $\text{Ca}^{2+}$  transients ( $\sim 25$  ms) (Kistamas et al., 2020; Gómez et al., 1996).

The link between action potential duration and the  $\text{Ca}^{2+}$  transient was addressed by Janczewski and colleagues in 2002 (Janczewski et al., 2002). They used an action potential clamp technique to compare  $\text{Ca}^{2+}$  fluxes and  $\text{Ca}^{2+}$  transients between voltage clamp wave forms representing ‘short’ and ‘long’ action potentials. The study showed that while longer action potentials have smaller magnitude of peak  $\text{Ca}^{2+}$  current than do shorter action potentials, and the total  $\text{Ca}^{2+}$  flux via the L-type  $\text{Ca}^{2+}$  current (represented by the integral of the current) was larger with longer action potentials. Moreover, they suggested that efflux via the  $\text{Na}^+/\text{Ca}^{2+}$  exchanger was smaller with longer action potential wave forms. Thus, the net sarcolemmal  $\text{Ca}^{2+}$  flux at each action potential would be greater with longer action potentials, and the resulting increase in SR  $\text{Ca}^{2+}$  load would have underpinned the larger  $\text{Ca}^{2+}$  transient amplitude with prolonged action potentials.

The free  $\text{Ca}^{2+}$  binds to troponin C in a concentration-dependent manner, which induces conformational changes (Figure 1.8B).  $\text{Ca}^{2+}$  displaces the troponin-tropomyosin complex and exposes the actin binding sites. Then, the formation of cross-bridges between myosin and actin produces the sliding of thick and thin filaments against each other (Ebashi et al., 1967). Myosin forms from the thick filament body with a thin fibrous tail region and head region (Figure 1.8B). The myosin head consists of an ATPase site which can trigger the binding of

adenosine triphosphate (ATP) and subsequently generate its hydrolytic products, for example, adenosine diphosphate (ADP) and phosphate (Hanson, 1989). The energy released from ATP by hydrolysis is transferred to the myosin which leads to a flexion of the myosin head. The motor change of the myosin head is responsible for shifting the thin filament (actin) and Z line towards the centre of the sarcomere and then allowing coupling of the action potential-mediated  $\text{Ca}^{2+}$  transients and muscle shortening and contraction.

During diastole, there are two mechanisms to remove the  $\text{Ca}^{2+}$  that enters the cell during action potentials. The first mechanism is the SR  $\text{Ca}^{2+}$  ATPase (SERCA) that is dependent on the ATP to actively re-uptake  $\text{Ca}^{2+}$  into the SR. The second mechanism is the  $\text{Na}^+/\text{Ca}^{2+}$  exchanger.  $\text{Na}^+/\text{Ca}^{2+}$  exchanger mediates reversibly efflux (forward mode) and influx (reverse mode) of  $\text{Ca}^{2+}$ , depending on the prevailing electrochemical driving force for  $\text{Na}^+$  and  $\text{Ca}^{2+}$ . This  $\text{Ca}^{2+}$  transporter mainly operates in forward mode, which uses the opposing  $\text{Na}^+$  electrochemical gradient to transports one  $\text{Ca}^{2+}$  ions out of the cell for three  $\text{Na}^+$  into the cell (Gambardella et al., 2017). Conversely, during “reverse mode” the  $\text{Na}^+/\text{Ca}^{2+}$  exchanger extrudes  $\text{Na}^+$  in exchange for  $\text{Ca}^{2+}$  influx. The mode in which  $\text{Na}^+/\text{Ca}^{2+}$  exchanger operates is governed by the Na and Ca gradients across the cell membrane, as well as the membrane potential ( $E_m$ ) (where  $E_{\text{Na}/\text{Ca}} = 3E_{\text{Na}} - 2E_{\text{Ca}}$ , where  $E_{\text{Na}}$  and  $E_{\text{Ca}}$  are the Na and Ca equilibrium potentials, respectively) (Blaustein and Lederer, 1999). In simpler terms, the positive membrane potential and high intracellular  $\text{Na}^+$  concentration mediate  $\text{Ca}^{2+}$  influx through the  $\text{Na}^+/\text{Ca}^{2+}$  exchanger, whereas high intracellular  $\text{Ca}^{2+}$  mediates  $\text{Ca}^{2+}$  efflux through the  $\text{Na}^+/\text{Ca}^{2+}$  exchanger. At rest, when  $E_m < E_{\text{Na}/\text{Ca}}$ ,  $\text{Na}^+/\text{Ca}^{2+}$  exchanger can extrude  $\text{Ca}^{2+}$  from the cell. At action potential upstroke, when  $E_m > E_{\text{Na}/\text{Ca}}$ ,  $\text{Na}^+/\text{Ca}^{2+}$  exchanger can bring  $\text{Ca}^{2+}$  into the cell.

Adrenaline and noradrenaline increase  $\text{Ca}^{2+}$  transient through two mechanisms (Levick, 2013). First, the increase in trigger  $\text{Ca}^{2+}$  current across the sarcolemma recruits more clusters of release channels, releasing a greater fraction of the  $\text{Ca}^{2+}$  store. Second, the raised  $\text{Ca}^{2+}$  current during the plateau increases the amount of  $\text{Ca}^{2+}$  available for subsequent uptake into the SR store, leading to an increase in the size of the  $\text{Ca}^{2+}$  store over several heartbeats. For example, L-type  $\text{Ca}^{2+}$  channels are regulated by cyclic adenosine monophosphate-dependent kinase (protein kinase A; PKA) downstream from the stimulation of  $\beta$  adrenergic receptor. PKA mediated phosphorylation of L-type  $\text{Ca}^{2+}$  channels, leading to an increase in the number

of channels in an active state and the permeability of the channel to pass  $\text{Ca}^{2+}$ , and thereby increases calcium release from the SR (Catterall, 2000b). In contrast, downregulation of intracellular cAMP inhibits L-type  $\text{Ca}^{2+}$  channels (Kamp and Hell, 2000). This pathway is coupled to muscarinic receptors ( $M_2$ ) and adenosine receptors ( $A_1$ ) that bind acetylcholine and adenosine released by parasympathetic nerves. The L-type  $\text{Ca}^{2+}$  channels can also be partially inhibited by  $\text{Ca}^{2+}$  channel blockers, such as verapamil and diltiazem (Levick, 2013).

Previous studies indicate that shortening of APD reduces the  $\text{Ca}^{2+}$  transient and prolongation of APD increases the  $\text{Ca}^{2+}$  transient (Clusin, 2008; Janczewski et al., 2002). For instance, the acute myocardial ischaemia reduces plateau duration, in response to the activation of the  $K_{\text{ATP}}$  channel (Levick, 2013). The increased  $K^+$  conductance induces early repolarization. This shortens the plateau, which in turn truncates  $\text{Ca}^{2+}$  influx. This may be helpful, in that it reduces the work of the  $\text{Ca}^{2+}$  pumps/exchangers, and thus reduces  $O_2$  demand during hypoxia. In contrast, chronic cardiac failure, ventricular hypertrophy and chronic infarction lengthen the plateau (Levick, 2013). This is due to the reduction in  $K^+$  channel expression, especially the transient outward  $K^+$  channel. The reduced  $K^+$  current leads to delayed repolarization, and therefore causes a prolonged plateau. A longer action potential favours net accumulation of  $\text{Ca}^{2+}$  in mammalian cardiac cells which may trigger cardiac arrhythmias (Zhang et al., 2016; Anderson, 2004). The effects on the  $\text{Ca}^{2+}$  transient of changing the duration of the repolarisation phase of the action potential was experimentally measured by using action potential clamp and the results suggest that stimulation of old rat cardiomyocytes with a short action potential-clamp reduces the  $\text{Ca}^{2+}$  transient amplitude (Janczewski et al., 2002).

The differences in ventricular repolarisation between rat and human ventricular myocytes has been referred to the different types of  $K^+$  currents that contribute to develop a repolarisation phase of action potential and counteract the developing of  $\text{Ca}^{2+}$  entry via the L-type  $\text{Ca}^{2+}$  current (Edwards and Louch, 2017). The repolarisation in rat myocytes proceeds so rapidly due to the dominant of transient outward current ( $I_{\text{to}}$ ) (Gralinski, 2003).  $I_{\text{to}}$  is considered as a rapidly developing repolarising currents, contributing to the early repolarisation in rat myocytes. The shorter duration of the action potential in rat cardiomyocytes is critically important determinant of  $\text{Ca}^{2+}$  entry via the L-type  $\text{Ca}^{2+}$  current (Yuan et al., 1996; Terracciano and MacLeod, 1997). Despite rat hearts exhibit lower  $\text{Ca}^{2+}$

sensitivity than those from human, SR  $\text{Ca}^{2+}$  is maintained due to the dominant of actively re-uptake  $\text{Ca}^{2+}$  into the SR by SERCA (Walweel et al., 2014). In contrast, the repolarisation in human myocytes proceeds so slowly due to the dominant of delayed rectifier potassium current such as  $I_{\text{Kr}}$  and  $I_{\text{Ks}}$ . This current exhibit much slower repolarising current development, contributing to prolonged the action potential duration. Therefore, more  $\text{Ca}^{2+}$  entered into human cells, and then triggered RyR opening and increased in releasable  $\text{Ca}^{2+}$  (Walweel et al., 2014; Edwards and Louch, 2017; Pieske et al., 2002). Although  $\text{Ca}^{2+}$  is expected to be quickly removed from SR in large species such as human, SR content increases with a faster pacing rate in failing heart.

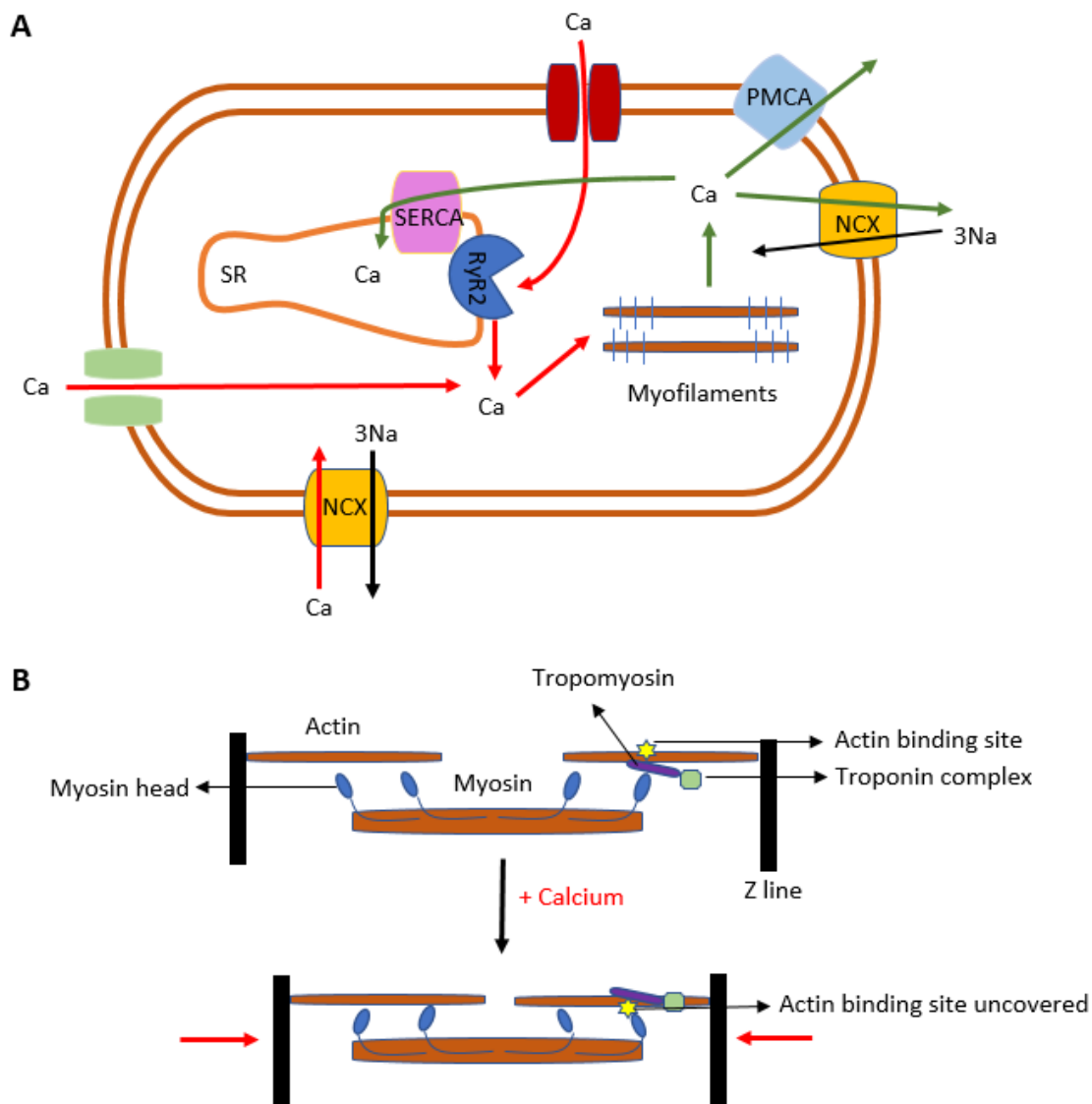


### Figure 1.8: Cardiac calcium cycling.

A,  $\text{Ca}^{2+}$  enters the cell through calcium channels which triggers  $\text{Ca}^{2+}$  release from the sarcoplasmic reticulum (SR). This process is called  $\text{Ca}^{2+}$ -induced  $\text{Ca}^{2+}$  release (CICR). The combination of  $\text{Ca}^{2+}$  influx and release raise the intracellular  $\text{Ca}^{2+}$  concentrations, allowing  $\text{Ca}^{2+}$  to bind to the myofilaments, which then induces cardiac muscle contraction. For relaxation to occur,  $\text{Ca}^{2+}$  transports out via the sarco/endoplasmic reticulum Ca-ATPase (SERCA), the  $\text{Na}^+/\text{Ca}^{2+}$  exchanger (NCX), and the plasma membrane  $\text{Ca}^{2+}$ -ATPase (PMCA). B, Sarcomere shortening via actin-myosin binding. At rest state, the actin binding sites are blocked by tropomyosin. During excitation, calcium displaces the troponin-tropomyosin complex, allowing the myosin head to form a crossbridge.

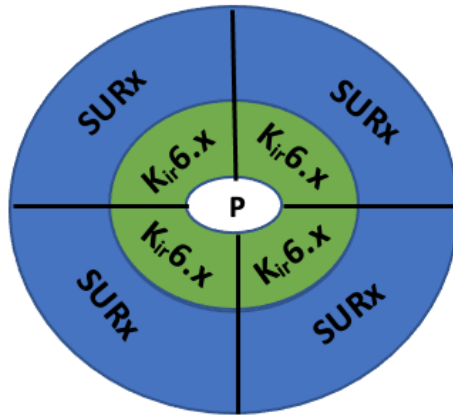
## 1.3 ATP sensitive potassium ( $\text{K}_{\text{ATP}}$ ) channel

ATP-sensitive potassium ( $\text{K}_{\text{ATP}}$ ) channels are widely expressed channels that are generally inhibited by normal physiological concentrations of ATP and activated by nucleotide diphosphates or a fall in ATP during ischaemia. The response to ATP and ADP means that the channels are metabolically sensitive and play a major role in responding to the metabolic state of the cell. In this section, the main characteristics of the channel subgroup will be outlined.

### 1.3.1 Molecular structure and the distribution of $\text{K}_{\text{ATP}}$ channels

The molecular structure of the  $\text{K}_{\text{ATP}}$  channel complex is hetero-octameric (Aguilar-Bryan and Bryan, 1999; Ashcroft and Gribble, 1998; Seino, 1999). This complex requires two unique subunits with different protein properties to reconstitute  $\text{K}_{\text{ATP}}$  channels, including the inward rectifier potassium channel family ( $\text{K}_{\text{ir}}6$ ) and the sulfonylurea receptor (SUR). To achieve a functional  $\text{K}_{\text{ATP}}$  channel, the outer ring is formed from four SURx which interact with four pore-forming subunits ( $\text{K}_{\text{ir}}6.x$ ) to form the inner ring (Shyng and Nichols, 1997; Li et al., 2017) (Figure 1.9A).

A)



B)

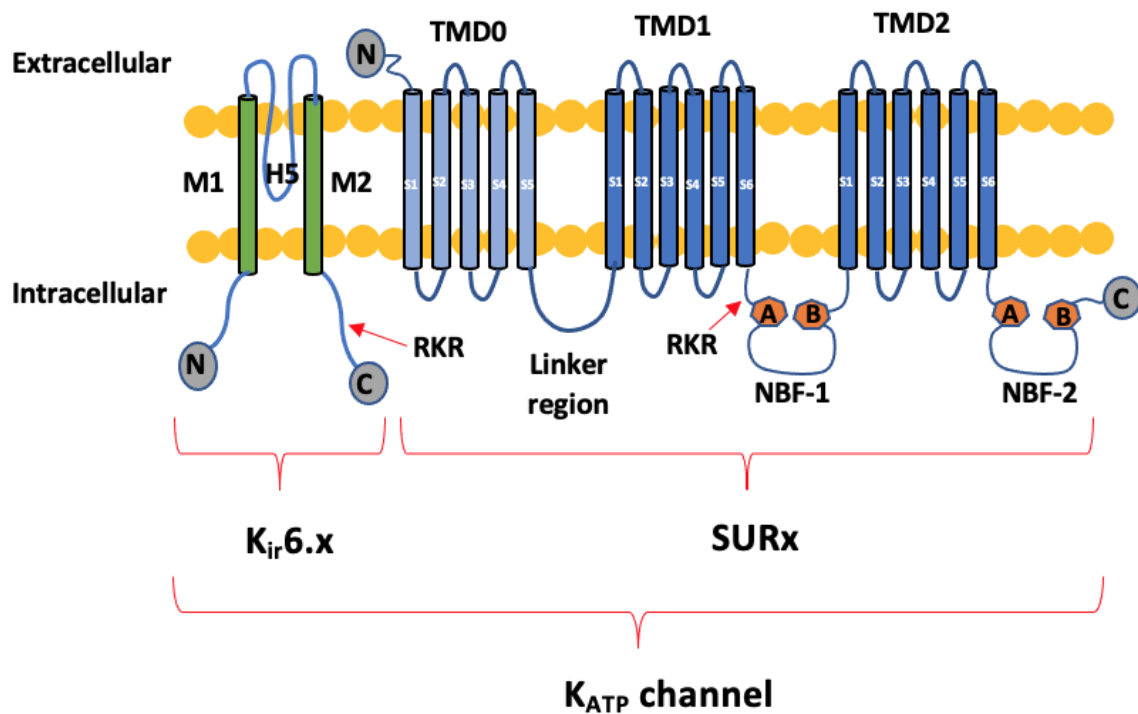


Figure 1.9: The molecular structure of K<sub>ATP</sub> channel.

A, A cross-section diagram of K<sub>ATP</sub> channel shows the octameric structure of K<sub>ATP</sub> channel. B, Diagram shows the molecular components of K<sub>ATP</sub> channel which are essentially required to achieve the physiological function of this protein. K<sub>i</sub>6 subunit forms from channel's pore (H5) with M1 and M2 (two transmembrane segments) and two terminal tails at intracellular side (N- and C-termini). SUR subunit is expressed with three transmembrane domains (TMD0, TMD1, and TMD2) with two nucleotide binding folds (NBF-1 and NBF-2) at cytoplasmic side. Abbreviations: P, pore-forming; RKR, endoplasmic reticulum retention signals of potassium channel; A and B, the Walker A and B motifs of NBF.

The pore-forming subunit of the  $K_{ATP}$  channel complex is  $K_{ir}6$ , of which there are three known isoforms:  $K_{ir}6.1$ ,  $K_{ir}6.2$ , and  $K_{ir}6.3$  (Inagaki et al., 1995b; Inagaki et al., 1995a; Zhang et al., 2006). As members of the inward rectifier potassium channel family, they have two transmembrane domains (M1 and M2) and one pore-forming loop (P-pore) with intracellular N and C termini (Figure 1.9B). The  $K_{ir}6$  channel resembles a part of the voltage-gated  $K^+$  channel which consists of S5, H5 and S6 segments. Importantly, the pore forming segment (H5) plays an essential role in  $K^+$  selectivity, with a glycine-phenylalanine-glycine (GFG) sequence within the pore similar to other known  $K^+$  channels with a glycine-tyrosine-glycine (GYG) motif. Although the  $K_{ir}$  family have analogous S5-H5-S6 membrane topology, they are not voltage-sensitive like the  $K_V$  family. This is due to the absence of voltage sensor region (S1-S4). The movement of  $K^+$  through this channel is regulated by intracellular substances such as  $Mg^{2+}$  or polyamines.

$K_{ir}6.1$  and  $K_{ir}6.2$  are present in most species, whereas  $K_{ir}6.3$  was only found in Zebrafish model (Zhang et al., 2006). The gene encoding the expression, and distribution of each subunit of  $K_{ATP}$  channel, has been summarised in

**Table 1.2.** In pancreatic cells, skeletal muscle and in cardiomyocytes, it was shown that the *KCNJ11* gene encodes the  $K_{ir}6.2$  (Miki and Seino, 2005; Fedele et al., 2013).  $K_{ir}6.1$  subunit expression, encoded by *KCNJ8*, was found in some cardiomyocytes and in smooth muscle cells (Miki and Seino, 2005; Bao et al., 2011; Delaney et al., 2012). The amino acid sequences between  $K_{ir}6.1$  and  $K_{ir}6.2$  show around 70% identity in their sequences and around 40% homology with other members of the inward rectifier potassium channel family (Inagaki et al., 1995b; Kono et al., 2000). Additionally, the intracellular N- and C-termini play an important role in generating a stable tetramer of globular domains of  $K_{ATP}$  channel (Nichols et al., 2013). By using cryoelectron microscopy, it has been found that the ATP binding sites was revealed on  $K_{ATP}$  channel, specifically on the surface of the C-terminal cytoplasmic domain (Li et al., 2017; Martin et al., 2017). Martin et al. (2017) reported that the C terminal domain of  $K_{ir}6.2$  is locked with L0 of SUR1 when the ATP binding, which inhibits the essential site to open the channel; between L0 of SUR1 and the N-terminal of  $K_{ir}6.2$ . Critically, most mutations in N- and C-termini actually alter ATP sensitivity of  $K_{ATP}$  and therefore affect the intrinsic open-closed equilibrium (Proks et al., 1999; Cukras et al., 2002; Tucker et al., 1997; Drain et al., 1998).

Previous studies report that the channel open probability increased in the presence of mutations in the C-terminus (Shyng et al., 1997; Tucker et al., 1998).

**Table 1.2:** The distribution of K<sub>ATP</sub> channels in the body by differing combinations of K<sub>i</sub>r6.x and SURx subunits.

Subunit/Gene	SUR1/ ABCC8	SUR2A/ ABCC9	SUR2B/ ABCC9
K <sub>i</sub> r6.1/ KCNJ8	1- Atrial and ventricular myocytes <sup>(1,2)</sup>	1- Smooth muscle cells <sup>(8)</sup>	1- Atrial and ventricular myocytes? <sup>(1,2)</sup> 2- Vascular smooth muscle cells <sup>(8,11)</sup>
K <sub>i</sub> r6.2/ KCNJ11	1- Pancreatic β-cells <sup>(3,4,5)</sup> 2- Neuronal cells in the brain <sup>(6,7)</sup>	1- Ventricular myocytes <sup>(9)</sup> 2- Skeletal muscle cells <sup>(10)</sup>	1- Non-vascular smooth muscle cells <sup>(12)</sup>

(Morrissey et al., 2005a)<sup>(1)</sup>; (Morrissey et al., 2005b)<sup>(2)</sup>; (Inagaki et al., 1997)<sup>(3)</sup>; (Tarasov et al., 2004)<sup>(4)</sup>; (Li et al., 2017)<sup>(5)</sup>; (Miki et al., 2001)<sup>(6)</sup>; (Liss et al., 1999)<sup>(7)</sup>; (Teramoto, 2006)<sup>(8)</sup>; (Inagaki et al., 1996)<sup>(9)</sup>; (Jovanović et al., 2016)<sup>(10)</sup>; (Yamada et al., 1997)<sup>(11)</sup>; (Isomoto et al., 1996)<sup>(12)</sup>

The second subunit of the K<sub>ATP</sub> channel complex is SUR which is integrated with the unrelated K<sub>i</sub>r6 subunit. The SUR is a member of a transporter protein family, the ATP-binding cassette (ABC) family (Linton and Higgins, 2007), playing a physiological role in all cell types by allowing different substrates to transport across the cell membrane. To date, two SUR accessory subunits have been reported, SUR1 and SUR2. SUR2 has two splice variants, SUR2A and SUR2B (Hambrock et al., 1999; Ashfield et al., 1999; Fujita et al., 2006; Flagg et al., 2008). The two isoforms of SUR are derived from different genes (

**Table 1.2**). The SUR1 subunit, from the ABCC8 gene, is found in atrial cells, neuronal tissue and in the pancreatic cells (Flagg et al., 2008; Nichols et al., 2007; Flanagan et al., 2009). The K<sub>i</sub>r6.2/SUR1 complex in the pancreas is perhaps the best characterised of all isoforms and has been the target for sulphonylurea therapies for type II diabetes. The SUR2 subunit, encoded by the ABCC9 gene, is present in cardiomyocytes, skeletal muscle and smooth muscle cells (Bienengraeber et al., 2004; Bryan et al., 2007; Nichols et al., 2013). The splice variants, SUR2A and SUR2B, differ only in the terminal 42 amino acids of the carboxy terminus (C-terminal tail)

(De Wet et al., 2010). This leads to differences in drug and nucleotide binding properties, and a lower ATPase activity of SUR2B comparing to SUR2A.

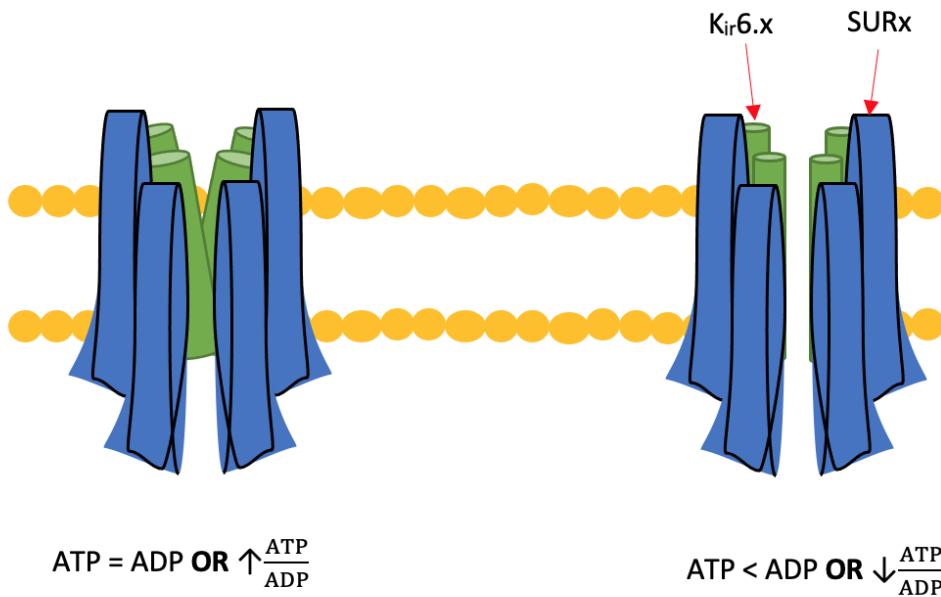
The SUR subunit general structure consists of three groups of domains with different numbers of transmembrane segments, including five (TMD0), six (TMD1), and six (TMD2) transmembrane helices (Nichols, 2006; Burke et al., 2008) (Figure 1.9B). The total number of transmembrane segments in each SUR subunit is 17 segments. Given that there are an odd number of transmembrane domains, the N-terminus is extracellular whilst the C-terminus is intracellular. The SUR subunit also has two nucleotide-binding folds (NBF-1 and NBF-2) with Walker A and Walker B motifs (Linton and Higgins, 2007). NBF-1 is located between TMD1 and TMD2 whereas NBF-2 is located between TMD2 and the C-terminus. Furthermore, TMD0 and TMD1 are connected to each other by a linker region. Both nucleotide binding folds interact to form two nucleotide binding sites (NBS), increasing the efficacy of ATP binding and hydrolysis.

The expression of  $K_{ATP}$  channels on the cell surface only occurs when both subunits are present due to endoplasmic reticulum retention signals (RKR motifs) within the primary sequence of both subunits, which were experimentally investigated by Zerangue et al. (1999) (Zerangue et al., 1999). A subunit that is not associated with the correct stoichiometry of other subunits is therefore maintained in the endoplasmic reticulum (ER) (Babenko et al., 1998). These signals are located in the C-terminal region in  $K_{ir}6.x$  and in the loop region between the last transmembrane segments of TMD1 and NBF-1 in SURx (Figure 1.9B). Importantly, the co-expression of two subunits of  $K_{ATP}$  channels masks these signals and so allows the complex to traffic to the membrane.  $K_{ir}6.2$  can be forced to express at the surface as a functional channel, however it requires the C-terminal 26 or 36 amino acids to be removed ( $K_{ir}6.2\Delta C26$ ,  $K_{ir}6.2\Delta C36$  mutants) to exclude the RKR motif (Tucker et al., 1997).

### 1.3.2 Properties of physiological function of $K_{ATP}$ channels

The composition of the pore forming  $K_{ir}6.x$  members with the members of SURx confers different channel regulatory mechanisms such as gating and pore properties (Figure 1.10). These subunits provide critical binding sites with intracellular ATP and ADP and so it is often

stated that the K<sub>ATP</sub> complex couples the cellular metabolic state with electrical excitability (Antcliff et al., 2005; Nichols, 2006; Ortiz et al., 2013; Sun and Feng, 2013). In general, K<sub>ATP</sub> channels are inhibited under normal conditions due to the presence of high intracellular ATP (~4.7 mM), and therefore the opening of channels occurs primarily under pathophysiological conditions such as during ATP depletion or metabolic stress. To achieve the channel inhibition at normal physiological condition, ATP inhibits at the pore-forming of K<sub>i6</sub> subunits and therefore forming four inhibitory sites at that subunit; while MgATP and MgADP activate at the nucleotide binding sites of SUR subunits, performing eight stimulatory sites. Consequently, the nucleotide regulation of the closed state of the channel is determined by a balance between the activation and inhibition events at the 12-nucleotide binding sites on the channel complex. However, mutation of these channels may cause them to have more prolonged opening in disease conditions due to the imbalance between the activation and inhibition effects; for example, congenital hyperinsulinism (HI), permanent and transient neonatal diabetes (PNDM, TNDM), septic shock and hypoxia induced lactic acidosis (Pelletier et al., 2000; Alejandro et al., 2009). In these physiological conditions, the ATP level falls and causes a lack of nucleotide binding to K<sub>i6</sub> inhibitory sites, whereas MgADP can bind to the nucleotide binding sites of the SUR subunits (NBF-1 and NBF-2). This imbalance of binding stimulates the channel to open.



#### $K_{ATP}$ channels close at:

- 1- Normal physiological condition
- 2- Hyperglycemic condition

#### $K_{ATP}$ channels open at:

- 1- Congenital hyperinsulinism (HI), leading to hypoglycemia.
- 2- Permanent and transient neonatal diabetes mellitus (PNDM) (TNDM).
- 3- Septic shock.
- 4- Hypoxia induced lactic acidosis.

**Figure 1.10:** The functional role of  $K_{ATP}$  channel subunits by control the close and open states in the response to alteration of the intracellular ATP/ADP level.

$K_{ATP}$  channels are blocked by normal physiological concentrations of ATP or under hyperglycemia. However, these channels are opened under ATP depletion or metabolic stress, including hypoglycemia, ischaemia and hypoxia.

#### 1.3.2.1 ATP sensitivity

The primary site for ATP binding to block the  $K_{ATP}$  channel is located in the C-terminal domain of the  $Kir6.x$  subunit (Tucker et al., 1997). Truncating the C terminal 36 amino acids ( $Kir6.2\Delta C36$ ), in the absence of SUR subunits, forms a functional surface expressed channel, however it shows a 10-fold reduction in ATP sensitivity ( $K_i = \sim 120 \mu M$ ). These findings suggest that the  $Kir6.2$  subunit contains an ATP binding site that is distinct from the SUR. Co-expression with the SUR increases the ATP sensitivity to an  $IC_{50}$  of  $\sim 20 \mu M$ , suggesting either a second inhibitory site on the SUR, or an enhancement of ATP binding to the  $Kir6.2$ . The intracellular

ATP has two vital functions to regulate the mechanical function of this  $K_{ATP}$  channel (Takano et al., 1990; Findlay and Dunne, 1986). The first function of ATP is achieved by binding of ATP to  $K_{ATP}$  channels, acting as an inhibitory ligand. This block is maintained as long as this intracellular nucleotide is attached to the channel. The second function of ATP occurs by binding of ATP to intracellular  $Mg^{2+}$  through the hydrolysis process, thereby is known as a hydrolysis-dependent action.

Functional  $K_{ATP}$  channels in the body are characterised by different biophysical properties (Table 1.3). Overall, the inhibition of the  $K_{ATP}$  channel in smooth muscle cells by ATP binding is low and often the  $K_{ir}6.1$ -containing channels are suggested to be ATP-insensitive (Teramoto, 2006).  $K_{ir}6.1$  cannot be easily investigated in excised patches as the current runs down rapidly, and so ATP concentration-response profiles cannot be readily measured. What is known is that the smooth muscle  $K_{ATP}$  complex, most often associated with a  $K_{ir}6.1$  pore, is constitutively active, modulated by protein kinases and highly sensitive to activation by nucleotide diphosphates (NDP's) and was often referred to as  $K_{NDP}$  (Nucleotide diphosphate-dependent potassium channel) in older literature (Teramoto, 2006; Davies et al., 2010).

**Table 1.3:** Biophysical properties of different types of  $K_{ATP}$  channels, including the single-channel conductance in inside-out patches in ~140 mM symmetrical of  $K^+$  concentrations, ATP sensitivity and ADP sensitivity.

$K_{ATP}$ channels	Single-channel conductance	ATP sensitivity ( $IC_{50}$ )	ADP sensitivity
<b>Cardiac cells (<math>K_{ir}6.2/SUR2A</math>)</b>	~80 pS <sup>(1)</sup>	$IC_{50}= 20\text{-}30 \mu M$ , with or without $Mg^{2+}$ <sup>(6,7,8)</sup>	$EC_{50}= \sim 250 \mu M$ (with $Mg^{2+}$ ) $IC_{50}= \sim 275 \mu M$ (without $Mg^{2+}$ ) <sup>(15)</sup>
<b>Pancreatic <math>\beta</math>-cells (<math>K_{ir}6.2/SUR1</math>)</b>	~76 pS <sup>(2,3)</sup>	$IC_{50}= \sim 5 \mu M$ (without $Mg^{2+}$ ) $IC_{50}= \sim 30 \mu M$ (with $Mg^{2+}$ ) <sup>(9,10,11)</sup>	$IC_{50}= \sim 64$ to $\sim 115 \mu M$ (without $Mg^{2+}$ ) <sup>(16,17)</sup>
<b>Smooth muscle cells (<math>K_{ir}6.1/SUR2A</math>)</b>	~35 pS <sup>(4)</sup>	$IC_{50}= \sim 190 \mu M$ <sup>(12)</sup>	—
<b>Vascular smooth muscle cells (<math>K_{ir}6.1/SUR2B</math>)</b>	~35 pS <sup>(4)</sup>	Insensitive to ATP inhibitor <sup>(4)</sup>	$EC_{50}= \sim 96 \mu M$ $IC_{50}= \sim 1.9 \mu M$ <sup>(18)</sup>

<b>Non-vascular smooth muscle cells (Kir6.2/SUR2B)</b>	~75 pS <sup>(4,5)</sup>	IC <sub>50</sub> = ~57 to ~300 μM <sup>(5,13)</sup>	EC <sub>50</sub> = ~28 μM (with Mg <sup>2+</sup> ) <sup>(19)</sup>
<b>Miscellaneous tissue (Kir6.1/SUR1)</b>	~35 pS <sup>(4)</sup>	IC <sub>50</sub> = ~300 μM <sup>(14)</sup>	–

(Inagaki et al., 1996)<sup>(1)</sup>; (Inagaki et al., 1995b)<sup>(2)</sup>; (Sakura et al., 1995)<sup>(3)</sup>; (Teramoto, 2006)<sup>(4)</sup>; (Isomoto et al., 1996)<sup>(5)</sup>; (Lodwick et al., 2014)<sup>(6)</sup>; (Terzic et al., 1995)<sup>(7)</sup>; (Ashcroft and Ashcroft, 1990)<sup>(8)</sup>; (Kang et al., 2008)<sup>(9)</sup>; (Ashcroft, 2005)<sup>(10)</sup>; (Ashcroft and Kakei, 1989)<sup>(11)</sup>; (Aggarwal et al., 2013)<sup>(12)</sup>; (Aziz et al., 2012)<sup>(13)</sup>; (Takano et al., 1998)<sup>(14)</sup>; (Lederer and Nichols, 1989)<sup>(15)</sup>; (Dabrowski et al., 2003)<sup>(16)</sup>; (Ribalet et al., 2003)<sup>(17)</sup>; (Davies et al., 2010)<sup>(18)</sup>; (Matsushita et al., 2002)<sup>(19)</sup>

Interestingly, both K<sub>ATP</sub> channels in smooth muscle cell share a single type of SUR2B, however, inhibitory sensitivities by intracellular ATP were varied. The conductance of single K<sub>ATP</sub> channels in smooth muscle cells is ~35 pS for channels containing from Kir6.1 and is ~75 pS for channels with Kir6.2 providing a clear mechanism for distinguishing the two populations of channels (Teramoto, 2006; Isomoto et al., 1996). Several studies have proposed that K<sub>ATP</sub> channel can functionally heteromultimerise with Kir6.1 and Kir6.2 co-assembled in one channel complex with members of SUR family (Babenko et al., 2000; Cui et al., 2001; Kono et al., 2000), however there is no evidence for this occurring *in vivo*. In heteromultimeric channels, often forced to co-express by synthesising fusion proteins, the electrophysiological properties show intermediate single channel conductance with homomeric Kir6.1 having the smallest and the homomeric Kir6.2 having the largest conductance (Babenko et al., 2000). Furthermore, the presence of a single Kir6.2 subunit conferred Kir6.2-levels of ATP inhibition in any of the heteromeric fusion proteins (Babenko et al., 2000).

### 1.3.2.2 ADP sensitivity

Intracellular nucleoside diphosphates (NDPs) are considered as a crucial regulator factor of K<sub>ATP</sub> channels; for example, adenosine diphosphate (ADP). One of the first studies of the primary site of NDP binding to SUR subunits of K<sub>ATP</sub> channels was by Bernardi et al. (1992), which was achieved by using the binding sites of the purified SUR from pig brain cells. The location of this binding site is within the nucleotide binding domain on SUR subunit which forms from the co-localisation of two nucleotide binding folds (NBF-1 and NBF-2) on the SUR subunit (Bernardi et al., 1992). Importantly, there are three motifs in each NBF which involve the regulation of K<sub>ATP</sub> by providing a hydrolysis reaction (Gribble et al., 1997) (Figure 1.9). For instance, each NBF contains from a walker A (W<sub>A</sub>) motif, a walker B (W<sub>B</sub>) motif, and the linker region which involve in the providing the conformational changes in the opening state of K<sub>ATP</sub>.

channel. There are two functions of ADPs: attenuating the inhibitory effect of  $K_{ATP}$  channel by intracellular ATP and enhancing the opening activity of  $K_{ATP}$  channels (Terzic et al., 1994; Beech et al., 1993). Under normal physiological conditions, this stimulatory effect by Mg-ATP is masked by the blocking action of the free-acid form of ATP. Previous studies have documented that the mutation in any particular motif of SUR subunit have detrimental impacts on the functional regulation of  $K_{ATP}$  channel; for example, the activation role by binding of MgATP is diminished and the inhibition effect by ATP is increased (Chang et al., 2011; Gribble et al., 1997).

In smooth muscle cells, the majority of  $K_{ATP}$  channels are highly sensitive to ADPs while the sensitivity of ATP in that channel appears very low. This  $K^+$  channel was defined as a  $K_{NDP}$  channel which is opened in response to NDPs with a small amount of  $K^+$  conductance (Beech et al., 1993). The sensitivity of  $K_{ATP}$  channel to intracellular ADP depends on the binding with intracellular  $Mg^{2+}$  (Ashcroft and Gribble, 1998). ADP acts as an inhibitor factor in the absence of intracellular  $Mg^{2+}$ , the presence of Mg enhances the ADP to be a potent stimulator factor for this channel. For instance, in vascular smooth muscle cells, the presence of  $Mg^{2+}$  enhances the channel stimulation with  $EC_{50} \approx 96 \mu M$ , however, and the  $IC_{50}$  value is reported  $\approx 1.9 \mu M$  in absence of  $Mg^{2+}$  (Davies et al., 2010).

### 1.3.2.3 The physiological role of the $K_{ATP}$ channel in pancreatic $\beta$ -cells

The functional role of the  $K_{ATP}$  channel is the best characterized in pancreatic  $\beta$ -cells (Cook et al., 1988; Ashcroft and Rorsman, 1989). The  $K_{ATP}$  channel of pancreatic  $\beta$ -cells is composed of  $K_{ir}6.2$  and SUR1 (Inagaki et al., 1997; Tarasov et al., 2004; Li et al., 2017). The electrical activity on pancreatic  $\beta$ -cells plays an essential role in the regulation of insulin secretion (Figure 1.11). This is achieved by elevation of blood glucose level which is metabolized and thereby increases the ATP concentration (Tarasov et al., 2004). The high level of ATP within the pancreatic cells block the  $K_{ATP}$  channels, producing a depolarization of cell membrane potential. Therefore, the voltage-dependent calcium channels (VDCCs) are activated, allowing  $Ca^{2+}$  currents to move inside the cells. Increasing the intracellular concentration of  $Ca^{2+}$  provides the electrical excitability and the calcium required to which triggers calcium-dependent vesicular release of insulin-containing granules. Accordingly, this  $K_{ATP}$  channel is closed as a response to the metabolic sensor and consequently regulates the insulin

secretion. For several years great effort has been devoted to the study of the essential role of  $K_{ATP}$  channels in the pancreatic  $\beta$ -cells, using pharmacological and genetic manipulation on that channel. For instance, the generation of the dominant-negative  $Kir6.2$  in pancreatic  $\beta$ -cells is represented with hypoglycaemia due to the loss of  $K_{ATP}$  function and thereby causes depolarization, increasing the entry of  $Ca^{2+}$  ions and finally creating a high level of insulin secretion (Miki et al., 1997; Koster et al., 2000). As a consequence, the insulin secretion from the pancreas depends critically on the  $K_{ATP}$  channel.

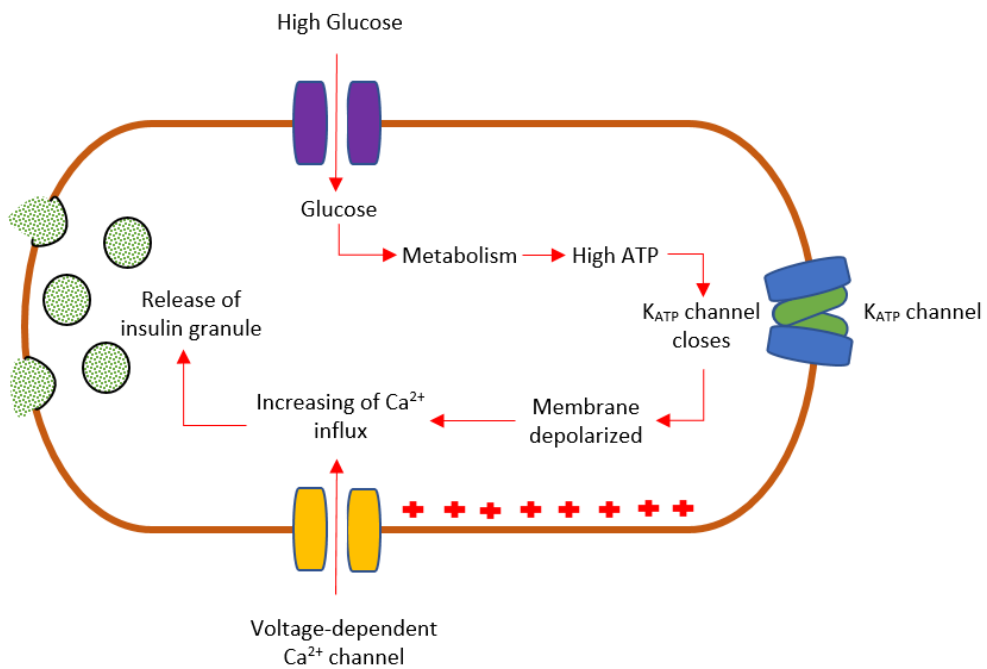


**Figure 1.11:** The role of  $K_{ATP}$  channel in the pancreatic  $\beta$ -cell.

*At the high blood glucose level, the intracellular metabolic rate increases, leading to increase the ATP level. The elevation of ATP triggers  $K_{ATP}$  channel to close which contributes to depolarize the cell membrane. This stimulates the opening of voltage-gated  $Ca^{2+}$  channel which enhances the insulin secretion from granule in a response to high concentration of intracellular  $Ca^{2+}$ .*

#### 1.3.2.4 The physiological role of $K_{ATP}$ channel in skeletal muscle cells

Skeletal muscle cells also contain  $K_{ATP}$  channels, comprising  $Kir6.2$  and  $SUR2A$  (Spruce et al., 1985). This channel is normally closed at the resting condition whereas is activated during muscle fatigue (Light et al., 1994; Tricarico et al., 2016). In this work, the authors observed that the genetic deletion of the  $Kir6.2$  subunit lead to increased resting tension due to the loss of functional  $K_{ATP}$  channels. As a result, there is a critical protective role of the  $K_{ATP}$  channels

in skeletal cells during the severe muscle exercised, consistent with a reduction in the intracellular  $\text{Ca}^{2+}$  handling and reduction in glucose uptake.

### 1.3.3 The physiological role of $\text{K}_{\text{ATP}}$ channel in cardiac muscle

The cardiac muscle undergoes a variety of energy demands to maintain contractile function during rest and in conditions of exercise. Importantly, it is essential to maintain a balance between a cardiac workload and energy consumption. Under stressed conditions such as myocardial ischaemia, the cardiac muscle experiences serious alterations in cardiac energy metabolism in a response to the reduction of oxygen supply. If the high demand for energy causes a depletion of ATP, this stimulates the opening of cardiomyocyte  $\text{K}_{\text{ATP}}$  channels, similar to skeletal  $\text{K}_{\text{ATP}}$  channels (Inagaki et al., 1996). This channel, comprised of  $\text{K}_{\text{ir}}6.2/\text{SUR}2\text{A}$  subunits, is often referred to as the sarcolemmal  $\text{K}_{\text{ATP}}$  channel (Sarco $\text{K}_{\text{ATP}}$ ) and plays a significant role during ischaemic and hypoxic conditions by increased  $\text{K}^+$  efflux (Figure 1.12) (Suzuki et al., 1999; Singh et al., 2003; van Bever et al., 2004; Rainbow et al., 2004).

Cardiac  $\text{K}_{\text{ATP}}$  channels have been linked with the phenomenon of cardioprotection as activators of cardiac  $\text{K}_{\text{ATP}}$  have been shown to be protective, whilst blockers appear cardiotoxic (Tinker et al., 2014). This has been previously investigated in our laboratory where the role of  $\text{K}_{\text{ir}}6.2/\text{SUR}2\text{A}$  was investigated in cardioprotection imparted by PKC activity (Brennan et al., 2015). In this study, it was found that the time to activation of the cardiac  $\text{K}_{\text{ATP}}$  channel was delayed following cardioprotection, but that direct inhibition of PKC reversed this effect (Brennan et al., 2015). The conclusion of this study was that the early opening of  $\text{K}_{\text{ir}}6.2/\text{SUR}2\text{A}$  channels was not part of the PKC-dependent cardioprotective pathway as evidenced by a *delayed* opening of  $\text{K}_{\text{ATP}}$ . It was concluded, therefore, that the channel opening during ischaemia was a powerful supporter of the protection to spare the remaining ATP, rather than to be a primary cardioprotective factor. In the open state, a severe shortening of action potential duration (APD) was achieved, leading to decreased  $\text{Ca}^{2+}$  influx. The reduction of intracellular  $\text{Ca}^{2+}$  overload contributes to energy sparing. The maintenance of a considerable amount of energy protects the cardiac muscle from further fatal damage during ischaemic conditions.

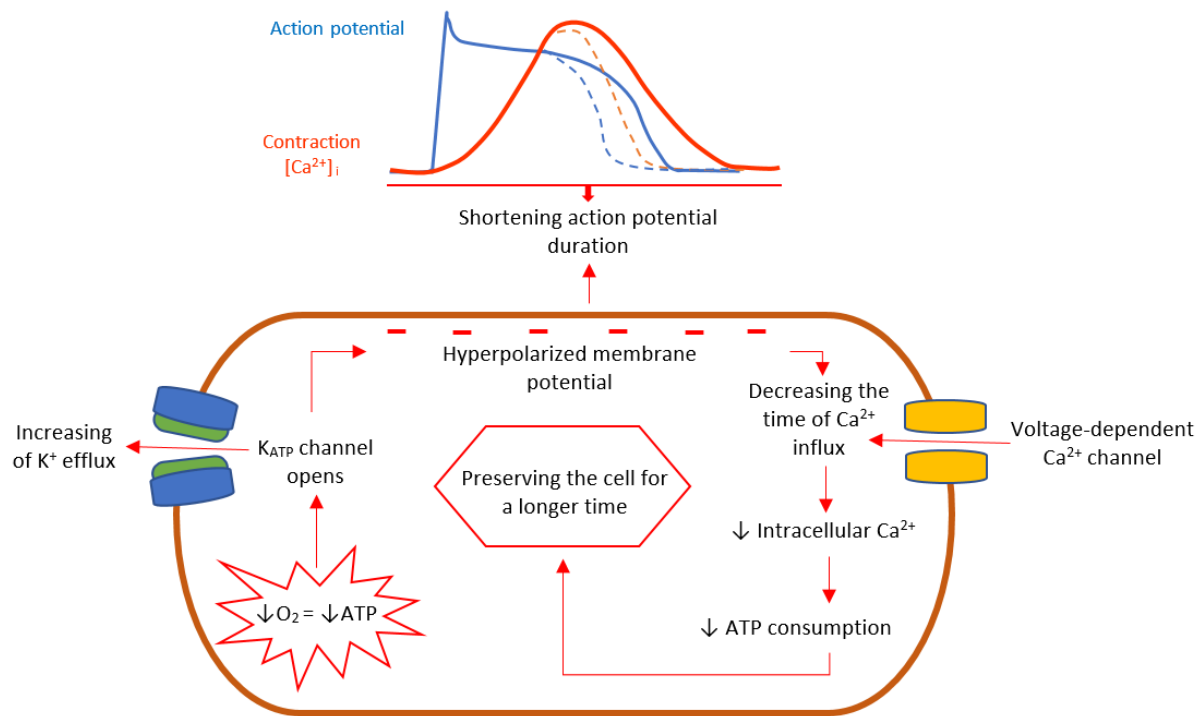


**Figure 1.12:** The role of  $K_{ATP}$  channel in cardiomyocytes.

This  $K_{ATP}$  channel couples the metabolic change to the electrical activity.  $K_{ATP}$  channel is open with the depletion of ATP as a consequence of insufficient oxygen supply during ischaemia. The opening of  $K_{ATP}$  channels triggers membrane hyperpolarization that prevents electrical excitation and therefore action potential duration is shortened, consequently, decreasing the  $Ca^{2+}$  entry via voltage-dependent  $Ca^{2+}$  channel. This leads to a reduction in the intracellular  $Ca^{2+}$  concentration and energy saving. As a result, the  $K_{ATP}$  channel can generate a protective role through decreasing calcium loading during ischaemic conditions.

To clarify the role of this cardiac  $K_{ATP}$  channel on  $Ca^{2+}$  handling, a pharmacological activator was examined in  $K_{ir}6.2$  knockout animals (Suzuki et al., 2002). Pinacidil was used as a specific activator of the sarcolemmal  $K_{ATP}$  channel, increasing the outward  $K^+$  currents and consequently shortening the APD in control mice, however was not seen  $K_{ir}6.2$ -KO mice (Suzuki et al., 2002). These findings suggest that the cardiac  $K_{ATP}$  channels plays an important cardioprotective role in the heart by responding to near complete ATP depletion to preserve the cardiomyocyte, but its role in ischaemic preconditioning or other cardioprotective interventions is still unclear.

Gain of function mutations of  $KCNJ8$  have been identified that cause a paradoxical effect of increasing myocardial L-type  $Ca^{2+}$  current. In patients suffering from Cantu syndrome, the

myocardium has been shown to have an increased excitability, which is potentially an adaptation to a reduced vascular tone caused by more active  $K_{ir}6.1$  channels (Levin et al., 2016). A gain-of-function point mutation, S422L, has also been associated with early ventricular repolarisation and atrial fibrillation, presenting particularly in patients with J-wave syndromes (Delaney et al., 2012).

### 1.3.4 The pharmacological modulation of $K_{ATP}$ channels

#### 1.3.4.1 Pharmacological blockers of $K_{ATP}$ channels

The  $K_{ATP}$  channel complex is a well-established target for drug therapies. The presence of the large SUR subunit provides a number of drug binding sites to modulate channel function. Sulphonylurea drugs can be activators (such as pinacidil, nicorandil or iptakalim) or blockers (such as glibenclamide and tolbutamide). Potassium channel openers (KCOs) of this channel, such as nicorandil, have been used therapeutically for angina (Kitakaze et al., 2007; Wu et al., 2013; Campo et al., 2017).

The group of sulphonylurea blocking drugs have an important site for binding in TMD2 of SURx subunits especially the region between S4 and S5 of TMD2 (Ashfield et al., 1999; Babenko et al., 1999). In a recent paper by Li et al., sulphonylureas also bind to TMD0 (Li et al., 2017). Sulfonylureas blockers include glucose-lowering agents such as glibenclamide and tolbutamide, enhancing glucose-induced insulin secretion by blocking of pancreatic  $K_{ATP}$  channels (Ashcroft and Ashcroft, 1990; Findlay, 1992; Beech et al., 1993; Stephan et al., 2006; Lodwick et al., 2014). Another interesting  $K_{ATP}$  blocking drug is PNU37883A which provides a direct inhibitor effect as a  $K_{ir}6.1$ -selective pore blocker, and is defined as non-sulphonylureas (Wellman et al., 1999). This inhibitor is mainly selective for  $K_{ATP}$  channels on vascular smooth muscle (Cui et al., 2003). In addition to smooth muscle, our unpublished experimental data suggest that there is a significant inhibitory effect of PNU37883A in cardiac cells, either by acting on  $K_{ir}6.2/SUR2A$ , or as has been demonstrated in the lab, but blocking cardiac surface  $K_{ir}6.1$  channels. The blocking contribution of the  $K_{ATP}$  channel by PNU37883A originally occurs on the pore structure of this channel such as the  $K_{ir}6.1$  subunit in the vascular smooth muscle (Kovalev et al., 2004; Cui et al., 2003).  $K_{ATP}$  channels are also blocked by another non-sulphonylurea drug with a similar effect as PNU, rosiglitazone. Rosiglitazone is a PPAR $\gamma$

agonist used to treat type-II diabetes, but was withdrawn from the market for cardiotoxicity. It is clear from the experimental study that both PNU and rosiglitazone are acting as selective inhibitors for  $K_{ir}6.1$  rather than  $K_{ir}6.2$  (Yu et al., 2012). The tissue target and  $IC_{50}$  values for several pharmacological inhibitors are illustrated in Table 1.4.

**Table 1.4:** Pharmacological properties by using a selective openers and blockers of  $K_{ATP}$  channels in major tissues with different subunit combinations.

Tissue with $K_{ATP}$ channels	Glibenclamide ( $IC_{50}$ )	Tolbutamide ( $IC_{50}$ )	PNU37883A ( $IC_{50}$ )	Rosiglitazone ( $IC_{50}$ )	5-HD ( $IC_{50}$ )	HMR1098 ( $IC_{50}$ )	Pinacidil ( $EC_{50}$ )	Diazoxide ( $EC_{50}$ )
<b>Pancreatic <math>\beta</math>-cells (<math>K_{ir}6.2/SUR1</math>)</b>	~5-30 nM <sup>(1)</sup>	~ 5-20 $\mu M$ <sup>(1)</sup>	No effect <sup>(6)</sup>	~45 $\mu M$ <sup>(8)</sup>	~81 $\mu M$ <sup>(9)</sup>	~5 $\mu M$ <sup>(9)</sup>	>500 $\mu M$ <sup>(1)</sup>	~20-102 $\mu M$ <sup>(1)</sup>
<b>Cardiac cells (<math>K_{ir}6.2/SUR2A</math>)</b>	~3 nM <sup>(2)</sup>	~400 $\mu M$ <sup>(4)</sup>	$\geq$ 100 $\mu M$ <sup>(7)</sup>	~37 $\mu M$ <sup>(8)</sup>	No effect <sup>(9)</sup>	~0.36 $\mu M$ <sup>(9,10)</sup>	10-30 $\mu M$ <sup>(11)</sup>	No effect or inhibited at 500 $\mu M$ <sup>(13)</sup>
<b>Vascular Smooth muscle cells (<math>K_{ir}6.1/SUR2B</math>)</b>	~50 nM <sup>(3)</sup>	~350 $\mu M$ <sup>(5)</sup>	~5 $\mu M$ <sup>(7)</sup>	~10 $\mu M$ <sup>(8)</sup>	No effect <sup>(9)</sup>	No effect <sup>(9)</sup>	~0.5 $\mu M$ <sup>(12)</sup>	~40 $\mu M$ <sup>(12)</sup>

(Ashcroft and Ashcroft, 1990)<sup>(1)</sup>; (Lodwick et al., 2014)<sup>(2)</sup>; (Stephan et al., 2006)<sup>(3)</sup>; (Findlay, 1992)<sup>(4)</sup>; (Beech et al., 1993)<sup>(5)</sup>; (Surah-Narwal et al., 1999)<sup>(6)</sup>; (Cui et al., 2003)<sup>(7)</sup>; (Yu et al., 2012)<sup>(8)</sup>; (Liu et al., 2001)<sup>(9)</sup>; (Rainbow et al., 2005)<sup>(10)</sup>; (Escande et al., 1989)<sup>(11)</sup>; (Quayle et al., 1995)<sup>(12)</sup>; (Faivre and Findlay, 1990)<sup>(13)</sup>

### 1.3.4.2 Pharmacological openers of $K_{ATP}$ channels

KCOs of  $K_{ATP}$  channels, include diazoxide, pinacidil, nicorandil, and cromakalim. These pharmacological treatments maintain  $K_{ATP}$  channels in the open configuration. The opening state of  $K_{ATP}$  channels is stabilised via an interaction of these drugs with nucleotide diphosphates and an enhanced ATP hydrolysis at NBF-2 in combination with binding of Mg-ATP to SUR subunits (Bienengraeber et al., 2000). These pharmacological modulations elicit a negative inotropic effect by stabilising the opening state of  $K_{ATP}$  channels, reducing  $Ca^{2+}$  influx and thereby preserving energy by reducing the requirement to remove intracellular  $Ca^{2+}$  (Ashcroft and Gribble, 2000). Several studies have confirmed a protective effect of KCOs. One of the first examples of the significant effects of  $K_{ATP}$  channel openers on the protection from myocardial damage was presented using pinacidil and cromakalim in dog models, which

showed a reduction of infarct size (Grover et al., 1990). Concentrations of these openers were between 300 nM and 10  $\mu$ M, providing a cardioprotective effect of  $K_{ATP}$  opening. Different  $K_{ATP}$  channel isoforms show varying sensitivities to KCOS; pancreatic  $K_{ATP}$  channels are strongly activated by diazoxide ( $EC_{50} = 20\text{-}102 \mu M$ ), however, very weakly activated by pinacidil ( $EC_{50} > 500 \mu M$ ) (Ashcroft and Ashcroft, 1990). The activity of cardiac  $K_{ATP}$  channels is seen on application of 10  $\mu M$  pinacidil ( $EC_{50} = 10\text{-}30 \mu M$ ), but is not affected by diazoxide (Escande et al., 1989; Faivre and Findlay, 1990).  $K_{ATP}$  channels in smooth muscle cells are activated in response to both opening agents (Quayle et al., 1995). These findings were examined in mesenteric arteries of the rabbit model, activated by diazoxide ( $EC_{50} = \sim 40 \mu M$ ), and also by pinacidil ( $EC_{50} = 0.5 \mu M$ ). Indeed, diazoxide is considered as a powerful pharmacological activator for SUR1 and SUR2B, however, this activator is only effective in the presence of MgADP for SUR2A containing  $K_{ATP}$  channels (D'hahan et al., 1999). As a result,  $K_{ATP}$  channels in various tissues are considered as a pharmacological target, using selective blockers or openers.

### 1.3.5 Mitochondrial $K_{ATP}$ channels

#### 1.3.5.1 The physiological role of mitochondrial $K_{ATP}$ channels

Since the link between mitochondrial function,  $K_{ATP}$  channel modulators such as diazoxide, and cardioprotection was established, a mitochondrial  $K_{ATP}$  channel has been postulated. One of the first examples of a report suggesting the presence functional  $K_{ATP}$  channels in the inner membrane of mitochondria was reported by Inoue et al., 1991, using fused giant mitoplast prepared from rat liver mitochondria (Inoue et al., 1991). Similarly, Dahlem et al., also suggested the presence of mito $K_{ATP}$  channels in the human T-lymphocytes by using pharmacological treatments (Dahlem et al., 2004). The difficulties for confirming a role for the mitochondrial  $K_{ATP}$  channel is that, to date, no definitive evidence for a known  $K_{ATP}$  subunit has been identified in the mitochondria.

Under symmetrical 150 mM KCl conditions, a  $K^+$  channel with a single channel conductance of around 16 pS has been identified (Yarov-Yarovoy et al., 1997). It has been hypothesised that the mitochondrial function can be controlled by the modulation of mito $K_{ATP}$  channels, through activating or inhibiting of this channel (Garlid, 1988), therefore contributing to the

regulation of mitochondrial matrix volume, membrane potential and oxygen consumption (Pucek et al., 1992; Dębska et al., 2001; Debska et al., 2002). The fundamental role of mitoK<sub>ATP</sub> channels depends on the K<sup>+</sup> uptake in the mitochondrial matrix which leads to depolarization of the inner membrane potential (Figure 1.13). As the potential differences across the cell membrane occur, the K<sup>+</sup> efflux is obtained to the intermembrane space through K<sup>+</sup>/H<sup>+</sup> antiporter, producing H<sup>+</sup> ion inside the mitochondrial matrix (Garlid, 1996). Therefore, this H<sup>+</sup> ion is transferred through respiratory enzyme complexes which is identified as an electron transport chain (ETC) (Guo et al., 2018). As a result, the activity of mitoK<sub>ATP</sub> channels may also be a response to the mitochondrial energetic state which is inhibited by the presence of ATP and ADP.

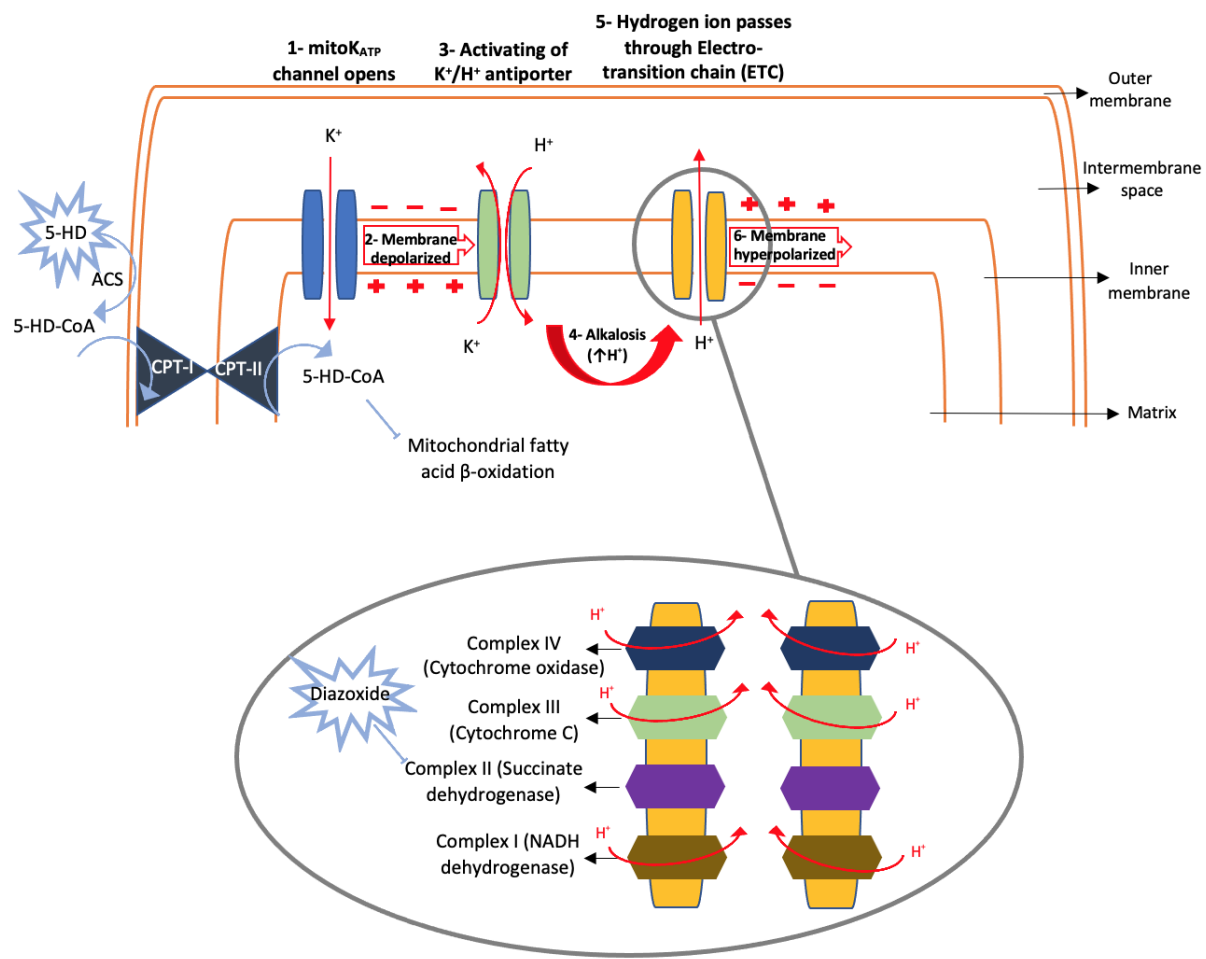


**Figure 1.13:** The mechanical function thought to be involved in the opening of mitoK<sub>ATP</sub> channel.

*The mitochondrial K<sup>+</sup> cycle consists of K<sup>+</sup> uptake and K<sup>+</sup> efflux across the inner membrane. The K<sup>+</sup> influx through the mitoK<sub>ATP</sub> depolarizes the inner membrane. Excess K<sup>+</sup> is ejected by the K<sup>+</sup>/H<sup>+</sup> antiporter in exchange with H<sup>+</sup> resulting in a state of alkalosis. The electron transport chain (ETC) ejects protons,*

*leading to the inner membrane hyperpolarization. The channel activity was increased by diazoxide, inhibiting Succinate dehydrogenase (SDH), and thus leads to attenuate oxidant stress on the heart and have a cardioprotective effect. This cardioprotective effect was reversed by 5-HD. 5-HD is metabolised by acyl-CoA synthetase and enters the β-oxidation pathway.*

### 1.3.5.2 The molecular composition of mitochondrial K<sub>ATP</sub> channels

Although several studies have aimed to identify the molecular structure of mitoK<sub>ATP</sub> channels, these observational findings are still lacking and have not clearly identified the subunits involved. Suzuki et al., showed that the mitochondrial fraction from rat liver and skeletal muscle suggested that K<sub>iR</sub>6.1 was expressed in the mitochondria through staining by immunofluorescent agent (Suzuki et al., 1997). These findings concluded that mitoK<sub>ATP</sub> channels are blocked by administration of 5-HD and are opened using diazoxide (Garlid et al., 1997; Bajgar et al., 2001). Consequently, identification of these pharmacological properties indicated that the subunits of mitoK<sub>ATP</sub> channels were different from the sarcoK<sub>ATP</sub> channel, suggesting that K<sub>iR</sub>6.2 is not involved.

Although previous results suggested the mitochondrial localization of K<sub>iR</sub>6.x subunit, the K<sub>iR</sub>6.x subunit was not identified as a functional part of the mitoK<sub>ATP</sub> complex. Seharaseyon et al. (2000) identified that the mitochondrial activity was not altered when dominant negative constructs of K<sub>iR</sub>6.1 or K<sub>iR</sub>6.2 were introduced into rat cardiomyocytes (Seharaseyon et al., 2000). In agreement with these findings and by using K<sub>iR</sub>6.x null animals, Ng et al. (2010) showed that the generation of ROS by the opening of mitoK<sub>ATP</sub> channels is maintained, despite the deletion of K<sub>iR</sub>6.x gene (Ng et al., 2010).

The most recent study in the molecular identification of mitoK<sub>ATP</sub> channels was conducted by Foster et al., which provides a novel target to modulate the functional role of this channel (Foster et al., 2012; Foster and Coetzee, 2016). Using cell imaging, the inner membrane of mitochondria of bovine heart identified K<sub>iR</sub>1.1 subunits. This is defined as a splice variant of the renal outer medullary potassium channel (ROMK) which is encoded by KCNJ1 gene. At the molecular level, the ROMK subunit is characterized by the presence of ATP binding site on the C-terminus (McNICHOLAS et al., 1996). Therefore, this channel has a similar role to K<sub>ATP</sub> in cellular protection which is inhibited by ATP and activated by the presence of Mg<sup>2+</sup>.

Additionally, the main hallmark of mitoK<sub>ATP</sub> channels can be activated by PIP<sub>2</sub> and regulated by PKC and pH which (McNicholas et al., 1998; Lin et al., 2002; Bednarczyk et al., 2008; Wojtovich et al., 2010). There are several ROMK isoforms which are distributed in the body, and have been reported to involve in mitoK<sub>ATP</sub> activity (Ho et al., 1993). In the heart, ROMK1 and ROMK2 are highly expressed in isolated cardiomyocytes of adult rat while the differences between them was found by the presence of extra 19 amino acid at N terminus of ROMK1 isoform as compared with ROMK2 (Kondo et al., 1996). Previous studies indicated that these variations in length of the N-terminal ends of ROMK isoforms affect neither ion permeation nor channel gating in both human and rat (Shuck et al., 1994; Zhou et al., 1994; Boim et al., 1995). While ROMK channels, and in particular ROMK2 isoform was showed an inhibition with administration of glibenclamide in the absence of SUR auxiliary subunit, the sensitivity to this pharmacological inhibitor was increased when the co-expression of ROMK2 with SUR2B subunit to form glibenclamide-sensitive channel ( $IC_{50} = 0.6 \mu M$ ) (Tanemoto et al., 2000; Jabůrek et al., 1998). On the basis of the recent findings presented in this paper (Foster et al., 2012), work on remaining issues with genetic approaches will be required to prove that the ROMK subunit forms an effective pore-gating component of mitoK<sub>ATP</sub> channels. However, since this initial manuscript in 2012, there has been no further expansion on the potential for ROMK to form a subunit for the putative mitoK<sub>ATP</sub> channel (Foster et al., 2012).

### 1.3.5.3 Effects of different pharmacological modulators of mitochondrial K<sub>ATP</sub> channels and their role in cardioprotection

There are several pharmacological agents which are suggested to be involved in the activating and inhibiting of mitoK<sub>ATP</sub> channels. This channel is activated by diazoxide and isoflurane, whereas the channel is inhibited by hydroxy derivative of decanoate (5-HD) and glibenclamide (Bednarczyk et al., 2005; Nakai et al., 2001; Zhang et al., 2001). These pharmacological treatments also contribute to the differentiation between sarcoK<sub>ATP</sub> and mitoK<sub>ATP</sub> channels due no discernible effect of diazoxide and 5-HD on cardiac sarcolemmal K<sub>ATP</sub> channels (Grover and Garlid, 2000). The potency of diazoxide was experimentally measured by Garlid et al. (1997) which suggested that activation of the mitoK<sub>ATP</sub> channel by diazoxide was 1000 times greater than that of the sarcoK<sub>ATP</sub> channel (Garlid et al., 1997).

Despite the suggestion that the mitoK<sub>ATP</sub> channel was activated by diazoxide, the incidence of sudden death was increased substantially in mice lacking the K<sub>i</sub>r6.1 gene (Miki et al., 2002). In agreement with these findings using dominant negative K<sub>i</sub>r6.1 subunits, Ng et al. (2010) suggested that the generation of ROS by the opening of mitoK<sub>ATP</sub> channels is maintained during use of diazoxide, despite the deletion of K<sub>i</sub>r6.x gene (Ng et al., 2010). Accordingly, the K<sub>i</sub>r6.1 subunit may not be a functional part of the mitoK<sub>ATP</sub> complex (Seharaseyon et al., 2000). Additionally, other studies indicate that diazoxide is able to inhibit Succinate dehydrogenase (SDH), which leads to oxidation of the mitochondrial flavoproteins and inhibition of the energetic production of citric acid cycle (Figure 1.13) (Guo et al., 2018). Furthermore, the mitochondrial matrix volume was suggested to be elevated during the opening of mitoK<sub>ATP</sub> due to high K<sup>+</sup> influx accompanied with high acidity level in the matrix and thus followed by the movement of water via osmosis (Grover and Garlid, 2000). Importantly, Suzuki et al. (2002) studied the cardioprotective role of diazoxide and showed that there was a lack of cardioprotective effect in K<sub>i</sub>r6.2 knockout mice (Suzuki et al., 2002). According to these points, the cardioprotective effect by using of diazoxide may not reflect the opening of a mitoK<sub>ATP</sub> channel.

5-hydroxydecanoate (5-HD) was suggested to be a selective blocker of the mitoK<sub>ATP</sub> channel that could reverse diazoxides effect on the oxidation of mitochondria (Liu et al., 1998). It was found that the administration of 5-HD blocks K<sub>i</sub>r6.2/SUR2A channel with an IC<sub>50</sub> of 28.7 μM in the presence of 1 μM ATP (Notsu et al., 1992).

Despite many studies in this area, there are significant inconsistencies in the literature on the effects of diazoxide and 5-HD on the putative mitoK<sub>ATP</sub> channel. There are other alternative pathways which can be involved in the production of deleterious substances from the mitochondria during the use of 5-HD. Firstly, 5-HD shares a similar basic pathway with fatty acid substrates which are activated via acyl-CoA synthetase and converted into 5-hydroxydecanoyl-CoA (5-HD-CoA) (Figure 1.13) (Hanley et al., 2002; Lim et al., 2002). This activation occurs in the outer membrane surface, and can be moved into the matrix via carnitine palmitoyltransferase (CPT-I and CPT-II) and be oxidized (Lim et al., 2002; Bartlett and Eaton, 2004). Secondly, the accumulation of 5-HD-CoA in the matrix stimulates fatty acid oxidation, reducing the contractile recovery after myocardial ischaemia (Hanley et al., 2005).

## 1.4 Slowly activating delayed rectifier potassium current ( $I_{Ks}$ )

### 1.4.1 The KCNQ family

#### 1.4.1.1 Molecular structure of KCNQ family

The KCNQ channel is a voltage-gated potassium channel which is encoded by the KCNQ gene. This gene plays an important role in controlling the shape of action potential. Therefore, the alteration of this gene contributes to deleterious impacts such as long-QT syndrome and epilepsy (Wang et al., 1996b). There are five members of Kv channel which are classified by their gene name: KCNQ1 to KCNQ5. All members of the KCNQ gene family encode a  $K^+$  channel with voltage-gated properties, also termed the Kv7 family which has 5 members, Kv7.1 (KCNQ1) to Kv7.5 (KCNQ5).

Despite the variation in  $K^+$  channel subunits which are encoded by the KCNQ family genes, all of these  $K^+$  channels have an identical structure with a tetrameric shape to form a functional Kv channel (Wei et al., 1996). Each subunit consists of six trans-membrane segments (S1-S6) which are constructed to form  $\alpha$  subunit (Figure 1.14). As with other Kv channels, the first four transmembrane segments (S1-S4) are considered the voltage-sensing domain (VSD) (Van Horn et al., 2011), and the final two segments (S5-S6) serve as a pore-forming section of the  $\alpha$  subunit. The primary voltage sensor of each Kv7 channel is the S4 segment which allows the channel to be activated in response to alterations of membrane potential (Jensen et al., 2012). The S4 trans-membrane domain (TMD) of all KCNQ subunits contains six repeated motifs of positively-charged residues. However, the S4 segment of the KCNQ1 subunit exhibits four positively-charged amino acid residues. Due to a lower net positive charge in KCNQ1 than other voltage-gated  $K^+$  families, the S4 of KCNQ1 can be converted to a voltage-independent, constitutively active, and leak channel which is attributable to the leak of  $K^+$  ions through the pore of KCNQ1 channel (Panaghie and Abbott, 2007; Schroeder et al., 2000b). All  $K^+$  channel proteins have an intracellular C- and N-terminus (Schroeder et al., 2000b; Schroeder et al., 2000a; Schwake et al., 2000). The C-terminus for KCNQ proteins consists of four helical domains (A, B, C & D) which are considered as effective sites for protein tetramer assembly and binding with different regulatory modulators such as calmodulin (CaM) and phospholipids (Haitin and Attali, 2008; Soldovieri et al., 2011; Thomas et al., 2011; Yus-Najera et al., 2002). Functional reduction of  $I_{Ks}$  (KCNQ1/KCNE1 protein complex) have

been documented in patients carrying Long QT mutations causing disruption of the intracellular C-terminus of KCNQ1 (Ghosh et al., 2006; Wiener et al., 2008). For instance, helix A mutations in C-terminal domain disrupt calmodulin binding and therefore reduce  $I_{Ks}$  function (Shamgar et al., 2006). Importantly, calcium/calmodulin-dependent protein kinase II (CaMKII), mediates a pathological function of  $I_{Ks}$  through phosphorylation at a residue in the region that connects the calmodulin-binding domains in helices A and B, resulting in prolonged action potential duration during sustained  $\beta$ -adrenergic receptor stimulation. Kv7.1 has a distinctive feature compared to the other Kv7 proteins which is the existence of a glycosylation on the extracellular loop between TM5 and TM6 (Barhanin et al., 1996b; Wang et al., 1996b). Protein kinase A phosphorylation sites have been found on the N-terminal of Kv7.1 and Kv7.2, however, it has been identified on the Kv7.5 C-terminus.

In addition to long-QT mutations caused by a loss of function, there are also gain-of-function mutations in *KCNQ1* that can result in a short-QT syndrome (Campbell et al., 2013). A single point mutation (S140) in the KCNQ1 gene leads to a gain-of-function mutation (Campbell et al., 2013). This changes the kinetics and the voltage dependence of the channel with the channel becoming rapidly activating and more like KCNQ1 expressed in the absence of KCNE1. This mutation is believed to be the mechanism underlying an autosomal dominant familial AF (Chen et al., 2003).

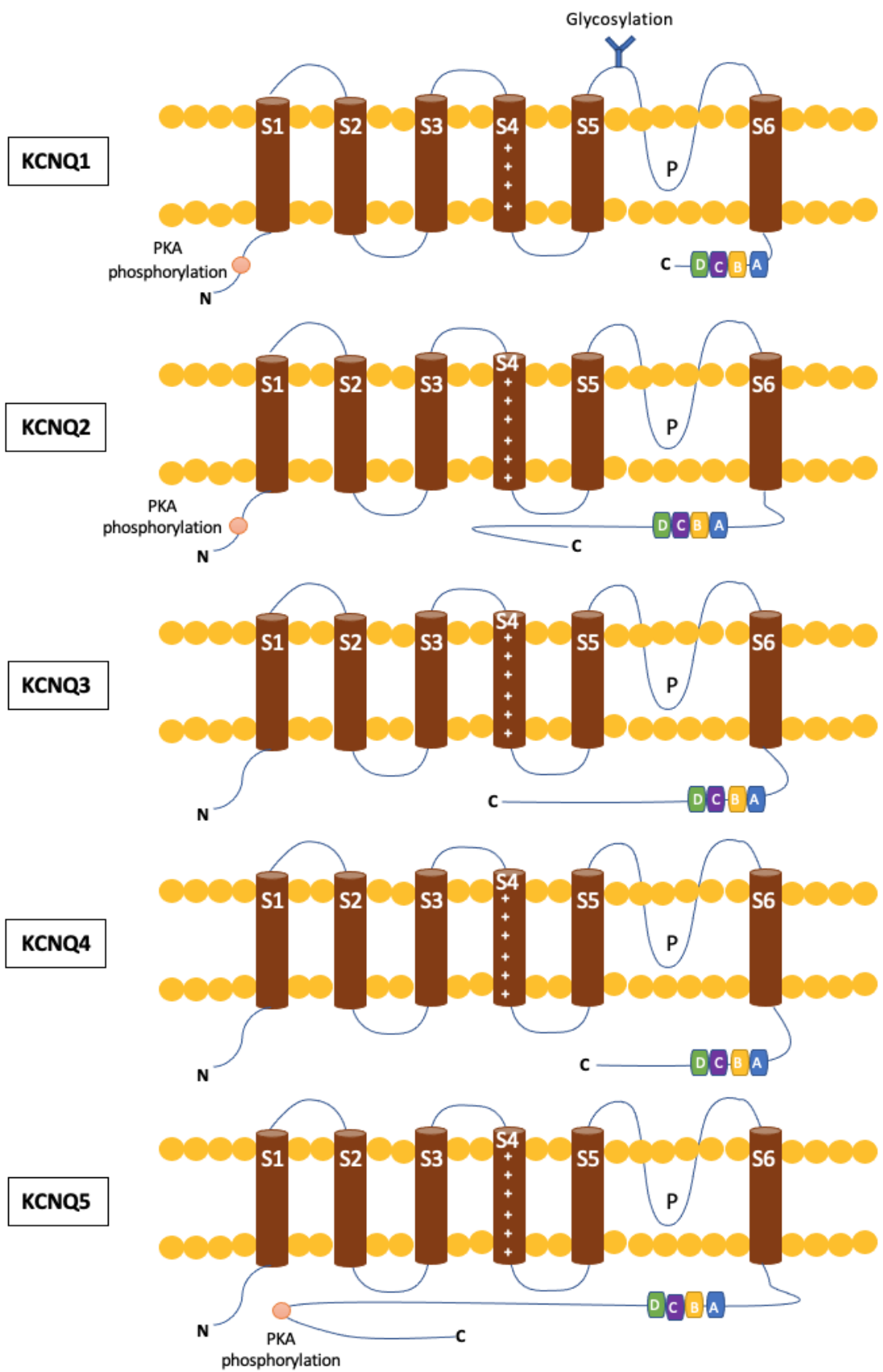


**Figure 1.14:** Molecular structure of KCNQ  $\alpha$ -subunits.

All types contain six TM segments (1-6), a pore-forming region (P), C-terminal domain with four distinct helices (A, B, C, D), and N-terminal domain. Glycosylation site is located on the extracellular area of KCNQ1. Protein kinase A phosphorylation sites (PKA) are existed for KCNQ1, KCNQ2, and KCNQ5. (Diagrams adapted from (Barrese et al., 2018; Robbins, 2001)).

The biophysical properties of each Kv7 sub-family are varied, depending on their expression system, whether expressed with identical protein subunit (homomultimers) or expressed with other Kv7 subunits (heteromultimers) (Table 1.5). Overall, KCNQ1 currents are identified as outward-rectifying  $K^+$  currents which play an important role in the heart repolarization. The activation kinetic properties of homotetramer Kv7.1 channels are sigmoidal activation and require 100-200 ms of channel activation to achieve 90% of repolarization with subthreshold membrane potential at -53 mV. However, the expression of Kv7.1 channels in mammalian cell lines gives rise to a more rapid current activation than those in the coassembly of Kv7.1 and KCNE  $\beta$ -subunit, which reaches a steady state within 1 s (Yang et al., 1997). The Kv7.1 subfamily is characterised by not being associated with other members of the Kv7 family, but it is commonly co-expressed with the KCNE1 (Barhanin et al., 1996a; Haitin and Attali, 2008; Sanguinetti et al., 1996). Kv7.2 homomultimeric channels have different current characteristics, depending on their expression in numerous cell types (Table 1.5). Kv7.2 can co-assemble with Kv7.3 subunits to form heteromultimeric channels (Main et al., 2000; Wang et al., 1998). This summation increases the amplitude of currents by 10 times and is referred to as the M-current in neuronal tissue. However, Kv7.2 cannot be co-expressed with Kv7.4 or Kv7.5 (Kubisch et al., 1999; Schroeder et al., 2000a). The biophysical parameters of homotetramer Kv7.4 channels seems to depend on the expression system (Table 1.5). The expression of Kv7.4 with Kv7.3 for heterotetramer channels yields currents with a significant large amplitude (Kubisch et al., 1999). Predominantly, Kv7.4 and Kv7.5 form heteromeric channels which are highly expressed in vascular tissues (Chadha et al., 2014; Brueggemann et al., 2014).

Table 1.5: Kv7 family genes and proteins and their properties expressed as homotetramers.

Kv7 member ( $\alpha$ -Subunit)	Half -activation voltage ( $V_{0.5}$ ) (mV)	Single-channel conductance (pS)	Voltage-dependent activation at threshold (mV)
Kv7.1	-10 to -29 <sup>(1)</sup>	1-4 <sup>(8)</sup>	-53
Kv7.2	-14 (CHO) <sup>(2)</sup> , -21 (HEK) <sup>(3)</sup> , -37 (Oocytes) <sup>(4)</sup> , -38 (COS) <sup>(5)</sup>	2-9 <sup>(9)</sup>	-60 to -50
Kv7.3	-37 <sup>(2)(4)</sup>	8.5 <sup>(9)</sup>	-60
Kv7.4	-19 (CHO) <sup>(2)</sup> , -10 (Oocytes) <sup>(6)</sup>	2 <sup>(9)</sup>	-60
Kv7.5	-46 to -48 <sup>(7)</sup>	2-9 <sup>(9)</sup>	-60 to -50

(Barhanin et al., 1996b; Shamgar et al., 2008)<sup>(1)</sup>; (Selyanko et al., 2000)<sup>(2)</sup>; (Shapiro et al., 2000)<sup>(3)</sup>; (Yang and Sigworth, 1998)<sup>(4)</sup>; (Tinel et al., 2000b)<sup>(5)</sup>; (Kubisch et al., 1999)<sup>(6)</sup>; (Schroeder et al., 2000a)<sup>(7)</sup>; (Sesti and Goldstein, 1998)<sup>(8)</sup>; (Fermini and Priest, 2008)<sup>(9)</sup>

#### 1.4.1.2 Different expression and their physiological roles of KCNQ family

KCNQ proteins have a relatively negative voltage dependence which regulates the functional activity of many excitable tissues by the opening at a small membrane depolarization (Robbins, 2001). The reduction of electrical excitability is achieved by allowing the outward movement of K<sup>+</sup> currents, which contributes to the stabilization of resting membrane potentials. The functional role of KCNQ channels was discovered in certain cell types such as cardiomyocytes, epithelial cells, neurons and smooth muscle cells and are not uniformly expressed in the body. KCNQ1 was first discovered by Wang et al. (1996) and was found in cardiomyocytes in association with KCNE1. The impact of KCNE1 on cardiac KCNQ1 subunits is well characterised and includes slowing activation by 5-10 fold, depolarisation of the voltage-dependence of activation by about +50 mV, stabilisation of the open pore of KCNQ1, increasing the K<sup>+</sup> current by 4-fold increasing single-channel conductance and delaying deactivation kinetics (Sanguinetti et al., 1996; Werry et al., 2013). The co-assembly of KCNE1 with KCNQ1 forming I<sub>Ks</sub>, together with hERG channel (I<sub>Kr</sub>) form a main repolarising currents of cardiac action potential (Barhanin et al., 1996b; Wang et al., 1996b; Abbott et al., 1999). Specifically, KCNQ1/KCNE1 complex contributes to create a “repolarising reserve” during

tachycardia to generate a large repolarising current which shortens the action potential and facilitates ventricular diastolic filling before the next heartbeat. It was also suggested that KCNE1 may contribute in the regulation of hERG channel which is the dominant repolarising current in human ventricles (Silva and Rudy, 2005). KCNQ1/KCNE1 combinations are also expressed in cochlea (Neyroud et al., 1997). The co-expression of KCNQ1/KCNE2 was identified in the thyroid gland, which plays a role in the regulation of thyroid hormone production (Fröhlich et al., 2011; Purtell et al., 2012). A KCNQ1/KCNE3 protein complex can be found in pancreas, trachea, small intestine and colon crypt cells which markedly contributes to Cl<sup>-</sup> secretion (Grahammer et al., 2001a; Grahammer et al., 2001b). KCNQ2 and KCNQ3 are substantially expressed in the central and peripheral nervous system which generates M-type currents and subsequently prevents neuronal hyperexcitability (Prole and Marrion, 2004; Robbins, 2001; Wang et al., 1998). KCNQ2/KCNQ3 channels are also expressed in skeletal muscle, particularly in human brachial biceps (Iannotti et al., 2010). The expression of KCNQ4 was reported to play a crucial physiological role for normal hearing; therefore, it is mainly expressed in outer hair cells of the cochlea (Kubisch et al., 1999; Rennie et al., 2001). Additionally, KCNQ4 is well located in several other tissues, including the gastrointestinal tract, smooth muscle cells, skeletal muscles, cardiac mitochondria, brain and nervous tissues (Iannotti et al., 2010; Jepps et al., 2009; Kharkovets et al., 2000; Stott et al., 2014; Testai et al., 2015). KCNQ5 is mainly expressed in neurons, which contributes to regulating the electrical activity of these neurons (Tzingounis et al., 2010). Expression of KCNQ5 is also identified in skeletal muscle (Schroeder et al., 2000a) . Moreover, the combination of KCNQ5/KCNQ4 has been detected in smooth muscle cells which contributes to mediating vasodilation (Chadha et al., 2014; Mani et al., 2016).

#### 1.4.2 The KCNE family

The KCNE proteins are a non-pore forming β-subunit with single transmembrane domain (Lundby et al., 2010; Wrobel et al., 2012). The KCNE subunit is encoded by members of the KCNE gene family (MinK-related peptides), including five proteins (KCNE1 to KCNE5) (Abbott and Goldstein, 1998; Abbott et al., 1999; Piccini et al., 1999). These β-subunits co-assemble with KCNQ channel α-subunits to alter their biophysical properties. The electrophysiological properties of all Kv7 channels are modified when they co-assemble with KCNE protein in

different aspects such as activation rate, deactivation kinetics, conductance properties and their sensitivity to pharmacological treatments. Table 1.6 presents a summary of the effects of the KCNE family when they are co-expressed with KCNQ  $\alpha$ -subunits of the Kv7 family.

**Table 1.6:** Functional implications of the interaction of KCNE1-5 auxiliary subunits with Kv7 channel  $\alpha$ -subunits

	KCNQ1	KCNQ2	KCNQ3	KCNQ4	KCNQ5
<b>KCNE1</b>	1-Slow activation kinetic (5-10 fold) <sup>(1,2,3)</sup> 2-Remove inactivation <sup>(4,5)</sup> 3- $\uparrow$ the amplitude of K <sup>+</sup> currents <sup>(6)</sup> 4- $\uparrow$ channel conductance (4 fold) <sup>(6)</sup> 5- $\uparrow$ the expression of Kv7 channels on the cell surface <sup>(7)</sup>	1- $\downarrow$ KCNQ2 current density <sup>(15,18)</sup> 2-Slowed activation and deactivation kinetics <sup>(15,18)</sup>	1- $\downarrow$ KCNQ2 current density <sup>(15)</sup> 2-Slowed activation <sup>(15)</sup>	1- $\uparrow$ the amplitude of K <sup>+</sup> currents <sup>(12,13)</sup> 2- shifted the voltage for half-maximal activation (V <sub>0.5</sub> ) in the negative direction <sup>(12)</sup> 3-slows the rates of Kv4.2 activation and inactivation <sup>(17)</sup>	1-Slow activation <sup>(13)</sup> 2- $\downarrow$ current magnitude in oocytes <sup>(13)</sup> 3- $\uparrow$ the current density in HEK293 cells <sup>(14)</sup>
<b>KCNE2</b>	1-Constitutively active currents <sup>(8,9)</sup> 2- $\downarrow$ the current density, when the KCNE2 subunit presents with KCNQ1-KCNE1 protein complex <sup>(1)</sup>	1- $\downarrow$ KCNQ2 current density <sup>(15,18)</sup> 2-Slowed activation and deactivation kinetics <sup>(15,18)</sup>	1-No significant effect on the current density <sup>(19)</sup> 2- $\uparrow$ deactivation kinetics when the KCNE2 subunit presents with KCNQ2-KCNQ3 protein complex <sup>(19)</sup>	1- $\uparrow$ the amplitude of K <sup>+</sup> currents <sup>(12,13)</sup> 2- shifted V <sub>0.5</sub> in the negative direction <sup>(12)</sup>	No effect <sup>(14)</sup>
<b>KCNE3</b>	1-Constitutively active currents <sup>(8)</sup> 2- $\uparrow$ the current density when the KCNE3 subunit presents with KCNQ1-KCNE1 protein complex <sup>(10)</sup>	$\downarrow$ currents <sup>(15)</sup>	1- $\downarrow$ currents <sup>(15)</sup> 2- alters the gating of KCNQ3 <sup>(16)</sup>	Current suppression <sup>(12,13)</sup>	Current suppression in oocytes and HEK293 cells <sup>(13, 14)</sup>
<b>KCNE4</b>	1- Slow activation kinetic <sup>(11)</sup> 2- Small current at physiological ranges <sup>(11)</sup>	Unaffected by co-expression with KCNE4 <sup>(20)</sup>	Unaffected by co-expression with KCNE4 <sup>(20)</sup>	1- $\uparrow$ the amplitude of K <sup>+</sup> currents <sup>(12,13)</sup> 2- $\downarrow$ ion selectivity 3- shifted V <sub>0.5</sub> in the negative direction <sup>(12)</sup>	No effect <sup>(14)</sup>
<b>KCNE5</b>	1- Slow activation kinetic <sup>(11)</sup> . 2- Small current at physiological ranges <sup>(11)</sup> .	No effect <sup>(22)</sup>	No effect <sup>(21)</sup>	No effect <sup>(12)</sup>	No effect <sup>(14)</sup>

(Wu et al., 2006)<sup>(1)</sup>; (Barhanin et al., 1996b)<sup>(2)</sup>; (Sanguinetti et al., 1996)<sup>(3)</sup>; (Pusch et al., 1998)<sup>(4)</sup>; (Seeböhm et al., 2003b)<sup>(5)</sup>; (Sesti & Goldstein 1998)<sup>(6)</sup>; (Tristani-Firouzi and Sanguinetti, 1998)<sup>(7)</sup>; (Schroeder et al., 2000b)<sup>(8)</sup>; (Tinel et al., 2000a)<sup>(9)</sup>; (Melman et al., 2002)<sup>(10)</sup>; (Bendahhou et al., 2005)<sup>(11)</sup>; (Strutz-Seeböhm et al., 2006)<sup>(12)</sup>; (Schroeder et al., 2000a)<sup>(13)</sup>; (Roura-Ferrer et al., 2009)<sup>(14)</sup>; (McCrossan et al., 2003)<sup>(15)</sup>; (Abbott and Goldstein, 1998)<sup>(16)</sup>; (Zhang et al., 2001)<sup>(17)</sup>; (McCrossan et al., 2009)<sup>(18)</sup>; (Tinel et al., 2000b)<sup>(19)</sup>; (Grunnet et al., 2002)<sup>(20)</sup>; (Angelo et al., 2002)<sup>(21)</sup>; (Abbott, 2016)<sup>(22)</sup>

### 1.4.3 The $I_{Ks}$ complex in cardiac cells

#### 1.4.3.1 The Molecular structure of $I_{Ks}$

The first reported expression of the slowly activating delayed rectifier potassium ( $I_{Ks}$ ) current in cardiac cells was made by Noble and Tsien (1969), using multicellular sheep cardiac Purkinje fibre model (Noble and Tsien, 1969). In cardiac myocytes, the functional  $I_{Ks}$  is achieved by co-expression of KCNQ1 (Kv7.1) subunit with the KCNE1 auxiliary subunit (Barhanin et al., 1996b; Sanguinetti et al., 1996) (Figure 1.15A). The number of KCNQ1 bound to KCNE1 is varied, with 4:1, 4:2, and 4:4 as a KCNQ1:KCNE1 ratio having been identified (Murray et al., 2016; Hou et al., 2017). The  $K^+$  Current activation becomes progressively slower as more KCNE1 subunit bound to KCNQ1 subunits. A full saturated KCNQ1/KCNE1 protein complex (4:4) has the slowest activation kinetics and the most positive half-activation curve (Wang et al., 2020). Most recent evidence from expression studies in recombinant systems suggests this complex is mostly closely modelled with a ratio of 4 KCNQ1:2 KCNE1 (Nakajo et al., 2010; Abbott, 2016; Kobertz, 2014; Plant et al., 2014). This  $I_{Ks}$  complex was also referred to as KvLQT1, by linking a deficiency of this  $I_{Ks}$  and the incidence of long QT1 syndrome (Wang et al., 1996a). Membrane depolarization activates the  $I_{Ks}$  with slow increase of outward  $K^+$  currents during the action potential which only significantly contributes to repolarization at the end of the plateau phase (Figure 1.15B). This current is considered as a repolarization reserve which only substantially participates to returning the membrane to its resting potential in the presence of sympathetic stimulation (Jost et al., 2005; Roden, 1998). Some studies have suggested that because the KCNE1 subunit exerts a crucial role in the regulation of ion conductance through the channel's gating, KCNE1 may bind directly to the pore domain of the KCNQ1 subunit (Tapper and George Jr, 2000; Melman et al., 2004). Other reports in the literature have suggested that the KCNE1 binds to the voltage sensor domain of KCNQ1 subunit using voltage clamp fluorometry (Osteen et al., 2010; Nakajo et al., 2010; Werry et al., 2013).

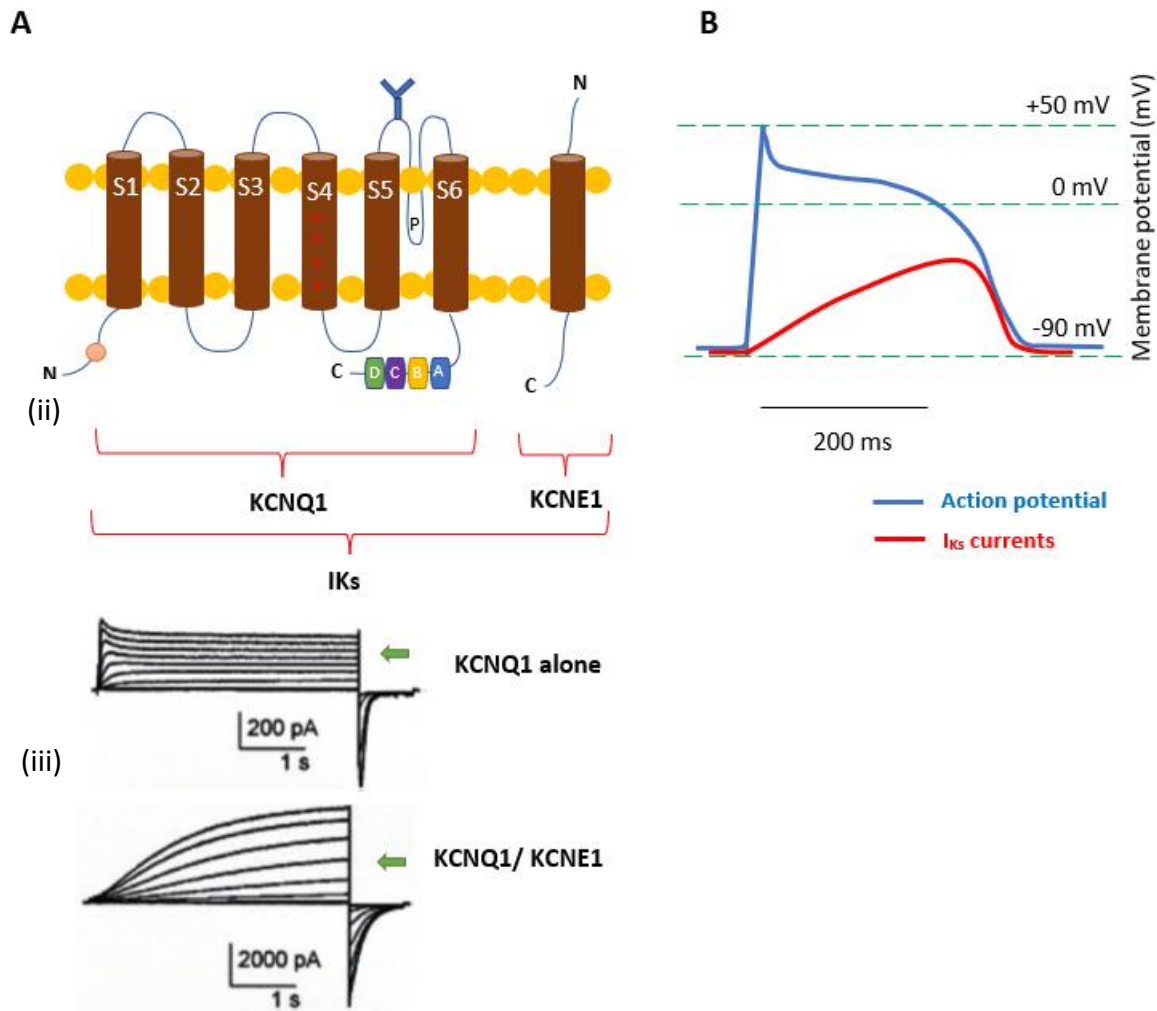


**Figure 1.15:** The molecular component and the electrophysiological characteristic of KCNQ1 in the absence and presence of KCNE1.

*A, (i) Diagram showing the general structure of the KCNQ1 and KCNE1 subunits. Electrical currents can be recorded from the expression of (ii) KCNQ1 alone and (iii) co-expression of KCNQ1 and KCNE1. Currents were evoked in CHO cells by voltage steps between -80 mV and +80 mV. The transfection of KCNQ1 with the accessory subunit KCNE1 protein complex alters biophysical properties of outward  $K^+$  currents, producing larger current amplitude than with KCNQ1 alone, and slows the activation kinetics; Adapted from (Zheng et al. 2010). The co-expression of KCNQ1/KCNE1 yields a current that resembles native cardiac  $I_{Ks}$  currents. B, A diagram showing the time course of the action potential in a ventricular cell (blue line) and the corresponding current amplitude of  $I_{Ks}$  (red line).*

#### 1.4.3.2 The physiological role of $I_{Ks}$

Although the expression of KCNQ1 subunit without KCNE1 can generate functional rapidly activating outward  $K^+$  currents, the co-expression with accessory  $\beta$ -subunit KCNE1 modulates

the biophysical kinetics by delaying the opening of the pore-forming KCNQ1 subunit, giving rise to the characteristic slow kinetics of channel activation and deactivation (Chen et al., 2009; Sanguinetti et al., 1996) (Figure 1.15). This property of the  $I_{Ks}$  contributes to cardiac repolarization by increasing the  $K^+$  efflux towards the end of the plateau phase. Interestingly, some studies have demonstrated that the functional role of  $I_{Ks}$  was absent in isolated cardiomyocytes from a non-diseased human heart (Iost et al., 1998). This finding is in agreement with incidences of long QT syndrome ( $I_{Ks}$  mutations) often appearing to be subclinical, and only manifesting on heavy exercise or with extreme stress. KCNQ1 and KCNE1 protein expression has also been detected in the rat ventricular myocytes using various imaging techniques including immunofluorescence and immunocytochemistry (Wu et al., 2006; Tsevi et al., 2005). In the study by Wu and colleagues, isolated rat ventricular myocytes were immunolabelled with anti-KCNQ1 and anti-KCNE1 antibodies, and their distribution and co-localisation analysed (Wu et al., 2006). KCNQ1 and KCNE1 proteins were found throughout the membrane and cytoplasm of rat myocytes and were also found to co-localise with each other. Electrophysiological recordings by the same group, using whole-cell patch clamp recordings were also shown to produce an outward current component at depolarised voltages that resembled that of the described the slowly activating delayed rectifier ( $I_{Ks}$ ) in rat ventricular myocytes (Wu et al., 2006). However, unlike human,  $I_{Ks}$  within the rat is generally considered to be small and is not a main repolarisation current under normal condition. It is proposed that this contributes to ventricular repolarisation in this species under some conditions such as chronically stressed conditions (Jiang et al., 2017; Wang and Fitts, 2020; Olgar et al., 2022).

Under physiological condition with significant sympathetic stimulation, the electrical excitability of the sinoatrial node (SAN) increases which triggers an elevation in heart rate (Rocchetti et al., 2006). At the same time, the sympathetic nervous system activates  $\beta$ -adrenergic receptor which augments the  $I_{Ks}$  through activation of G-protein  $\alpha$  ( $G\alpha$ ) (Kurokawa et al., 2003; Nicolas et al., 2008). The  $\beta$ -adrenergic receptor is a G-protein coupled receptor which activates adenylyl cyclase (AC), increases cAMP, and hence activates PKA and phosphorylates the Kv7.1 channel  $\alpha$ -subunit at the N-terminus (Figure 1.16) (Terrenoire et al., 2009). The summation of actions of these proteins can phosphorylate this channel, which augments channel activation to enhance cardiac repolarization and to prevent deleterious impacts of hyperexcitability during sympathetic stimulation. In addition to that,  $I_{Ks}$  can be

regulated by phosphatidylinositol 4,5-biophosphate (PIP<sub>2</sub>) which stabilises the channel's gating, maintaining the channel in the opening state during the plateau phase (Li et al., 2011; Sun et al., 2012; Choveau et al., 2012). It also was observed that the co-expression of KCNE1 increases KCNQ1 sensitivity to PIP<sub>2</sub> by approximately 100-fold compared to KCNQ1 expressed alone (Li et al., 2011). As a result, the activation of  $\beta$ -adrenergic receptor and PIP<sub>2</sub> are considered as major regulators to control the physiological function of the KCNQ1/KCNE1 protein complex in cardiomyocytes. An additional interesting feature of KCNQ1 is that its activation is affected by other modulators such as, polyunsaturated fatty acids (PUFA), Calmodulin (CaM), and the serum- and glucocorticoid-inducible kinase 1 (SGK1). PUFA are lipid molecules, that bind to KCNQ1 via the lipid head group and consequently cause the activation of KCNQ1 channel through this electrostatic interaction (Liin et al., 2018). CaM is the cytosolic Ca<sup>2+</sup>-binding protein and Ca<sup>2+</sup> signalling mediator that binds to the C-terminal of KCNQ1 and plays an essential role in facilitating activation of KCNQ1 (Chang et al., 2018). SGK1 is a gene abundant in cardiac tissue and regulated by a stress hormone, cortisol, and therefore its activation stimulates I<sub>Ks</sub> to increase ventricular repolarisation time during stress reaction (Strutz-Seeböhm et al., 2009).

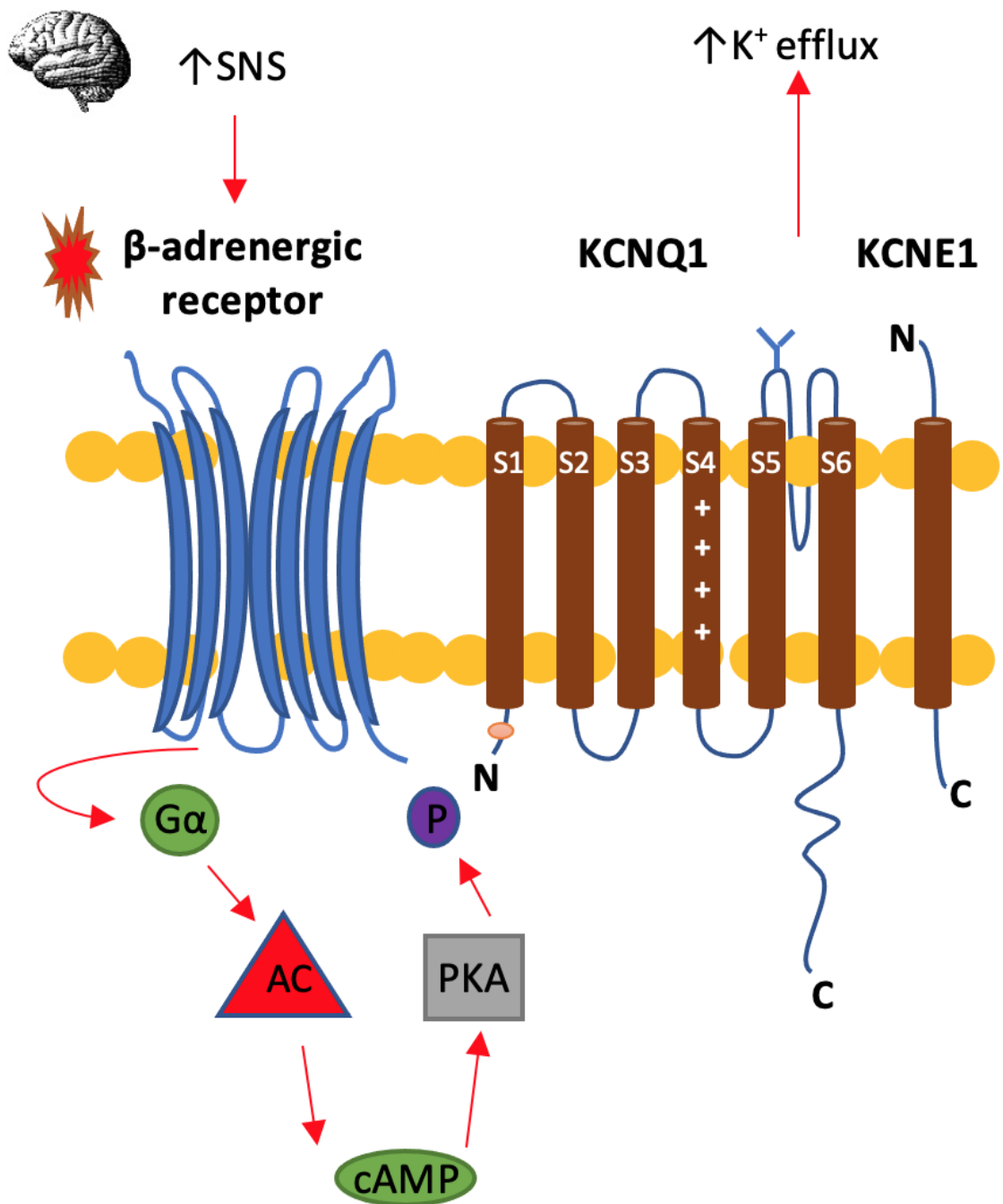


**Figure 1.16:** The functional role of Kv7 channel in cardiac myocytes.

The cardiac  $I_{Ks}$  channel is composed from KCNQ1 and KCNE1 subunits. Activation of the  $\beta$ -adrenergic receptor in the signal transduction pathway leading to potentiation of Kv7.1 channel currents.  $G\alpha$  activates adenylyl cyclase, increase cAMP, which activates PKA which phosphorylates the Kv7.1 channel  $\alpha$ -subunit at the N-terminus. As a result, activating of this channel contributes to the accelerate repolarization of action potential via increased  $K^+$  efflux. (Adapted from (Chen et al., 2005)).

#### 1.4.4 The pharmacological modulation of $I_{Ks}$

The Kv7 family of channels has been shown to have important roles in the regulation of different excitable cells, including cardiomyocytes, neuronal and vascular tissue. The focus of the present study has been on pharmacological modulation of the cardiac  $I_{Ks}$ , for which, both blockers and activators exist. In addition, other members of the KCNQ family have also been successfully used as drug targets, such as KCNQ2/3 for epilepsy (Retigabine) and pain management (Fluripitine) (summarized in Table 1.7).

##### 1.4.4.1 Pharmacological blockers of the $I_{Ks}$ complex

Given the known deleterious impact of inhibition of  $I_{Ks}$ , specific blockers are not currently used clinically. In early clinical studies, QT prolongation, leading to torsades de pointes, was reported after administration of  $I_{Ks}$  blockers such as mibepradil, indapamide and propafenone (Gläser et al., 2001; Guzzini et al., 1990; Hii et al., 1991). These blockers, however, remain useful tools that can be used in pre-clinical research to investigate the role of  $I_{Ks}$  in the regulation of cardiac function. Chromanol 293B was considered the first compound for  $I_{Ks}$  block which selectively inhibits KCNQ1 with  $IC_{50}$  value of 6.9  $\mu M$  in Xenopus oocytes (Busch et al., 1996; Gerlach et al., 2001; Lerche et al., 2007). The efficacy of Chromanol 293B is increased by the co-expression of  $\beta$ -subunit with KCNQ1  $\alpha$ -subunit, including KCNE1 and KCNE3 subunits (Bett et al., 2006). Chromanol 293B showed a 30-fold greater blockage of the  $I_{Ks}$  with the presence of KCNE3 than KCNE1. Recently, it has also been found that 100  $\mu M$  chromanol 293B enhances insulin secretion in mouse pancreas (Liu et al., 2014), however given the high concentration, it is likely that this has off-target effects at this concentration. A more powerful and selective blocker of the  $I_{Ks}$  is HMR1556 which inhibits  $I_{Ks}$  with an  $IC_{50}$  of 0.074  $\mu M$  (Gerlach et al., 2001). This pharmacological compound is 100 times more potent in blocking the  $I_{Ks}$  channel than chromanol 293B. Recently, attention has been paid to investigate the inhibitory effect of JNJ303, reported as a selective blocker of  $I_{Ks}$ , with an  $IC_{50}$  of 0.064  $\mu M$  (Towart et al., 2009). The interaction between JNJ303 and the KCNQ1/KCNE1 channel was first examined by Worbel et al. (2013) which found that the inhibitory effect of this pharmacological compound depends on the presence of KCNE1 subunit but their effect are abolished when KCNQ1  $\alpha$ -subunit is expressed alone (Worbel, 2013). This is due to a conformational change when co-expressed with KCNE1 which provides a binding site for

JNJ303. Accordingly, JNJ303 binds to this inhibitory site and does not block the pore-forming section of the  $\alpha$  subunit of KCNQ1. Therefore, this result suggests that JNJ303 leads to incomplete  $I_{Ks}$  block by stabilising a closed state via this inhibitory site. Linde et al (2010) showed that the administration of JNJ303 contributes to produce a major prolongation of QT-interval in *in vivo* anesthetized dogs, minipigs and guinea pigs, leading to Torsades de Pointes (TdP) arrhythmia (Van der Linde et al., 2010). Albrecht (2017) offers contradictory findings about using JNJ303 in *in vitro* experiments, suggesting that there is a lack of prolongation of APD, but with significantly reduced  $Ca^{2+}$  influx (Albrecht, 2017). However, much uncertainty still exists about the relation between  $Ca^{2+}$  influx and  $I_{Ks}$  blockade to generate cardiac arrhythmia. There are also some suggestions that clofilium can act as an  $I_{Ks}$  blocker, causing TdP arrhythmia in anesthetized rabbits (Varnum et al., 1993; Batey and Coker, 2002). Interestingly, the effect of this drug also appears to block other members of KCNQ family such as KCNQ2, KCNQ5, and KCNQ2/KCNQ3 (Batey and Coker, 2002; de los Angeles Tejada et al., 2012).

#### 1.4.4.2 Pharmacological activators of the $I_{Ks}$ complex

The first selective, and currently the most potent, activator of the Kv7.1 channel is ML277. As reported by Yu et al (2013), the effect of this pharmacological compound was examined using a CHO cell line with different expressed ratios for the KCNQ1:KCNE1 complex (Yu et al., 2013b). The results presented by Yu et al. (2013) showed a significant effect of ML277 on KCNQ1 channel subunits expressed alone with an  $EC_{50} = 0.26 \mu M$  whereas the augmentation effect of ML277 was less significant with progressive increases in KCNQ1:KCNE1 stoichiometry. It has been hypothesised that the presence of KCNE1 may decrease the efficacy of ML277 binding. Similarly, Xu et al (2015) found that ML277 led to an augmented activation of  $I_{Ks}$  and subsequently shortening APDs using human-induced pluripotent stem cell (iPSC)-derived cardiomyocytes and guinea pig cardiomyocytes (Xu et al., 2015). A recent study of the effects of ML277 on KCNQ1 have highlighted the electrophysiological alterations in cardiomyocytes, including modulation in voltage-dependence of activation, inactivation kinetics, and the permeability of  $K^+$  efflux (Hou et al., 2019). The sensitivity of  $I_{Ks}$  in cardiomyocytes to ML277 suggests that the native  $I_{Ks}$  are not always saturated with KCNE1 and therefore this pharmacological compound could be considered as a therapeutic approach to treat long QT syndrome (Hou et al., 2019). Other  $I_{Ks}$  activators, 4,40-

diisothiocyanatostilbene-2,20-disulfonic acid (DIDS) and mefenamic acid, have been identified as chloride channel inhibitors and can increase  $I_{Ks}$  in Xenopus Oocytes (Abbott et al., 1999; Busch et al., 1994; Abitbol et al., 1999).  $I_{Ks}$  properties are significantly changed by ML277, including a negative shift in the voltage-dependence of activation by  $\sim$ 17 mV, and slowed inactivation of KCNQ1 currents. Importantly, applying these agents in the presence of KCNE1 with KCNQ1 subunits leads to strong amplification of electrophysiological changes. For instance, there has been a reported increase of  $I_{Ks}$  amplitude by  $\sim$ 2.5 times and a shift in the voltage-dependence of activation to more negative by  $\sim$ 30 mV (Abitbol et al., 1999).

Other pharmacological activators include R-L3 or L-364 373, benzodiazepines (Salata et al., 1998; Seeböhm et al., 2003a) and zinc pyrithione (ZnPy) (Surti and Jan, 2005). These drugs, however, activate the KCNQ1 channel and could affect other members of the Kv7 channel, but their effects are limited when KCNQ1 is co-expressed with KCNE1, consequently, these compounds may have limited effects on the cardiac  $I_{Ks}$ .

**Table 1.7:** Pharmacological modulators acting on Kv7 channels, including blockers and activators.

Pharmacological agent	Target channels	Effects	Experimental application in <i>in vivo</i> and their clinical uses
<b>Pharmacological blockers</b>			
Chromanol 293B	KCNQ1+KCNE1, KCNQ1+KCNE3, KCNQ1 alone (less efficacy)	-Inhibit 90% of KCNQ1 at 30 $\mu$ M -Inhibit 10% of other members of KCNQ family at 100 $\mu$ M	enhance insulin secretion in mice <sup>(1)</sup>
HMR1556	KCNQ1+KCNE1, KCNQ1 alone (less efficacy)	$IC_{50}$ of 0.074 $\mu$ M	no longer clinically used <sup>(2)</sup>
JNJ303	KCNQ1+KCNE1, KCNQ1 alone (less efficacy)	$IC_{50}$ of 0.064 $\mu$ M	prolongation of QT-interval in <i>in vivo</i> anesthetized dogs, minipigs and guinea pigs <sup>(3,4)</sup>
Clofilium	KCNQ1+KCNE1, KCNQ2, KCNQ5, KCNQ2/KCNQ3		causing TdP arrhythmia in anesthetized rabbits <sup>(5,6)</sup>
XE991	All KCNQ family	At different ranges $IC_{50}$ =0.8 $\mu$ M (KCNQ1), 0.71 $\mu$ M (KCNQ2), <50 $\mu$ M (KCNQ3), 2.4 $\mu$ M (KCNQ4), 65 $\mu$ M (KCNQ5), 0.6 $\mu$ M (KCNQ2/KCNQ3)	neurotransmitter release enhancer <sup>(7,8,9)</sup>

Linopirdine	All KCNQ family	At different ranges IC <sub>50</sub> =8.9 μM (KCNQ1), 4.8 μM (KCNQ2), 4.8 μM (KCNQ3), 14-200 μM (KCNQ4), 16-51.3 μM (KCNQ5); 4.0 μM (KCNQ2/KCNQ3)	Increase vascular resistance and blood pressure, useful to treat dementia <sup>(10,11)</sup>
<b>Pharmacological activators</b>			
ML277	KCNQ1+KCNE1 (The effect is gradually attenuated with progressive increase in KCNQ1:KCNE1 stoichiometry)	EC <sub>50</sub> = 0.26 μM	Anti-arrhythmic <sup>(12)</sup>
DIDS and Mefenamic acid (Cl <sup>-</sup> channel blockers)	KCNQ1, KCNQ1+KCNE1	Current potentiation	<ul style="list-style-type: none"> <li>- not clinically used</li> <li>- negative shift in the voltage-dependence of activation by ~17 mV, and slow the inactivation (in the presence of KCNQ1 alone).</li> <li>- ↑current amplitude by ~2.5 times and shifting the voltage-dependence of activation to more negative by ~30 mV (in the presence of KCNQ1+KCNE1). <sup>(13)</sup></li> </ul>
R-L3 or L-364 373	KCNQ1 alone, KCNQ1+KCNE1 (less efficacy)	Current potentiation	<ul style="list-style-type: none"> <li>- not clinically used</li> <li>- hyperpolarizing shift in the voltage-dependence of activation and slow the inactivation kinetic <sup>(14,15)</sup></li> </ul>
zinc pyrithione (ZnPy)	All KCNQ family except KCNQ3, KCNQ2/KCNQ3	Current potentiation, primarily an ionophore for zinc	<ul style="list-style-type: none"> <li>- not clinically used</li> <li>- hyperpolarizing shift in the voltage-dependence of activation by ~25 mV and slow the deactivation kinetic <sup>(16,17)</sup></li> </ul>
Retigabine	All KCNQ family except KCNQ1, KCNQ2/KCNQ3	At different ranges EC <sub>50</sub> =2.51 μM (KCNQ2), 0.6 μM (KCNQ3), 5.25 μM (KCNQ4)	Many clinical uses (such as antidepressant <sup>(18)</sup> , anxiolytic <sup>(19)</sup> , antimanic <sup>(20)</sup> , antihypertensive <sup>(21)</sup> , attenuation inflammation pain <sup>(22)</sup> , decrease stroke induced brain damage <sup>(23)</sup> )
Flupirtine	All KCNQ family except KCNQ1		Many clinical uses (such as antidepressant <sup>(18)</sup> , reduce memory damage <sup>(24)</sup> , reduce the addiction to cocaine <sup>(25)</sup> , decrease pulmonary hypertension <sup>(26,27)</sup> , decrease

			stroke induced brain damage (28)
--	--	--	----------------------------------

(Liu et al., 2014)<sup>(1)</sup>; (Gerlach et al., 2001)<sup>(2)</sup>; (Towart et al., 2009)<sup>(3)</sup>; (Van der Linde et al., 2010)<sup>(4)</sup>; (Varnum et al., 1993)<sup>(5)</sup>; (Batey and Coker, 2002)<sup>(6)</sup>; (Wang et al., 2000)<sup>(7)</sup>; (Song et al., 2009)<sup>(8)</sup>; (Zaczek et al., 1998)<sup>(9)</sup>; (Chorvat et al., 1998)<sup>(10)</sup>; (Mackie and Byron, 2008)<sup>(11)</sup>; (Hou et al., 2019)<sup>(12)</sup>; (Abitbol et al., 1999)<sup>(13)</sup>; (Salata et al., 1998)<sup>(14)</sup>; (Seeböhm et al., 2003a)<sup>(15)</sup>; (Surti and Jan, 2005)<sup>(16)</sup>; (Xiong et al., 2007)<sup>(17)</sup>; (Friedman et al., 2016)<sup>(18)</sup>; (Korsgaard et al., 2005)<sup>(19)</sup>; (Redrobe and Nielsen, 2009)<sup>(20)</sup>; (Fretwell and Woolard, 2013)<sup>(21)</sup>; (Hayashi et al., 2014)<sup>(22)</sup>; (Bierbower et al., 2015)<sup>(23)</sup>; (Huang et al., 2015)<sup>(24)</sup>; (Mooney and Rawls, 2017)<sup>(25)</sup>; (Morecroft et al., 2009)<sup>(26)</sup>; (Sedivy et al., 2015)<sup>(27)</sup>; (Block et al., 1997)<sup>(28)</sup>

## 1.5 The modulation of cardiac action potential in disease conditions

### 1.5.1 Acute coronary syndrome

Acute coronary syndrome (ACS) is a broad term referring to several clinical symptoms, including unstable angina (UA), myocardial infarction (MI) and sudden cardiac death (SCD) (Kumar and Cannon, 2009). In general, coronary artery disease (CAD) is the most serious cardiac disorder that leads to ACS. The pathophysiological mechanism of CAD involves the rupture of atherosclerotic plaques on the internal surface of the coronary lumen, which triggers the activation of platelets and the coagulation cascade (Naghavi et al., 2003). This atherosclerotic plaque consists of cells, connective tissues, lipid, immune cells and blood-borne inflammatory cells. This occlusion interrupts blood flow into the downstream myocardial tissue, which causes deleterious effects on the cardiac muscle, such as reduced efficiency of cardiac contractility and electrical instability. These effects are due to insufficient oxygen supply and increase of energy consumption.

UA is caused by transient and partial blockage of the coronary artery due to spasms, leading to a reduction in blood flow. On the other hand, MI is caused by narrowing of the coronary artery due to a fixed atherosclerotic plaque. Generally, MIs are classified into two types: ST-segment elevation myocardial infarction (STEMI), which occurs as a result of a completely occluded coronary artery, and non-ST-segment elevation myocardial infarction (NSTEMI), which is due to intermittent coronary occlusion. To differentiate between MI types, electrocardiograms (ECGs) can be used to diagnose the presence or absence of elevation in the baseline between the S and T segments on ECG leads.

ACS is the leading cause of mortality and morbidity worldwide, especially among patients with risk factors such as diabetes and hypertension (O'gara et al., 2013). In 2019, the World Health

Organization (WHO) reported that approximately 17.9 million people died from sudden occurrences of cardiovascular disease (WHO, 2021). Specifically, in the United Kingdom, over 160,000 people die per year, with more males than females affected (BHF, 2021). According to the latest statistical study by the British Heart Foundation (BHF), the mortality rate declining by more than half due to the effective use of preventative therapies and advanced control of risk factors (Ibáñez et al., 2015; BHF, 2021). Despite a downward trend in the incidence of CAD, 50% of patients are classified as being at a high risk of death as time progresses. This is a consequence of damage resulting from ongoing intermittent ischaemia and reperfusion (I/R) injury. Hence, it is essential to protect the cardiac muscle from damage that could continue in the myocardium, even after the initial ischaemic insult.

## 1.5.2 Ischaemic and reperfusion injury

### 1.5.2.1 Ischaemic injury

During ischaemia, the cardiac muscle is subjected to inadequate blood perfusion, resulting in an insufficient supply of nutrient- and oxygen-containing blood. As a consequence, the intracellular adenosine triphosphate (ATP) level declines due to a lack of oxygen and metabolic substrates, leading to the impairment of ion homeostasis and therefore causing contractile dysfunction (Dutta et al., 2017; Klabunde, 2017). To maintain the ATP level required for muscular contraction, anaerobic glycolysis becomes the main source of ATP instead of the aerobic metabolic pathway (Xiao and Allen, 1999). Although this anaerobic pathway produces ATP, intracellular lactate and acidosis ( $H^+$ ) is increased, which activates the sodium/hydrogen exchanger (NHE) to extrude  $H^+$ . However, this causes an elevation of intracellular  $Na^+$ . Additionally, the reduction in ATP levels lowers the activity of ATP-dependent ion pumps, including  $Na^+/K^+$  ATPase, sarco/endoplasmic reticulum  $Ca^{2+}$  ATPase (SERCA) and plasma membrane  $Ca^{2+}$  ATPase (PMCA). The inhibition of the  $Na^+/K^+$  ATPase pump causes elevations in intracellular  $Na^+$  and extracellular  $K^+$ . The rise in extracellular  $K^+$  shifts the membrane potential to a more positive level, rapidly reaching the threshold for activation and causing ventricular depolarisation (Kleber, 1983). Elevation of intracellular  $Na^+$  due to the impairment of  $Na^+/K^+$  ATPase activates a reverse mode of the sodium-calcium exchanger (NCX), in which the efflux of  $Na^+$  ions is coupled with the influx of  $Ca^{2+}$  ions in a 3:1 ratio. This  $Ca^{2+}$  influx, in combination with the impaired function of SERCA and PMCA, results

in an increase in intracellular  $\text{Ca}^{2+}$  concentrations. The accumulation of intracellular  $\text{Ca}^{2+}$  with ATP depletion during ischaemia contributes to large ischaemic insults, which result in irreversible cell injury and tissue death.

#### 1.5.2.2 Reperfusion injury

The restoration of blood perfusion into the stenosed coronary artery is known as reperfusion, which is essential to minimise the harmful impacts of myocardial ischaemia (Ye et al., 2019). The rapid application of reperfusion therapy limits myocardial damage after a period of ischaemic conditions. The reperfusion therapy can be performed via two methods: pharmacological and mechanical. For patients presenting with MI, the most effective method is mechanical reperfusion, which is achieved by providing percutaneous coronary intervention (PCI). PCI is considered an invasive therapeutic technique that leads to reopening of the occluded artery and provides rapid restoration of coronary perfusion. According to the European Society of Cardiology (ESC), successful outcomes are achieved when PCI is performed within 90 minutes after a positive ACS diagnosis (Ibáñez et al., 2015). For patients with UA, NSTEMI or those with a delay in implementing PCI, thrombolytic/fibrinolytic therapy could be considered within 30 minutes of diagnosis. According to randomised control trials (RCTs) in a large sample of acute MI patients treated with fibrinolytic agents, this pharmacological approach reduced short-term mortality by approximately 25% (Trialists, 1994).

Although successful outcomes are often reported in ACS patients after mechanical and pharmacological reperfusion therapy, around 20% of patients suffer from recurrent myocardial damage, which is termed reperfusion injury (Figure 1.17) (Yellon and Hausenloy, 2007). The myocardial reperfusion injury can manifest as any of four forms of damage: reperfusion-induced arrhythmias, myocardial stunning, microvascular obstruction (MVO) and reperfusion-induced necrotic cells (Hausenloy and Yellon, 2013).

Reperfusion-induced arrhythmias result from the restoration of ATP production. This restores the activity of the SERCA pump, allowing excess intracellular  $\text{Ca}^{2+}$  to be pumped into the sarcoplasmic reticulum (SR). Subsequently, the excessive intracellular  $\text{Ca}^{2+}$  leaves the SR via the opening of ryanodine receptor 2 (RyR2). The large quantities of intracellular  $\text{Ca}^{2+}$  trigger the NCX current, which depolarises the diastolic membrane potential via the permission of

$\text{Ca}^{2+}$  efflux. This transient depolarisation is known as a delayed afterdepolarisation (DAD) (Liu et al., 2015). The second form of reperfusion injury is myocardial stunning, which is a reversible contractile dysfunction after reopening of the coronary artery after a long period of ischaemia. The third form, MVO, results from ongoing obstruction of the coronary microcirculation. The microcirculatory network comprises branching vessels, which play a critical role in the myocardial supply of nutrients and oxygen. Patients may suffer from recurrent stenosis due to embolisation or microvascular impairment. These microemboli lead to occlusion of the microcirculation, resulting in ongoing intermittent ischaemia and reperfusion injury. The last form of reperfusion injury, which is the most serious and lethal form, manifests as the death of viable cells, even though these cells were functionally contractile at the end of the initial ischaemic event. In the heart, the vast majority of this cell death occurs due to opening of the mitochondrial permeability transition pore (mPTPs), which causes cell swelling and apoptosis (Halestrap et al., 2004). These detrimental impacts of I/R injury suggest that the essential targets for cardioprotection should be against ischaemia; these follow a common underlying mechanism of reducing cellular excitability and understanding the cellular mechanisms behind I/R injury with the aim of exploring the potential of new cardioprotective drugs.

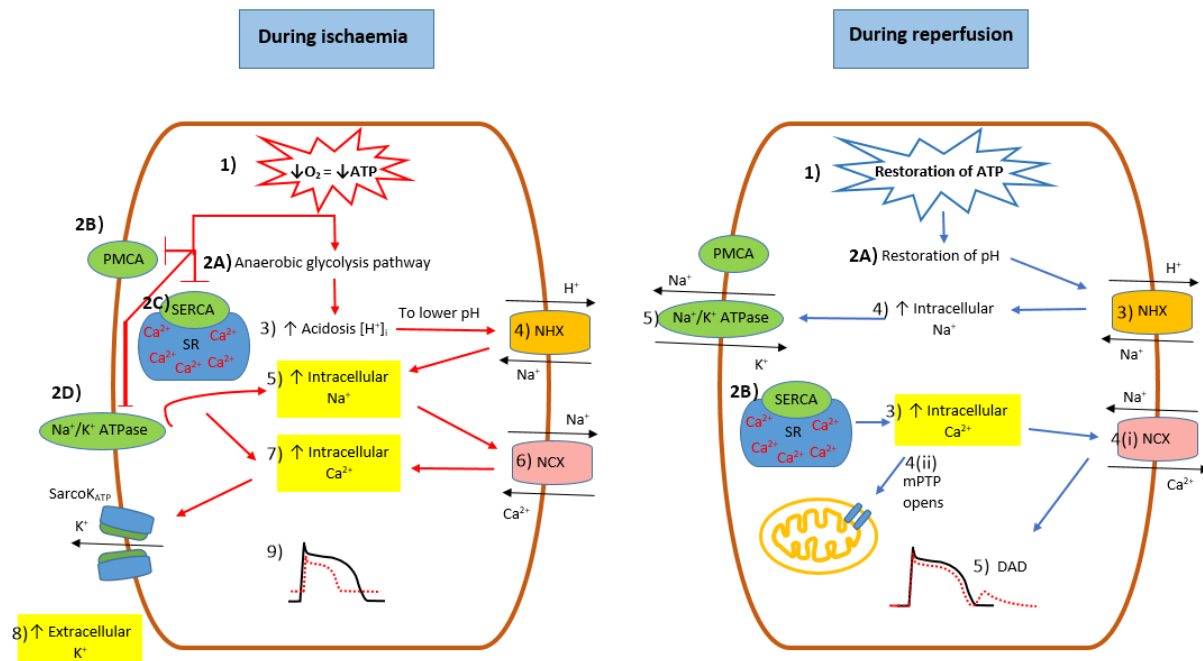


**Figure 1.17:** The modulation of ion homeostasis and therefore cardiac action potential during ischaemic and reperfusion injury.

*During acute myocardial ischaemia, the absence of oxygen (1) switches cell metabolism to anaerobic glycolysis (2A), resulting in the production of lactate and a reduction in intracellular pH (3). This induces the  $\text{Na}^+/\text{H}^+$  exchanger (4) to extrude  $\text{H}^+$  and results in intracellular  $\text{Na}^+$  overload (5), which activates the NCX exchanger (6) to function in reverse to extrude  $\text{Na}^+$  leading to intracellular  $\text{Ca}^{2+}$  overload (7). The PMCA (2B), SERCA (2C) and  $\text{Na}^+/\text{K}^+$  ATPase (2D), cease to function in ischaemia, exacerbating intracellular  $\text{Na}^+$  overload and result in intracellular  $\text{Ca}^{2+}$  overload. Therefore, this  $\text{Ca}^{2+}$  overload activates sarco $\text{K}_{\text{ATP}}$  channels to extrude  $\text{K}^+$ , resulting hyperkalemia (8) and arrhythmogenesis (9). The acidic conditions during ischaemia prevent the opening of the mitochondrial permeability transition pores (mPTP) and cardiomyocyte hypercontracture at this time.*

*During reperfusion, the electron transport chain is reactivated (1), resulting in the restoration of intracellular pH (2A). Generation of ROS mediates myocardial reperfusion injury by inducing the opening of the mPTP. This contributes to intracellular  $\text{Ca}^{2+}$  overload (3) which activates the NCX exchanger (4(i)) to function in forward mode to extrude  $\text{Ca}^{2+}$ . The reactivation of the  $\text{Na}^+/\text{H}^+$  exchanger (3) in washout of lactic acid, resulting in the rapid restoration of physiological pH, which releases the inhibitory effect on mPTP opening (4(ii)) and cardiomyocyte contracture. The reactivation of SERCA (2B) contributes to SR  $\text{Ca}^{2+}$  overload in reperfusion which may induce spontaneous  $\text{Ca}^{2+}$ -release events. The  $\text{Na}^+/\text{K}^+$  ATPase (5) in reperfusion works to restore the  $\text{Na}^+$  and  $\text{K}^+$  gradients, but may play a role in arrhythmogenesis by restoring the  $\text{Na}^+$  gradient so increasing the driving force on  $\text{Na}^+$  influx. (Adapted from (Hausenloy and Yellon, 2013)).*

## 1.6 Cardioprotection

### 1.6.1 Definition

Myocardial protection is achieved by different cardioprotective interventions to attenuate the injury resulting from myocardial ischaemia and to maximise the benefits of reperfusion therapy. The term cardioprotection is defined as any stimulus which activates intracellular signalling pathways to protect the heart from damage due to a major ischaemic event. There are different methods of conferring cardioprotection and limiting the size of the myocardial infarct, including ischaemic pre-conditioning (IPC), ischaemic post-conditioning (IPostC), remote ischaemic conditioning (RIC) and certain cardioprotective drugs.

### 1.6.2 Ischaemic conditioning

#### 1.6.2.1 Ischaemic preconditioning

The cardioprotection phenomenon was first described in pre-clinical animal models by Murry et al. (1986), who used short periods of ischaemia prior to a major ischaemic event to impart protection. They determined that there are two windows of protection: an early window,

which continues for several hours after the initial period of reperfusion, and a delayed second window of protection, which lasts 24 to 72 hours. This experimental phenomenon is known as IPC, which is triggered by repeated cycles of five minutes of coronary artery occlusion and five minutes of reperfusion before a sustained occlusion of the same coronary artery for 40 minutes (Murry et al., 1986). The cardioprotective effect is observed as a reduction in infarct size following the major ischaemic insult.

This preconditioning is believed to occur due to a delay in ATP depletion, a reduction in oxygen consumption and preservation of the intracellular structure of cardiomyocytes (Murry et al., 1986; Kitakaze, 2010). This result is in good agreement with observational studies on patients suffering multiple recurrent episodes of myocardial angina prior to an acute myocardial infarction, which showed delays in cell death after the onset of complete coronary occlusion (Ahmed et al., 2012; Lønborg et al., 2012b). However, the application of IPC is limited in the clinical setting among ACS patients because these clinical conditions are unpredictable events; therefore, research has focused on understanding the mechanisms of IPC. Despite nearly 40 years of research, the complete mechanisms of IPC are not fully understood and have not been translated into cardioprotective benefits in a clinical setting. A potential reason for the poor translation of the preclinical data is that results obtained from animal models did not undergo a stress response that would be seen in humans because these models are in controlled conditions. In clinical settings, patients with acute myocardial infarction undergo immense stress as they are rarely sedated prior to an infarct, and therefore cellular pathways could be altered by this stress response. This preconditioning is believed to occur due to a delay in ATP depletion, a reduction in oxygen consumption and preservation of the intracellular structure of cardiomyocytes (Murry et al., 1986; Kitakaze, 2010). This result is in good agreement with observational studies on patients suffering multiple recurrent episodes of myocardial angina prior to an acute myocardial infarction, which showed delays in cell death after the onset of complete coronary occlusion (Ahmed et al., 2012; Lønborg et al., 2012b). However, the application of IPC is limited in the clinical setting among ACS patients because these clinical conditions are unpredictable events; therefore, research has focused on understanding the mechanisms of IPC. Despite nearly 40 years of research, the complete mechanisms of IPC are not fully understood and have not been translated into cardioprotective benefits in a clinical setting. A potential reason for the poor

translation of the preclinical data is that results obtained from animal models did not undergo a stress response that would be seen in humans because these models are in controlled conditions. In clinical practices relating, patients with acute myocardial infarction undergo immense stress as they are rarely sedated prior to an infarct, and therefore cellular pathways could be altered by this stress response.

#### 1.6.2.2 Ischaemic postconditioning

The technique of applying intermittent short periods of ischaemia during the reperfusion period was investigated by Zhao et al. (2003) and is termed ischaemic postconditioning (IPostC). This form of protection was applied after three hours of total coronary occlusion, using a protocol of three repeated cycles of 30 seconds of reperfusion and 30 seconds of re-occlusion. The cardioprotective effect was achieved by attenuating the reperfusion injury's effect on infarct size.

With regard to the use of IPostC at the time of reperfusion, its translation into clinical use has been the primary goal of research in recent years. To evoke IPostC clinically, rapid repetitive ischaemia is performed by inflating a balloon multiple times at the onset of reperfusion during PCI and subsequently assessing biomarker levels. A recent systematic review and meta-analysis suggested that IPostC confers cardioprotection via reduction of final infarct size as evaluated by biomarkers of myocardial injury, such as the area under the serum creatine kinase curve (CK-AUC) (Touboul et al., 2015). Although the benefits of IPostC have been documented in humans, its cardioprotective effects can only be realised by patients who undergo reperfusion by PCI and not by those who achieve reperfusion using thrombolytic therapy.

#### 1.6.2.3 Remote ischaemic conditioning

The application of a brief period of ischaemia and subsequent reperfusion in a limb (such as the forearm) or internal organs (such as via the renal or mesenteric arteries) provides cardioprotective effects, and this is known as remote ischaemic conditioning (RIC) as it is “remote” to the organ intended for protection (Hausenloy and Yellon, 2008). Recently, cardioprotective effects of RIC have been observed in animal models, which showed a

reduction in infarct size after applying transient ischaemia to organs or limbs at a distance from the heart (Bromage et al., 2017). In the setting of human patients undergoing coronary artery bypass graft (CABG) surgery, the application of RIC via three intermittent cycles of inflation of an automated cuff on the right upper arm, followed by three cycles of cuff deflation, induces a cardioprotective signal in the myocardium. This beneficial effect is documented as reductions in infarct size, troponin T release and reperfusion arrhythmias (Hausenloy and Yellon, 2008). Despite the promising effects of RIC in both animal models and human patients, recent clinical outcome data from the Effect of Remote Ischaemic Conditioning in Coronary Artery Bypass Graft (ERICCA) study suggested that application of the transient arm ischaemia-reperfusion protocol did not confer a cardioprotective effect (Hausenloy et al., 2016b).

#### 1.6.2.4 Cardioprotective drugs

Cardioprotective drugs can be used to target various endogenous signalling pathways pharmacologically to reduce I/R injury. Several therapeutic agents may mimic endogenous ischaemic conditions and have been tested in animals and humans. Most of their pre-clinical studies have yielded positive results in terms of improvement of infarct size. However, many of the pharmacological agents (summarised in Table 1.8) that were initially shown to be beneficial in animal models subsequently failed to be translated into routine clinical practice for cardioprotection. This poor translation reflects the complexity of understanding the mechanisms of cardioprotection. Several barriers exist which may account for the failure of translation. The vast majority of pre-clinical studies was done at *ex vivo* models which leads to a lack of physiological interaction such as intact nervous system and a circulation required to ideally model ischaemic tolerance. Critically, animal studies most commonly use juvenile, healthy animals. These may be a poor representative of the elderly diabetic, hypertensive, vascular disease patients who are at increased risk of acute myocardial infarction. The cardiac ion channels distribution and function show most similarity among large mammals, such as dog, pig, rabbit and human (Joukar, 2021). However, the high costs of working on large mammals, and the ethical implications, mean that many studies are limited to the use of rodents in many cardioprotective research studies. So, the best model for cardioprotection is large mammals, and *in vivo* models of disease.

**Table 1.8:** A summary of preclinical and clinical trials for certain potentially cardioprotective drugs aimed at mimicking ischaemic conditioning

Agent	Indication/ Mechanisms	Pre-clinical testing	Clinical testing
<b>Cyclosporine A</b>	Immunosuppressant drug which inhibits T-cell activation and the opening of mPTP	Most animals studied had a reduction in final infarct size <sup>(1,2)</sup>	A recent large study suggested that there was no beneficial effect on the infarct size when administrated to patients prior to PCI <sup>(3,4)</sup>
<b>Adenosine</b>	Nitric oxide and protein kinase G (PKG)	When given prior to an ischaemic event, it reduced infarct sizes <sup>(5)</sup>	1. The AMISTAD trial demonstrated the cardioprotective effect of adenosine (via intravenous infusion with thrombolysis) on infarct size <sup>(6)</sup> 2. The AMISTAD-II trial showed no clinical benefit of adenosine when given at the time of reperfusion, although it did reduce anterior infarct size <sup>(7)</sup> 3. Administration of adenosine with intracoronary boluses at the time of PCI did not show cardioprotective effects <sup>(8)</sup> Despite large clinical trials on the cardioprotective effect of adenosine, no studies to date have demonstrated that the effective dose of adenosine causes a meaningful effect on infarct size.
<b>Nicorandil</b>	K <sub>ATP</sub> channel opener and vasodilator, used as a second-line therapy for angina	Animal studies have documented a reduction in infarct size when Nicorandil is administered <sup>(9,10,11)</sup>	Nicorandil showed a possible effect in humans by reducing heart failure and myocardial arrhythmia but had no impact on infarct size <sup>(12,13,14)</sup>
<b>Glucagon-like peptide-1 (GLP-1) (E.g., exenatide)</b>	Incretin hormone that reduces plasma glucose levels	Exenatide reduces the infarct size in isolated hearts in an animal model <sup>(15,16)</sup>	In some clinical studies, it has been documented that exenatide reduced infarct size by 30% if given to patients who had suffered a brief ischaemic event <sup>(17)</sup> . Additionally, exenatide improved myocardial salvage by 15% <sup>(18)</sup> . However, it was later shown that exenatide failed to provide a protective effect in ACS patients <sup>(19)</sup> .
<b>Glucose-insulin-potassium (GIK)</b>	Induction of the glycolysis pathway	Some pre-clinical studies suggested that GIK has a cardioprotective effect by slowing the progression of I/R injury <sup>(20)</sup>	The IMMEDIATE trial tested the administration of pre-hospital suspected ACS patients with GIK infusion, showing a reduction in infarct size but no effect on mortality <sup>(21)</sup> . In contrast, the largest clinical trial (CREATE-ECLA) testing the effect of GIK on mortality in ACS patients concluded that GIK had no benefit in this group <sup>(22)</sup> . Therefore,

			the clinical outcome of GIK-mediated cardioprotection remains controversial and incomplete.
<b>Metoprolol</b>	Beta-blocker therapy	The administration of metoprolol caused a reduction in infarct size in animal hearts (23)	The METOCARD-CNIC trial showed a reduction in infarct size and preserved left ventricular function if given in the ambulance prior to PCI or prior to reperfusion (24,25). However, the EARLY BAMI trial, which tested the effect of metoprolol when administrated by an intravenous catheter immediately prior to PCI, demonstrated no beneficial effect on infarct size (26).

(Argaud et al., 2005)<sup>(1)</sup>; (Lim et al., 2012)<sup>(2)</sup>; (Piot et al., 2008)<sup>(3)</sup>; (Cung et al., 2015)<sup>(4)</sup>; (Liu et al., 1991)<sup>(5)</sup>; (Mahaffey et al., 1999)<sup>(6)</sup>; (Ross et al., 2005)<sup>(7)</sup>; (Desmet et al., 2011)<sup>(8)</sup>; (Mizumura et al., 1996)<sup>(9)</sup>; (Imagawa et al., 1998)<sup>(10)</sup>; (Lenz et al., 2021)<sup>(11)</sup>; (Kitakaze et al., 2007)<sup>(12)</sup>; (Wu et al., 2013)<sup>(13)</sup>; (Campo et al., 2017)<sup>(14)</sup>; (Sonne et al., 2008)<sup>(15)</sup>; (Timmers et al., 2009)<sup>(16)</sup>; (Lønborg et al., 2012a)<sup>(17)</sup>; (Lønborg et al., 2012c)<sup>(18)</sup>; (Roos et al., 2016)<sup>(19)</sup>; (Grossman et al., 2013)<sup>(20)</sup>; (Selker et al., 2012)<sup>(21)</sup>; (Mehta et al., 2005)<sup>(22)</sup>; (Ibanez et al., 2007)<sup>(23)</sup>; (Ibanez et al., 2013)<sup>(24)</sup>; (Pizarro et al., 2014)<sup>(25)</sup>; (Roolvink et al., 2016)<sup>(26)</sup>

### 1.6.3 The mechanisms of cardioprotection

The mechanisms of cardioprotection are still not completely understood, but a large amount of research has been carried out in an attempt to elucidate these mechanisms. Although the mechanisms underlying these mediators of protection are still unclear, it is agreed that protein kinase C (PKC) plays a central role (Eisen et al., 2004). The PKC isoforms believed to be involved in cardioprotection include PKC $\epsilon$ , which is activated prior to ischaemia to impart protection, and PKC $\delta$ , which is inhibited at the onset of reperfusion to prevent damage from reperfusion injury; these isoforms are both from the “novel” family. This notion is supported by several studies revealed that cardioprotection was abolished in animals after deleting cardiac PKC $\epsilon$ , as demonstrated by the absence of improvement in final infarct size (Ytrehus et al., 1994; Inagaki et al., 2005; Weinbrenner et al., 2002). Therefore, the protection is mediated by PKC $\epsilon$ -induced regulation of SarcoK<sub>ATP</sub> channels, MitoK<sub>ATP</sub> channels and connexin (Cx)43 (Budas et al., 2007). The opening of SarcoK<sub>ATP</sub> channels can provide protection via the reduction of Ca<sup>2+</sup> accumulation by allowing K<sup>+</sup> efflux and shortening cardiac action potentials (Noma, 1983). Additionally, the opening of MitoK<sub>ATP</sub> channels can impart cardioprotection by different methods, including reduction of mitochondrial Ca<sup>2+</sup> overload, inhibition of mPTP

opening and generation of ROS. Furthermore, PKC $\epsilon$  can inhibit Cx43, which is the main component of gap junctions, and can therefore inhibit the progression of myocardial injury. Thus, the PKC signalling pathway is the main target of cardioprotection, leading to reductions in infarct size, necrosis and apoptosis (Hausenloy et al., 2009).

Ischaemic conditioning activates three main signalling pathways to initiate cardioprotection, including the cyclic guanosine monophosphate/cGMP-dependent protein kinase (cGMP/PKG) pathway, the reperfusion injury salvage kinase (RISK) pathway, and the survivor activating factor enhancement (SAFE) pathway (Burley et al., 2007; Hausenloy and Yellon, 2004; Lecour, 2009) (Figure 1.18). These pathways are activated at different time post myocardial ischaemia which in turn support myocardial survival: early and late cardioprotective factors. In the following sections, the mechanisms of these signalling pathways are discussed.

#### 1.6.3.1 The cyclic guanosine monophosphate/cGMP-dependent protein kinase (cGMP/PKG) pathway

During the early phase (several hours) of myocardial ischaemia, several ligands are released, including adenosine, bradykinin, opioids, angiotensin, acetylcholine and catecholamines (Hausenloy et al., 2016a). These ligands can act on G-protein-coupled receptors (GPCR) to activate intracellular signalling pathways, including phosphoinositide 3 kinase (PI3K), PKC, and mitochondrial K<sub>ATP</sub> which play an essential role in the suppression of cell death and improve the cell survival (Vinten-Johansen et al., 2007; Krieg et al., 2002). For instance, adenosine is rapidly accumulated during myocardial ischaemia which can interact with GPCR and activate the phosphoinositide-specific phospholipase C (PLC) signalling pathway (Liu, 2007). PLC enzymes hydrolyse phosphatidylinositol-4,5-bisphosphate (PIP<sub>2</sub>) and generate the messengers, diacylglycerol and inositol-1,4,5-trisphosphate (IP<sub>3</sub>) which resulting in increase in intracellular calcium and activation of PKC (Weernink et al., 2007).

In either case, there is increased in the production of exogenous NO which has been recently shown to play an important role in imparting cardioprotection against ischaemia/reperfusion injury (Sun et al., 2007). NO activates soluble guanylyl cyclase (sGC), localised in the cytosol, which generates cyclic guanosine 3', 5'-monophosphate (cGMP) from cytosolic purine nucleotide guanosine triphosphate (GTP) (Lucas et al., 2000). cGMP is an intracellular second

messenger which plays an important role in the regulation of physiological process in the myocardium. Once produced, cGMP targets cGMP-dependent protein kinases (PKGs) to reduce I/R injury (Hofmann et al., 2000). PKG interacts with PKC to mediate the opening of mitochondrial K<sub>ATP</sub> channels with subsequent inhibiting of mPTP (Burley et al., 2007).

#### 1.6.3.2 The reperfusion injury salvage kinase (RISK) pathway

Following the early period of myocardial ischaemia, there are late cardioprotective factors activated within several days after myocardial ischaemia. The definitive mechanism by which this occurs is unclear, however, its known to involve a number of growth factors and may contribute to cardioprotection from ischaemic injury and enhancing myocardial reperfusion via activating cell survival mechanisms (Torella et al., 2007; Ellison et al., 2006). The first group of pro-survival protein kinases was described by Yellon's group, often referred to as the Reperfusion Injury Salvage Kinase (RISK) pathway (Hausenloy et al., 2011; Rossello and Yellon, 2018; Schulman et al., 2002). The RISK pathway refers to a group of late-phase cardioprotective factors which combines two parallel cascades: the phosphatidylinositol 3-kinase-protein kinase B (PI3K-AKT) and extracellular signal-regulated kinase 1/2 (ERK1/2). These kinases are initially stimulated by the activation of GPCRs or EGFR, which ultimately regulates downstream components such as glycogen synthase kinase 3β (GSK-3β) and endothelial nitric oxide (eNOS). The phosphorylation of eNOS via PI3K-AKT is pivotal in PKCε activation to impart cardioprotection (Le Good et al., 1998). Similarly, the importance of phosphorylation of GSK-3β via ERK1/2 signalling pathway was documented in ischaemic conditioning, which ultimately acts to inhibit mPTP and therefore promoting myocardial reperfusion (Hausenloy et al., 2003).

#### 1.6.3.3 The survivor activating factor enhancement (SAFE) pathway

The survivor activating factor enhancement (SAFE) pathway was discovered as a second group of pro-survival signalling pathway which activated specifically at the time of reperfusion (Lecour et al., 2005; Lecour, 2009). The SAFE pathway is initiated by binding of Tumour necrosis factor alpha (TNF-α) to TNF receptor 2 (TNFR2) on the cell surface, leading to activation of Janus kinase (JAK) and the subsequent phosphorylation of the single transducer and activator of transcription 3 (STAT-3). TNF-α is a proinflammatory cytokine that released

from inflammatory cells. Although the presence of TNF- $\alpha$  has been linked to pathological conditions in the heart, its activation can contribute to the activation of downstream protective signalling pathways (Dörge et al., 2002; Lecour, 2009). Phosphorylation of STAT-3 mediates cardioprotection in two ways; firstly, by translocation to the nucleus where it up-regulates several cardioprotective factors such as Bcl-2 and vascular endothelial growth factor; and secondly, by phosphorylation of GSK-3 $\beta$  to inhibit mPTP (Boengler et al., 2010; Boengler et al., 2013; Meier et al., 2017; Lacerda et al., 2009).

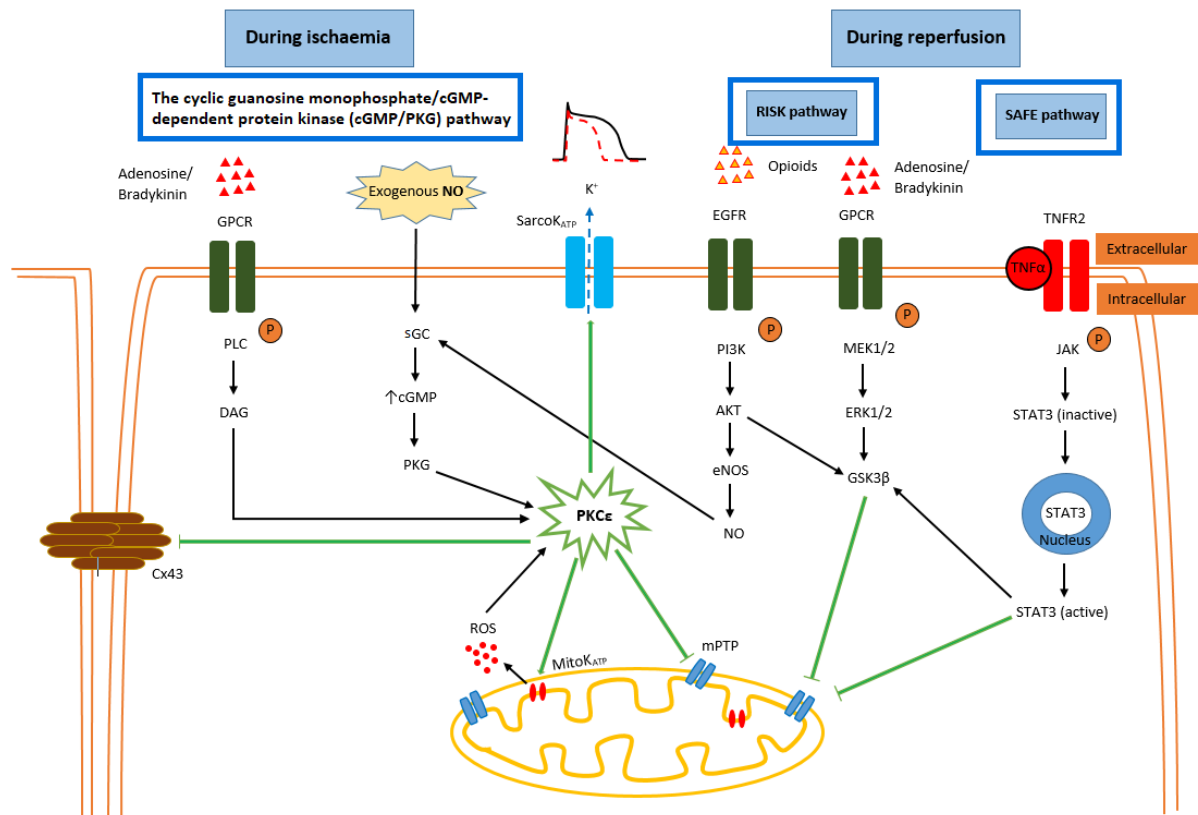


**Figure 1.18:** The early- and late- phase cardioprotective signalling pathways in ischaemic conditioning.

There are several signalling pathways which are involved to impart protection against ischaemia/reperfusion injury, including the cyclic guanosine monophosphate/cGMP-dependent protein kinase (cGMP/PKG) pathway, the reperfusion injury salvage kinase (RISK) pathway, and the survivor activating factor enhancement (SAFE) pathway. Cardioprotective factors activated during the early phase (several hours) are a group of small molecules from injured cells in response to myocardial ischaemia. These factors include, adenosine, opioids, and bradykinin which act on G-protein coupled receptors (GPCR) to activate protein kinase C-epsilon (PKC $\epsilon$ ). cGMP-dependent protein kinases (PKG) also phosphorylates at the early phase post myocardial ischaemia, which interacts with PKC $\epsilon$  to impart cardioprotection. Cardioprotective factors activated during the late phase (several days) post

*myocardial ischaemia/or at reperfusion are a group of growth factors and cytokines. These factors include RISK and SAFE pathways. These cardioprotective factors act through GPCR or receptor tyrosine kinases (RTK) to activate the RISK pathway, or through inflammatory cytokines via tumour necrosis factor receptor (TNFR) to activate the SAFE pathway. All of these signalling pathways result in the inhibition of the mitochondrial permeability transition pore (mPTP) which contribute to attenuate the damage from ischaemic and reperfusion injury. (Adapted from (Hausenloy et al., 2016a)).*

## 1.7 Aims and hypotheses

The overall aim of the present study was to examine the effects of direct channel modulators in imparting cardioprotection. By using isolated ventricular myocytes and intact whole-heart, this study will be able to investigate whether direct modulation of cardiac potassium currents using pharmacological treatments induce changes in the cardiac function by increasing repolarising currents and shortening cardiac action potential, and so reducing calcium overload in myocardial ischaemia.

To achieve this goal, the Wistar male rat was used as the primary model. The rat heart, despite the differences with the human heart in the pattern of K<sup>+</sup> channel activation during repolarisation, has remarkably similar cardioprotective signalling to humans (Joukar, 2021; Behzadi et al., 2018). Guinea pig cardiomyocytes have a much more human-like action potential compared to rat, however their coronary circulation is much more branched than in humans. It is therefore, very difficult to record coronary ligation-type data in a guinea pig compared to rat. Cardioprotection has not, therefore, been widely studied in the guinea pig model. Previous studies confirmed that, similar to humans, the heart rhythm and electrical signals changes in rats following various pharmacological treatments such as antidepressant and vasodilators are similar to human (Farraj et al., 2011).

Previous studies reported that the reduction in the electrical excitability to improve Ca<sup>2+</sup> accumulation following ischaemic preconditioning imparts cardioprotection which has been observed as a slightly shortened action potential duration in cardioprotected cells compared to control cells (Murry et al., 1986). So, it has been hypothesised that direct ion channel modulators, particularly that modulating repolarising outward K<sup>+</sup> currents will mimic the

changes seen in electrical activity of cardioprotective stimuli as a mechanism for directly imparting cardioprotection pharmacologically.

Hypotheses:

Activation/potentiation of  $K_{ir}6.1$  containing  $K_{ATP}$  current and/or  $I_{Ks}$  in cardiac cells is cardioprotective by shortening the cardiac action potential to reduce  $Ca^{2+}$  overload and thus could preserve cellular ATP during myocardial ischaemia.

These hypotheses will be examined in the following sections:

- 1- Pharmacological manipulation of cardiac  $K_{ir}6.1$  containing  $K_{ATP}$  modulates action potential duration to impart protection (as investigated in Chapter 3)

Patch clamp cell-attached recording will be used under normal physiological conditions to record the presence of a second  $K_{ATP}$  channel in the cardiac ventricular myocytes, with a  $K_{ir}6.1$ -pore, other than the classical  $K_{ir}6.2/SUR2A$  channel, which may be associated with imparting cardioprotection in the early stages of metabolic stress. Patch clamp whole-cell recording will be used to measure the cardiac action potential and current modulate by appropriate concentrations to pharmacologically activate and block  $K_{ir}6.1$  selectively (such as pinacidil and PNU37883). The effect of modulating  $K_{ir}6.1$  containing  $K_{ATP}$  with pharmacological manipulation on calcium homeostasis will then be investigated. The effectiveness of selective  $K_{ir}6.1$  activator and inhibition as a cardioprotective/cardiotoxic target will be investigated in cellular and whole heart models of ischaemia and reperfusion.

- 2- Pharmacological potentiation of  $I_{Ks}$  modulates the cardiac action potential (as shown in Chapter 3)

In this section of work, initial characterisation will involve pharmacological activation and inhibition of  $I_{Ks}$ , such ML277 and JNJ303, to record action potential shortening/prolongation using patch clamp whole-cell recording. The modulation of  $I_{Ks}$  on currents and calcium homeostasis will also be investigated.

- 3- Pharmacological potentiation of  $I_{Ks}$  imparts cardioprotection (as examined in Chapter 4)

To investigate the cardioprotective effects of  $I_{Ks}$  potentiation, pharmacological activation of the current, such as ML277, will be used to assess to the cellular measures of cardioprotection whilst blocker, such as JNJ303, could abolish it. The effect of selective  $I_{Ks}$  potentiation on infarct size will be assessed in a whole heart *ex vivo* coronary ligation and reperfusion model. This study will be the first to selectively activate this current to impart pharmacological cardioprotection against myocardial ischaemia/reperfusion injury.

## Chapter 2 General methods

### 2.1 Solutions

Isolated cardiomyocytes were maintained at room temperature in 2 mmol/L Ca<sup>2+</sup> Tyrode's solution (2 CaT). The Tyrode's solution was comprised of, in mmol/L, 135 NaCl, 5 KCl, 0.33 NaH<sub>2</sub>PO<sub>4</sub>, 10 N-[2-hydroxyethyl]piperazine-N'-[2-ethanesulphonic acid] (HEPES), 5 Glucose, 15 Mannitol, 5 Na pyruvate, 2 CaCl<sub>2</sub>, and 1 MgCl<sub>2</sub>, at pH of 7.4 using NaOH. During cell isolation, a nominally Ca<sup>2+</sup> free Tyrode's solution (0-CaT) was used that was similar to 2CaT, however with no added CaCl<sub>2</sub> and 0.6 mM EGTA added to the solution. Substrate-free metabolic inhibition Tyrode's solution (SFT-MI) was used as part of a metabolic inhibition solution. This solution contained, in mmol/L, 140 NaCl, 5 KCl, 0.33 NaH<sub>2</sub>PO<sub>4</sub>, 10 HEPES, 20 Sucrose, 1 MgCl<sub>2</sub>, 2 CaCl<sub>2</sub>, pH to 7.4 with NaOH. Metabolic inhibition was used to simulate ischaemia (Brennan et al., 2015; Rainbow et al., 2004). To achieve this, 2 mM cyanide and 1 mM iodoacetic acid was added to SFT-MI solution on the day of the experiment. Sodium cyanide is responsible for blocking ATP synthesis at the level of oxidative phosphorylation and iodoacetic acid inhibits glycolysis (by inhibition of GAPDH) (Wink, 2010).

### 2.2 Isolation of cardiomyocytes

Adult male Wistar rats were used between 300 to 400 g. Animals were killed by concussion and cervical dislocation in accordance with the UK Animals (Scientific Procedures) Act 1986. To excise the heart, an extended midline surgical incision was performed toward the abdominal surface to expose the ribcage. A cut was made along the diaphragm and then along the ribs to expose the heart. The heart was then cut out and placed immediately in Ca<sup>2+</sup> free Tyrode's solution. The heart was cannulated via the ascending aorta to perfuse the heart in retrograde fashion on a Langendorff-type apparatus, using the aortic valve to push solution into the coronary circulation (Figure 2.1). The heart was perfused at 37°C at a rate of 8.5 ml/min. Initially, the heart was perfused with 0-CaT solution for ~6 min to clear the blood and to prevent contractions. A 3F polypropylene catheter (Portex, Kent, UK) was inserted in the left atrium to the apical part of the left ventricle, allowing drainage to limit pressure build-up. The solution was exchanged with enzyme mix in 0-CaT solution 0.5 mg/ml collagenase type II

(Sigma), 1.66 mg/ml BSA from factor V albumin and 0.6 mg/ml protease (type XIV 15 % Ca<sup>2+</sup>) for 7-15 min. Good enzymatic perfusion was indicated by swelling of the heart and an increasing viscosity of the perfusate. Typically, the enzymatic solution was perfused for 4 or 8 minutes depending on the cardiac size and quality of the perfusion through the heart. On the appearance of rod-shaped cardiomyocytes in the perfusate, the solution was switched back to 0CaT for 3 minutes. The heart was then cut into several pieces to increase the surface area, and the solution exchanged for 2CaT solution. This solution was discarded, and the tissue placed into a conical flask with fresh 2CaT solution, the flask transferred to a shaking water bath at 37°C in order to disperse the cardiac cells. After 5 minutes, the cell suspension was decanted to a fresh flask, and fresh 2CaT solution was added to the residual tissue. This process was repeated until the tissue was completely dispersed. The cell suspension was filtered, and placed into 15 ml Falcon™ tubes for 10-15 minutes, allowing living cells to separate from dead cells by depositing at the bottom of the tubes. The supernatant containing dead cells was removed. This wash was repeated by adding 5-10ml of NT and left for 10 minutes, and resuspended cells were transferred to dishes with 5-10ml of NT. This protocol yielded around 70% rod-shaped cells, these were stored at room temperature and used on the day of isolation.

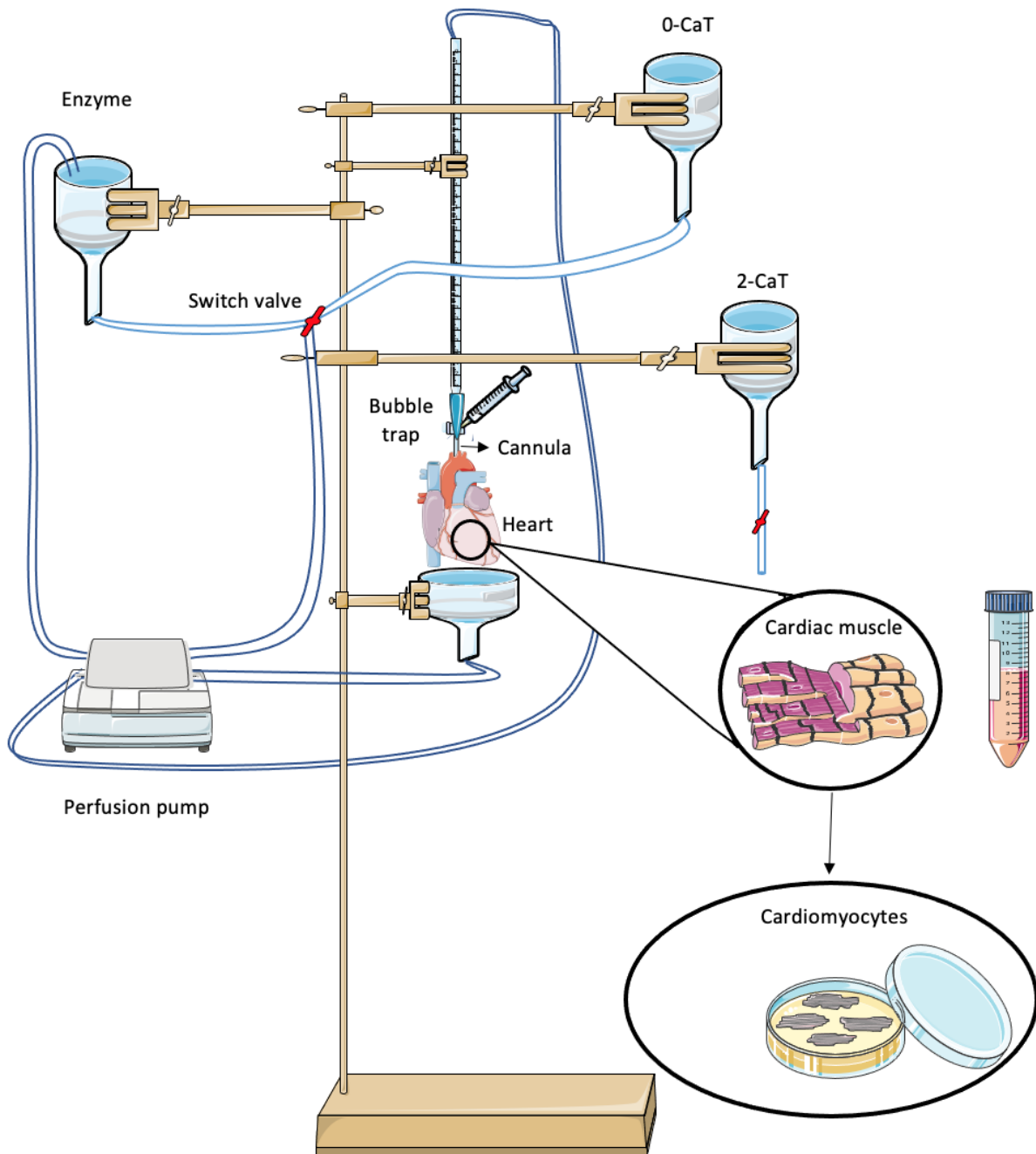


Figure 2.1: Diagram to demonstrate the Langendorff perfusion mode for enzymatic isolation of ventricular myocytes.

*The Langendorff apparatus was used for the collection of cells from the tissue. A fully digested heart was removed from the Langendorff apparatus and then transferred into a Falcon tube to be dissociated in a shaking water bath, allowing the cardiomyocytes to be released from the tissue. Following isolation, cardiomyocytes were stored in dish containing NT solution at room temperature (using smart servier medical art, <https://smart.servier.com/>).*

## 2.3 Patch clamp electrophysiology

The patch clamp technique allows us to measure the membrane potential or the membrane currents (Figure 2.2) (Neher and Sakmann, 1976). This is achieved by using an electrolyte-filled micropipette that can be used to record currents on the surface of the cell (cell-attached patch), from the whole cell (the whole cell configuration) or from an isolated patch of membrane (excised patch). All of these configurations have in common a micropipette formed from a glass capillary with a tip diameter about 1  $\mu\text{m}$ . Micropipettes were pulled from thick-walled borosilicate filamented glass (Narishige PC-10, Japan) in a 2-step process. The microelectrodes were filled (approximately 1/3<sup>rd</sup>) with a pipette solution appropriate to the experiment being carried out. For whole cell recording the pipette solution approximates the intracellular environment, and in the experiments described here contained, in mM, 140 KCl, 5 EGTA, 10 HEPES, 1 MgCl<sub>2</sub>, 0.61 CaCl<sub>2</sub> (20 nM free Ca<sup>2+</sup>, calculated using Webmaxchelator), 1 ATP, 0.1 ADP and 0.1 GTP, KOH was used to titrate pH to 7.4. Extracellular perfusion in these experiments was achieved using the standard 2 mM Ca<sup>2+</sup> Tyrode's solution, outlined in section 2.1. These solutions give an E<sub>K</sub> of ~-88 mV (assuming 140 mM intracellular K<sup>+</sup> ([K<sup>+</sup>]<sub>i</sub>)), an E<sub>Na</sub> of ~63 mV (assuming 12 mM [Na<sup>+</sup>]<sub>i</sub>), and an E<sub>Ca</sub> of ~130 mV (assuming 100 nM [Ca<sup>2+</sup>]<sub>i</sub>). For cell-attached patch recording the solution does not come into contact with the intracellular solution. The potassium concentration for the pipette solution was 140 mM, to ensure that the E<sub>K</sub> for the experiment was ~0 mV. The cell-attached solution contained, in mM, 140 KCl, 5 HEPES, 2 CaCl<sub>2</sub>, 1 MgCl<sub>2</sub>, and KOH was used to titrate pH to 7.4.

The recording electrode was formed from a silver/silver chloride wire in the patch pipette, whilst the circuit is completed with a Silver/Silver chloride bath electrode. Recordings were made using an Axopatch 200B amplifier (Scientifica, UK), with the signal from amplifier digitised using a DigiData 1550 (Scientifica, UK). Data was recorded to computer using pCLAMP10 software (Scientifica, UK). The electrode was positioned using a Siskiyou micromanipulator (Siskiyou, Japan). Cardiomyocyte (~50  $\mu\text{l}$  of cell suspension) was placed into a heated perfusion chamber (HW-30, Dagan Corp, USA) for ~10 minutes prior to experimentation to adhere to the glass coverslip. Cells were perfused at a rate of ~5 ml/min at 30-32°C. With the Dagan HW-30 perfusion system, temperatures of 37 °C caused a number of bubbles to form within the perfusion chamber, which would knock cells during patch-clamp

recording. This did not happen when the temperature was reduced to 30 - 32°C (Rainbow et al., 2004)(Rainbow et al., 2004).

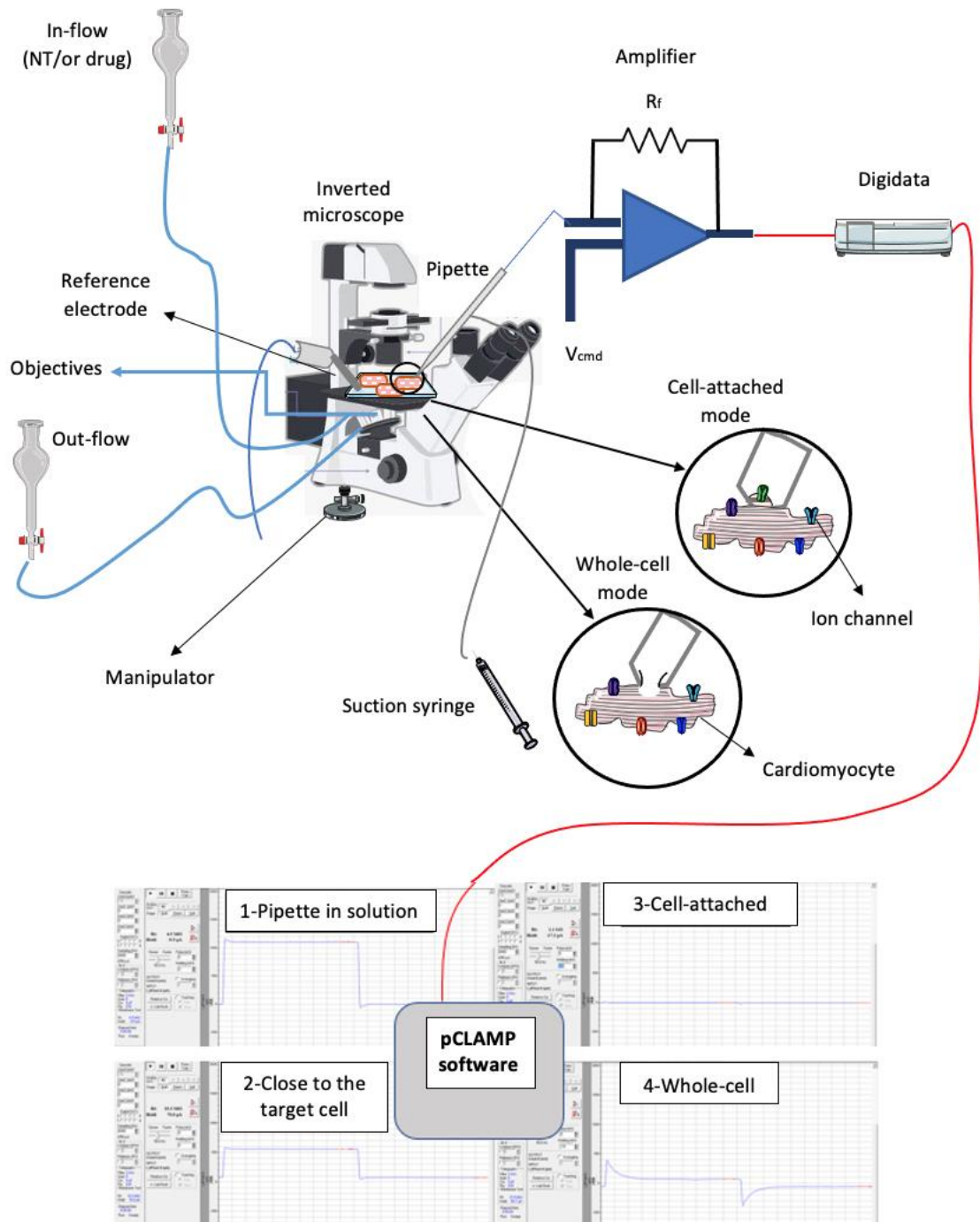


**Figure 2.2:** Diagram to illustrate the arrangement of instruments that were used for patch clamp recording.

*Figure showing the outline of the patch-clamp apparatus used in this study. Firstly, the patch-clamp amplifier, connected to the digitizer interface, is connected to the computer to record the signals. The patch clamp amplifier is then connected via the patch pipette to the cells mounted in the microscope. The cells are perfused within the perfusion chamber mounted on the microscope. pCLAMP software which provides a membrane test window to detect the quality of the seal. Briefly, a square pulse reflected that the pipette position in the solution bath (1), the square pulse getting smaller (2) indicated that the electrode down on to the cell which increases the electrical resistance, A near flat line represented a good seal and is termed as cell-attached configuration (3), the appearance of significant charge and discharge capacitance spikes (4) with additional syringe suction reflected that the whole-cell access has been achieved (using smart servier medical art, <https://smart.servier.com/>).*

### 2.3.1 Cell attached patch recording

In the cell attached configuration, the patch electrode is pushed up to the cell membrane and a tight electrical seal between the pipette and the cell membrane is made. A “good” seal is recorded in the  $G\Omega$  range and this cell-attached patch is the starting point for all patch clamp configurations. In this project, the cell-attached configuration was also used to record  $K_{ir}6.1$  and  $K_{ir}6.2$  channel activity in cardiomyocytes. Having achieved a  $G\Omega$  seal, the patch electrode was held at +40 mV. In the cell attached recording mode, the patch electrode does not control the whole membrane, and so only the patch of membrane in the tip of the electrode is controlled. The holding potential across the patch of membrane is the sum of the whole cell resting membrane potential and the pipette potential. With a holding potential of +40 mV, the inside of the cell is -40 mV, plus an assumed membrane potential of ~-70 to -80 mV means that the holding potential on the patch of membrane is ~-110 to -120 mV. At this negative potential there should be limited activity of any voltage-gated currents. Kir current, however, will be active at these potentials and can be distinguished by their conductance.  $K_{ir}6.1$  has a conductance of ~40 pS,  $K_{ir}6.2$  ~80 pS and  $K_{ir}2.x$  ~20-30 pS (Bao et al., 2011; Isomoto et al., 1996; Repunte et al., 1999; Roepert, 2001).

### 2.3.2 Whole cell recording of currents

From a  $G\Omega$  seal in the cell-attached configuration, other recording modes are derived by disruption of the cell membrane in the patch pipette to obtain the whole cell configuration

where the pipette solution and cytoplasm are continuous. Once the pipette solution and the intracellular solution are continuous then the membrane potential of cell can be recorded, or controlled, via the patch pipette. To record currents, the membrane of the cell is controlled, often in a series of voltage steps to activate voltage-gated currents, and the currents recorded to computer.

The interaction of electrode and the interior solution of the cell causes resistance of the recording electrode in series with the cell membrane which introduces voltage errors and unwanted filtering. This electric resistance is named as a series resistance. To minimise this issue, the amplifier can compensate for the series resistance to obtain a correction of the sum of all the resistances between the membrane resistance and the electrode resistance. The voltage error is caused when there is any current flowing through the electric resistance and therefore, the pipette voltage will be not equal to the actual membrane voltage. This difference can be minimised by making the input resistance as low as possible to increase the peak capacity current and improves the recording of the membrane potential to be closer to the voltage at the patch pipette, as predicted by Ohm's law ( $v = \frac{I}{R}$ ). The electrodes had resistances of 3-6 M $\Omega$  when the conductive pathway develops between the electrodes filled with internal solution and the cell (Hamill et al., 1981; Rainbow et al., 2005). The unwanted filtering is caused when there is insufficient current to charge the membrane voltage and is mainly established on large cells. To minimise this error, the capacitance of the cell membrane should be considered by adding a voltage pulse to correct for the membrane capacitance. Using the membrane test function in pCLAMP, the values given were entered into the amplifier to ensure that the capacitance compensation was as good as possible. Changes in the capacitance spike during the recordings, or broadening of the sodium current, were used to signify a degrading whole cell recording.

### 2.3.3 Action potential recording

Once the whole cell configuration has been achieved, the current or the membrane potential can be recorded in voltage- or current-clamp respectively. Action potentials were recorded from cells stimulated at 1 Hz using a 5 ms current pulse via the patch pipette. The depolarising stimulus was set for each cell at 130% of the level required to trigger an action potential.

## 2.4 Metabolic inhibition and reperfusion (MI/R) model and contractile function measurements

A metabolic inhibition and washout protocol was used to investigate the effects of pharmacological treatments on freshly isolated cardiomyocytes (Figure 2.3). This technique enables the contractile function of the cells to be monitored throughout the simulated ischaemia and reperfusion. Ischaemia was simulated in cardiomyocytes chemically with iodoacetic acid and cyanide, as described in section 2.1 which inhibit glycolysis and oxidative phosphorylation. These chemicals were added to substrate free Tyrode's (SFT) solution, creating a metabolic inhibition solution (SFT-MI). Cardiomyocytes were then perfused with NT solution containing glucose and pyruvate which is simulated a reperfusion condition. This protocol was used as a screening method to determine whether the cells had been cardioprotected during pharmacological treatment.

Firstly, isolated cardiomyocytes were placed into a heated perfusion chamber and allowed to adhere to the glass coverslip in the chamber for 10 minutes prior to experimentation. Cells were perfused with NT solution using a Gilson Evolution Peristaltic pump at rate of 5 ml/min with the temperature controlled using a Heatwave-30 system (Dagan Corp, USA) at 30-32°C. Cells were stimulated to contract at 1 Hz, using electric field stimulation (EFS) (Digitimer, Stimulator DS92, UK). Isolated cardiomyocytes that contract in the time with the electric field stimulation were captured by a JVC CCD camera and recorded to DVD for offline analysis.

In this

The metabolic inhibition and washout protocol consisted of 3 min of perfusion with NT, 7 min with SFT-MI solution to mimic ischaemia followed by 10 min of washout to simulate reperfusion. At the end of reperfusion, these cells were stained with 50 µl of Trypan blue, where staining with Trypan blue is an indicator of cell death.

At the end of the experiment, the contractile function of cells was visualised via JVC CCTV camera. Cardiomyocytes which showed contractile function synchronous with electric field

stimulation following reperfusion were identified as recovered cells and then the percentage of contractile recovery and also the percentage of cell survival identifying by Trypan blue were compared in the absence and presence of pharmacological treatments. Several parameters were recorded including, 1) the time to contractile failure in metabolic inhibition, 2) the time to rigor contracture, 3) the time to hypercontracture and 4) the time to contractile recovery in reperfusion. The field of view obtained from each stage was recorded onto DVD for later analysis. Analysis was then carried out using Microsoft Excel and GraphPad Prism 7.

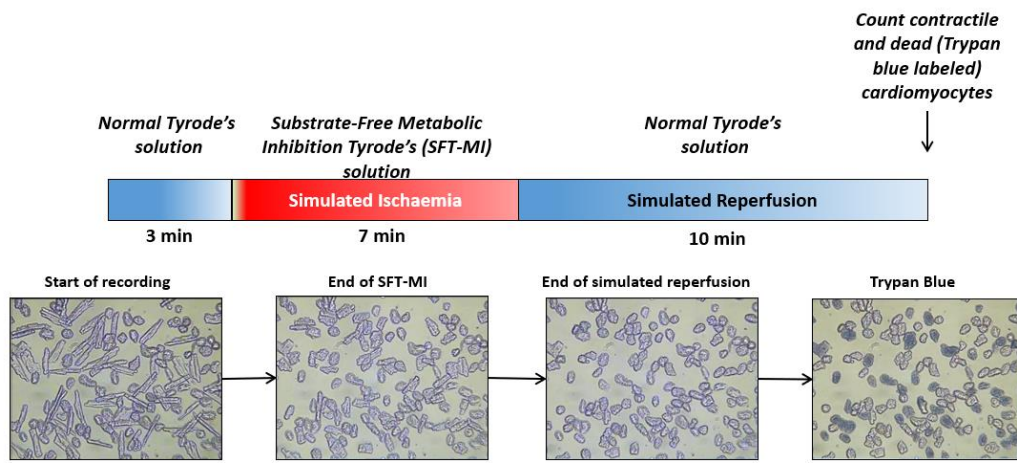


**Figure 2.3:** The metabolic inhibition and washout protocol was used to simulate ischaemia and reperfusion.

*The images show the morphology of cardiomyocytes at different stages of this protocol. At the beginning of the recording, cardiomyocytes in the NT solution appear rod-shaped. At the end of SFT-MI, cardiomyocytes start lose contractile activity and then enter a state of rigor contracture due to ATP depletion. At the end of reperfusion, cardiomyocytes may recover their contractile function however, some cells can enter a state of hypercontracture due to overload of calcium (can be seen to shorten further with further reduction in the length to width ratio). When hypercontracture occurs, membranes often bleb and rupture, therefore, allowing Trypan blue to stain dead cells.*

## 2.5 Fluorescence imaging

To examine the effects of ion channel modulation on cardiac cell function, a fluorescent indicator was used, Fura-2-AM. In this study, fluorescent imaging was used to measure changes in calcium during the use of specific pharmacological inhibitors and activators.

### 2.5.1 Calcium measurements

Fura-2-AM, which is in an acetoxyethyl (AM) ester form, was used to measure changes in intracellular  $\text{Ca}^{2+}$  and changes in  $\text{Ca}^{2+}$  transients after perfusion with pharmacological treatments. This dye is ratiometric where recordings were achieved by using excitation wavelengths of 340 nanometres (nm) ( $\text{Ca}^{2+}$  bound)/ 380 nm ( $\text{Ca}^{2+}$  free) and emission signals collected at wavelengths greater than 520 nm. An advantage of Fura-2 for cardiac cells is that during contraction, both excitation signals of Fura-2-AM would change simultaneously, therefore minimising movement artefacts due to the fact that data is expressed as a ratio of 340 and 380 nm excitations signals. Similarly, given prolonged excitation, there may be photo bleaching of the indicator, however both excitation signals would decay at the same rate and therefore the ratio would remain constant. The indicator crosses the sarcolemmal membrane of cardiomyocytes via the ester group, which is cleaved to form a free indicator. Once inside the cytoplasm, the free Fura-2 then binds to calcium ions, giving a change in the fluorescent molecule that can be detected using imaging methods.

Fura-2-AM was stored in 50  $\mu\text{L}$  dimethyl sulfoxide (DMSO) at 4°C. 0.5 mL of cardiomyocytes was diluted in 0.5 mL of Tyrode's solution, and this 1 mL suspension was incubated with 5  $\mu\text{L}$  of Fura-2-AM. The cardiomyocytes were placed into black microtubes for 20 minutes to fully load the dye. Fura-2-loaded myocytes were transferred to a glass coverslip and left to settle for 10 minutes. Isolated myocytes were perfused at a rate of 5 mL/min and then stimulated at 1 Hz. The field of view was visualised using a 20x objective with a Nikon (Eclipse TE200) inverted microscope. Myocytes were excited, using a DeltaRAM X monochromator controlled by Winfluor software (John Dempster, University of Strathclyde). In order to improve the acquisition rate of calcium transients, the exposure time was maintained at low level as possible, for 20 ms. Emission signals were captured to a Roper Cascade 512 B CCD camera (Photometrics, Arizona, USA) and using a 79001 – ET – Fura 2 Filter (Chroma Technology Corp, Vermont, USA). Images were analysed with Winfluor 4.0.2 software (Dr John Dempster, University of Strathclyde, Glasgow, UK) by drawing regions of interest around the contracting cells in response to electrical field stimulation. An average of 10 calcium transients were used in each cell to differentiate between the control and pharmacological treatment conditions.

## 2.6 Langendorff experimental protocol

A Langendorff perfused heart model was used to assess the effective treatments on the ischaemia-reperfusion injury. In this model, ischaemia was induced by ligating left anterior descending (LAD) coronary artery. Reperfusion was mediated by returning coronary blood flow into the region at risk by releasing the ligature. The infarct size following reperfusion was used as a targeted end point to evaluate the effects of the pharmacological treatments on the whole heart.

In this protocol, excised hearts were quickly cannulated via the aorta and then held in place via secured sutures prior to removal of the temporary holding clip, after sacrificing the animals via concussion and cervical dislocation (section 2.2). The hearts were retrogradely perfused with NT solution and submerged in a water jacket with NT solution that was warmed to 37°C to maintain normothermic conditions throughout the experiment. The hearts were equilibrated for 1 hour and perfused via the aorta at a rate of 8.5 mL/min with NT solution (Figure 2.4A). A curved needle with a 5-0 suture (USP, 1.0 metric) was inserted behind the left anterior descending coronary artery (Figure 2.4B). The ends of the thread were twisted together and then inserted into a cut yellow (200 µl) tip with a second tip inside which could be pushed together against the heart to temporarily occlude the blood vessels. This coronary ligation was maintained for 40 minutes to induce regional ischaemic damage. The ligature was released from yellow tips to allow the perfusion of the NT solution for 3 hours, which was used to simulate coronary reperfusion. At the end of reperfusion, the ends of the suture were tightened to mediate coronary re-occlusion. The perfusion pump was then stopped, and 1-2 mL of Evans blue (0.5 g in 20 mL Tyrode's solution) was injected into the heart via the syringe attached to the bubble trap to differentiate between the normally perfused myocardium and the area affected by ischaemia. The Evans dye coloured the non-affected zone dark blue, whereas, the area at risk zone remained pale pink because the dye does not perfuse into this area. The heart was then cut and frozen for 1-2 hours and subsequently sliced into several thin sections and placed into a 40 ml phosphate buffered solution containing 400 mg triphenyltetrazolium chloride (TTC) for 20 minutes in a shaking bath, which allows to distinguish between the infarct tissues and living tissues of area at risk. This buffer solution was made by combining 30 mL of Na<sub>2</sub>HPO<sub>4</sub> (0.1 M stock) and 10 mL NaH<sub>2</sub>PO<sub>4</sub> (0.1 M stock) at

pH 7.4 using NaH<sub>2</sub>PO<sub>4</sub> and warming the solution to 37°C. The TTC dye coloured the viable tissues in the area at risk red because the dehydrogenase enzymes in living tissues react with TTC, while the infarct tissue in the area at risk remains white (Figure 2.4C) (Bell et al., 2011). Heart slices were individually weighted, placed between two cover slips and scanned with 1200 dpi resolution. Image J software (National Institutes of Health) was used to quantify the areas for each cardiac section on both sides, allowing the infarct size and the area at risk to be calculated. The final results were obtained as a percentage of area at risk and a percentage of infarct size. To minimise the risk of detection of bias, the images were analysed by three researchers, including the experimenter. The experimenter provided the two additional researchers with the images in a blinded manner so they did not know the experimental conditions. The mean of the three analyses were used to give a single infarct size for each heart slice.

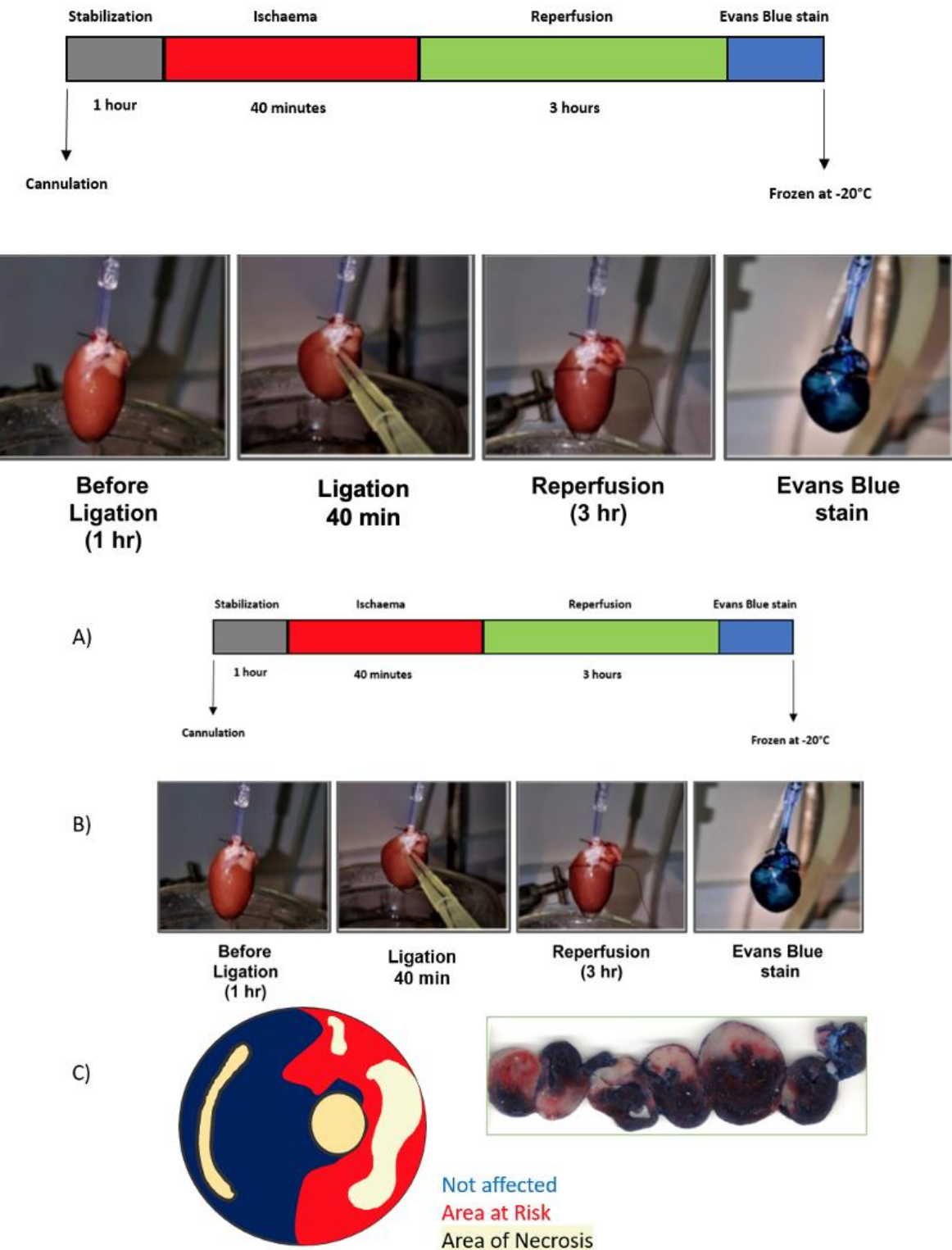


Figure 2.4: A Langendorff experimental model of ex vivo coronary ligation.

*A, Protocol designed to simulate myocardial ischaemia and reperfusion injury: isolated hearts were cannulated, stabilised for 1 hr with NT perfusion, ligated for the LAD coronary artery for 40 min to induce a regional ischaemia, and un-ligated for the coronary artery with NT perfusion for 3 hr to simulate reperfusion period. B, Representative single rat heart mounted in the Langendorff apparatus. Before the coronary artery ligation, heart was stabilised for 1 hr. Then the LAD was surrounded by the suture which is secured in place via two yellow tips. For coronary artery reperfusion, the yellow tips*

were removed to release the ligation. In the end of the reperfusion period, rat heart was injected with Evans blue. C, Representative image of slice hearts stained and presented different colour, containing blue region (unaffected area), red region (area at risk), white region (Necrosis area), and right- (RV) and left- (LV) ventricular holes. Representative heart slices of stained heart on the coverslip. (Adapted from (Brennan et al 2019)).

## 2.7 Statistical analysis

All electrophysiological data were recorded and analyzed by using pClamp10 (Axon Instruments) software and Excel 2019 software. Calcium fluorescence data were analysed using Winfluor4.1.1 software (Dr John Dempster, University of Strathclyde) and Excel 2019. Figures and statistical analysis were completed in GraphPad Prism 9 software (GraphPad Software, Inc., La Jolla, CA, 123 USA). Statistical significance was analysed using the paired t-test (for two groups), unpaired t-test and one-way ANOVA with Holm-Sidak post-test (for multiple comparisons versus control condition). A p-value of  $p<0.05$  was classified as statistically significant. The statistical tests used are identified in the figure legend for each dataset. These experimental data are reported as mean  $\pm$  standard error of mean (S.E.M).

# Chapter 3 The cardioprotective role of $I_{KATP}$ activation

## 3.1 Introduction

As described in the introduction, under normal physiological conditions,  $K_{ATP}$  channels remain closed, blocked by normal physiological ATP levels, but are opened during severe ATP depletion under ischaemic conditions to limit cardiac damage. Canonical cardiac  $K_{ATP}$  channels are composed of four  $K_{ir}6.x$  subunits and four SURx subunits, which form functional channels. Of these subunits,  $K_{ir}6.1$  and  $K_{ir}6.2$ , as well as SUR1, SUR2A and SUR2B are all found in different cell types in the heart in various combinations to form  $K_{ATP}$  channels (Inagaki et al., 1996; Miki et al., 2002; Morrissey et al., 2005b; Morrissey et al., 2005a). Previous research has documented how the major constituents of ventricular sarcolemmal  $K_{ATP}$  channels are  $K_{ir}6.2$  and SUR2A subunits in various mammalian species, including mouse, rat, guinea pig, and human hearts (Morrissey et al., 2005b; Fedorov et al., 2011). However, co-assembly of  $K_{ir}6.2$  and SUR1 generates atrial sarcolemmal  $K_{ATP}$  channels (Glukhov et al., 2010). In the heart, the activation of  $K_{ir}6.2/SUR2A$  channels plays a vital role during severe metabolic depression in ischaemia, which leads to an increase of  $K^+$  efflux (Fujita and Kurachi, 2000). Consequently, this hyperpolarises the membrane potential, and it also shortens the duration of the cardiac action potential, which allows for the reduction of ATP consumption and  $Ca^{2+}$  accumulation.

The initial opening of cardiac  $K_{ATP}$  channels in response to a severe metabolic insult is cardioprotective. Consistently, pre-clinical studies show that intrinsic cardioprotective stimuli in response to preconditioning bursts of ischaemia prior to sustained ischaemia can also protect the heart under physiological conditions via an energy-saving mechanism (Murry et al., 1986; Kitakaze, 2010; Brennan et al., 2015). The results of these pre-clinical studies provide an exciting opportunity to investigate our hypothesis that reducing  $Ca^{2+}$  accumulation to preserve intracellular ATP could be a protective mechanism. Our group has carried out studies that suggest that this preservation of ATP and  $Ca^{2+}$  homeostasis would be unlikely due to  $K_{ir}6.2/SUR2A$  channel activation as might be expected. Recent results suggest that the time to activation of  $K_{ir}6.2/SUR2A$  channels is delayed following cardioprotective stimuli, which indicates that canonical  $K_{ir}6.2/SUR2A$  channels do not impart protection in the early stages of metabolic inhibition (Brennan et al., 2015). This feature led us to think of the  $K_{ir}6.2/SUR2A$

channels as a metabolic sensor rather than cardioprotective effector. The complication with this hypothesis stems from the findings that  $K_{ATP}$  channel openers have a cardioprotective effect, but don't seem to open this channel. Recently, our group have identified that there is a second  $K_{ATP}$  channel in the cardiac ventricular myocytes, with a  $K_{ir}6.1$ -pore. Therefore, the hypothesis tested in the present study is that this newly identified  $K_{ATP}$  channel, other than the classical  $K_{ir}6.2/SUR2A$  channel, may be associated with imparting cardioprotection in the early stages of metabolic stress.

Numerous studies have reported that  $K_{ir}6.1$ -containing  $K_{ATP}$  channels and SUR2B are predominantly expressed in vascular smooth muscles (Wang et al., 2003; Teramoto, 2006). However, research has been conducted on the expression of  $K_{ir}6.1$  subunit in cardiomyocytes (Singh et al., 2003; van Bever et al., 2004; Pu et al., 2008). The SUR2B subunit, which is mainly expressed in vascular smooth muscle cells, has also been found in cardiomyocytes (Singh et al., 2003; Morrissey et al., 2005a; Jovanović et al., 2016). Interestingly,  $K_{ir}6.1$  null mice are prone to cardiovascular disorders, such as sudden infant death syndrome, electrocardiographic J wave syndrome, and hypercontractility of coronary arteries (Miki et al., 2002; Tester et al., 2011; Nichols et al., 2013). This indicates a potential mechanism of  $K_{ir}6.1$ -containing channels in regulating cardiomyocyte function and the need to understand whether the opening of  $K_{ir}6.1$ -containing channels participates in controlling cardiac function in physiological resting conditions and cardioprotection.

It was hypothesised that  $K_{ir}6.1$ -containing channels expressed at the cardiomyocyte membrane surface remained open in normal physiological conditions.  $K_{ir}6.1$  in vascular smooth muscle shows constitutive activity with limited ATP sensitivity. The activity of this newly identified cardiac  $K_{ATP}$  channel was hypothesised to follow the properties in the vasculature, showing relatively insensitive to ATP depletion and may contribute to protecting the heart in the early stages of myocardial ischaemia. The protective role of these new  $K_{ATP}$  channels would be similar to canonical  $K_{ir}6.2/SUR2A$  channels via hyperpolarising the membrane potential and shortening the cardiac action potential duration to preserve the intracellular ATP and reduce calcium overload. Consequently, pharmacological shortening of the cardiac action potential duration via targeting this newly identified channel could reduce the damage from acute myocardial ischaemia.

In this chapter, pinacidil, a vascular  $K_{ATP}$  channel activator with well characterised effects in the vasculature, was tried to see whether it has a similar cardiac effect using both isolated ventricular cardiomyocytes and a whole heart model. In vascular smooth muscle cells, pinacidil is known to cause a relaxation of vascular smooth muscle due to pinacidil is associated with the opening of smooth muscle  $K^+$  channels (Bray et al., 1987). We proposed that pinacidil would have a similar  $K_{ATP}$  channel activating effect in cardiac cells, increasing  $K^+$  efflux, shortening the action potential duration and hence reducing  $Ca^{2+}$  entry. It is hypothesised that this action, if present, would be cardioprotective. Previous studies indicate that pinacidil was shown to open  $K_{ATP}$ -like channels at a concentration of 30 and 100  $\mu M$  (Satoh et al., 1998; Suzuki et al., 2001; Lodwick et al., 2014), so these concentrations were used to test its functionality on cardiac cells. In this study, the focus of attention was on  $K_{ir}6.1$  containing  $K_{ATP}$  channels, and therefore 10  $\mu M$ , 30  $\mu M$  and 50  $\mu M$  pinacidil were attended to use to activate  $K_{ir}6.1$  selectively. However, pinacidil at a concentration of 150  $\mu M$  and 200  $\mu M$  caused the activation of  $K_{ir}6.2$  containing  $K_{ATP}$  channels and was used to explore the efficacy of the canonical  $K_{ir}6.2/SUR2A$  opener in myocardial ischaemia compared to the newly identified channel containing  $K_{ir}6.1$  pore-forming subunits. First, to test the hypothesis that a different  $K^+$  channel other than the classical  $K_{ir}6.2/SUR2A$  channel opens in normal physiological conditions, we used cell-attached patch recording. To further investigate this, the patch clamp technique was used to assess 1) whether pinacidil shortens the action potential duration, 2) whether pinacidil increases  $K^+$  efflux, and 3) whether pinacidil improved calcium handling via measuring calcium transients.

PNU is a known vascular  $K_{ATP}$  channel blocker. It selectively blocks the pore of the vascular  $K_{ATP}$  channel ( $K_{ir}6.1/SUR2B$ ), resulting in depolarisation of vascular smooth muscle cell action potential (Humphrey et al., 1996). Previous electrophysiological experiments showed that PNU at a concentration up to 3  $\mu M$  had no significant effect on classical  $K_{ir}6.2/SUR2A$  channel, whereas the same concentration was sufficient to block the current carried by  $K_{ir}6.1$  containing  $K_{ATP}$  channels and was considered to be the half inhibition constant for PNU treatment (Meisheri et al., 1993; Khan et al., 1997; Cui et al., 2003; Kovalev et al., 2004) (Wellman et al., 1999). Moreover, PNU at a concentration of 10  $\mu M$  was shown to inhibit vascular  $K_{ir}6.1$  containing  $K_{ATP}$  current while having a little effect on the  $K_{ir}6.2/SUR2B$  (Kovalev

et al., 2004). The same study used PNU at a concentration of 3  $\mu$ M which still showed Kir6.1 containing  $K_{ATP}$  channels blocking effect. So, similar to testing pinacidil as a cardiac  $K_{ATP}$  channel opener, we examined PNU at the concentrations mentioned above as a cardiac Kir6.1 containing  $K_{ATP}$  blocker which could increase the action potential duration and  $Ca^{2+}$  influx and thus has deleterious cardiac effects. In this chapter, we tested whether 1) PNU prolongs action potential duration, 2) PNU reduces  $K^+$  efflux in rat cardiomyocytes, 3) Kir6.1 subunit is a component of classical Kir channels ( $I_{K1}$ ), and 4) PNU increases calcium accumulation.

In this chapter, we also tested the cardioprotective role of  $K_{ATP}$  channel activators and blockers, which were applied using a simulated ischaemia and reperfusion protocol and a whole-heart *ex vivo* coronary ligation model. In the simulated ischaemia and reperfusion protocol, the contractile function was assessed as the endpoint to investigate whether these pharmacological treatments had any effect on cellular injury in isolated myocytes. Further, a whole-heart *ex vivo* coronary ligation experiment was used to investigate the same cardioprotection with Kir6.1 subunit activation and cardiac damage via the inhibition of Kir6.1-containing channels. These experiments may identify the effect of direct modulating of the newly identified channel containing Kir6.1 pore-forming subunits and therefore provide insight into their effect on infarct size.

## 3.2 Results

### 3.2.1 Identification of a channel with a current with amplitude half of that compared to the Kir6.2/SUR2A cardiac $K_{ATP}$ current

Many studies have been published on the activity of  $K_{ATP}$  channel on the surface of ventricular myocytes (Inagaki et al., 1995a; Inagaki et al., 1995b; Noma, 1983; Babenko et al., 1998; Brennan et al., 2015). These studies reported that during metabolic inhibition, the canonical Kir6.2-containing channel is activated with a large conductance current of approximately 79 pS. Kir6.2/SUR2A  $K_{ATP}$  channels do not open under normal physiological conditions, as it requires an ATP-depletion to less than 100  $\mu$ M to start to see channel openings (Lodwick et al., 2014). This channel, therefore, acts as an ATP sensor; stimuli that slow ATP depletion also slow the time to activation of this metabolically-sensitive current. Metabolic inhibition activates the Kir6.2/SUR2A channel complex in every cell, with the timing of the activation

dependent on the ability of the cell to regulate its ATP consumption. The opening of the cardiac  $K_{ATP}$  ( $K_{ir}6.2/SUR2A$ ) channel in cardioprotected cells is markedly delayed following ischaemic preconditioning, which suggests that this channel does not impart protection in the early stages of metabolic inhibition and is only activated at severe ATP depletion to prevent calcium overload (Brennan et al., 2015). Therefore, it was hypothesised that there is unidentified  $K^+$  channel other than the classical cardiac  $K_{ATP}$  channel that may open and participate in the early stage of protection. To investigate this hypothesis, cell-attached patch experiments were used to record the activity of the channel current on the surface of ventricular cardiomyocytes during the absence and presence of metabolic inhibition.

To investigate the openings of ventricular  $K^+$  channel, the membrane potential of cardiomyocytes was held at around -110 mV, which was achieved by holding the pipette potential at +40 mV and assuming a resting membrane potential of ~-70 mV. At this negative membrane potential, inward rectifier  $K^+$  channels, such as  $K_{ir}2$  and the putative  $K_{ir}6$ , will be the primary open channels. These channels are readily differentiated by their single channel current amplitude and kinetics.  $K_{ir}2$  channels have a conductance of ~30 pS and so have a single channel current of ~3.5 pA in these conditions. The kinetics of the  $K_{ir}2$  channels show long openings that do not display a bursting pattern. The putative  $K_{ir}6.1$  channels show a bursting activity with a single channel current amplitude of 5.5 – 6 pA. When analysing these cell-attached records, the threshold for channel detection can be set to treat the opening of  $K_{ir}2$  as a shift in baseline.  $K_{ir}6.2$  channels, unlike the putative  $K_{ir}6.1$  channels, only open in metabolic inhibition when there is significant ATP depletion, triggering the activation of a larger (~75 pS) channel with a single channel current amplitude of 10 – 11 pA. The bursting behaviour of this channel gives a characteristic open and closed level with no obvious sub-conductance states, differentiating it from the opening of multiple  $K_{ir}6.1$  channels. With increasing openings of  $K_{ir}6.2$  channels, the single channel current may increase as the resting membrane potential of the cell becomes more hyperpolarised. The channels that underlie  $I_{Na}$ ,  $I_{Ca}$ ,  $I_{Ks}$  and  $I_{Kr}$  normally pass currents at positive membrane potentials and so these channels will be in a closed state at -110 mV. It is unlikely that these voltage-gated channels will make any contribution to the single channel activity in these cell-attached recordings.

Cells were perfused with normal Tyrode (NT) solution for 1 min, followed by administration of substrate-free metabolic inhibition Tyrode's solution (SFT-MI) to simulate ischaemia to activate the classical cardiac  $K_{ATP}$  current (Figure 3.1A). Figure 3.1A(i) shows an unidentified active  $K_{ATP}$ -like channel with a half amplitude current at  $\sim 5$  pA in resting conditions. By contrast, after simulated ischaemia with metabolic inhibition, the classical  $K_{ir}6.2/SUR2A$  channel opens, characterised by  $\geq 10$  pA of passing amplitude currents, as shown in Figure 3.1A(ii). To measure the open probability of the newly-identified, putative  $K_{ir}6.1$  channel, analysis was carried out of the cell-attached recording in Clampfit. Given that it was not possible to ascertain how many channels were contained within each cell-attached patch recording, the NPo was calculated. Channel opening events were measured using a threshold level search, with this level being set at 5 pA to limit detection of smaller conductance channels, such as  $K_{ir}2$ . Given the difficulties of assessing the true number of channels in the cell-attached patch, the NOpen (NPo) (where N, the number of the channels in the patch estimated from the maximum number of simultaneous openings) was used. This method of analysis does not take into account channels opening independently in "series" whilst other channels are closed, and so is most likely an underestimation of the number of channels in the cell-attached patch. Figure 3.1B shows no significant difference in the open probabilities of this newly-identified  $K_{ATP}$  channel between control and perfusion of SFT-MI [from  $0.076\pm 0.02$  ( $n=21$ ) in control to  $0.078\pm 0.02$  ( $n=21$ ,  $p=0.89$ ) in SFT-MI cells].

This cell-attached patch recording provides important evidence that under normal physiological conditions, there is a second type of  $K_{ATP}$  channel that plays an important role in the  $K^+$  ion conductance through the cardiac surface. Previous studies have reported that recombinant  $K_{ir}6.1/SUR2B$  channels in vasculature are characterised by ATP insensitivity (Koh et al., 1998; Beech et al., 1993; Zhang and Bolton, 1995). Therefore, it was hypothesised that this new  $K_{ATP}$  channel comprises of  $K_{ir}6.1$  subunit. This finding supports previous research that links the  $K_{ATP}$  channel, in particular  $K_{ir}6.1$  containing channel, and cardiovascular disorders (Miki et al., 2002; Tester et al., 2011; Nichols et al., 2013). Subsequent experimental studies in this chapter aimed to determine the extent to which the role of  $K_{ir}6.1$  containing channel in regulating cardiac function and whether modulation of this newly-identified  $K_{ATP}$  channel has a protective role, using a selective activator and blocker.

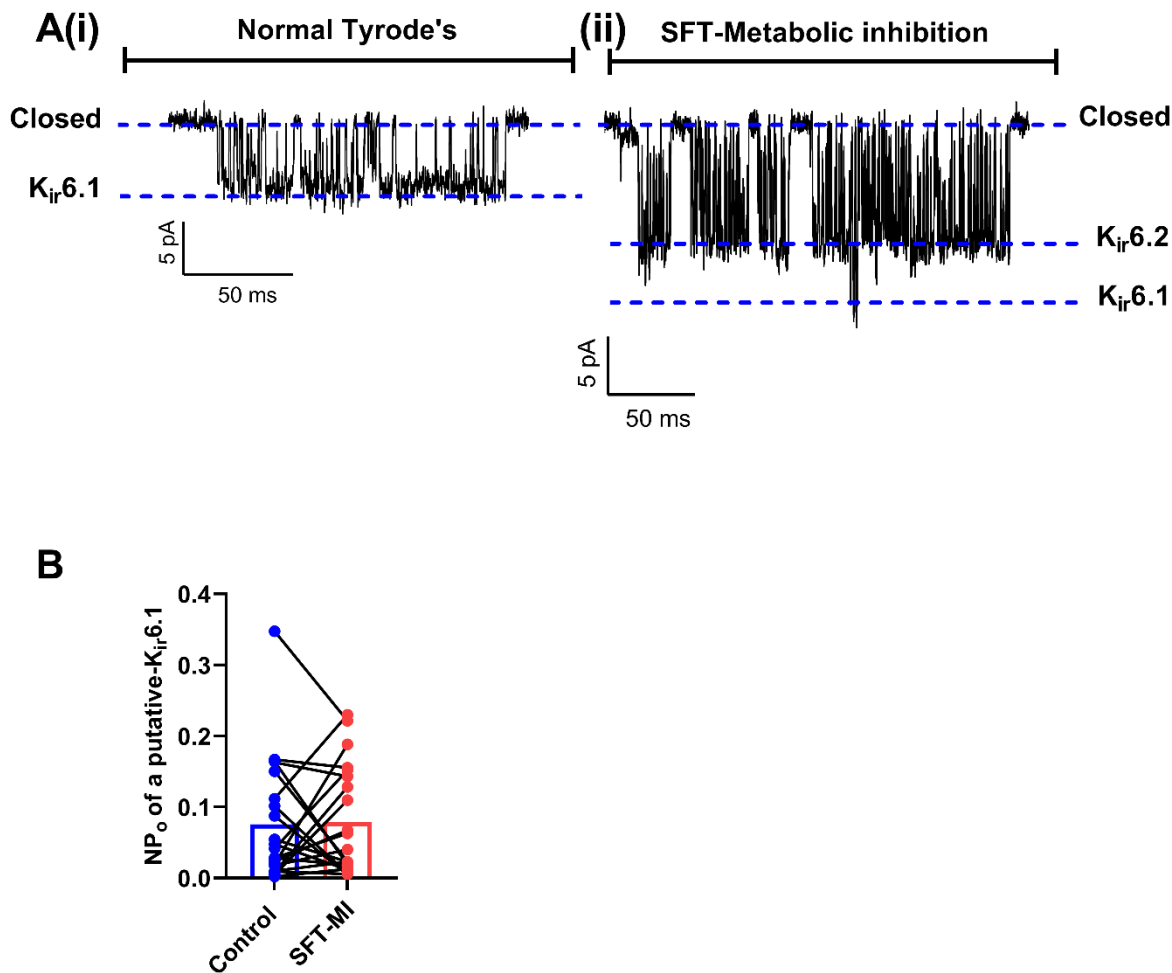


**Figure 3.1:** Identification a channel with a current with amplitude half of that compared to the K<sub>iR</sub>6.2/SUR2A cardiac K<sub>ATP</sub> current on the surface of ventricular myocytes.

*A, Representative traces of cell-attached patch recording showing the activity of cardiac sarcolemmal currents before and after the administration of metabolic inhibition. The patch pipette was held at +40 mV with the resting membrane potential of cardiomyocyte at -70 mV to maintain the cell membrane at -110 mV. A(i), Expanded trace showing the openings of an unidentified cardiac channel that allowed approximately 5 pA of current in resting condition. A(ii), Expanded trace showing a canonical sarcolemmal K<sub>ATP</sub> channel, K<sub>iR</sub>6.2/SUR2A that allowed approximately 10 pA of current in the presence of metabolic inhibition. B, Bar chart showing the number of openings of an constitutively active K<sub>ATP</sub>-like channel, in the absence and presence of SFT-metabolic inhibition. There was no significant difference in the open probabilities of this newly-identified K<sub>ATP</sub> channel between control and perfusion of SFT-MI (controls vs. SFT-MI, n=21, p=0.89) (paired t-test).*

### 3.2.2 $I_{KATP}$ activation with pinacidil causes a shortening of the action potential duration

The ventricular myocytes of rat models contain numerous  $K_{ATP}$  channels that present in a closed state during normal physiological conditions. These channels can be activated by two different methods: metabolic inhibition or pharmacological manipulation. During metabolic inhibition, such as myocardial ischaemia, the quantity of intracellular ATP is depleted resulting in contractile failure, caused by a failure of electrical activity (cardiac action potential) in the heart, due to the enhanced opening of  $K_{ATP}$  channels to preserve ATP levels. Figure 3.1 shows, in line with the results obtained by Brennan *et al.* (2015), that the time to activation of classic cardiac  $K_{ATP}$  ( $Kir6.2/SUR2A$ ) channels is delayed following cardioprotective stimuli (Brennan *et al.*, 2015), and therefore, this indicates the presence of a new  $K_{ATP}$  channel than canonical  $Kir6.2/SUR2A$  channels to impart early-stage protection. In a previous study, application of pinacidil at a concentration less than 150  $\mu M$  had a limited effect on the  $Kir6.2$ -containing  $K_{ATP}$  channels. Therefore, the present study considered 150  $\mu M$  pinacidil sufficient to cause pinacidil-induced vascular  $K_{ATP}$ -like channels ( $Kir6.1$  containing) (Satoh *et al.*, 1998; Suzuki *et al.*, 2001; Lodwick *et al.*, 2014). Action potentials from isolated cardiomyocytes were recorded using the whole-cell patch-clamp technique. To trigger action potentials, the cells were stimulated at a rate of 1 Hz via a patch pipette. Cardiomyocytes were perfused with NT solution for 3–5 min in the control recordings. Then, 150  $\mu M$  pinacidil was applied after 5 min of steady-state control recording to measure the change happening during  $K_{ATP}$ -like channel activation.

Figure 3.2A(i) presents representative trace of action potentials recorded before and after perfusion with 150  $\mu M$  pinacidil, which resulted in the shortening of action potential duration of cardiomyocyte. The role of the  $K_{ATP}$  activator in the resting membrane potential was also investigated.

The action potential duration to 90% ( $APD_{90}$ ) was measured in rat cardiomyocytes. The mean  $APD_{90}$  in Figure 3.2B(i) showed that 150  $\mu M$  pinacidil induced significant shortening of  $APD_{90}$  (from  $53.6 \pm 10.5$  ms to  $29.7 \pm 6.6$  ms;  $p=0.001$ ,  $n=5$ ), an effect that was lost with washout (with  $APD$  of  $50.3 \pm 8.5$  ms compared to control  $APD$ ;  $p=0.44$ ,  $n=5$ ). In these cardiomyocytes, there

was no effect on resting membrane potential, with  $-66.5 \pm 2.3$  mV in the control recording,  $-66.6 \pm 2.1$  mV after pinacidil treatment ( $n=5$ ,  $P=0.987$ ) and  $-67.1 \pm 2.8$  mV following washout ( $n=5$ ,  $P=0.987$ ) (Figure 3.2B(ii)).

$K_{ATP}$  channels pass a current that is weakly rectifying and, therefore, will affect the action potential across the voltage range. To investigate this, action potential durations for different levels of repolarisation were measured in the presence of  $150 \mu M$  pinacidil (Figure 3.2A(ii)). The application of  $150 \mu M$  pinacidil to isolated cardiomyocytes resulted in a significant shortening of APD at 50% repolarisation, from  $37.5 \pm 6.3$  ms at control to  $24.9 \pm 5.5$  ms at treatment conditions ( $p=0.003$ ) (Figure 3.2C(i)). Additionally, the mean  $APD_{50}$  ( $n=5$ ) did not significantly change following the washout of the drug, being  $35.6 \pm 5.0$  ms ( $p=0.49$ ). Moreover,  $150 \mu M$  pinacidil resulted in the shortening of APD at 10% repolarisation but was insignificant ( $p=0.08$ ), decreasing from  $13.1 \pm 3.3$  ms (control,  $n=5$ ) to  $10.4 \pm 4.0$  ms (pinacidil,  $n=5$ ) and to  $14.4 \pm 4.2$  ms following the washout of the drug ( $p=0.26$ ) (Figure 3.2C(ii)).

As pinacidil was dissolved in DMSO, control experiments were carried out in which DMSO alone was added to the cells to rule out any interference. As illustrated in Figure 3.2D, no differences were observed in  $APD_{90}$  and RMP between the mean data of the control value and the measurements taken after DMSO administration. Figure 3.2D(i) is a plot of the mean data ( $n=6$ ) of  $APD_{90}$  at  $62.9 \pm 11.3$  ms for control and  $63.5 \pm 12.5$  ms for DMSO ( $P=0.876$ ). Figure 3.2D(ii) demonstrates that there were no differences in membrane potential between control ( $-63.5 \pm 1.7$  mV) and DMSO ( $-64.1 \pm 1.3$  mV) ( $p=0.724$ ). These data suggested that activation of  $K_{ATP}$  channels affected all levels of repolarisation, which corresponds to the previous findings on the shortening of  $APD_{90}$  with the presence of  $150 \mu M$  pinacidil.

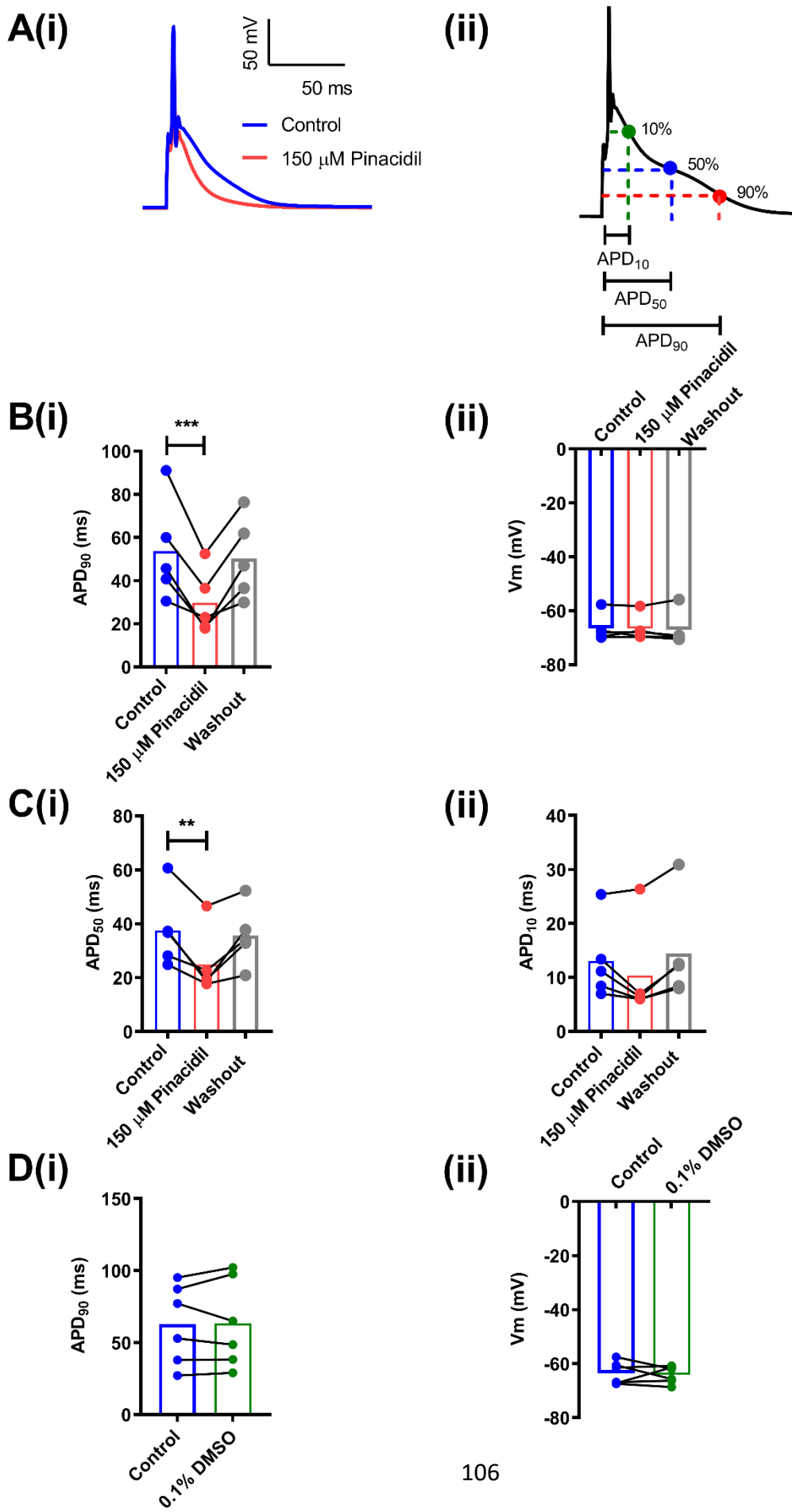


**Figure 3.2:** pinacidil causes shortening of action potential duration in rat cardiomyocytes.

*A(i), Representative traces of an action potential prior to perfusion with 150 µM pinacidil treatment (blue line) and during it (red line), showing shortening of the APD. A(ii), Sample trace of cardiac action potential duration, which identifies different points of repolarisation to investigate the effect of drugs at 10%, and 50% of repolarisation. B(i), Histogram showing 150 µM pinacidil shortened the mean APD<sub>90</sub> (n=5, \*\*\*p=0.001, for one-way ANOVA Holm-Sidak post-test), which increased again with the washout and shown no significant difference with the control (p=0.44). B(ii), Histogram showing no effect of 150 µM pinacidil on the membrane potential (n=5, p=0.99, one-way ANOVA Holm-Sidak post-test). C(i) Histogram showing 150 µM pinacidil shortened the mean APD<sub>50</sub> (n=5, \*\*p=0.003), which increased again with the washout and shown no significant difference with the control (n=5, p=0.49). C(ii), Histogram showing that APD<sub>10</sub> was not significantly changed with 150 µM pinacidil (n=5, p=0.08) or after washout (n=5, p=0.26). D, Diagram showing that 0.1% DMSO as a control has no effect on either the duration of action potential (i) or the resting membrane potential (ii) (n=6, p=0.876, p=0.724, respectively) (paired t-test).*

### 3.2.3 Activation of K<sub>ATP</sub> currents by different concentrations of pinacidil treatment in rat ventricular myocytes changes the inward rectifier potassium currents

As demonstrated above, a K<sub>ATP</sub> channel opener (K<sub>CO</sub>), particularly pinacidil, increased K<sup>+</sup> efflux by enhancing the shortening of cardiac APD. To investigate the effects of pinacidil on I<sub>K1</sub> and other potassium currents in cardiomyocytes, a protocol was used as shown in Figure 3.3. Initially, whole-cell currents were recorded by holding the cell membrane potential at -70 mV, followed by depolarisation to -30 mV to activate Na<sup>+</sup> and some Ca<sup>2+</sup> currents. Subsequently, the K<sup>+</sup> currents were recorded by applying 400 ms pulses between -100 mV and +60 mV. Throughout these voltage steps, the K<sup>+</sup> current, which is considered a major cardiomyocyte current across the voltage range, is classified into I<sub>K1</sub> and voltage-gated K<sup>+</sup> current (Noma, 1993; Huang et al., 2017). I<sub>K1</sub> is normally activated over a narrow potential range between -100 mV and -20 mV. The rectifying property at approximately -20 mV results in no conductance of I<sub>K1</sub> and limits the outward current at more positive membrane potentials to fire action potential, so this membrane potential was used to test the effect of K<sub>ATP</sub> channel opener on cardiac cells. Under metabolic stress, the flow of outward current is maintained via passing I<sub>KATP</sub>, which is important for adaption to stress. For the purpose of I<sub>KATP</sub> activation, K<sub>CO</sub> pinacidil treatment was used at different concentrations (30 µM and 150 µM).

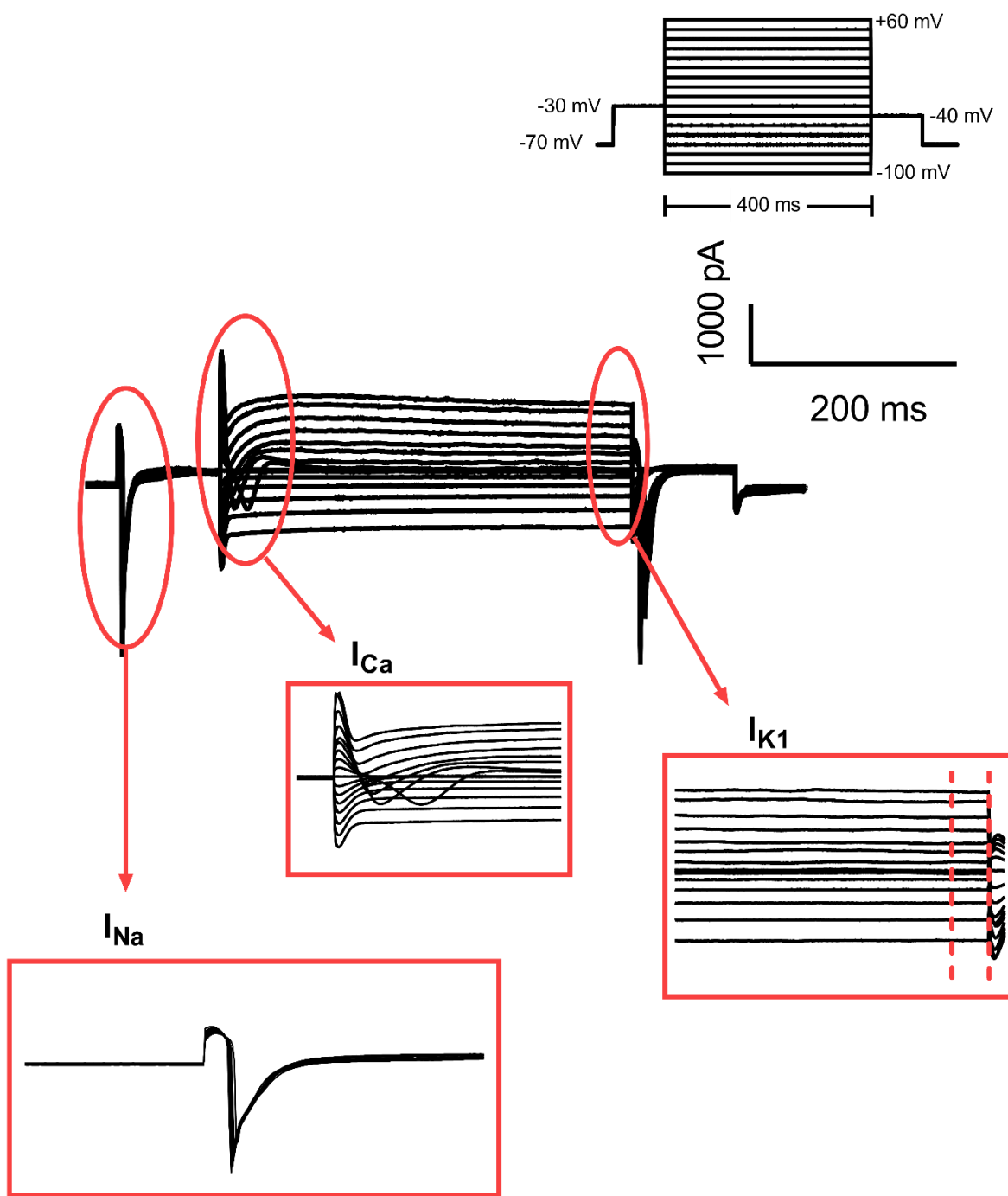
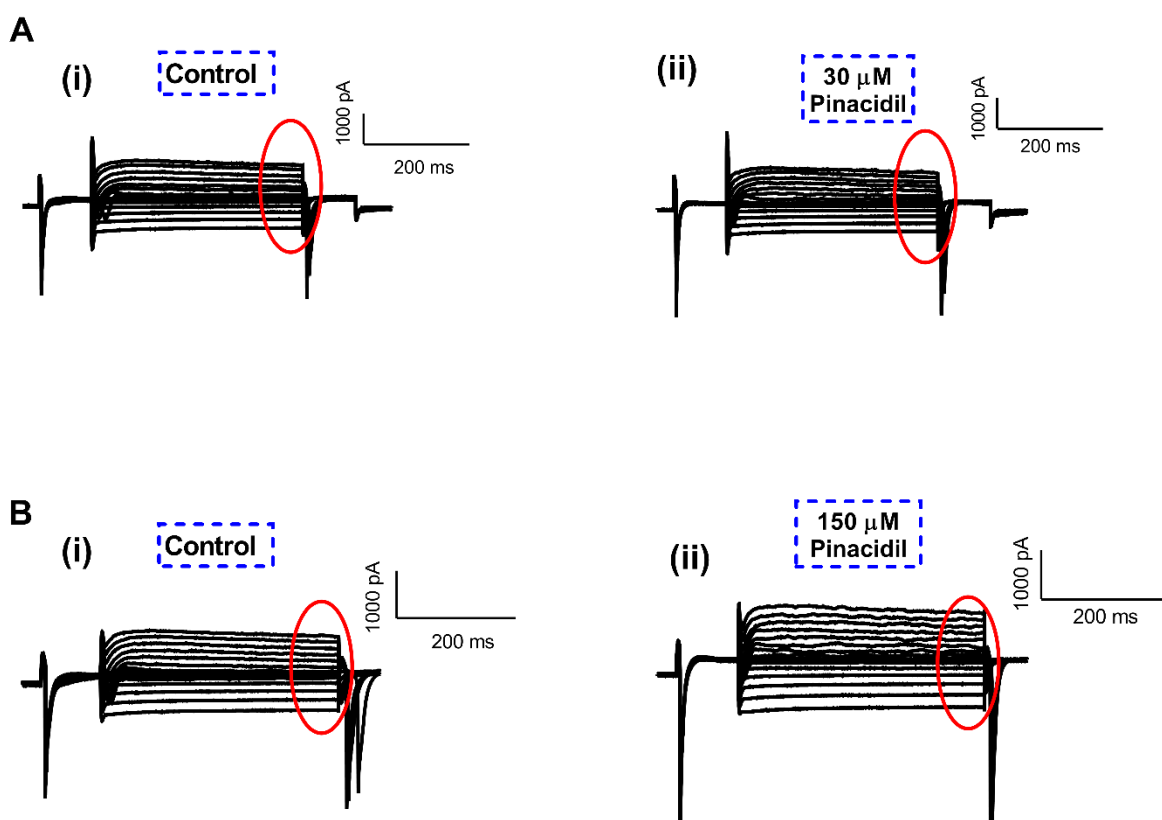


Figure 3.3: A designed protocol with a voltage clamp mode for whole-cell recording in rat ventricular myocytes.

The cell membranes were evoked by moving the cell membrane from a holding potential of -70 mV to -30 mV to activate  $\text{Na}^+$  channel, followed by 400 ms voltage steps between -100 mV and +60 mV (10 mV increments) to activate  $\text{Ca}^{2+}$  and  $\text{K}^+$  channels. This recording trace was obtained as described in the protocol above, showing different currents, for example,  $I_{Na}$ ,  $I_{Ca}$ , and  $I_{K1}$ .  $I_{K1}$  was measured by a series of depolarising steps between -100 mV and +60 mV. The inward potassium current was measured at specific regions which were represented between the two red cursors.  $I_{K1}$  was measured as mean current in the final 50 ms of each voltage step.

Representative traces showing the effect of low and high concentrations of pinacidil on K<sup>+</sup> current in the control and 4 min after pinacidil application are shown in Figure 3.4. From Figure 3.4A it can be seen that the administration of 30 µM pinacidil caused non-notable increased in K<sup>+</sup> currents. However, as shown in Figure 3.4(B) it is notable that 150 µM pinacidil causes elevation in K<sup>+</sup> current. This finding supports the idea that the activation of K<sub>ATP</sub> obtains by administrating pinacidil treatment at a high concentration (150 µM), and consequently leads to increase K<sup>+</sup> efflux.

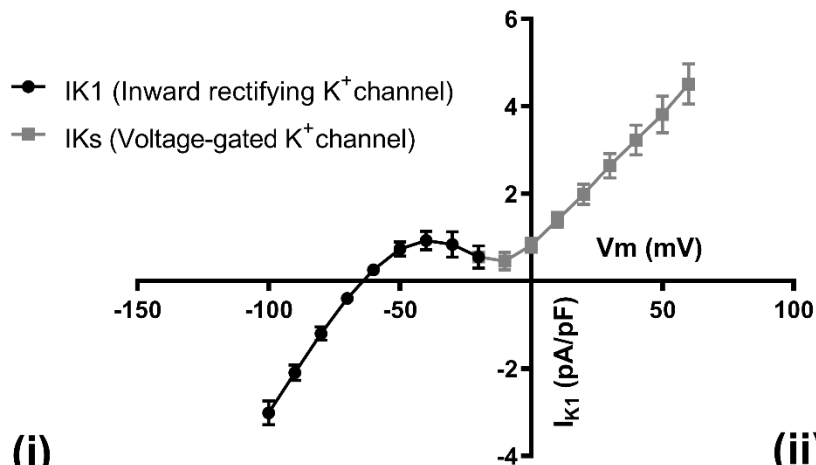
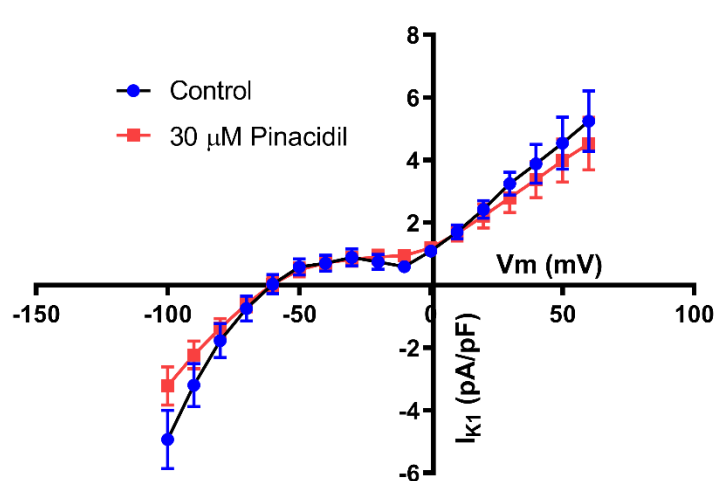
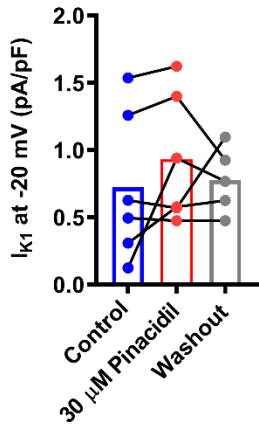
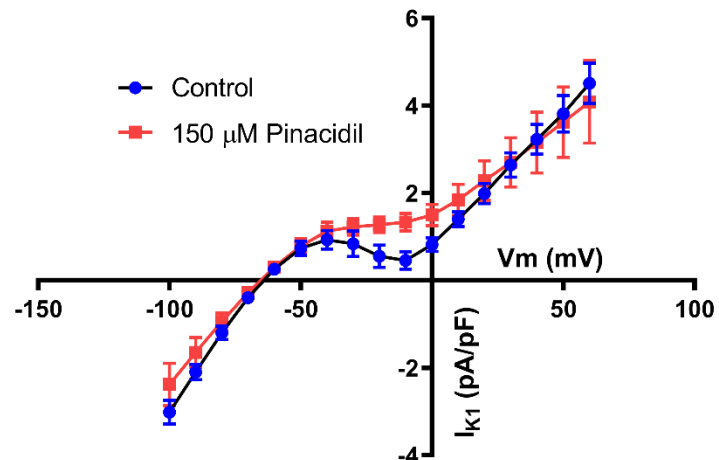
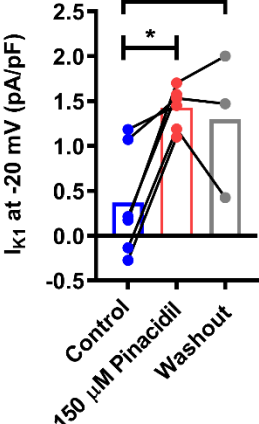


**Figure 3.4:** Comparison of whole-cell patch clamp recordings with a voltage clamp mode in the absence and presence of different concentrations of pinacidil treatments, highlighted with a red circle.

*A, Representative traces of isolated rat ventricular cells in the control condition (i) and after being perfused with 30 µM pinacidil (ii). B, Recording traces of single cardiomyocyte under control recordings (i) and after the administration of 150 µM pinacidil (ii), showing a noticeable increase of K<sup>+</sup> current with a high concentration of pinacidil.*

To demonstrate a current-voltage (I-V) relationship, the mean K<sup>+</sup> currents over the 400 ms depolarisation steps were measured. These currents were normalised to the cell capacitance. Across the voltage range tested here, there are two main potassium currents: the I<sub>K1</sub> are activated at greater negative voltage steps, and voltage-gated potassium currents are opened from -10 mV and gradually increase with positive depolarising steps (Figure 3.5A). The major effect of pinacidil treatment on the I<sub>K1</sub> was noticeable at -20 mV, a potential where I<sub>K1</sub> shows rectification. Opening of the weakly rectifying K<sub>ATP</sub> current yielded a significantly larger current at -20 mV. Figure 3.5B(i) is a plot of the application of 30 μM pinacidil versus the control conditions, showing no difference between the recordings. The mean I<sub>K1</sub> was recorded in the control condition at 0.72 ± 0.23 pA/pF and with the pharmacological treatment at 0.93±0.29 pA/pF (p=0.69, n=6) (Figure 3.5B(ii)). The mean I<sub>K1</sub> was not significantly different to the control conditions in the washout recordings, being 0.78±0.1 pA/pF (n=5, p=0.85). This finding suggested that at -20 mV, there were no significant changes in the I<sub>K1</sub> with 30 μM pinacidil. The administration of 150 μM pinacidil is shown in Figure 3.5(C(i)), demonstrating an increase in I<sub>K1</sub> at a -20 mV voltage step after treatment. As a result, the mean data of I<sub>K1</sub> at -20 mV significantly increased from 0.37±0.25 pA/pF in the control condition to 1.42±0.09 pA/pF with 150 μM pinacidil (n=6, p=0.01) (Figure 3.5C(ii)). After washout period, I<sub>K1</sub> at -20 mV did not return to control values (1.29±0.5 pA/pF, n=3, p=0.03, Figure 3.5B(ii)).

An explanation is that pinacidil at high concentration may not be completely washed compared to lower concentration. (Pelzmann et al., 2003) reported that pinacidil at a 30 μM concentration can be washed out completely. Pinacidil, being lipophilic may accumulate in the membrane where it interacts with the channel. This may take a longer duration to washout than anticipated to be returned to control values. Further cell-based washout experiments are needed.

**A****B (i)****(ii)****C (i)****(ii)**

**Figure 3.5:** Pinacidil at different concentrations changes I<sub>K1</sub>, which leads to maintaining K<sup>+</sup> efflux at the -20 mV voltage step.

*A, A recording trace shows the relationship between the I<sub>K1</sub> (black line) and the I<sub>Ks</sub> (gray line) in response to alterations in voltage steps. The voltage-current relationship of K<sup>+</sup> current is shown in the absence*

and in the presence of 30  $\mu$ M pinacidil (B(i)) and 150  $\mu$ M pinacidil (C(i)). The control condition is displayed with the blue line, while the red line represents the effect of pharmacological treatment. Histograms B(ii) and C(ii) show the mean data for the cardiomyocytes under the control conditions compared to the pinacidil treatments. The alteration of  $I_{K1}$  by this pharmacological treatment was detected at a -20 mV voltage potential. B(ii) There was no difference in the  $I_{K1}$  after the application of 30  $\mu$ M pinacidil and following the washout of the drug ( $n=6$ ,  $p=0.69$  and  $n=5$ ,  $p=0.85$ , respectively). C(ii) The application of 150  $\mu$ M pinacidil led to significantly increased  $I_{K1}$  ( $n=6$ ,  $*p=0.01$ ). Also, there was a significant increase in  $I_{K1}$  in washout recordings versus controls ( $n=3$ ,  $p=0.03$ ). (one-way ANOVA [non-pairing experimental design] with Holm-Sidak post-test).

### 3.2.4 Identification of a second $K_{ATP}$ channel in cardiomyocytes by the application of a selective $K_{ir}6.1$ blocker (PNU37883)

#### 3.2.4.1 PNU37883 prolongs the cardiac action potential

As mentioned in Section 3.1, that  $K_{ir}6.1$  null mice are prone to cardiovascular diseases. The classical cardiac  $K_{ATP}$  channel has been suggested to be an important player in protective mechanisms when there is severe depletion of intracellular ATP. However, studies have shown that the known cardiac  $K_{ATP}$  ( $K_{ir}6.2/SUR2A$ ) does not open early during metabolic stress to impart protection. Previous studies show that PNU37883 is an effective blocker of  $K_{ir}6.1/SUR2B$ , which mainly contributes as  $K_{ATP}$  channels in vasculature, and has partially inhibitory effects on  $K_{ir}6.2/SUR2A$  when applied at high concentration (10  $\mu$ M) (Cui et al., 2003; Kovalev et al., 2004). To identify the possibility of other  $K_{ATP}$  channel, in particular  $K_{ir}6.1$ -containing channel other than the classical cardiac  $K_{ir}6.2/SUR2A$  channel, a low concentration (3  $\mu$ M) PNU was used as a completely (100%) selective blocker for  $K_{ir}6.1$  subunit. Studies to identify the expression of other isoforms of  $K_{ATP}$  channels expressed in cardiomyocytes were undertaken to investigate the presence of other isoforms and to understand the molecular nature of these channel subunits using specific pharmacological blockers, PCR, and western blotting. To date, all  $K_{ATP}$  channel subunits have been identified in the heart, with compelling evidence suggesting that the  $I_{KATP}$  is comprised of subunits other than the widely accepted  $K_{ir}6.2/SUR2A$  cardiac sarcolemmal isoform.

To determine whether  $K_{ir}6.1$  subunits had a role in the ventricular  $K_{ATP}$  current, we assessed the effects of  $K_{ir}6.1$ -pore blocker, PNU (3  $\mu$ M), and pan- $K_{ATP}$  channel blocker glibenclamide (10  $\mu$ M) on the action potential measured in ventricular cardiomyocytes. Cells were first

perfused with NT solution, and APD was measured at steady-state recording, followed by measuring the alteration of different blockers following 5 min of application of each.

Figure 3.6A shows representative traces of action potentials recorded in the absence and presence of these pharmacological blockers, showing a prolongation of APD<sub>90</sub> in the presence of either PNU or Glibenclamide. The mean APD<sub>90</sub> (n=9) of ventricular cells perfused with 3 μM PNU showed a significant prolongation of APD<sub>90</sub> compared to control conditions (53.4±4.8 ms vs. 76.6±5.0 ms, p<0.0001), as shown in Figure 3.6B(i). The subsequent application of 10 μM glibenclamide caused further prolongation of APD<sub>90</sub>, from 53.4±4.8 ms (control) to 85.0±6.0 ms (pharmacological treatment) (n=9, p=0.0003) (Figure 3.6B(i)). After washout of these blockers, the mean APD<sub>50</sub> (n=9) returned nearly to control recordings (53.4±4.8 pA/pF vs. 66.3±5.7 pA/pF, p=0.051). There was a significant difference in the prolongation between PNU (76.6±5.0 ms) and glibenclamide (85.0±6.0 ms) (p=0.024), suggesting that the maximal block of I<sub>KATP</sub> had been achieved with the application of glibenclamide, a pan-K<sub>ATP</sub> blocker. Furthermore, treatment of cells with either PNU or glibenclamide did not result in any shift in resting membrane potentials compared to baseline values (-65.3±0.8 mV in control vs. -65.3±0.8 mV (p=0.94) and -65.5±0.8 mV (p=0.89) after application of PNU and glibenclamide, respectively) (Figure 3.6B(ii)). There was no statistically significant difference between the resting membrane potential in control recordings and after a washout period (-65.3±0.8 mV vs. -66.6±0.8 mV) (p=0.09). This suggests that K<sub>iR6.1</sub> inhibition prolongs the action potential duration of ventricular cardiomyocytes.

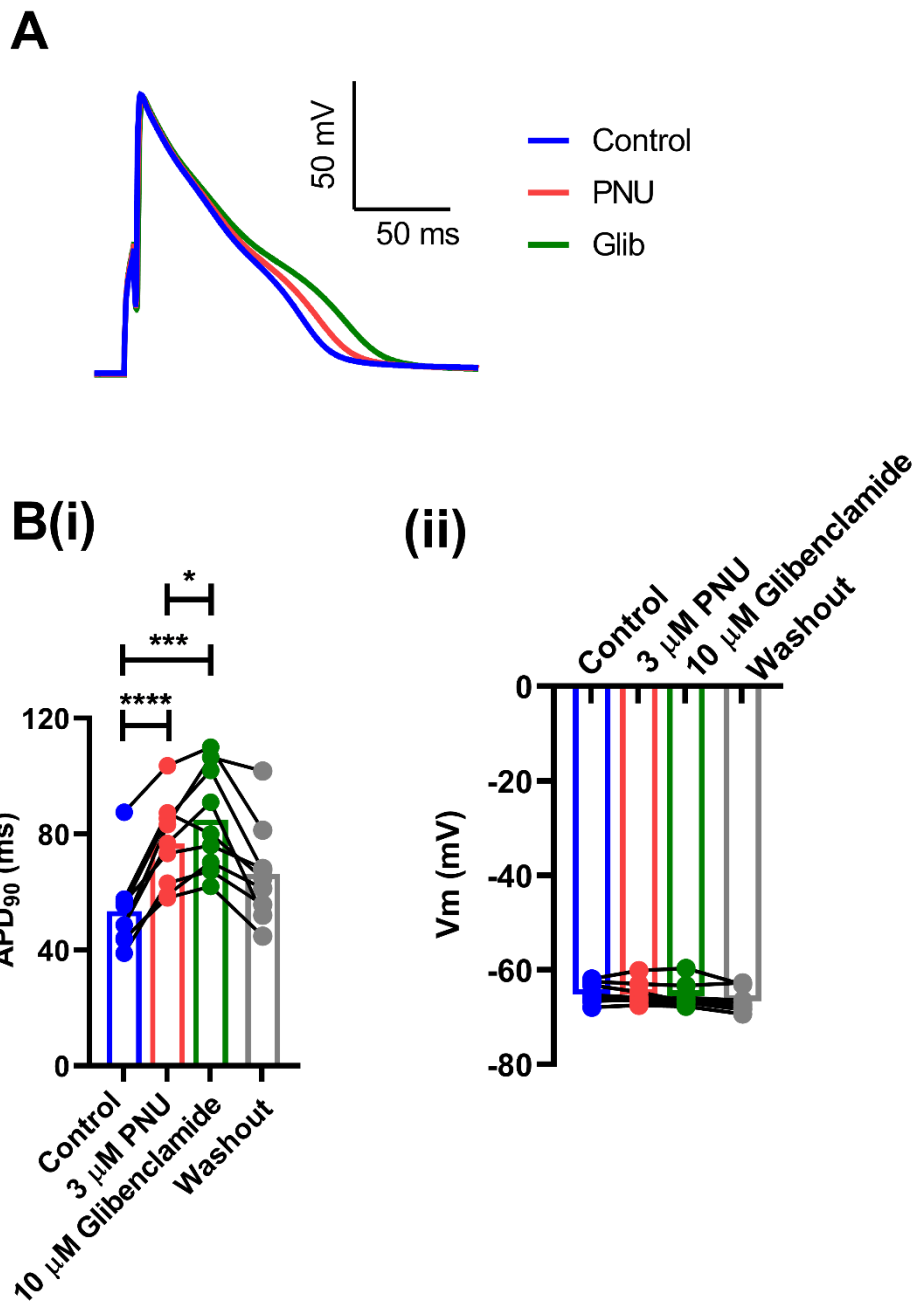


**Figure 3.6:** A selective blocker of  $K_{ir}6.1$  (PNU) prolongs the duration of cardiac action potential at 90% repolarisation.

*A, Recording traces show APD<sub>90</sub> (at control, 3  $\mu$ M PNU, and 10  $\mu$ M glibenclamide) of ventricular cells. B(i), Graphs showing the effect of 3  $\mu$ M PNU ( $K_{ir}6.1$  blocker), compared to control on APD<sub>90</sub>, displaying a significant increase in cardiac action potential ( $n=9$ , \*\*\* $p<0.0001$ ). Prolongation of APD<sub>90</sub> was also significant with 10  $\mu$ M glibenclamide (pan- $K_{ATP}$  blocker) ( $n = 9$ , \*\*\* $p=0.0003$ ). There was no significant change with washout recordings, compared to controls ( $n=9$ ,  $p=0.051$ ). A significant difference was found between PNU and glibenclamide (\* $p=0.024$ ). B(ii), Histograms show that these pharmacological blockers did not induce any change in the resting membrane potential of cardiomyocytes (one-way ANOVA Holm–Sidak post-test).*

### 3.2.4.2 PNU37883 blocks Kir6.1 currents in rat ventricular myocytes

Having demonstrated that the Kir6.1 blocker (PNU) caused a change in the action potential duration in ventricular cells, the contribution of PNU-sensitive K<sup>+</sup> currents in cardiomyocytes was investigated (section 3.2.4.1). Previous studies have shown 10 μM PNU is a selective blocker of the vascular form of K<sub>ATP</sub> channel (Kir6.1/SUR2B) and has a little effect on the Kir6.2/SUR2A (Kovalev et al., 2004). We next sought to examine the inhibition of K<sub>ATP</sub> currents by 10 μM PNU. Pharmacological inhibition of Kir6.1 was expected to be mostly observable in the I<sub>K1</sub>, because the Kir6.1 subunit, as with the I<sub>K1</sub>-carrying Kir2.x channel subunits, is a member of the inwardly rectifying K<sup>+</sup> channel family. Whole-cell recording was used based on the protocol shown in Figure 3.3. The I<sub>K1</sub> is normally activated over a narrow potential range, from -100 mV to about -20 mV, whereas voltage-gated K<sup>+</sup> current, in particular I<sub>Ks</sub>, is fully activated at +60 mV. Cardiomyocytes were initially perfused with NT solution, followed by administration of 10 μM PNU. To illustrate the result, an example experimental trace under a control condition (Figure 3.7A(i)) and after pharmacological administration (Figure 3.7A(ii)) are shown. The application of 10 μM PNU notably decreases the K<sup>+</sup> currents.

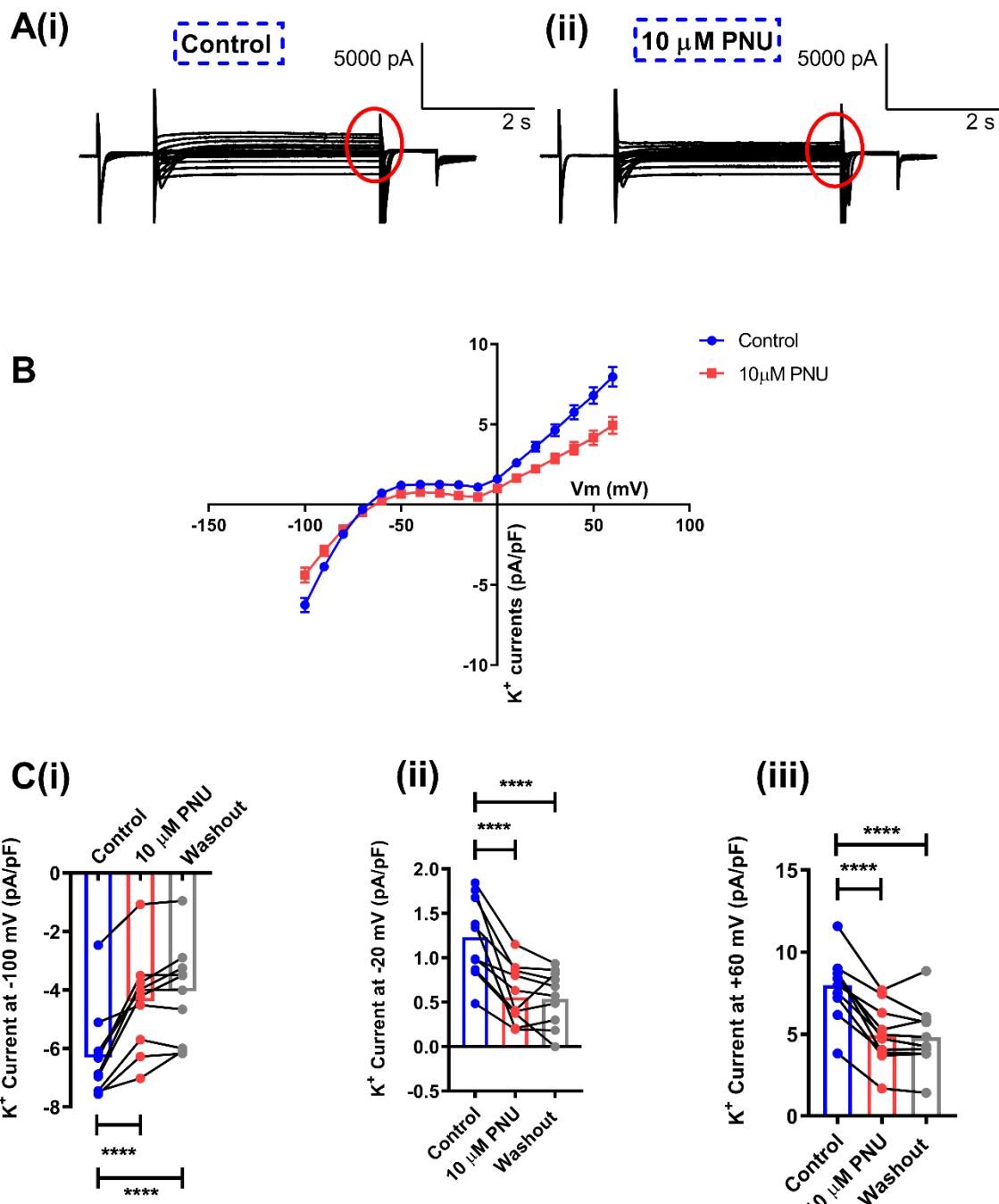


Figure 3.7: PNU reduces potassium currents at different membrane potentials.

A, Example recordings from whole-cell voltage-clamp experiments in control conditions (i) and following perfusion with 10  $\mu\text{M}$  PNU (ii); showing a reduction of  $\text{K}^+$  currents in the presence of PNU treatment. B, The current voltage relationship of  $\text{K}^+$  currents is shown in the absence (blue line) and in the presence of 10  $\mu\text{M}$  PNU (red line). C, bar charts show the mean data ( $n=11$ ) of isolated cardiomyocytes under control conditions and in the presence of PNU, demonstrating the block response at different membrane potentials. At a membrane potential of -100 mV (i), there is a significant reduction of  $\text{K}^+$  current in the presence of 10  $\mu\text{M}$  PNU ( $n=11$ ,  $****p<0.0001$ ) and following the washout of the drug ( $n=11$ ,  $****p<0.0001$ ). At -20 mV membrane potential (ii),  $\text{K}^+$  current was

*significantly reduced with 10 µM PNU (n=11, \*\*\*\*p<0.0001), and there was also a significant decrease in K<sup>+</sup> current in washout recordings compared to controls (n=11, \*\*\*\*p<0.0001). At +60 mV membrane potential (iii), there is also a significant reduction of K<sup>+</sup> current with 10 µM PNU (n=11, \*\*\*\*p <0.0001; paired T-test) and following washout of the drug (n=11, \*\*\*\*p<0.0001). (one-way ANOVA Holm–Sidak post-test).*

To examine the inhibitory effect of PNU on K<sup>+</sup> current at different voltage steps, a current-voltage (I-V) curve was plotted from the voltage steps to show the currents in control and PNU perfusion normalised to cell capacitance. The curves were measured before and after 10 µM PNU, showing the reduction of K<sup>+</sup> currents in response to this inhibitor (Figure 3.7B). This concentration was used to block as much K<sub>i</sub>6.1 as possible without causing inhibition of K<sub>i</sub>6.2 (Kovalev et al., 2004). As we expected the K<sub>i</sub>6.1 to be opened all through the action potential duration, the mean data for K<sup>+</sup> currents were measured at different voltage steps, including -100 mV, -20 mV, and +60 mV (Figure 3.7C). The mean data for the control condition were compared to the inhibited mean currents following pharmacological treatment. At -100 mV (Figure 3.7C(i)), the mean data for the K<sup>+</sup> current (n=11) was significantly decreased from -6.3±0.4 pA/pF in the control condition to -4.4±0.5 pA/pF with PNU treatment (p<0.0001). The mean K<sup>+</sup> current was significantly decreased compared to the control conditions in the washout recordings at -100 mV, being -4.0±0.5 pA/pF (n=11, p<0.0001, Figure 3.7C(i)). Further, the reduction of the mean K<sup>+</sup> current (n=11) at -20 mV was recorded as 1.2±0.1 pA/pF in the control condition and 0.6±0.1 pA/pF with 10 µM PNU (Figure 3.7C(ii)). This reduction in current at the -20 mV depolarising step was a significant response to pharmacological inhibition (p<0.0001). There was a significant decline in K<sup>+</sup> current at -20 mV following the washout of the drug (0.5±0.1 pA/pF), compared to control conditions (n=11, p<0.0001, Figure 3.7 C(ii)). Further, K<sup>+</sup> current at +60 mV significantly declined with PNU, from 7.9±0.6 pA/pF (control condition, n=11) to 4.9±0.5 pA/pF (10 µM PNU, n=11) (p<0.0001) (Figure 3.7C(iii)). K<sup>+</sup> current at +60 mV showed significant reduction, with 7.9±0.6 pA/pF for control versus 4.8±0.6 pA/pF for the washout condition (n=11, p<0.0001, Figure 3.7 C(iii)). For all washout recordings, the inhibitory effect on K<sup>+</sup> current was still observed. An explanation for this is that PNU treatment is characterised by a relatively slow time course of action which can result in a special type of slow recovery or irreversible inhibition (Wellman et al., 1999). Further research into time-matched recordings is still necessary before obtaining a definitive answer to whether decreases in K<sup>+</sup> current could be attributed to this compound or rundown.

These data suggest that the inward rectifier K<sup>+</sup> current ( $I_{K1}$ ) may also be formed from Kir6.1 in addition to the established Kir2.x subunits. These findings suggest that Kir6.1 in the heart may play a pivotal role in normal physiological conditions.

### 3.2.5 The classical K<sub>ATP</sub> channel (Kir6.2/SUR2A) remains inactive following HMR1098 (selective Kir6.2 blocker) treatment in cardiac muscle cells

HMR1098 has been reported as a potent cardio-selective K<sub>ATP</sub> channel (Kir6.2/SUR2A) blocker in cardiac muscle cells (Sato et al., 2000b; Manning Fox et al., 2002). As the canonical cardiac K<sub>ATP</sub> channel remains closed in resting conditions, it was hypothesised that application of pharmacological blockade of Kir6.2/SUR2A containing K<sub>ATP</sub> channel, HMR1098, would not affect K<sup>+</sup> currents of cardiomyocytes in control conditions. Additionally, PNU treatment was used to block Kir6.1-containing channel. To examine these pharmacological treatments, the effect of 1 μM HMR1098 and 3 μM PNU on potassium currents were measured, as shown in Figure 3.3. Whole-cell K<sup>+</sup> currents were initially recorded in control conditions using normal Tyrode's solution, followed by 1 μM HMR1098 for 4 min and then a solution containing both 1 μM HMR1098 and 3 μM PNU, recorded for 4 min. To demonstrate a current-voltage (I-V) relationship, the mean K<sup>+</sup> currents recorded in normal conditions and following the application of these inhibitors were measured and compared. These currents were normalised to the cell capacitance.

Figure 3.8A shows the curve of the mean data for K<sup>+</sup> currents in control conditions and following perfusion with different inhibitors. At -100 mV, the mean data of K<sup>+</sup> currents was significantly decreased by 1 μM HMR1098, from  $-5.48 \pm 0.33$  pA/pF to  $-4.24 \pm 0.47$  pA/pF (control vs. HMR1098, n=7, \*p=0.033). A further reduction was observed with a combination of both pharmacological inhibitors (1 μM HMR1098 and 3 μM PNU), recorded as  $-3.36 \pm 0.32$  pA/pF (n=7, \*\*p=0.003), as shown Figure 3.8B(i). Furthermore, the K<sup>+</sup> current at +60 mV did not significantly decline, being  $7.09 \pm 0.51$  pA/pF in the control condition,  $6.29 \pm 0.54$  pA/pF with HMR1098 (n=7, p=0.276), and  $5.84 \pm 0.52$  pA/pF with PNU+HMR1098 (n=7, p=0.215), as shown in Figure 3.8B(ii). As anticipated, the classical K<sub>ATP</sub> channel (Kir6.2/SUR2A) was not opened under normal physiological conditions, which was confirmed by maintaining the inactive mode following a selective pharmacological activator (HMR1098) at +60 mV.

Time-matched recordings were carried out to determine whether decreases in K<sup>+</sup> currents at -100 mV could be attributed to rundown. Figure 3.8C shows the mean K<sup>+</sup> currents in the presence of vehicle (DMSO) at time points equivalent to control, HMR1098 administration and with a combination of HMR1098 and PNU. At -100 mV, the mean K<sup>+</sup> currents was not altered from -4.4±0.4 pA/pF at baseline to -3.5±0.4 pA/pF at the equivalent time of drug addition, and to -3.2±0.4 pA/pF at time matched a combination of drug (n=8, p=0.14, p=0.06, respectively) (Figure 3.8C(i)). K<sup>+</sup> currents at +60 mV were also not significantly altered, recording from 5.8±0.4 pA/pF to 5.2±0.3 pA/pF and to 5.3±0.3 pA/pF (n=8, p=0.28, p=0.24, respectively, Figure 3.8C(ii)). Consequently, the control experiments at the time-matched fashion concluded that there is an absence of rundown in K<sup>+</sup> currents at -100 mV. These findings suggest that 3 µM PNU had effect on the whole-cell K<sup>+</sup> current at -100 mV.

In these experiments, 3 µM PNU had no effect on the whole-cell K<sup>+</sup> current, unlike the results shown earlier that PNU caused prolongation of APD<sub>90</sub> in 3.2.4.1. We now have included time matched control data for these experiments showing a little rundown in the presence of DMSO vehicle alone. These data in Figure 3.8 demonstrate a reduction in current at both -100 mV and +60 mV, however this does not reach significance at +60 mV. Currents at -100 mV will be almost exclusively inwardly rectifying potassium channels given that voltage-gated channels will be closed at this potential. At +60 mV, there will be influence from at least Kv7.1 channels and so detecting a change in current will be more difficult.

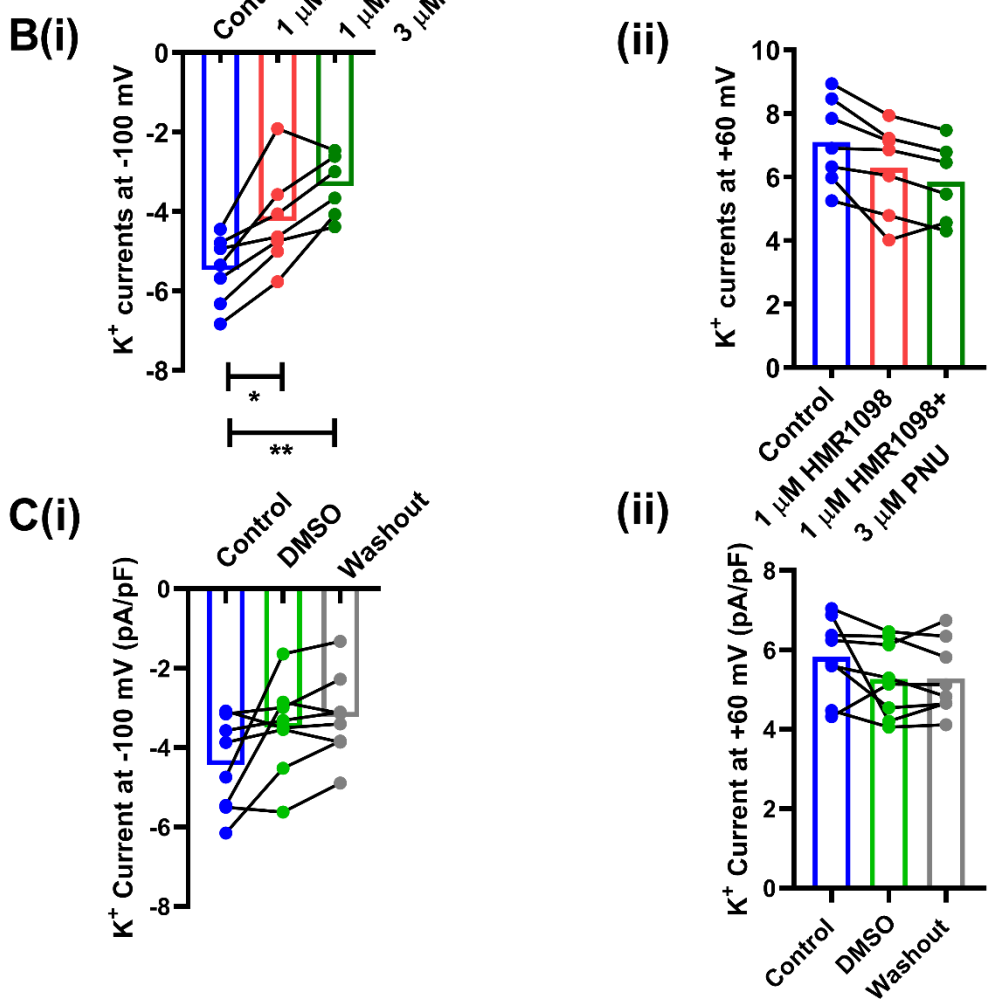
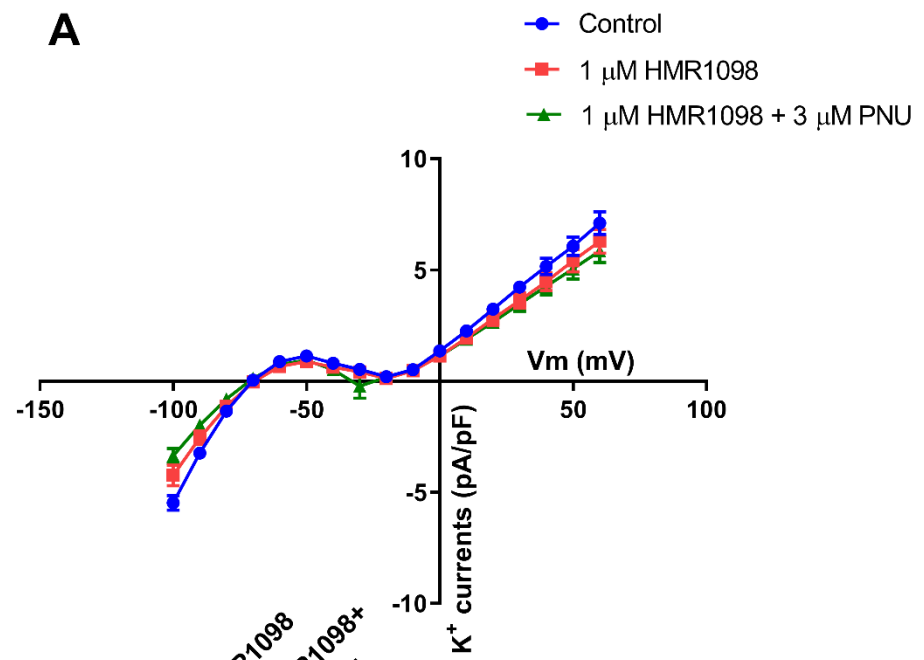


**Figure 3.8:** The classical K<sub>ATP</sub> channel (K<sub>iR</sub>6.2/SUR2A) maintains inactive following a selective pharmacological activator (HMR1098).

*A, The voltage-current curve of K<sup>+</sup> current is shown in the absence and in the presence of selective pharmacological inhibitors, the blue line defining the control condition, the red line representing the 1 μM HMR1098 treatment, and the green line representing a solution containing both 1 μM HMR1098 and 3 μM PNU. B, Histograms show the mean data (n=7) of isolated cardiomyocytes under normal conditions with different pharmacological treatments at different depolarisation steps. At -100 mV, 1 μM HMR1098 caused a significant reduction of K<sup>+</sup> current (\*p=0.033) (i), however; these results showed that there was no significant decrease in resting currents with 1 μM HMR1098 at +60 mV (n=7, p=0.276) (ii). The application of 1 μM PNU treatment + 1 μM HMR1098 caused a significant reduction at only -100 mV (n=7, \*\*p=0.003) (i), and no significant alteration at +60 mV (ii) (n=7, p=0.215) (one-way ANOVA Holm-Sidak post-test). C(i), Bar chart shows the mean K<sup>+</sup> current (n=8) at -100 mV at a time-matched fashion, being a non-significant change (n=8, p=0.14, p=0.06, respectively). C(ii), K<sup>+</sup> currents at +60 mV were not significantly affected by the run-down phenomena at time-matched corresponding measurements in the absence of the drug (n=8, p=0.28, p=0.24, respectively). (one-way ANOVA Holm-Sidak post-test).*

### 3.2.6 Identification of K<sub>iR</sub>6.1 as a component of the I<sub>K1</sub> in cardiomyocytes using selective blockers of K<sub>iR</sub>6.1 and K<sub>iR</sub>2.1

An important finding presented in Section 3.2.4.2 is that K<sub>iR</sub>6.1 appears to act as a component of the I<sub>K1</sub>, suggesting that K<sub>iR</sub>2.x subunits might not be solely responsible for I<sub>K1</sub>. To distinguish between these subunits in cardiomyocytes, a whole-cell configuration was used to record the responses of two different selective pharmacological blockers. Previous research has indicated that Ba<sup>2+</sup> is a selective blocker of the inward rectifier K<sup>+</sup> channel pore (K<sub>iR</sub>2.x-containing channel) and this channel pore is inhibited by <30 μM external Ba<sup>2+</sup> (Kubo et al., 1993; Robertson et al., 1996). The potency level of this Ba<sup>2+</sup> inhibition increases with membrane hyperpolarisation. Previous studies have reported that PNU is highly effective to block K<sub>iR</sub>6.1-containing channel and this channel is blocked by ≤10 μM PNU (Cui et al., 2003; Kovalev et al., 2004). An example protocol was designed with two subsequent voltage steps (Figure 3.9A). Recordings were measured from a holding potential at -70 mV and at a frequency of 1 Hz, followed by two depolarisation steps: the first step at -100 mV for 200 ms, followed by the second at -20 mV for 400 ms.

Whole-cell K<sup>+</sup> currents were initially recorded under control conditions using normal Tyrode's solution, followed by 10 μM PNU for 4 min and then a solution containing both 10 μM PNU

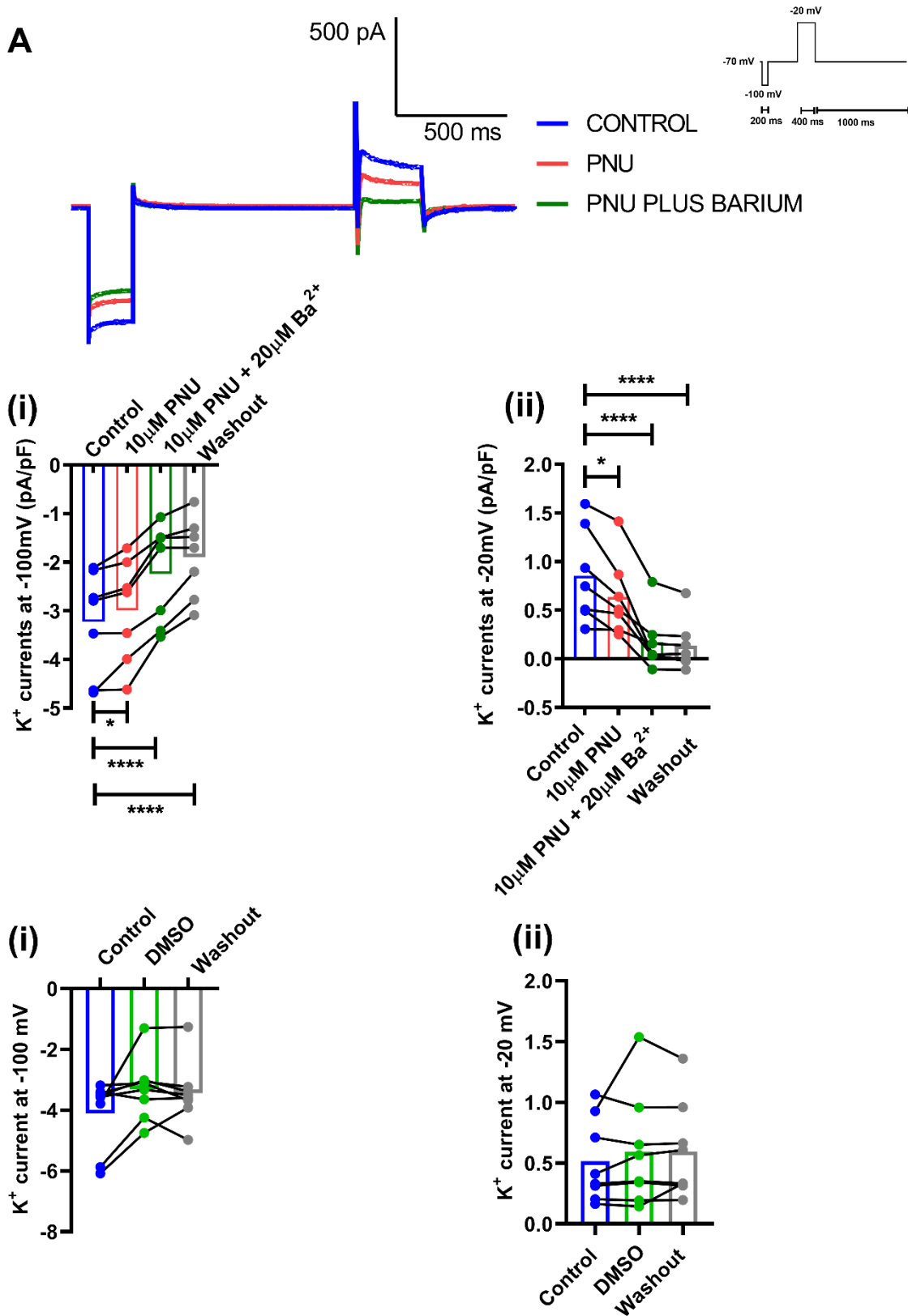
and 20  $\mu$ M Ba<sup>2+</sup>, recorded for 4 min. The K<sup>+</sup> currents recorded in normal conditions and following the application of these inhibitors were compared (Figure 3.9A). From this figure, the  $K_{ir}6.1$  selective blocker (PNU) reduced the size of the K<sup>+</sup> currents. Furthermore, the combination of blockers (PNU+Ba<sup>2+</sup>) blocked a greater proportion of the cardiac potassium inward rectifier currents. The reduction of K<sup>+</sup> currents was more notable at -20 mV than at -100 mV. This is of particular importance, as it is within the normal physiological range of the I<sub>K1</sub> in cardiomyocytes, where this current shows its rectification.

Figure 3.9B shows the mean data for inward rectifier currents in control conditions and following perfusion with different inhibitors. At -100 mV, the mean data of K<sup>+</sup> currents was significantly decreased by both pharmacological treatments from  $-3.2 \pm 0.4$  pA/pF at control to  $-2.9 \pm 0.4$  pA/pF with PNU treatment ( $p=0.04$ ), and a further reduction to  $-2.2 \pm 0.4$  pA/pF with a combination of Ba<sup>2+</sup> and PNU ( $p<0.0001$ ) ( $n=7$ ) (Figure 3.9B(i)). There was also a significant difference between these pharmacological inhibitors in the I<sub>K1</sub> at -100 mV ( $p=0.025$ ). In addition to that, the mean K<sup>+</sup> currents ( $n=7$ ) at -100 mV was decreased from the controls to  $-1.9 \pm 0.7$  pA/pF with washout ( $p<0.0001$ , Figure 3.9B(i)). Further, at -20 mV, a significant reduction of the mean K<sup>+</sup> currents was recorded as  $0.9 \pm 0.2$  pA/pF in the control condition and  $0.6 \pm 0.2$  pA/pF at 10  $\mu$ M PNU ( $p=0.05$ ) ( $n=7$ ), and an additional reduction was observed with a combination of 20  $\mu$ M Ba<sup>2+</sup> and 10  $\mu$ M PNU to  $0.2 \pm 0.1$  pA/pF ( $p<0.0001$ ) (Figure 3.9B(ii)). However, the reduction in the I<sub>K1</sub> at -20 mV was not significant between these pharmacological inhibitors ( $p=0.16$ ). The mean K<sup>+</sup> currents at -20 mV showed a further reduction following the washout of the pharmacological treatment, being  $0.1 \pm 0.1$  pA/pF ( $n=7$ ,  $p<0.0001$ , Figure 3.9B(ii)). Consequently, the washout recordings of pharmacological inhibitors concluded the presence of rundown in K<sup>+</sup> currents. This finding might be attributed to the presence of a residual block; however, the results should be applicable also to an identical time recording on this experimental protocol to verify whether modulation of this K<sup>+</sup> current has been resulted from rundown in these experiments or these could be not washed out completely.

Time-matched recordings were carried out to determine whether decreases in I<sub>K1</sub> could be attributed to rundown. Figure 3.9C shows the mean K<sup>+</sup> currents in the presence of vehicle (DMSO) at time points equivalent to control, PNU administration and with a combination of

$\text{Ba}^{2+}$  and PNU. At -100 mV, the mean  $\text{K}^+$  currents was not altered from  $-4.1 \pm 0.4 \text{ pA/pF}$  at baseline to  $-3.3 \pm 0.4 \text{ pA/pF}$  at the equivalent time of drug addition, and to  $-3.4 \pm 0.4 \text{ pA/pF}$  at time matched for the combination of drugs ( $n=8$ ,  $p=0.08$ ,  $p=0.23$ , respectively) (Figure 3.9C(i)).  $\text{K}^+$  currents at -20 mV were also not significantly altered, recording from  $0.5 \pm 0.1 \text{ pA/pF}$  to  $0.6 \pm 0.2 \text{ pA/pF}$  and to  $0.6 \pm 0.1 \text{ pA/pF}$  ( $n=8$ ,  $p=0.56$ ,  $p=0.38$ , respectively, Figure 3.9C(ii)). Consequently, the experiments with the time-matched controls concluded that the effects of rundown in  $\text{K}^+$  currents at -100 mV and -20 mV were negligible.

These findings suggest that the application of both PNU and  $\text{Ba}^{2+}$  have a cumulative effect on inhibiting  $I_{\text{K}1}$ . These data suggest that the external  $\text{Ba}^{2+}$  and PNU blocked different components of the  $I_{\text{K}1}$ . This provides evidence that the  $\text{K}_{ir6.1}$  current may contribute to the  $I_{\text{K}1}$ .



**Figure 3.9:** The  $K_{ir}6.1$  is a component of the  $I_{K1}$  in cardiomyocytes using selective blockers of  $K_{ir}6.1$  and  $K_{ir}2.1$ .

*A,  $I_{K1}$  was recorded at two membrane potentials using voltage-clamp from rat ventricular myocytes. A voltage step of -100 mV was first applied for 200 ms with a second step to -20 mV for 400 ms.  $I_{K1}$  were measured during NT solution for isolated ventricular myocytes (blue line), following 10  $\mu$ M PNU for 4 min (red line), finally with the addition of 20  $\mu$ M Ba<sup>2+</sup> for 4 min (green line). B(i), The bar chart shows a significant reduction in the mean  $I_{K1}$  at -100 mV with both 10  $\mu$ M PNU treatment and 20  $\mu$ M Ba<sup>2+</sup>+10  $\mu$ M PNU ( $n=7$ , \* $p=0.04$ , \*\*\*\* $p<0.0001$ , respectively). Additionally, there was a significant decrease in  $I_{K1}$  in washout recordings versus controls ( $n=7$ , \*\*\* $p<0.0001$ ). B(ii), This graph shows the mean data ( $n=7$ ) of  $I_{K1}$  at -20 mV in the absence and the presence the same manner of inhibitor drugs, demonstrating gradual reduction of  $I_{K1}$  and did change following washout of inhibitor drugs ( $n=7$ , \* $p=0.05$ , \*\*\* $p<0.0001$ , and \*\*\*\* $p<0.0001$ , respectively). C(i), Histograms show the mean  $I_{K1}$  ( $n=8$ ) at -100 mV of isolated cardiomyocytes in a time-matched fashion, showing non-significant change ( $n=8$ ,  $p=0.08$ ,  $p=0.23$ , respectively). C(ii),  $I_{K1}$  at -20 mV were not significantly affected by the run-down phenomena at time-matched corresponding measurements in the absence of the inhibitors ( $n=8$ ,  $p=0.56$ ,  $p=0.38$ , respectively). (one-way ANOVA Holm–Sidak post-test).*

### 3.2.7 Calcium transients are shortened by $K_{ir}6.1$ activation in rat ventricular myocytes

We hypothesised that activation of  $K_{ATP}$  channels in ventricular myocytes, which are formed from both  $K_{ir}6.2$  and  $K_{ir}6.1$  as pore-forming subunits (Morrissey et al., 2005b; Li et al., 2013; Aziz et al., 2017), shortens the cardiac action potential, as presented in Section 3.2.2. The opening of  $K_{ATP}$  channels was achieved by the application of pinacidil at a range from 10  $\mu$ M to 300  $\mu$ M (Cole et al., 1991; Glukhov et al., 2010). Therefore, this markedly shortening of APD could impart cardioprotection by limiting calcium accumulation during each systolic interval, thus reducing cellular energy. The hypothesis tested in this section is whether the calcium transients could be regulated by potentiation of  $K_{ir}6.2$  and  $K_{ir}6.1$ -containing  $K_{ATP}$  channels in cardiac muscle cells in the presence of a low (50  $\mu$ M) and high (200  $\mu$ M) concentration of pinacidil treatment.

Isolated cardiomyocytes were loaded with Ca<sup>2+</sup> sensitive dye Fura-2 for 20 min. Cardiac action potentials are triggered by stimulating the cells at 1 Hz. Cardiomyocytes were perfused with NT solution for 2 min, followed by separately exposing the cells for 3 min to 50  $\mu$ M pinacidil and a solution containing 200  $\mu$ M pinacidil treatment. The Ca<sup>2+</sup> transients were recorded for 30 s at the end of each stage.

Figure 3.10A shows representative traces of  $\text{Ca}^{2+}$  transients for cardiomyocytes in the NT solution (control), 50  $\mu\text{M}$  pinacidil, and 200  $\mu\text{M}$  pinacidil, illustrating a notable decrease of  $\text{Ca}^{2+}$  transients. In some cardiomyocytes pre-treated with a high pinacidil concentration, 200  $\mu\text{M}$ , showed a complete loss of the  $\text{Ca}^{2+}$  transients. A possible explanation might be that 200  $\mu\text{M}$  pinacidil can cause complete action potential failure in some cells via  $\text{K}_{ir6.2}$  containing  $\text{K}_{ATP}$  activation. This complete failure of cardiac action potential might provide a final step in the cardioprotection that can be afforded to the myocardium during severe ATP depletion. For the analysis, the ratio of emission signals (340:380) was measured together with the area under the curve. A significant decline in the amplitude of  $\text{Ca}^{2+}$  transients was recorded from  $0.05 \pm 0.002$  (Controls, n=142) to  $0.04 \pm 0.003$  (50  $\mu\text{M}$  pinacidil, n=65, \*\*\*p<0.0001) and  $0.03 \pm 0.002$  (200  $\mu\text{M}$  pinacidil, n=77, \*\*\*p<0.0001), as shown in Figure 3.10B(i). Figure 3.10B(ii) demonstrates that pinacidil induced a significant reduction in the AUC of the  $\text{Ca}^{2+}$  transient, from  $0.02 \pm 0.001$  (controls, n=142) to  $0.011 \pm 0.001$  (50  $\mu\text{M}$  pinacidil, n=65, \*\*\*p<0.0001) and  $0.007 \pm 0.001$  (200  $\mu\text{M}$  pinacidil, n=77, \*\*\*p <0.0001). There was a significant difference in the alteration in AUC of  $\text{Ca}^{2+}$  transients between low-concentration (50  $\mu\text{M}$ ) pinacidil and high-concentration (200  $\mu\text{M}$ ) pinacidil treatments (\*\*p=0.01), however; a reduction in the amplitude of  $\text{Ca}^{2+}$  transients was not significant between these concentrations of pinacidil treatment (p=0.06). Additionally, a significant decrease in the duration of the  $\text{Ca}^{2+}$  transients was recorded with pinacidil in concentration-dependent (n=142 for control, n=65 for 50  $\mu\text{M}$  pinacidil, n=77 for 200  $\mu\text{M}$  pinacidil, \*\*\*p<0.0001, \*\*p<0.01, respectively), as shown in Figure 3.10B(iii). Further time-match control experiments or recovery of the  $\text{Ca}^{2+}$  transient amplitude following washout of pinacidil treatments will be needed to exclude photobleaching and/or extrusion of Fura-2 from the cells. However, with Fura-2, rather than single wavelength indicators, such as Fluo-4, the photobleaching would tend to occur in both wavelengths simultaneously. This leaves the ratio unchanged and therefore suggests that any decrease in signal is due to an effect of a drug rather than a photobleaching effect.

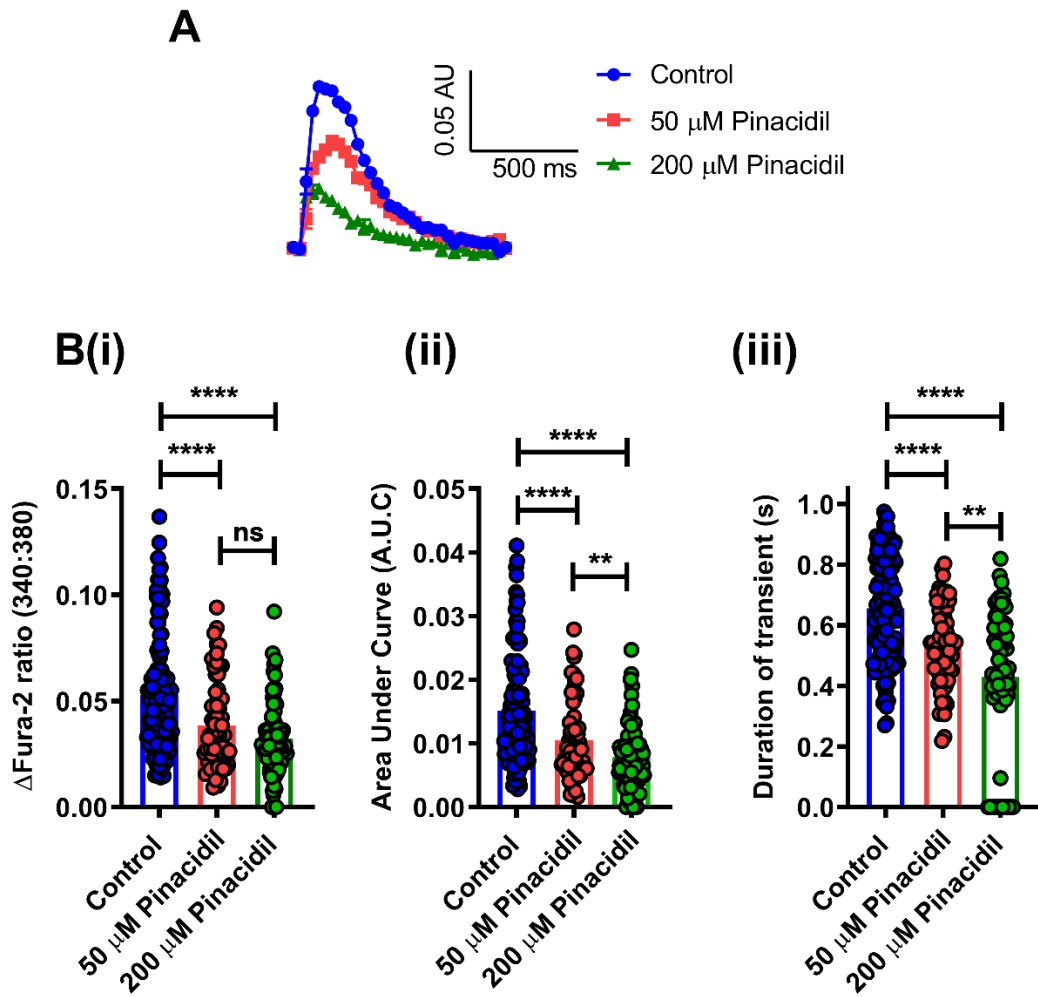


Figure 3.10: Pinacidil treatment at different concentrations reduced  $\text{Ca}^{2+}$  transients.

*A, Representative traces showing  $\text{Ca}^{2+}$  transients during cardiac action potentials in rat cardiomyocytes using Fura-2-AM as an intracellular calcium indicator, from control (blue line) to 50  $\mu\text{M}$  pinacidil (red line) and 200  $\mu\text{M}$  pinacidil (green line). B(i), Histograms show the peak of  $\text{Ca}^{2+}$  transients which is significantly reduced with pinacidil treatment ( $n=142$  for control,  $n=65$  for 50  $\mu\text{M}$  pinacidil,  $n=77$  for 200  $\mu\text{M}$  pinacidil,  $****p<0.0001$  for both concentrations). B(ii), Graphs showing that pinacidil led to a significant concentration-dependent decrease in the area under the curve of the  $\text{Ca}^{2+}$  transients ( $n=142$  for control,  $n=65$  for 50  $\mu\text{M}$  pinacidil,  $n=77$  for 200  $\mu\text{M}$  pinacidil,  $****p<0.0001$ ,  $**p<0.01$ , one-way ANOVA Holm–Sidak post-test). B(iii), Graphs showing that pinacidil led to a significant concentration-dependent decrease in the duration of the  $\text{Ca}^{2+}$  transients ( $n=142$  for control,  $n=65$  for 50  $\mu\text{M}$  pinacidil,  $n=77$  for 200  $\mu\text{M}$  pinacidil,  $****p<0.0001$ ,  $**p<0.01$ , one-way ANOVA Holm–Sidak post-test).*

### 3.2.8 Calcium transients are prolonged by Kir6.1 inhibition in rat ventricular myocytes

The previous results, shown in Section 3.2.4.1, suggested that Kir6.1 inhibition prolonged the action potential duration of ventricular cardiomyocytes. Therefore, we examined the hypothesis of whether blockade of Kir6.1 using PNU indeed increases Ca<sup>2+</sup> accumulation in cardiomyocytes. Isolated cells were loaded with Ca<sup>2+</sup>-sensitive dye, Fura-2, for 20 min and stimulated at 1 Hz. Isolated cardiomyocytes were perfused with NT solution for 2 min to record a steady state of Ca<sup>2+</sup> transients and then followed by recording the same field of cells following exposure to a solution containing 3 μM PNU for 3 min. At the end of each stage, Ca<sup>2+</sup> transients were recorded for 30 s.

The Ca<sup>2+</sup> transient recordings in the control condition and after the application of PNU treatment are shown in Figure 3.11A. Ca<sup>2+</sup> transients at the end of PNU treatment exhibited a significantly higher amplitude compared to control conditions, with 0.065±0.01 for controls versus 0.073±0.01 for 3 μM PNU (n=43, \*\*\*p=0.0002) (Figure 3.11B(i)). The effect was also measured on the AUC of Ca<sup>2+</sup> transients which showed a significant increase to 0.025±0.004 following PNU treatment (3 μM PNU, n=43, \*\*\*p=0.0003) compared to the control conditions 0.022±0.003, Figure 3.11B(ii). Figure 3.11B(iii) demonstrates that 1 μM PNU caused a significant prolongation of the duration of the Ca<sup>2+</sup> transients (n=43, \*\*p=0.038). These data showed that selective blockade of cardiac Kir6.1 containing channels enhanced the accumulation of intracellular Ca<sup>2+</sup>. However, future work including time-match controls will be needed to exclude possible photobleaching and/or extrusion of Fura-2 from the cells. However, as mentioned previously, photobleaching is unlikely with Fura-2.

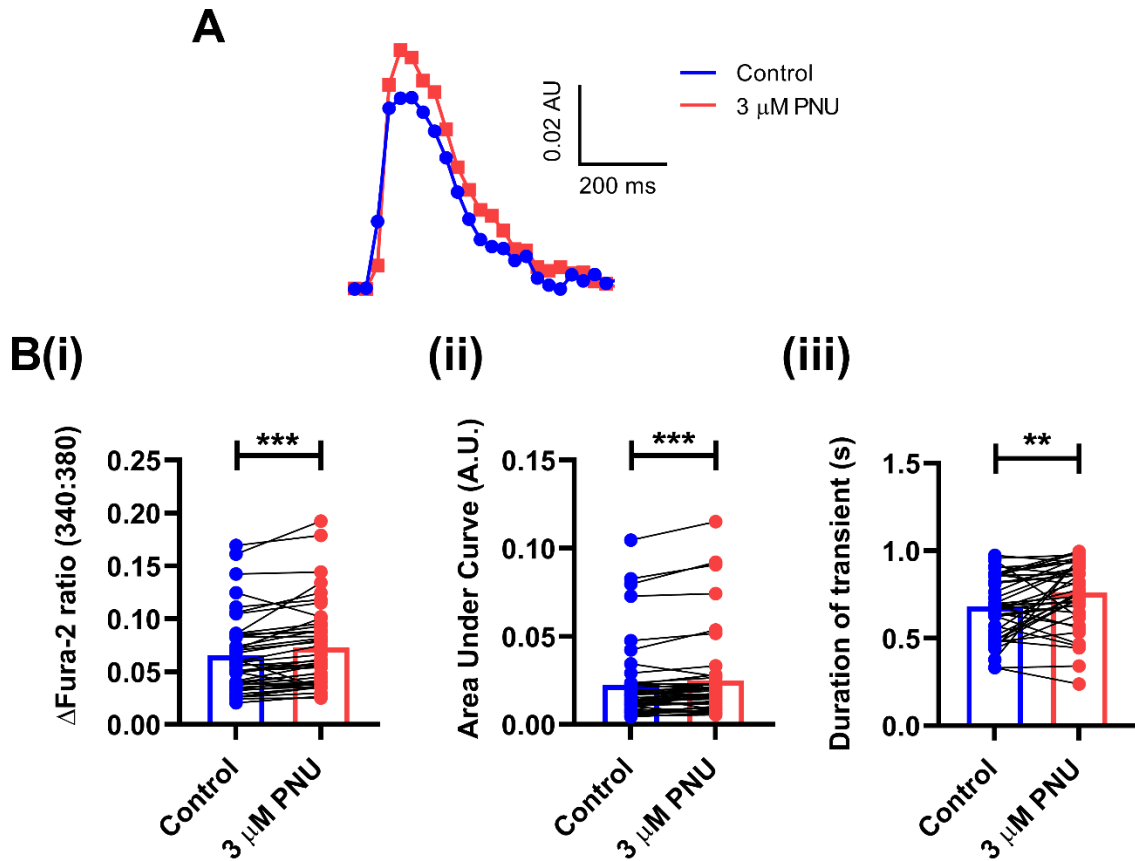


**Figure 3.11:** PNU treatment increased  $\text{Ca}^{2+}$  transients, which may have a cardiotoxic effect to cardiac muscle cells during metabolic stress.

*A, Representative traces of  $\text{Ca}^{2+}$  transients during cardiac action potentials in rat cardiomyocytes using Fura-2-AM as a sensitive intracellular calcium indicator, from control (blue line) to pharmacologically pre-treated myocytes (red line). B(i), Graph showing 3  $\mu$ M PNU caused a significant rise in the peak of  $\text{Ca}^{2+}$  transients ( $n=43$ , \*\*\* $p=0.0002$ ; paired t-test). B(ii), Graph showing that 1  $\mu$ M PNU increased the AUC of the  $\text{Ca}^{2+}$  transients ( $n=43$ , \*\*\* $p=0.0003$ ; paired t-test). B(iii), graphy showing that 1  $\mu$ M PNU caused a prolongation of the transient duration ( $n=43$ , \*\* $p=0.038$ ; paired t-test).*

### 3.2.9 Potentiation of ventricular $K_{ir6.1}$ channels with pinacidil delays $K_{ir6.2}$ channel openings during metabolic inhibition

Cardioprotected cells differ from unprotected cells via a delay in the time taken to activate the cardiac  $K_{ATP}$  ( $K_{ir6.2}/SUR2A$ ) current following metabolic inhibition, which is caused by ATP depletion during metabolic stress (Brennan et al., 2015). Based on the previous results, we hypothesised that activation of  $K_{ir6.1}$  containing channels in cardiomyocytes shortened the cardiac action potential and reduced calcium overload to limit the utilisation of cellular ATP.

To investigate a delay in the time for  $K_{ir}6.2/SUR2A$  activation after perfusion with selective activation of  $K_{ir}6.1$ , cell-attached patch recording was used. In control experiments, cells were perfused with NT for 1 min, and then exposed to substrate-free metabolic inhibition Tyrode's solution (SFT-MI) containing cyanide and iodoacetic acid to inhibit glycolysis and the electron transport chain, respectively, to activate the classic cardiac  $K_{ATP}$  current (Figure 3.12A). Cardiomyocytes were perfused with 100  $\mu M$  pinacidil for 5 min prior to exposure to the metabolic inhibition to activate  $K_{ir}6.1$  containing channels (Figure 3.12A). In metabolic inhibition, the opening of  $K_{ir}6.2/SUR2A$  channel for longer than 100 ms was used as a surrogate marker of ATP depletion, displaying an amplitude of  $\sim 10$  pA in the recording conditions described. To investigate the effect of selective potentiation of  $K_{ir}6.1$  current, we measured the time difference from the beginning of the metabolic inhibition to the first burst of  $K_{ir}6.2/SUR2A$  activity greater than 100 ms in duration.

Figure 3.12B(i) shows a representative trace of cardiac  $K_{ATP}$  current activity on the cell membrane for cardiomyocytes in NT solution and after perfusion with metabolic inhibition, demonstrating two levels of the cardiac  $K_{ATP}$  current amplitude:  $\sim 5$  pA in the control condition (ATP-insensitive  $K_{ir}6.1$  channel), and  $\sim 10$  pA following the introduction of the metabolic inhibitor (ATP-sensitive  $K_{ir}6.2$  channel) as shown in Figure 3.12B(ii) and (iii), respectively.

Pre-treating with 100  $\mu M$  pinacidil led a significant delay in the  $K_{ir}6.2/SUR2A$  opening, from  $245.2 \pm 14.1$  s (control,  $n=31$ ) to  $305 \pm 20.4$  s (100  $\mu M$  pinacidil,  $n=20$ , \* $p=0.016$ , Figure 3.12C(i)). The effect of 100  $\mu M$  pinacidil on  $K_{ir}6.1$  channel can be visualised using amplitude histograms in control conditions and in the presence of pharmacological treatment. Representative amplitude histograms of the  $K_{ir}6.1$  channel open probability during control and 100  $\mu M$  pinacidil, showed values close to 0 pA (the shut level or closed state) and  $\sim 5.5$  pA (the opening level of  $K_{ir}6.1$ ) (Figure 3.12C(ii)). The increase in  $K_{ir}6.1$  channel opening with pinacidil treatment is shown as an increase in the peak at  $\sim 5.5$  pA, compared with control conditions (Figure 3.12C(ii)). Additionally, the amplitude histogram shows a second peak of opening level of  $K_{ir}6.1$  channel in the presence of 100  $\mu M$  pinacidil, at  $\sim 11$  pA which indicates multiple openings of the same channel type. Finally, the peak indicating the closed state of the channel suggests that the  $K_{ir}6.1$  activity spends less time in the closed state in the presence of pinacidil.

Figure 3.12C(iii) shows the mean data for the  $K_{ir}6.1$  channel open probability ( $NP_o$ ) in control conditions and following perfusion with pinacidil and SFT-MI. The application of pinacidil as a pre-treatment prior to metabolic inhibition resulted in a significant increase in  $NP_o$  of the  $K_{ir}6.1$  channel. This was recorded with 100  $\mu M$  pinacidil treatment, from  $0.09 \pm 0.02$  (control,  $n=19$ ) to  $0.18 \pm 0.04$  (100  $\mu M$  pinacidil,  $n=19$ ,  $p=0.001$ ). However, the  $NP_o$  of the  $K_{ir}6.1$  channel was not significantly different to control following metabolic inhibition ( $0.09 \pm 0.02$  vs  $0.07 \pm 0.02$ ,  $n=19$ ,  $p=0.43$ ). This indicates that a 100  $\mu M$  pinacidil induced a marked increase in channel open probability of the  $K_{ir}6.1$  with an amplitude of  $\sim 5.5$  pA. At the single channel level, no  $K_{ir}6.2$  activity was observed until SFT-MI was applied.

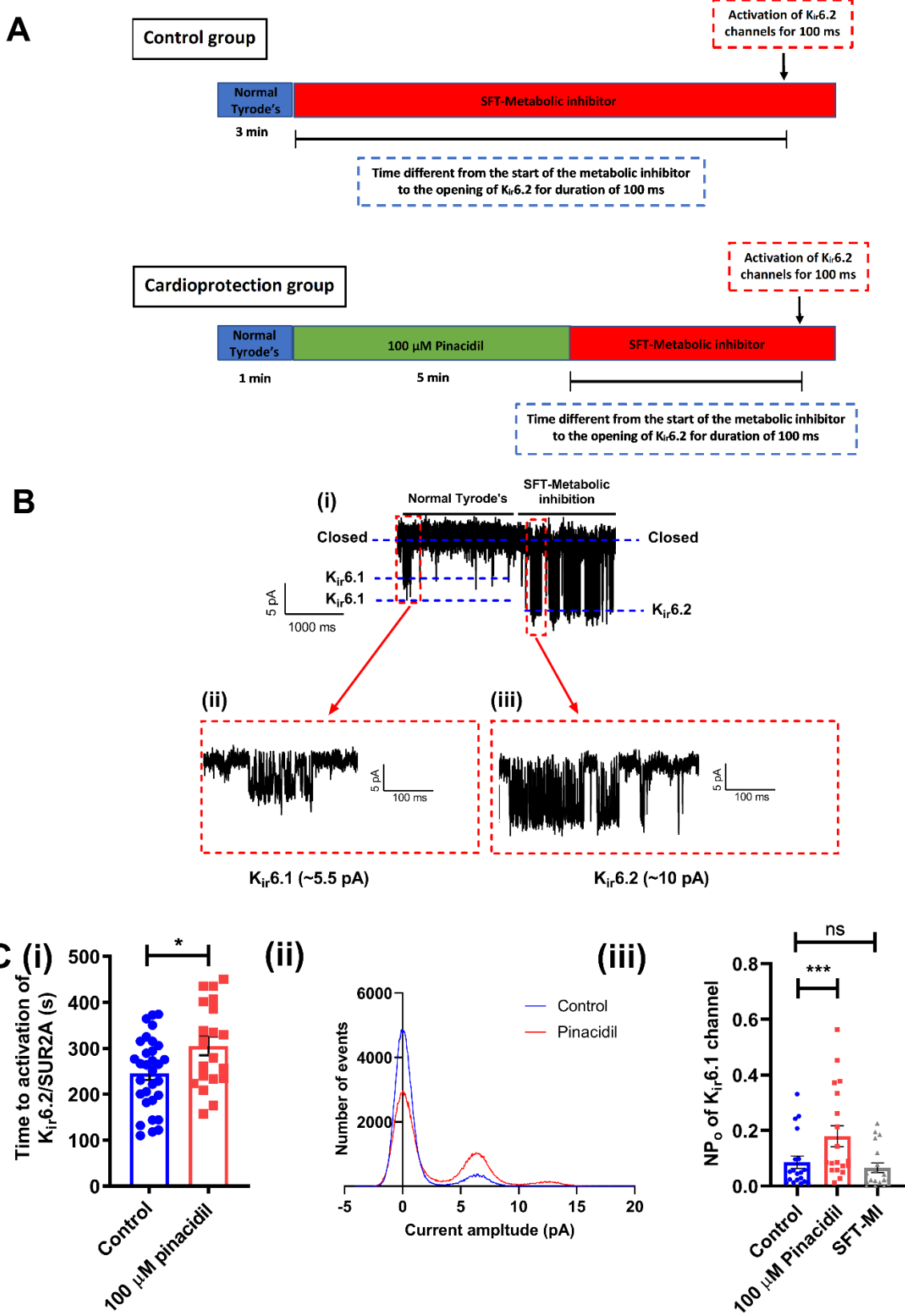


**Figure 3.12:** Potentiation of  $K_{ir}6.1$  led to a delay in the opening of  $K_{ir}6.2/SUR2A$  channels and consequently delayed time to ATP depletion.

*A, Protocols to measure the time to opening of  $K_{ir}6.2/SUR2A$  channels in cell attached recording. The time difference between the beginning of the metabolic inhibition to the first burst of activity greater than 100 ms was measured. B, Representative traces of cardiac  $K_{ATP}$  current activity in the cell attached patch recordings, showing ~5 pA in the control condition (ii), and ~10 pA following the introduction of the metabolic inhibitor (iii). C(i), Bar chart showing the time to activation of cardiac  $K_{ATP}$  ( $K_{ir}6.2/SUR2A$ ) current was significantly delayed (control, n=31 vs. 100  $\mu$ M pinacidil, n=20, \*p=0.016) (unpaired t-test). C(ii), Representative amplitude histograms of a 1 min interval assessed in the absence and presence of 100  $\mu$ M pinacidil, showing increased in the peak of opening level of  $K_{ir}6.1$  at ~5.5 pA in the presence of pinacidil. C(iii), Graphs showing the mean  $NP_o$  of  $K_{ir}6.1$  channels in control cells, in cells treated with 100  $\mu$ M pinacidil and following the perfusion of SFT-metabolic inhibition. There was a significant increase in  $NP_o$  following perfusion with pinacidil, however, there was no significant difference in  $NP_o$  following the perfusion of SFT-metabolic inhibition, compared to controls (n=19, p=0.001, p=0.43, respectively) (One-way ANOVA with Holm-Sidak post-test).*

### 3.2.10 Potentiation of ventricular $K_{ir}6.1$ channels by pre-treatment with pinacidil imparts cardioprotection in isolated rat ventricular myocytes

The previous results showed that  $K_{ATP}$  activation caused a shortening of APD so presumably limiting  $Ca^{2+}$  channel activation so reducing  $Ca^{2+}$  transients (Section 3.2.2 and 3.2.7). It was hypothesised that pharmacological modulation of  $K_{ATP}$  channel could impart protection to cardiomyocytes. To investigate this hypothesis, isolated cardiomyocytes were subjected to metabolic inhibition and reperfusion protocols under control conditions and pharmacological treatments (protocol outlined in Figure 3.13A). Isolated cardiomyocytes were perfused with NT for 3 min, followed by perfusion with SFT-MI for 7 min to simulate ischaemia, and then for 10 min with NT to simulate reperfusion injury. The contractile function of cardiomyocytes was examined by stimulating cells at 1 Hz via electric field stimulation (EFS) throughout this protocol. For the analysis, several parameters were measured: the time for contractile failure (as a measure of the time to ATP depletion), the percentage of cells recovering their contractile function, and the percentage of cell survival (as measured using trypan blue exclusion).

Figure 3.13B(i) shows the time course of the effects of metabolic inhibition on contractile function and contractile recovery. This figure suggests that pinacidil imparted

cardioprotection, as seen with an increasing recovery of contractile function for pinacidil-treated compared to untreated cardiomyocytes. It was also noted that prior to perfusion with metabolic inhibition, cardiomyocytes treated with 200  $\mu$ M pinacidil had a decrease in the percentage of contractile cells compared to control cardiomyocytes (~60% of contractile cells with 200  $\mu$ M pinacidil vs. ~80% of contractile cells with NT). The possible loss of contractile function following perfusion of high pinacidil could be explained by an activation of  $K_{ir}6.2$ -containing channels normally involved in late-stage protection via severe shortening or complete failure of the cardiac action potential.

To examine pinacidil pre-treatment-induced cardioprotection, the time from the onset of metabolic inhibition to the time when the cells failed to contract was measured, as shown in Figure 3.13B(ii). The application of pinacidil as a pre-treatment prior to metabolic inhibition resulted in a significant delay in the time to contractile failure. This was most pronounced with 50  $\mu$ M pinacidil treatment, from  $152.4 \pm 1.1$  s (control, n=23) to  $249 \pm 8.4$  s (50  $\mu$ M pinacidil, n=6, \*\*\*\*p<0.0001),  $212.5 \pm 14.8$  s (100  $\mu$ M pinacidil, n=6, \*\*\*\*p<0.0001), and  $184.2 \pm 4.9$  s (200  $\mu$ M pinacidil, n=6, \*\*\*p=0.0002), as shown in Figure 3.13B(ii).

An increased contractile recovery following metabolic inhibition is another hallmark of cardioprotection. To confirm pinacidil-induced cardioprotection, the percentage of cells regaining contractile function at the end of the washout period was assessed. In the control conditions,  $23.9 \pm 1.3\%$  of cardiomyocytes recovered their contractile function following 10 min of reperfusion (n=23) (Figure 3.13B(iii)). Pre-treatment with pinacidil tended to increase the percentage of cardiomyocytes regaining contractile function, and this was pinacidil concentration-dependent. Contractile function increased from  $23.9 \pm 1.3\%$  (control, n=23) to  $66.7 \pm 2.3$  (50  $\mu$ M pinacidil, n= 6, \*\*\*\*p<0.0001),  $77.9 \pm 4.1\%$  (100  $\mu$ M pinacidil, n=6, \*\*\*\*p<0.0001), and  $84.5 \pm 5.0\%$  (200  $\mu$ M pinacidil, n=6, \*\*\*\*p<0.0001), as shown in Figure 3.13B(iii).

As a further indicator of cardioprotection at the end of the reperfusion period, trypan blue was used to stain dead cells and thus indicate the percentage of cell survival. Figure 3.13B(iv) shows that pinacidil treatment increased cell survival from  $69.0 \pm 0.8\%$  (control, n=23) to

$93.7 \pm 1.2\%$  (50  $\mu\text{M}$  pinacidil,  $n=6$ ,  $****p<0.0001$ ),  $95.3 \pm 0.6\%$  (100  $\mu\text{M}$  pinacidil,  $n=6$ ,  $****p<0.0001$ ), and  $100 \pm 0.00\%$  (200  $\mu\text{M}$  pinacidil,  $n=6$ ,  $****p<0.0001$ ).

Together, these data suggest that isolated cardiomyocytes treated with pinacidil were able to maintain contractile function for longer during metabolic inhibition, and showed increased contractile recovery and cell survival, an outcome that was concentration-dependent. This suggests that potentiation of ventricular  $K_{\text{ATP}}$  channels, whether containing of  $K_{\text{ir}}6.1$  subunit or  $K_{\text{ir}}6.2$  subunit, imparts cardioprotection.

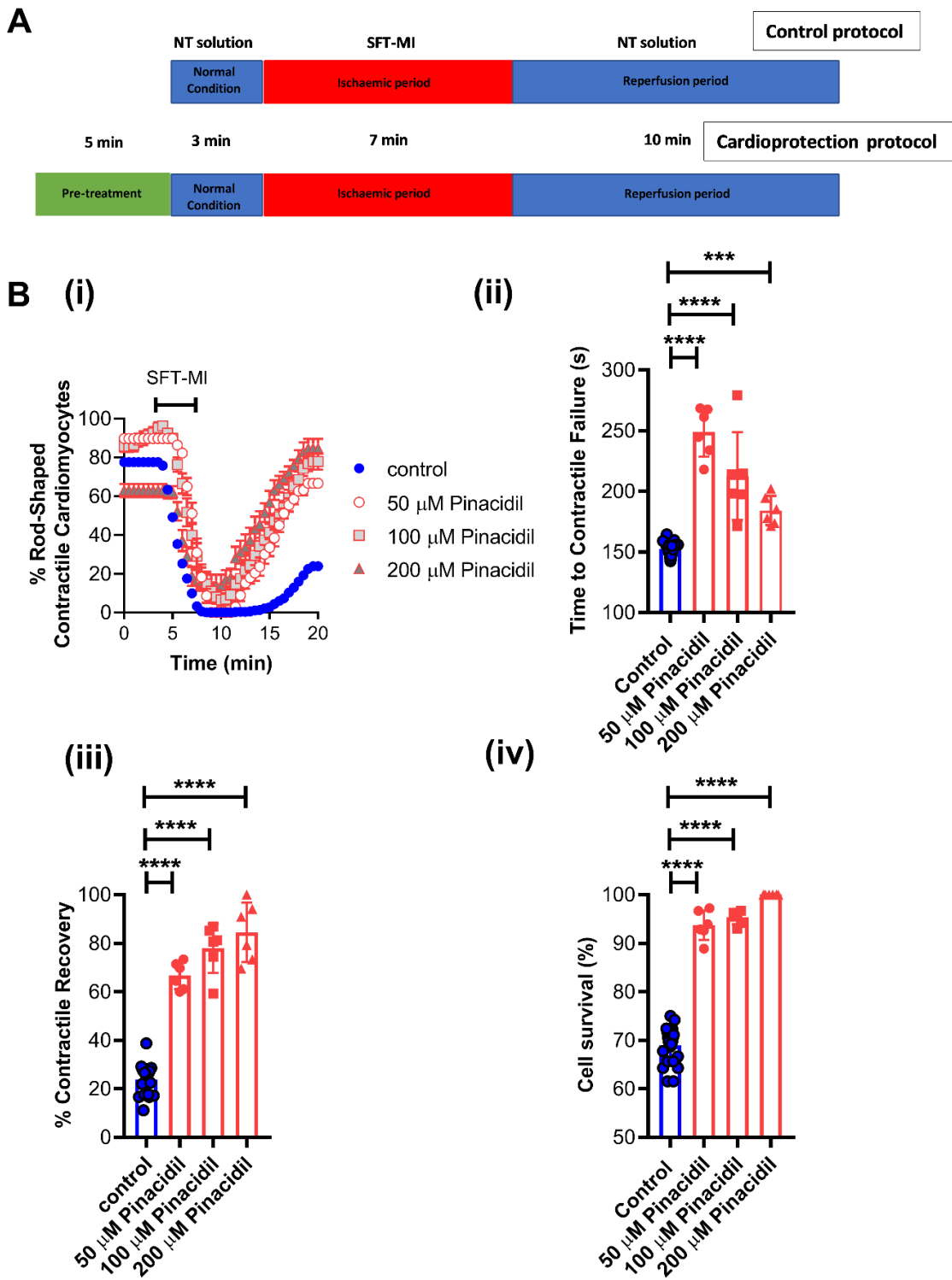


**Figure 3.13:** Pre-treatment with pinacidil imparts cardioprotection in isolated cardiomyocytes.

*A, Example of the protocols used in these experiments. B(i), Example time course showing the percentage of rod-shaped contractile cells throughout the protocol. B(ii), Time to contractile failure (\*\*\*\*p<0.0001, \*\*\*p<0.0001, \*\*p=0.0002, for 50 µM, 100 µM and 200 µM pinacidil). B(iii), The percentage of cardiomyocytes regaining contractile function at the end of reperfusion, (\*\*\*\*p<0.0001 for all concentrations). B(iv), Bar chart showing the mean percentage of cell survival (\*\*\*\*p<0.0001 for all concentrations) (one-way ANOVA with Holm–Sidak post- test).*

### 3.2.11 PNU37883 is cardiotoxic to cells during metabolic inhibition protocol

As documented previously, PNU tended to prolong the cardiac action potential by blocking ventricular  $K_{ir}6.1$  channels, and we also documented that this treatment caused a significant increase of  $Ca^{2+}$  transients (Section 3.2.4.1 and 3.2.8). To investigate whether blocking  $K_{ir}6.1$  is cardiotoxic, the effects of PNU during simulated ischaemia and reperfusion were investigated. For the control group, isolated cardiomyocytes were perfused with NT for 3 min, followed by perfusion with SFT-MI for 7 min to simulate ischaemia, and then for 10 min with NT to simulate reperfusion injury. In the pharmacological treatment group, isolated cardiomyocytes were exposed to a solution containing SFT-MI and 3  $\mu M$  PNU to determine whether this pharmacological blocker could attenuate ischaemic cardioprotection. We used the protocol outlined in Figure 3.14A. As with the pinacidil recordings from the metabolic inhibition and washout protocols, similar parameters were used to examine the effect of PNU on contractile function, including the time to contractile failure, the percentage of contractile recovery, and the percentage of cell survival.

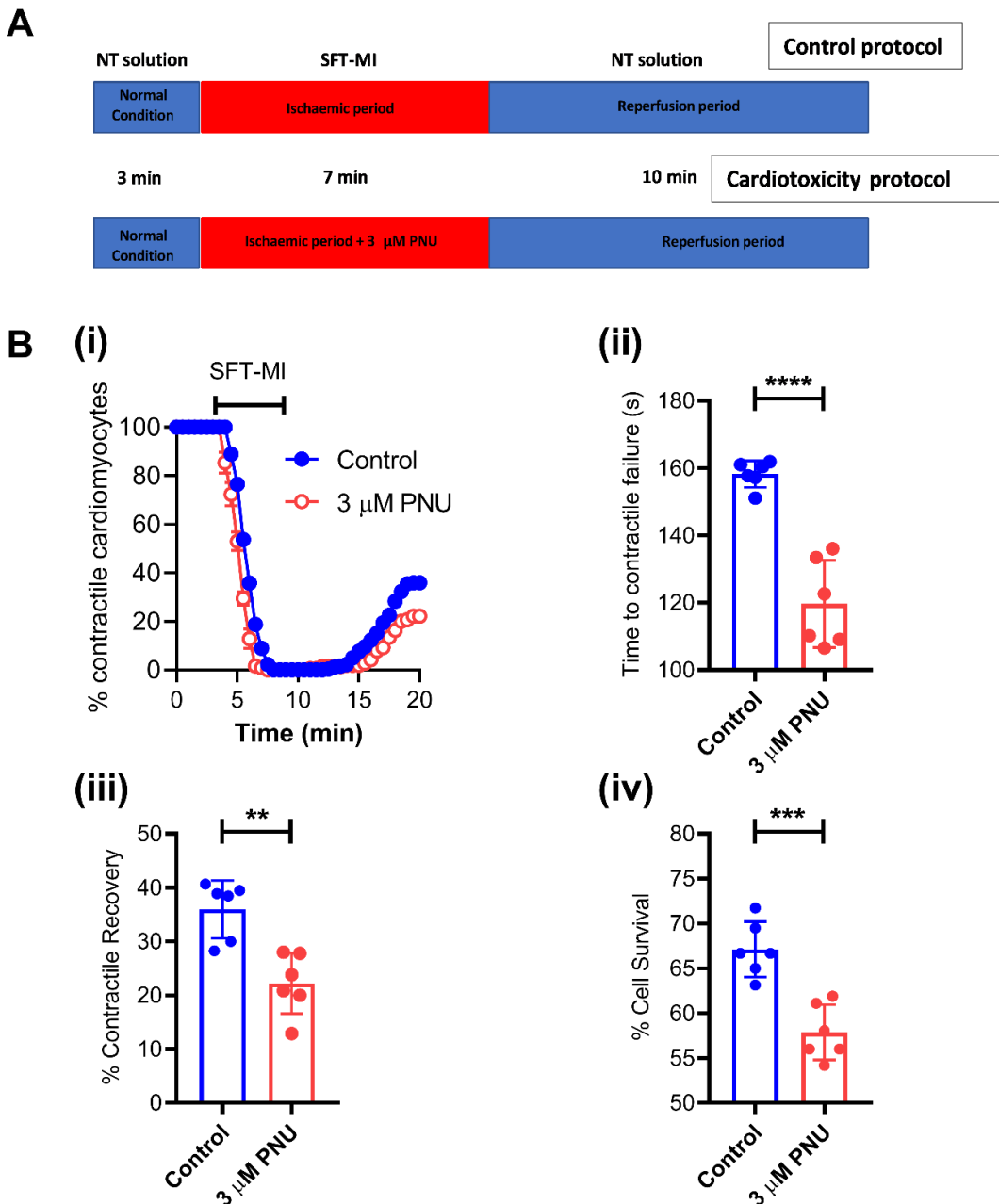
The percentage of contractile isolated cardiomyocytes in response to metabolic inhibition and the regaining of contractile function on reperfusion is shown in Figure 3.14B(i), for both controls and PNU treatments.

Figure 3.14B(ii) shows the time to contractile failure, which was measured from the onset of metabolic inhibition to the time of loss of contractility of cardiomyocytes, to examine the cardiotoxicity of  $K_{ir}6.1$  inhibition. The application of 3  $\mu M$  PNU treatment caused a significantly shortened time to contractile failure, from  $158.3 \pm 1.6$  s (control, n=6) to  $119.7 \pm 5.3$  s (3  $\mu M$  PNU, n=6, \*\*\*p<0.0001).

To further confirm the cardiotoxic effect of PNU treatment, the percentage of cardiomyocytes regaining contractile function after 10 min of reperfusion was measured. The 3  $\mu M$  PNU treatment significantly worsened contractile recovery compared to the control myocytes, from  $36.0 \pm 2.2\%$  (control, n=6) to  $22.2 \pm 2.3\%$  (3  $\mu M$  PNU, n=6, \*\*\*p=0.002), as shown in Figure 3.14B(iii).

Figure 3.14B(iv) shows that the treatment with 3  $\mu$ M PNU attenuated the percentage of cell survival, showing significantly decreased viable cardiomyocytes from 67.1 $\pm$ 1.3% in the control group to 57.9 $\pm$ 1.3% in the PNU group (n=6, \*\*\*p=0.0004).

All three measurement strategies indicated the deleterious impact of 3  $\mu$ M PNU treatment on the contractile function of cardiomyocytes. The application of a K<sub>i</sub>r6.1 blocker in isolated cardiomyocytes had a cardiotoxic effect, evidenced by the accelerated time to contractile failure, as well as the worsening contractile recovery and cell survival at the end of reperfusion.



**Figure 3.14:** The application of PNU treatment leads to cardiotoxic effects on isolated cardiomyocytes during the metabolic inhibition protocol.

*A, Metabolic inhibition and reperfusion protocols for the control group and cardiotoxicity group used in this study (3 min with NT, 7 min with SFT-MI, and treatment was washed out for 10 min with NT in the control; and 3 min with NT, followed by 7 min with SFT-MI+3  $\mu$ M PNU, and then washed out for 10 min with NT in the cardiotoxicity group). B(i), Time course traces showing the percentage of isolated cardiac myocytes in response to the stimulator throughout the protocol in the control and 3  $\mu$ M PNU. B(ii), Time to contractile failure was measured from the onset of the metabolic inhibition period that shows a significant reduction ( $***p<0.0001$ ; unpaired T-test). B(iii), The percentage of cardiomyocytes with 3  $\mu$ M PNU which recovered contractile function, significantly decreased ( $n=6$ ,  $***p=0.0015$ ; unpaired t-test). B(iv), The mean percentage of cell survival at the end of reperfusion for cardiomyocytes was documented which showed a reduction in the number of cell surviving ( $***p=0.0004$ ; unpaired t-test).*

### 3.2.12 The presence of 10 $\mu$ M pinacidil reduced infarct size in a whole heart *ex vivo* coronary ligation model via potentiation of ventricular $K_{ir}6.1$ channels

In the previous section (Section 3.2.10), we showed that pre-treatment with pinacidil tended to improve the contractile recovery of cardiomyocytes during ischaemia and reperfusion. To investigate whether the application of pinacidil had beneficial effects on infarct size following ischaemia and reperfusion, we employed a whole-heart preparation that used a coronary ligation model on a Langendorff system. The rat hearts were stabilised for 1 h, the hearts underwent ischaemia by ligation of the coronary artery for 40 min, and then ligation was released for 3 h to simulate the reperfusion period (the protocol is outlined in Figure 3.15A). Heart slices were stained with Evans blue and TTC: blue indicated non-affected regions (Evans blue dye), red indicated areas at risk, and white indicated necrotic tissue (stained with TTC), as described in Section 2.6. To determine the cardioprotective potential of pinacidil, this pharmacological treatment was perfused throughout the experimental protocol, and the infarct size was measured.

Figure 3.15B shows representative images of sliced rat hearts for the control group and hearts treated with 10  $\mu$ M pinacidil. The percentage of infarct size was significantly reduced in hearts treated with 10  $\mu$ M pinacidil compared to untreated hearts, at  $32.6\pm1.1\%$  (control, n=19) to  $21.3\pm2.2\%$  (10  $\mu$ M pinacidil, n=10, \*\*\* $p<0.0001$ ) (Figure 3.15C). These data suggest that potentiation of  $K_{ir}6.1$  channels provides a cardioprotective effect against damage from ischaemic insult.

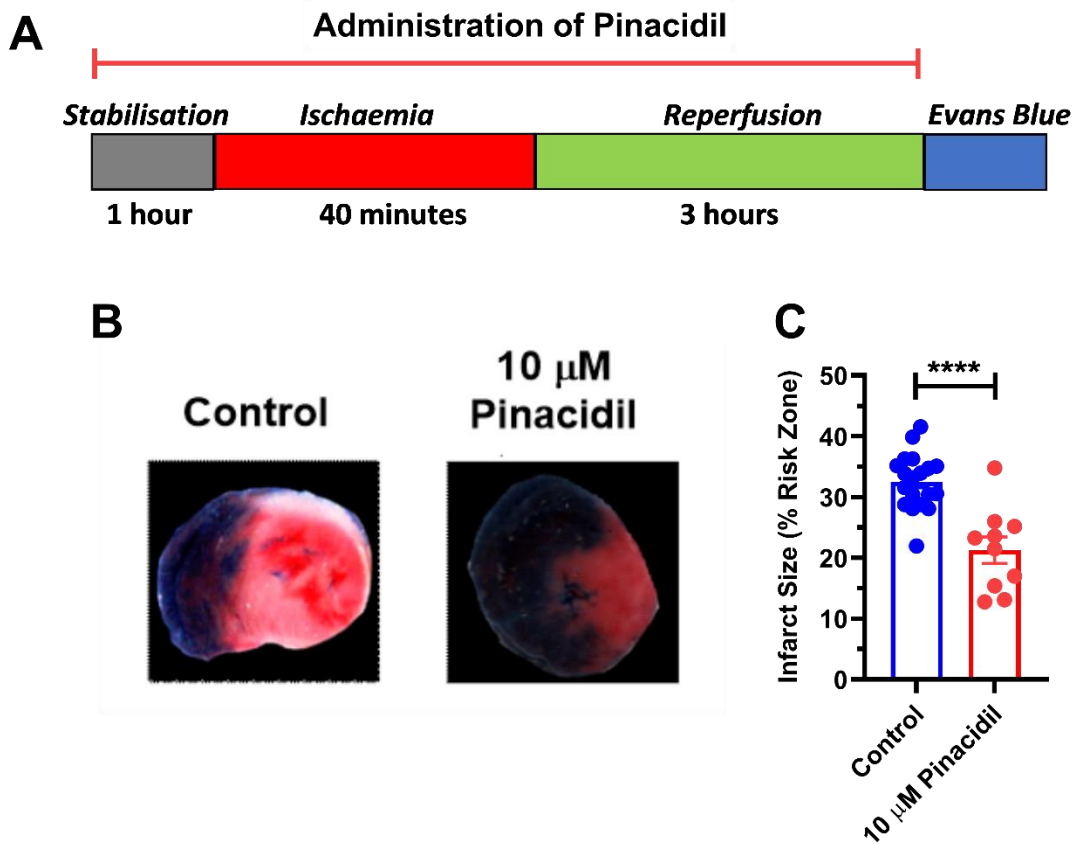


**Figure 3.15:** Pinacidil imparts cardioprotection by reducing infarct size in the whole heart after coronary ligation via potentiation of ventricular  $K_{ir}6.1$  channels.

*A, Protocol designed to examine the effect of  $K_{ir}6.1$  potentiation on the damage from myocardial ischaemia and reperfusion injury: rat hearts were stabilised for 1 h with NT perfusion, and ischaemia was induced by coronary ligation for 40 min, followed by 3 h of reperfusion with NT. Pinacidil was perfused throughout this protocol. B, Representative scanned images of stained hearts during control and 10  $\mu$ M pinacidil which demonstrate reduction of infarct size with pinacidil treatment. C, Bar chart showing that the mean infarct size was significantly reduced after perfusion with 10  $\mu$ M pinacidil (\*\*\*\* $p<0.0001$ ; unpaired t-test).*

### 3.2.13 Selective inhibition of $K_{ir}6.1$ with PNU37883 increased infarct size in a whole heart *ex vivo* coronary ligation model

As previously described, perfusing isolated cardiomyocytes with the  $K_{ir}6.1$  pore-blocker (PNU) (section 3.2.11) caused cardiotoxic effects. We hypothesised that the application of PNU in a whole-heart *ex vivo* coronary ligation model would have a cardiotoxic effect by increasing infarct size. Figure 3.16 shows the protocol used to assess the effects of PNU. To measure the detrimental impact on the size of the infarct area, PNU was perfused during the coronary

ligation period. As with the pinacidil experiments from whole hearts, similar parameters were used to examine the effect of PNU on infarct size and were then compared with the control hearts.

Representative images of slice-stained hearts are shown in Figure 3.16B. Figure 3.16C shows the mean data of infarct size in the absence and presence of 3  $\mu$ M PNU, which indicated a significant increase in the infarct size, from 32.6 $\pm$ 1.1% (control, n=19) to 50.4 $\pm$ 3.7% (3  $\mu$ M PNU, n=6, \*\*\*\*p<0.0001). These results suggest that exposure to  $K_{ir}6.1$  blocker led to extending the infarct size, causing a cardiotoxic effect during myocardial ischaemia.

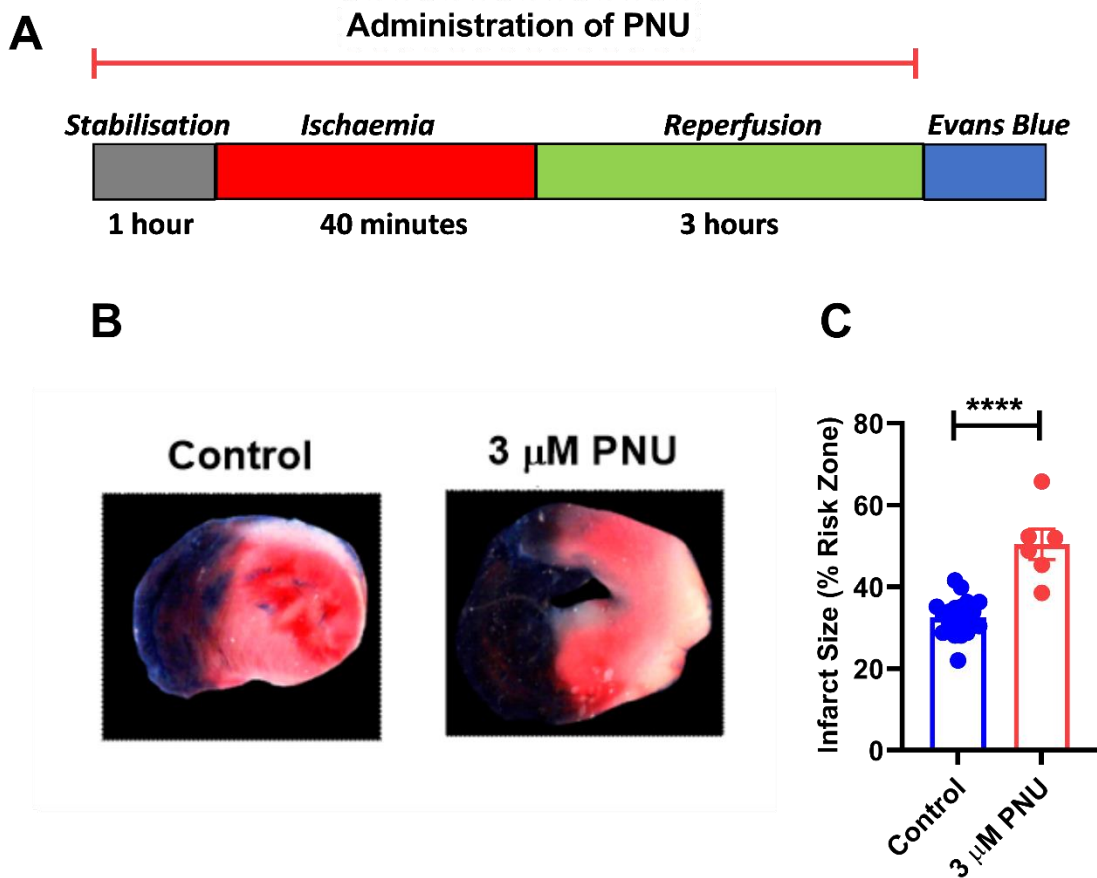


**Figure 3.16:** PNU treatment causes a cardiotoxic effect via inhibition of  $K_{ir}6.1$  channel, increasing the infarct size in whole-heart preparation.

*A, Protocol used to investigate the effect of PNU on infarct size: hearts were stabilised for 1 h with NT perfusion and ischaemia was induced by coronary ligation for 40 min, followed by 3 h of reperfusion with PNU perfused during the coronary ligation period in the same experimental protocol for the treatment group. B, Representative images of stained hearts during control and 3  $\mu$ M PNU which*

demonstrate a larger infarct size with PNU treatment compared to that in the normal untreated heart. C, Histogram showing a larger mean infarct size during PNU perfusion (\*\*\*\* $p<0.0001$ ; unpaired t-test).

### 3.3 Discussion

In the present study, we identified a ventricular SarcoK<sub>iR</sub>6.1 channel by recording current activity on the cell membrane for cardiomyocytes, based on our hypothesis that K<sub>iR</sub>6.1-containing K<sub>ATP</sub> channels and cardiac K<sub>iR</sub>6.2-containing K<sub>ATP</sub> channels are expressed in ventricular muscles. As described previously, the cardiac K<sub>ATP</sub> (K<sub>iR</sub>6.2/SUR2A) channel is considered a metabolic sensor, detecting ATP depletion during myocardial ischaemia, which leads to shortening and ultimately failure of the action potential and consequently sparing of intracellular ATP. This newly identified channel, similar to the canonical K<sub>iR</sub>6.2/SUR2A channel, was hypothesised to be very important in modulating normal physiological process by having a role in altering the action potential duration. Confirming the identity of this K<sub>ATP</sub> channel has been extensive with a publication in preparation for submission. Part of my role in the characterisation of this channel was to use cell-attached patch clamp electrophysiology to record the activity of K<sub>iR</sub>6.1-containing channels, and use metabolic inhibition to distinguish from the canonical cardiac K<sub>ATP</sub> channel (K<sub>iR</sub>6.2/SUR2A). This newly identified channel was characterised by a single current amplitude of ~5pA, which when the single channel conductance was investigated using the IV relationship gave a conductance of 39 pS.

To investigate the physiological role of K<sub>iR</sub>6.1-containing channels at the ventricular cell surface, patch clamp recording was used to measure alterations in the electrophysiological properties, and the effects of specific pharmacological agents that target the K<sub>iR</sub>6.1 subunit. A key finding, was that activation of K<sub>iR</sub>6.1 subunit by pinacidil occurred at concentrations used in previous studies, but that had little to no effect on the canonical K<sub>iR</sub>6.2/SUR2A (<100 μM) but did lead to a delay in the time for opening K<sub>iR</sub>6.2/SUR2A. It was also found that potentiation of this K<sub>iR</sub>6.1 current with a lower concentration of pinacidil than would normally be used in cardiomyocytes (normally up to 200 μM) improved the contractile function of cells following metabolic inhibition and washout. The low concentration of pinacidil (10 μM) can reduce infarct size following an ischaemic insult, however it should be noted that this concentration of pinacidil is known to activate the vascular K<sub>ATP</sub> current (Suzuki et al., 2001;

Kovalev et al., 2004; Selvam et al., 2010). Similarly, although the selective blocker of this newly discovered  $K_{ATP}$  channel had a cardiotoxic effect, the caveat to this is that 3  $\mu M$  PNU37883A could significantly block vascular channels to cause vasoconstriction and so worsen perfusion to the cardiac tissue.

### 3.3.1 Identification of $K_{ir6.1}$ containing channels expressed in sarcolemmal cardiomyocytes and their role in regulation of the cardiac electrophysiology

$K_{ATP}$  channels have been found to be expressed in different tissues with different combinations of various  $K_{ir6.x}$  and SURx subunits, contributing to a variety in their biophysical properties and their sensitivities to pharmacological agents (Foster and Coetze, 2016). This chapter mainly focuses on identifying the functional role of the two known mammalian pore-forming subunits of  $K_{ATP}$  channels in ventricular muscle. The probability of their opening in response to the physiological ATP concentration as an endogenous modulator varies.  $K_{ATP}$  channels in cardiac ventricular myocytes was first identified by Noma (Noma, 1983). Previous research suggests that the opening of the cardiac  $K_{ATP}$  ( $K_{ir6.2}/SUR2A$ ) channels was involved in cardioprotection. It has been proposed that  $K_{ATP}$  openers impart protection by enhancing repolarising potassium current and therefore causing a shortening of APD. This shortening of APD contributes to limiting  $Ca^{2+}$  influx, reducing  $Ca^{2+}$  release so sparing intracellular ATP that would be required to restore  $Ca^{2+}$  levels in diastole (D'Alonzo et al., 1992). There is a consensus that  $K_{ir6.2}$  null mice are prone to cardiotoxicity measured as a worsening the infarct size *in vivo* coronary ligation models (Suzuki et al., 2001; Du et al., 2014).

The findings by Brennan *et al.* (2015) agree with a key role for  $K_{ir6.2}$  in cardioprotection, however do not entirely support the role of cardiac  $K_{ATP}$  ( $K_{ir6.2}/SUR2A$ ) channels in  $K_{ATP}$  agonist-induced cardioprotection (Brennan et al., 2015). This study found that following cardioprotective stimuli, rather than opening earlier to limit electrical excitability, the time to the opening of cardiac  $K_{ir6.2}/SUR2A$  channels was delayed. These findings were rather surprising and suggested that canonical  $K_{ATP}$  channels at the ventricular surface do not impart protection in the early stages of metabolic stress, rather they act as a metabolic sensor of significant ATP depletion. This led to the hypothesis that there was another cardioprotective ion channel that could be active in imparting early-stage protection.

The literature has documented that Kir6.1 pore-forming K<sub>ATP</sub> channels are normally found in vascular smooth muscle cells, and play a unique electrophysiological role in the conduction system controlling the heart rate from the sinoatrial node and inducing vasodilatation (Aziz et al., 2018; Aziz et al., 2014). However, few studies have suggested that it is also expressed in ventricular myocytes and plays an effective role in cardiac function (Singh et al., 2003; van Bever et al., 2004; Pu et al., 2008). These results agree with the findings of other studies, in which Kir6.1 null mice are prone to cardiovascular disorders, such as sudden infant death syndrome, electrocardiographic J wave syndrome, and hypercontractility of coronary arteries (Miki et al., 2002; Tester et al., 2011; Nichols et al., 2013). Furthermore, prior studies have documented a strong relationship between Kir6.1-containing K<sub>ATP</sub> channels and cardiovascular disease such as Cantu syndrome, which is characterised by a gene mutation in Kir6.1 subunit, and this contributes to cardiomyopathy and hypercontractility of cardiac muscles (Huang et al., 2018; Ye et al., 2018). The most interesting finding, which may indicate the functional role of Kir6.1-containing channels in ventricular myocytes, is the absence of ST-segment elevation among animals with deletion of vascular-specific Kir6.1 pore-forming subunits, whereas ST-segment elevation was reported among mice with deletion of the global Kir6.1 subunit (Aziz et al., 2014; Miki et al., 2002; Dart, 2014). According to these data, we can infer that two types of K<sub>ATP</sub> channel may be expressed on the surface of ventricular cardiomyocytes.

In addition to literature demonstrating an importance for Kir6.1 subunit in the heart, the data presented in this chapter support the hypothesis that in Kir6.1-containing channels are present in the ventricular membrane surface and that both pore-forming subunits of K<sub>ATP</sub> channels contribute to ventricular electrophysiology. The current of Kir6.1 pore-forming subunit was identified by using a cell-attached patch holding the pipette potential at +40 mV to maintain the membrane potential of cardiomyocyte at ~-110 mV. The activity of Kir6.1-containing K<sub>ATP</sub> channels passed a current of ~5 pA in amplitude at rest, whereas Kir6.2-containing K<sub>ATP</sub> channels passed a current of ~10 pA in amplitude and were only active following metabolic inhibition. As shown in Figure 3.1, there was a clear difference in the current amplitude between these subunits during recording of cardiac K<sub>ATP</sub> current activity on the cell membrane of rat cardiomyocytes, which suggests the presence of K<sub>ATP</sub>-like channel on ventricular myocytes. The data presented here suggest that Kir6.2-containing K<sub>ATP</sub> channels

are a metabolic sensor that responds to significant ATP depletion, demonstrated by exposing isolated cardiomyocytes to substrate-free metabolic inhibition Tyrode's solution (SFT-MI) containing cyanide and iodoacetic acid to inhibit glycolysis and the electron transport chain, respectively. Although  $K_{ir}6.2$ -containing  $K_{ATP}$  is not thought to be active under rest physiological conditions due to inhibition under normal intracellular ATP ( $\sim 4.7$  mM), the data from this experimental study suggest that this newly identified pore-forming subunit carries a similar characteristic ATP-insensitive  $K_{ir}6.1$  channel. The data presented from cell-attached recordings are consistent with previous literature, which suggests that  $K_{ir}6.1$ -containing  $K_{ATP}$  channels in vascular smooth muscle cells contribute to regulating membrane potential under resting conditions (Teramoto, 2006; Yamada et al., 1997). To confirm that conventional cardiac  $K_{ATP}$  ( $K_{ir}6.2/SUR2A$ ) remains inactive in resting conditions, a reportedly selective  $K_{ir}6.2/SUR2A$  blocker (1  $\mu$ M HMR1098) (Sato et al., 2000a; Manning Fox et al., 2002) was used (Figure 3.8). Under the experimental resting physiological condition, no apparent inhibition of the constitutively active channel was seen.  $K_{ir}6.2/SUR2A$  in whole cell recordings activated by 200  $\mu$ M pinacidil was inhibited by HMR1098, but this could not be tested in cell attached recording activated by metabolic inhibition as HMR1098 has been reported to have reduced efficacy in the presence of elevated ADP as seen in metabolic inhibition (Rainbow et al., 2005). These findings support previous evidence from the literature that  $K_{ir}6.2/SUR2A$  is found to be closed in normal physiological ATP. If this small conductance  $K_{ir}6.1$ -like channel is like the vascular smooth muscle  $K_{ir}6.1/SUR2B$  channel, then this could also be a relatively ATP-insensitive.

Several attempts have been made to investigate  $K_{ir}6.x$  subunit in the functional ion channels in rodent ventricular myocytes by calculating the channel conductance of  $K_{ir}6.x$  isoform because the passing current is largely dependent on this subunit. A greater unitary conductance of  $\sim 80$  pS was found in  $K_{ir}6.2$ -containing  $K_{ATP}$  channels, whereas a low unitary conductance of  $\sim 35$  pS was recorded in  $K_{ir}6.1$ -containing  $K_{ATP}$  channels (Bao et al., 2011; Isomoto et al., 1996; Repunte et al., 1999; Rooper, 2001). The intermediate unitary conductance of  $\sim 58$  pS was investigated in the presence of a heteromultimeric pore-forming channel ( $K_{ir}6.1/K_{ir}6.2$ ) and a debate continues about the expression of  $K_{ir}6.1/K_{ir}6.2$  complex as a native channel in ventricular myocytes (Baron et al., 1999; Seharaseyon et al., 2000). As a result, it is believed that the newly discovered  $K_{ATP}$  channels are formed from a  $K_{ir}6.1/SUR2B$

or Kir6.1/SUR2A complex. The first possible reason may be due to the characteristic of newly identified K<sub>ATP</sub> channels mimicking vascular smooth muscle type K<sub>ATP</sub> channels, which are maintained open under resting conditions to allow vasodilatation. Another possible explanation for this is the single channel current amplitude presented in the resting condition compared to Kir6.2-containing K<sub>ATP</sub> channel (double current amplitude).

Further investigation to characterise the newly identified Kir6.1-containing K<sub>ATP</sub> channel in ventricular myocytes was conducted using a specific pharmacological activator and inhibitor of Kir6.1. Pinacidil is a well-recognised K<sub>ATP</sub> channel opener that leads to increase K<sup>+</sup> efflux, and therefore causes membrane hyperpolarisation (Kowaltowski et al., 2001; Quayle et al., 1994). It was reported that the EC<sub>50</sub> of pinacidil is ~0.2 μM for Kir6.1/SUR2B and ~40 μM for Kir6.2/SUR2A (Grover and Garlid, 2000; Lodwick et al., 2014). Although pinacidil activates all types of K<sub>ATP</sub> channels, the maximum level of Kir6.2/SUR2A activity was not reached at a pinacidil concentration of 100 μM (Satoh et al., 1998). In this study, a pinacidil concentration (≤150 μM) was used to activate Kir6.1-containing K<sub>ATP</sub> channels, which may also cause some brief activation of Kir6.2-containing. We revealed in Figure 3.5 that 150 μM pinacidil had the ability to significantly increase the K<sup>+</sup> current at -20 mV. The effects of 150 μM of pinacidil on the outward current indicated that pinacidil had a significant effect on the cardiac action potential duration. Figure 3.2 showed that 150 μM pinacidil induced a 23.9% shortening of APD<sub>90</sub> in rat ventricular myocytes. This finding is in agreement with Nakayama et al.'s (1990) findings, which showed APD<sub>90</sub> was shortened after application of 150 μM pinacidil in guinea pig cardiomyocytes (Nakayama et al., 1990). The new K<sub>ATP</sub>-like channel is a weakly-rectifying K<sup>+</sup> channels, and therefore the effect of pinacidil on the action potential right across the voltage range was investigated. The findings in Figure 3.2 suggest that pinacidil induced shortened APD at 50% (APD<sub>50</sub>) and 10% (APD<sub>10</sub>) repolarisation by ~12.6% and ~2.7%, respectively. From these observations, a selective opener of Kir6.1 appeared to affect all different levels of repolarisation, and therefore, this Kir6.1-containing K<sub>ATP</sub> channels may be a component of what we know as the I<sub>K1</sub> in ventricular myocytes.

We therefore hypothesised that Kir2.x subunits might not be solely responsible for I<sub>K1</sub>, and Kir6.1 subunit may contribute to I<sub>K1</sub> in cardiac sarcolemma. To test this hypothesis, the reduction of K<sup>+</sup> currents was measured at -20 mV and -100 mV after perfusion with

extracellular Ba<sup>2+</sup> (Kir2.x pore-blocker) (Kubo et al., 1993; Robertson et al., 1996; Zhao et al., 2003) and PNU (Kir6.1 pore-blocker). This served as a pharmacological tool to distinguish between the link of the two pore-forming subunits and the current from I<sub>K1</sub>. A significant inhibition was found from the two different pore types containing channels on I<sub>K1</sub>, as shown in Figure 3.9. These data suggest that the Kir6.1-containing K<sub>ATP</sub> channels play an important physiological role in resting conditions by contributing to I<sub>K1</sub>, which is responsible for maintaining the membrane close to E<sub>K</sub>.

To further investigate the newly identified K<sub>ATP</sub> channel, isolated cardiomyocytes were perfused with PNU37883A (PNU) to examine the pore-forming subunit of this channel. PNU is well documented as a selective Kir6.1 pore-blocker (Kovalev et al., 2004; Ploug et al., 2008). Current inhibition by PNU has been observed in truncated K<sub>ATP</sub> channels that lacked SUR subunits and were expressed on the cardiac cell surface with only pore-forming subunit. This finding suggests that PNU blocks the pore sites of K<sub>ATP</sub> channels. PNU is also known as a non-sulphonylurea K<sub>ATP</sub> blocker. To avoid potential off-target effects of high concentrations of PNU, less than 10 μM was used to assess the role of Kir6.1 in cardiac cells. This was followed by the application of a pan-K<sub>ATP</sub> blocker, glibenclamide (sulphonylurea inhibitor). First, the relationship between the blockade of Kir6.1-containing K<sub>ATP</sub> channels and current was investigated using a whole-cell recording configuration, followed by an investigation of the effect of this pharmacological agent on the cardiac APD. The data in Figure 3.7 showed that the current was significantly reduced following 10 μM PNU treatment, for ~1.9%, ~0.6%, and ~3.0% at -100 mV, -20 mV and +60 mV, respectively. The observed reduction in K<sup>+</sup> current at different voltage steps could be attributed to the presence of Kir6.1 pore-forming channels in active states right across the voltage range of cardiac action potential, which supports the finding documented in Figure 3.2. The APD was prolonged by 23.2% following treatment with 3 μM PNU, with a further 31.6% prolongation of APD<sub>90</sub> with 10 μM glibenclamide treatment, as shown in Figure 3.6. The application of these pharmacological inhibitors did not result in any shift in resting membrane potential. From these findings, it is possible to hypothesise that Kir6.1 pore-forming K<sub>ATP</sub> channels play an important role in regulating cardiac action potential in resting conditions.

### 3.3.2 The modulation of $K_{ir}6.1$ -containing channels alters calcium influx by limiting the opening time of the L-type calcium channel

We hypothesised that a direct modulation of  $K_{ir}6.1$  containing channel in cardiac sarcolemma results in reduced cell excitation via shortening of cardiac action potential and ultimately reducing intracellular  $Ca^{2+}$ , presumably by causing L-type channels to close more quickly, as part of the cardioprotective mechanism. L-type channels are known to mediate the  $Ca^{2+}$  influx during the depolarization phase of the cardiomyocyte action potential (Levick, 2013; Nilius et al., 1985). Previous studies have reported the activation of cardiac  $K_{ATP}$  channels during hypoxia to limit ATP depletion via reduced L-type calcium current entry to reduce toxic calcium loading during each systolic beat (Korchev et al., 2000; Suzuki et al., 2001; Shimoda and Polak, 2011). In the present study, the levels of  $Ca^{2+}$  transients in control conditions and during perfusion with a selective  $K_{ir}6.1$  activator and blocker were measured. Figure 3.10 shows, in line with previous literature, that activation of cardiac  $K_{ATP}$  ( $K_{ir}6.2/SUR2A$ ) channels following a high pinacidil concentration (200  $\mu M$ ) led to a severe reduction or abolished of  $Ca^{2+}$  transients. The findings observed in this figure mirror those of the previous studies that have found the opening of cardiac  $K_{ir}6.2/SUR2A$  channel imparts late-stage protection to preserve the remnant intracellular ATP for a long time through severe reduction of cardiac contractility. Potentiation of  $K_{ir}6.1$  by application of 50  $\mu M$  pinacidil significantly shortened the  $Ca^{2+}$  transients but the limiting of cardiac contractility was lower than the shortening effect in high pinacidil concentration treatment, as shown in Figure 3.10. Given these findings, it is possible that the newly identified  $K_{ir}6.1$ -containing  $K_{ATP}$  channels could contribute to imparting energy-sparing mechanisms during the early stage of metabolic stress. By contrast, selective blockade of the cardiac  $K_{ir}6.1$  subunit (3  $\mu M$  PNU) caused a significant prolongation of  $Ca^{2+}$  transients, as shown in Figure 3.11. The findings presented in this figure may suggest that inhibition of cardiac  $K_{ir}6.1$  containing channels have a toxic effect on cardiomyocytes during metabolic stress, via loading intracellular calcium.

### 3.3.3 Activation of Kir6.1 imparts protection to cardiomyocytes and isolated hearts

The link between the potentiation of Kir6.1-containing K<sub>ATP</sub> channels and cardioprotection was a further objective of this chapter. It is well documented in the literature that K<sub>ATP</sub> channels openers and ischaemic preconditioning are a cardioprotective mechanism (Kitakaze, 2010; Wojtovich et al., 2010; Brennan et al., 2015). While there is a fall in intracellular ATP during simulated ischaemia, cardioprotected cells show a delay in action potential and contractile failure to maintain the cardiac function for longer during the ischaemic insult and a corresponding delay in the opening of the cardiac K<sub>ATP</sub> (Kir6.2/SUR2A) channel. Consequently, a delayed opening of this classic cardiac K<sub>ATP</sub> has been suggested as one of the hallmarks of ischaemic preconditioning. The study by Brennan *et al.* (Brennan et al., 2015) indicated that during cardioprotective stimuli, the time to opening the canonical Kir6.2/SUR2A channels is delayed, which indicates that this channel provides a late-protection with severe ATP depletion. This observation supports the hypothesis about the presence of another cardiac K<sub>ATP</sub> channel that may be involved in imparting the early stage of protection. In accordance with our hypothesis, previous studies have demonstrated that during normal physiological conditions, mice with Kir6.2 deletion did not exhibit modulation in the cardiac action potential, whereas mice with Kir6.1 deletion exhibited sudden death and ST segment elevation (Suzuki et al., 2001; Miki et al., 2002). It is possible, therefore, that the activation of Kir6.1-containing K<sub>ATP</sub> channels may act during resting conditions and contribute to the effect on the time to activation of canonical Kir6.2/SUR2A channels. To investigate this, a cell-attached patch recording was used to measure the effect of Kir6.1 potentiation on the time required to activate known cardiac K<sub>ATP</sub> (Kir6.2/SUR2A) channels. In experiments with pre-treating isolated cardiomyocytes with 100 μM pinacidil, the time to Kir6.2/SUR2A channels activation following metabolic inhibition was significantly delayed, as shown in Figure 3.12. This finding indicates that Kir6.1-containing K<sub>ATP</sub> channels play an important role in cardioprotection by delaying ATP depletion.

The question that remains is how potentiation of cardiac Kir6.1-containing K<sub>ATP</sub> channels may result in cardioprotection. To investigate this hypothesis, the metabolic inhibition and reperfusion protocol was used to examine the contractile function of isolated cardiomyocytes

following pinacidil treatment and the time to contractile failure at this point, as well as the percentage of contractile recovery and cell survival at the end of reperfusion. The present findings provide evidence of the cardioprotective role of Kir6.1 pore-forming K<sub>ATP</sub> channels against damage from metabolic inhibition and reperfusion injury. This is shown in Figure 3.13; with pre-treatment with pinacidil to potentiate the Kir6.1 activity, the time to contractile failure, which is reflected in the time to ATP depletion, and the rate of contractile recovery increased with an increase in cell survival at the end of the reperfusion period. Different concentrations of pinacidil treatment were applied separately to target different pore-forming subunits of K<sub>ATP</sub> channels in the cardiac membrane surface; both 50 µM and 100 µM pinacidil caused marked activation of Kir6.1 pore-forming channels, whereas 200 µM pinacidil led to marked opening of Kir6.2 pore-forming channels. The contractile function before the application of the metabolic inhibitor was noticeably reduced in cardiomyocytes pre-treated with 200 µM pinacidil compared to controls and pre-treatment with other concentrations of pinacidil (as shown in the time-course trace in Figure 3.13B(i)). A possible explanation for these findings might be that activation of the known cardiac K<sub>ATP</sub> (Kir6.2/SUR2A) channels with 200 µM pinacidil is sufficient to limit the ability of the electric field stimulation to reach the threshold for activating an action potential, therefore reducing the proportion of contractile cells at the start of the experiment.

The protective effect of Kir6.1 activation was investigated in this chapter using whole-heart *ex vivo* coronary ligation. The findings indicate that hearts treated with 10 µM pinacidil exhibited a significant reduction in infarct size, as shown in Figure 3.15. The observed protection of the heart following an application of 10 µM pinacidil treatment could be attributed to dilation of the coronary arteries. Despite the demonstrated cardioprotective effect of pre-treatment with Kir6.1 potentiation against damage after myocardial ischaemia, it is necessary to investigate this pharmacological potentiator during ischaemia and reperfusion by simulating human hearts undergoing myocardial infarction in the clinical setting. Based on the findings of isolated cardiomyocytes and isolated whole hearts, we could infer that the cardioprotective effect against damage after myocardial ischaemia is a result of the opening of the newly identified Kir6.1 containing K<sub>ATP</sub> channel.

### 3.3.4 Blockade of Kir6.1 causes cardiotoxicity to cardiomyocytes and isolated hearts

As mentioned in previous studies, mice with Kir6.1 deletion exhibit a larger infarct size following hypoxia (Miki et al., 2002; Aziz et al., 2017). Mice with global knockout of Kir6.1 have shown ST-segment elevation, an outcome that was absent in mice with vascular deletion of Kir6.1 (Miki et al., 2002; Aziz et al., 2014). Figure 3.14 shows, in line with previous literature, that the blockade of cardiac Kir6.1 containing  $K_{ATP}$  channels has a deleterious impact on the contractile function of isolated cardiomyocytes following 3  $\mu$ M PNU treatment. This finding was evidenced by the accelerated time to contractile failure as well as the reduced rate of contractile recovery and cell survival at the end of reperfusion. This is consistent with our hypothesis in that Kir6.1-containing channels impart protection in ventricular myocytes by either indirectly mediating vasodilatation of the coronary artery to reduce infarct size or directly modulating the physiological function of cardiomyocytes.

We further determined the effect of Kir6.1 inhibition on the infarct size of whole-heart preparation using a coronary ligation model. The findings from this experiment indicate that hearts treated with Kir6.1 inhibition (3  $\mu$ M PNU) caused a significant increase in infarct size, as shown in Figure 3.16. It seems possible that the cardiotoxicity following PNU treatment is due to this pharmacological inhibitor having effects on the coronary circulation. Together, the findings in isolated cardiomyocytes and isolated hearts suggest that the blockade of cardiac Kir6.1 pore-forming channels has a cardiotoxic effect after metabolic stress.

At the beginning of this chapter, we postulated that increased Kir6.1 activity in ventricular myocytes could impart cardioprotection by shortening the cardiac action potential, limiting calcium overload, and thus preventing ATP depletion. The data presented here suggest that the potentiation of Kir6.1 may act as a novel effector of cardioprotection. These observations suggest that there may be two types of  $K_{ATP}$  channel on the surface of ventricular cardiomyocytes, including the canonical cardiac  $K_{ATP}$  channel (Kir6.2/SUR2A) and the second ventricular SarcoKir6.1, possibly with a SUR2B subunit. The newly identified cardiac Kir6.1 containing  $K_{ATP}$  channel may be involved in fine-tuning of the resting potential and action potential of ventricular myocytes and may also impart early-stage protection, whereas

$K_{ir}6.2/SUR2A$  channel is a metabolic sensor by opening during prolonged ischaemia to impart late-stage protection. However, further studies should be performed to explore the link between cardiac  $K_{ir}6.1$ -containing  $K_{ATP}$  channels and protection against the damage of myocardial ischaemia and reperfusion injury.

# Chapter 4 Characterisation of $I_{K_s}$ in the heart

## 4.1 Introduction

Despite the initial identification of ischaemic preconditioning as a cardioprotective intervention nearly 40 years ago, its underlying mechanisms are still not fully understood. More disappointingly, the cardioprotective stimuli that are effective in pre-clinical models have not successfully translated to efficacy in humans (Rossello and Yellon, 2016). The ability to activate the intrinsic cardioprotective mechanisms within the heart to protect against ischaemic and reperfusion damage has thus far eluded us.

Studies have shown that cardioprotective interventions, such as ischaemic preconditioning and adenosine treatment, cause changes in the functional behaviour of cardiomyocytes. It has been observed that cardioprotected cells have a slightly shortened action potential duration, while in simulated ischaemia, they have a prolonged time to ATP depletion and a corresponding delay of the opening of the known cardiac  $K_{ATP}$  ( $Kir6.2/SUR2A$ ) channel. This delay in the opening of this large hyperpolarising current means that there is a delay in action potential and contractile failure, meaning that they maintain function for longer during the ischaemic insult. Finally, the cells maintain their intracellular calcium homeostasis for longer during metabolic stress, which also suggests that intracellular ATP is preserved for longer (Murry et al., 1986; Kitakaze, 2010; Brennan et al., 2015). In short, cardioprotected cells appear to be able to maintain their intracellular calcium homeostasis for longer than non-cardioprotected cells via a mechanism that is most likely dependent on them having a reduced or more efficient use of ATP.

It was hypothesised that the slight shortening of the action potential duration seen in the cardioprotected cell shortened the time that L-type channels permitted the influx of calcium, thus limiting the accumulation of cytoplasmic calcium during each contractile cycle. This would reduce the ATP consumption of the cell, as there would be less calcium to remove from the cytoplasm during diastole.

In this chapter, the compound ML277, which is a known  $Kv7.1$  (KCNQ1) selective activator with an  $EC_{50}$  260 nM (Mattmann et al., 2012; Yu et al., 2013a), was used to shorten the action potential duration to assess whether potentiation of the repolarisation reserve current in

resting conditions impart cardioprotection. We used ML277 at a concentration of 1  $\mu$ M. Previous studies indicate that ML277 at this concentration increased the peak of  $I_{Ks}$  (Yu et al., 2013a; Xu et al., 2015; Hou et al., 2019). ML277 is an activator of KCNQ1 currents and its effectiveness is reduced at saturating levels of KCNE1 expression (Yu et al., 2013a).

Blockade of  $I_{Ks}$  was achieved by using JNJ303. JNJ303 was developed from the initial compound JNJ423 which is a potent inhibitor of 11 $\beta$ -hydroxysteroid dehydrogenase-1 (HSD1) enzyme being profiled as an anti-obesity/diabetes drug (Towart et al., 2009). JNJ303 has selectivity at the  $I_{Ks}$  complex rather than solely KCNQ1 (Yu et al., 2013a). JNJ303 binds to a unique pocket when the KCNQ1 and KCNE1 subunits are co-assembled, with an  $IC_{50}$  value of 64 nM. JNJ303 at a concentration of 1  $\mu$ M was shown to inhibit the KCNQ1/KCNE1 channel current by about 80% (Wrobel, 2013), so we used this concentration in our experiments. The inhibitory effect of JNJ303 increases with higher expression level of  $\beta$ -subunit KCNE1 (Wrobel, 2013). In order for JNJ303 to bind to  $K_v7.1$  it requires the co-assembly with the accessory subunit, KCNE1, to form a pocket in the structure that JNJ303 can bind to (Wrobel, 2013). This does not rule out any additional effects of JNJ303 on other proteins or ion channels. There is literature that suggests JNJ303 had an effect on  $K_v11.1$ , causing QT prolongation in the anaesthetised guinea-pig model when JNJ303 was intravenously applied at dose of 0.63 and 1.25 mg/kg (Towart et al., 2009). This suggests that JNJ303 might have effects on other ion channels.

To investigate the cardioprotective/cardiotoxic effects of  $I_{Ks}$  modulation, several different techniques were used. Firstly, patch clamp recording was done to assess 1) whether ML277 shortens the action potential duration via potentiating of the voltage-gated current component in rat cardiomyocytes, 2) whether ML277 had any additional effects on other currents to ensure it was selective for  $I_{Ks}$ , and 3) the calcium transients in cardiomyocytes to determine whether ML277 did indeed reduce calcium accumulation. Isolated cardiomyocytes were treated with JNJ303 to investigate whether 1) JNJ303 prolongs cardiac action potential, 2) JNJ303 reduces the peak amplitude of  $I_{Ks}$  and their effect on other cardiac ion channels, and 3) JNJ303-induced calcium accumulation.

## 4.2 Results

### 4.2.1 ML277 (a selective activator of the $I_{Ks}$ ) shortens the cardiac action potential

Previous studies have shown that, ML277 is a potent potentiator of the cardiac  $I_{Ks}$  at the ratio of 4 KCNQ1: 2KCNE1 found in native  $I_{Ks}$  (Yu et al., 2013a; Xu et al., 2015). The potent potentiation by ML277 of the  $I_{Ks}$  makes it a promising pharmacological target which causes a shortened duration of cardiac action potentials. To examine this pharmacological effect, the action potentials of isolated rat cardiomyocytes were measured. These recordings were carried out using current-clamp recordings, as outlined in Section 2.3.3. Cardiomyocytes were first perfused with NT solution. The action potential was stimulated at a rate of 1 Hz via a patch pipette. The cells were recorded in NT solution for 2 min to allow the action potential duration to reach a steady state before the addition of drugs. Once equilibrated, 1  $\mu$ M ML277 in NT solution was applied for 5 min.

Figure 4.1A shows a representative recording of an action potential in control conditions and during the perfusion of ML277. For the analysis, the action potential duration (APD) was measured together with the resting membrane potential. The APD was measured at three time points, 10%, 50% and 90% repolarised, to investigate the effects of ML277 (Figure 4.1B). It was anticipated that ML277 activation of  $I_{Ks}$  would have the greatest effect on the  $APD_{90}$ , given that  $I_{Ks}$  is a slowly activating current. In the presence of ML277, the  $I_{Ks}$  retains its slow-acting phenotype.

ML277 led to a significant shortening of the  $APD_{90}$  in ventricular myocytes, from  $62.19 \pm 2.9$  ms (control condition, n=16) to  $50.1 \pm 3.2$  ms (ML277, n=16, p<0.0001) and that there was not a significant change at washout to  $56.8 \pm 4.6$  ms (p=0.142) (Figure 4.2A(i)). Figure 4.2A(ii) showed  $APD_{90}$  variability was reduced after exposing cardiomyocytes with a solution containing 1 $\mu$ M ML277 as compared to  $APD_{90}$  variability of control conditions. In these cardiomyocytes, there was no effect on resting membrane potential, with  $-68.8 \pm 1.5$  mV in the control recording,  $-70.6 \pm 1.7$  mV after ML277 treatment (n=8, P=0.35) and  $-68.9 \pm 2.6$  mV following washout (n=8, P=0.99) (Figure 4.2A(iii)).

As anticipated, the effects of ML277 on APD<sub>10</sub> and APD<sub>50</sub> were limited (Figure 4.2B). The mean APD<sub>50</sub> (n=7) did not significantly alter from 61.4±5.1 pA/pF at baseline to 56.9±5.6 pA/pF with ML277 treatment and to 58.4±5.6 pA/pF following the washout of the drug (p=0.52, p=0.66, respectively) (Figure 4.2B(i)). In addition to that, APD<sub>10</sub> did not significantly change, recording from 20.3±5.1 pA/pF at control to 19.2±3.9 pA/pF with ML277 treatment and to 20.5±4.1 pA/pF following the washout of the drug (p=0.80, p=0.90, respectively) (n=7), as shown in Figure 4.2B(ii).

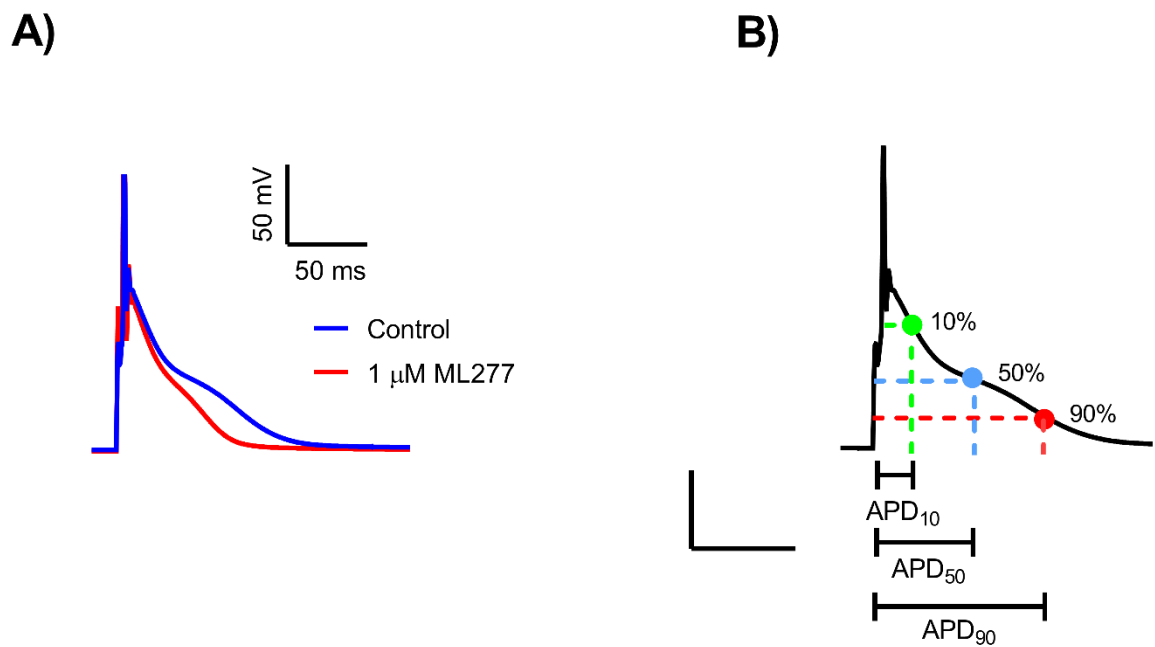


**Figure 4.1:** The representative effect of ML277 on action potential duration (APD) in a rat ventricular myocyte compared to the control condition.

*A, Representative traces of an action potential prior to (blue line) and during perfusion with 1  $\mu$ M ML277 (red line), showing shortening of the action potential during the pharmacological treatment. B, A representative trace of APD at different points of the repolarisation at 10% (green dot), 50% (blue dot) and 90% (red dot).*

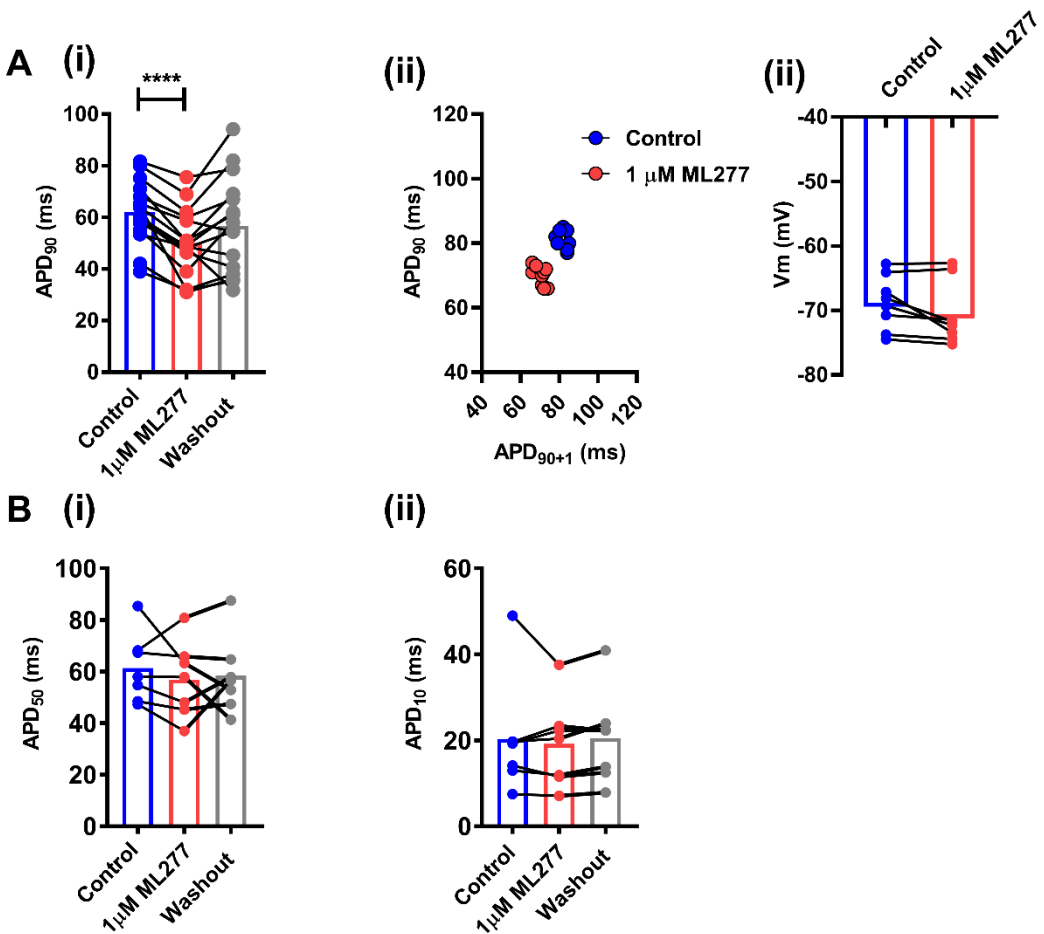


**Figure 4.2:** ML277 treatment shortened action potential duration (APD) with no effect on resting membrane potential.

*A(i), Graph showing that  $1\text{ }\mu\text{M ML277}$  shortened the mean  $APD_{90}$  with non-significant change compared to washout recordings ( $****p < 0.0001$ ,  $p = 0.142$ , respectively for one-way ANOVA Holm-Sidak post-test) ( $n=16$ ). A(ii), Poincare plot showing the action potential variability in control and ML277. Data plotted for 10 action potentials in each condition. A(iii), Histogram showing no effect of  $1\text{ }\mu\text{M ML277}$  on the membrane potential ( $n=8$ ,  $P=0.35$ ,  $p=0.99$ , one-way ANOVA Holm-Sidak post-test). B(i),  $APD_{50}$  was not altered in the presence of ML277 and following the washout ( $p=0.52$ ,  $p=0.66$ , respectively for one-way ANOVA Holm-Sidak post-test) ( $n=7$ ). B(ii),  $APD_{10}$  was also not significant change with ML22 and washout recordings, compared to controls ( $p=0.81$ ,  $p=0.90$ , respectively for one-way ANOVA Holm-Sidak post-test) ( $n=7$ ). Data are presented as mean  $\pm$  SEM.*

#### 4.2.2 JNJ303 (a selective $I_{Ks}$ blocker) did not prolong cardiac action potentials

JNJ303 has been reported to be a selective blocker of the  $I_{Ks}$  (Section 1.4.4.1) (Towart et al., 2009). It was hypothesised that if the hyperpolarising effect of the  $I_{Ks}$  was removed, then the action potential would be longer, as is seen in  $I_{Ks}$  mutations associated with long QT syndrome

(Heijman et al., 2012). We therefore hypothesised that  $I_{Ks}$  inhibition would have a cardiotoxic effect on cardiomyocytes.

To examine this pharmacological effect, the action potentials of isolated rat cardiomyocytes were measured. As with the ML277 recordings, once a steady state of APD was reached (after ~2 min), the solution was exchanged for ones containing 1  $\mu$ M or 300 nM JNJ303 to enable us to assess changes in APD.

Figure 4.3 shows the action potential in the control condition and during the perfusion of JNJ303. There was a small but insignificant prolongation of the  $APD_{90}$  at different concentrations of JNJ303 (1  $\mu$ M and 300 nM), with no effect on the RMP.

In the cardiomyocytes, the  $APD_{90}$  was measured. The  $APD_{90}$  increased from  $50.6 \pm 5.6$  ms to  $56.3 \pm 7.9$  ms, albeit insignificantly (control vs 1  $\mu$ M JNJ303,  $n=6$ ,  $p=0.265$ , Figure 4.3B(i)). Investigation of the membrane potential showed a non-significant depolarisation of RMP from  $-68.3 \pm 0.74$  mV to  $-67.2 \pm 1.0$  mV (control vs 1  $\mu$ M JNJ303,  $n=6$ ,  $p=0.162$ , Figure 4.3B(ii)). Similarly, at a low concentration of JNJ303 (300 nM), the alteration of  $APD_{90}$  was not significant, changing from  $74.9 \pm 10.2$  ms to  $73.3 \pm 10.3$  ms (control vs. 300 nM JNJ303,  $n=7$ ,  $p=0.560$ , Figure 4.3C(i)). Figure 4.3C(ii) showed no change in RMP from  $-48.5 \pm 2.4$  mV (control,  $n=7$ ) to  $-50.6 \pm 2.6$  mV (300 nM JNJ303,  $n=7$ ,  $p=0.126$ ). These data of JNJ303 at different concentrations suggested that the prolongation of  $APD_{90}$  was not significant due to  $I_{Ks}$  not being the major current for repolarisation in rat cardiomyocytes.

Given that  $I_{Ks}$  only makes a minor contribution to repolarisation in rat ventricular myocytes (Edwards and Louch, 2017), it was not expected that JNJ303 would have a significant effect on the APD. In these experiments, no significant prolongation of APD was seen, although washout data were not recorded in these experiments. Future experiments could be required to further investigate this.

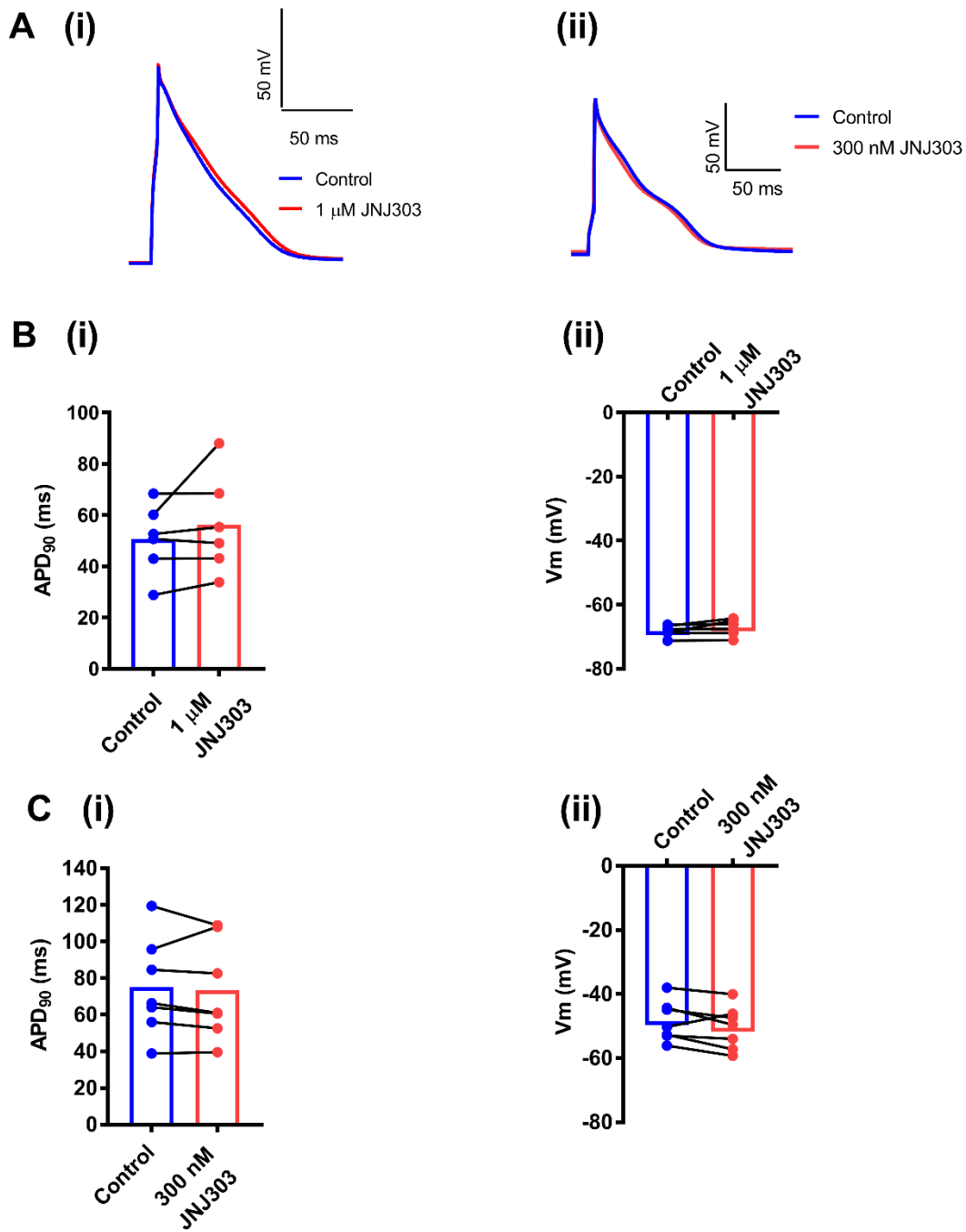


**Figure 4.3:** The effect of JNJ303 on action potential duration (APD) from a rat ventricular myocyte compared to the control condition.

*A, Representative traces of an action potential prior to (blue line) and during perfusion with 1  $\mu$ M JNJ303 (i) or 300 nM JNJ303 (red line) (ii), showing a slight prolongation/an abolished alteration of the action potential during the pharmacological treatment. B, Graph showing that 1  $\mu$ M JNJ303 did not change the mean APD<sub>90</sub> ( $p=0.265$  for the paired t-test), or the resting membrane potential when compared to the control condition ( $p=0.162$ ,  $n=6$ ). C, mean data showing that 300 nM JNJ303 did not prolong the mean APD<sub>90</sub> ( $p=0.560$  for the paired t-test) and had no effect on RMP ( $p=0.126$  for the paired t-test,  $n=7$ ).*

#### 4.2.3 ML277 selectively activates the $I_{Ks}$ in rat cardiomyocytes

The hypothesis under investigation in this chapter is that the selective potentiation of the  $I_{Ks}$  shortens the cardiac action potential and that this reduces calcium loading during each contractile cycle to preserve energy. To confirm this hypothesis, it is important to first understand whether  $I_{Ks}$  is indeed selectively potentiated by ML277, or whether ML277 has effects on other cardiac ion channels. To investigate this, whole-cell recordings were used to measure different cardiac currents using a voltage-clamp protocol. This protocol was designed to measure several currents, including  $I_{K1}$ ,  $I_{Ca}$ ,  $I_{Na}$  and  $I_{Ks}$ , as shown in Figure 4.4. Currents were evoked by depolarising the membrane to different voltages from a holding potential at -70 mV. In the cardiac myocytes, inward currents were activated at different voltages, including, sodium current ( $I_{Na}$ ) and calcium ( $I_{Ca}$ ) current (more positive than -50 mV) (Figure 4.4). The outward movement of  $K^+$  in rat ventricular myocytes occurs via different currents, including the transient outward current ( $I_{to}$ ) and the slowly activating  $K^+$  currents ( $I_{Ks}$ ) (Figure 4.4). The inwardly rectifying  $K^+$  currents formed from  $K_{ir}2$  and  $K_{ir}6$  subunits will pass inward currents negative to  $E_K$  (~-90 mV) and outward currents at potentials positive to  $E_K$  (Figure 4.4). The  $I_{K1}$  current, conventionally considered to be due to the activity of  $K_{ir}2$  subunits, was measured from -100 to -45 mV giving both inward and outward currents across the voltage range. The duration of depolarisation step was maintained for 6 s where other currents such as  $I_{Na}$ ,  $I_{Ca}$  and  $I_{to}$  would be inactivated, whilst  $I_{K1}$  blocked by its rectification properties, at the end of this long protocol. It would be anticipated that at the end of this depolarising step,  $I_{Ks}$  would be a significant part of the current active. It would also be expected that there would be a  $K_{ATP}$  current component,  $K_{ir}6.1$ -containing  $K_{ATP}$  channels, as described in the previous chapter.

The main limitation of the experimental protocol (Figure 4.4) is that does not isolate  $I_K$  from other potassium currents (Himmel et al., 1999). For example, the end-pulse current under these recording conditions will include a non-inactivating steady-state outward current ( $I_{ss}$ ) with properties inconsistent with the properties of  $I_{Ks}$ . In this experiment, we used a highly selective KCNQ1 activator, ML277 (Mattmann et al., 2012), and then we investigated their

effect at the end of the depolarisation step with a duration around 6 s where  $I_{Ks}$  would be a significant part of the current active.

To test whether ML277 had an effect on  $I_{K1}$ , the current was recorded by applying 100 ms steps from -100 mV to -45 mV (Figure 4.4).  $I_{Na}$  typically activated when conditions were more positive than resting membrane potential ( $\sim$  -40 mV) and peaked within a few milliseconds of the start of the depolarisation (Figure 4.4). This fast and transient current was fully inactivated by the end of a 100 ms pulse to -40 mV. The final depolarising steps (from -50 mV to +60 mV in 10 mV increments) were to activate  $Ca^{2+}$  currents and  $I_{Ks}$ .  $I_{Ks}$  were assessed at the end of the duration of depolarisation steps (6 s) due to their slow kinetics of activation.

Initially, the cells were perfused with NT solution for 2 min to measure the control conditions (Figure 4.5A). After running the recording protocol twice, cardiomyocytes were perfused with an NT solution containing 1  $\mu$ M ML277. Application of ML277 led to a notable increase in  $I_{Ks}$  compared to the control solution (Figure 4.5B).

To compare the currents between cells, the currents were normalised to their cell capacitance (Figure 4.6). The mean data for the  $I_{Ks}$ ,  $I_{K1}$  and  $I_{Ca}$  were compared, as shown in Figure 4.6. Figure 4.6A(i) shows that the I-V relationship of  $I_{Ks}$  had increased current amplitude in the presence of 1  $\mu$ M ML277 when compared to control conditions. At a membrane potential of +60 mV, the mean  $I_{Ks}$  ( $n=16$ ) increased from  $3.6\pm0.2$  pA/pF at baseline to  $4.7\pm0.3$  pA/pF with ML277 treatment ( $n=16$ ,  $p<0.0001$ , Figure 4.6B(i)). The mean  $I_{Ks}$  was not significantly different to the control conditions in the washout recordings, being  $4.0\pm0.2$  pA/pF ( $n=16$ ,  $p=0.09$ ). This finding suggested that there was no rundown of  $I_{Ks}$  at +60 mV.

The I-V curves of  $I_{K1}$  at -100 mV was recorded in the control condition at  $-5.9\pm0.4$  pA/pF and with the pharmacological treatment at  $-5.7\pm0.4$  pA/pF ( $n=16$ ,  $p=0.22$ ) as shown in Figure 4.6B(ii). However, there was a significant decline in  $I_{K1}$  at -100 mV following the washout of the drug ( $-5.1\pm0.4$  pA/pF), compared to control conditions ( $n=16$ ,  $p=0.02$ , Figure 4.6B(ii)). A possible explanation for this finding might be rundown of  $I_{K1}$  over time at -100 mV. Although the calculated  $E_K$  for these solutions is -88 mV, in reality, the reversal potential of a  $K^+$  current, in the absence of any selective ion channel blockers, in a cardiac myocyte is unlikely to be

strictly at  $E_K$ . This is partially due to potential ion flux through non-selective leak currents and transporters that may contribute to an  $\text{Na}^+$  influx.

$I_{\text{Ca}}$  at -10 mV showed no significant alterations, with  $-3.8 \pm 0.6 \text{ pA/pF}$  for control versus  $-3.8 \pm 0.5 \text{ pA/pF}$  for 1  $\mu\text{M}$  ML277 and  $-3.8 \pm 0.5 \text{ pA/pF}$  for the washout condition ( $n=16$ ,  $p=0.99$  and  $p=0.98$ , respectively) (Figure 4.6B(iii)). This finding indicates that  $I_{\text{Ca}}$  at -10 mV were not rundown.

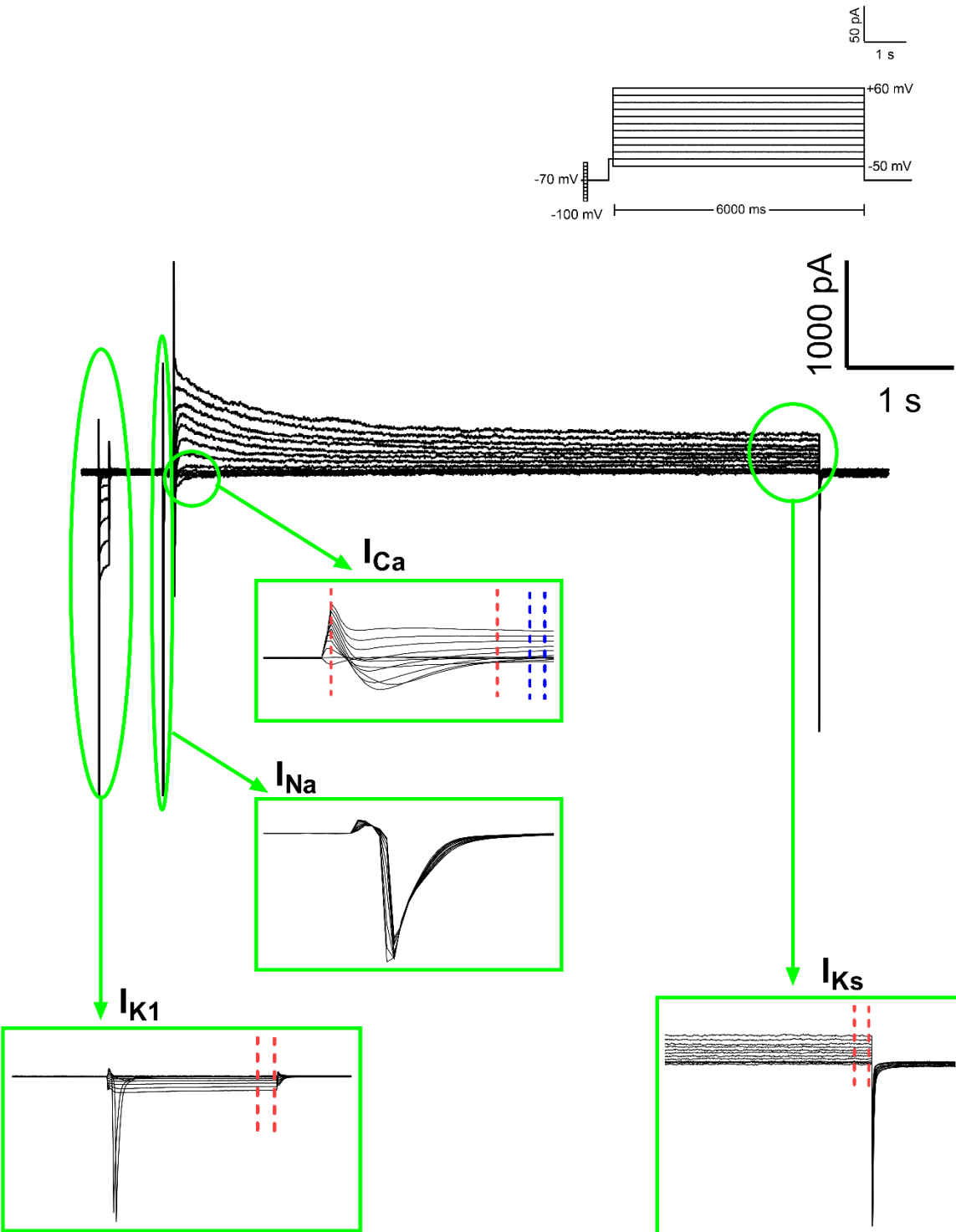


**Figure 4.4:** Representative trace from multi-current protocol used for whole-cell recording from rat ventricular myocytes which was illustrated the currents measured.

The cardiac membrane currents were measured using the voltage step protocol outlined above.  $I_{K1}$  was measured by a series of depolarising steps between -100 and -45 mV. Measurements of inward currents such as  $I_{Na}$  and  $I_{Ca}$ , were carried out by depolarizing the membrane to more positive voltage than -50 mV. Voltage steps from -50 to +60 mV for 6 s were applied, and the start of the depolarisations were used to record  $Ca^{2+}$ current and the very end of this depolarisation step was used to measure  $I_{Ks}$ .

The current was measured at specific regions which were represented between the two red cursors.  $I_{K1}$  was measured as mean of final 20 ms of each sweep.  $I_{Ca}$  was measured when the peak negative of calcium current (between the two red cursors) are subtracted from the potassium current (between the two blue cursors).  $I_{Ks}$  was measured as mean of the end 6 s of each recording. Data was normalized to cell capacitance to allow comparison between cells.

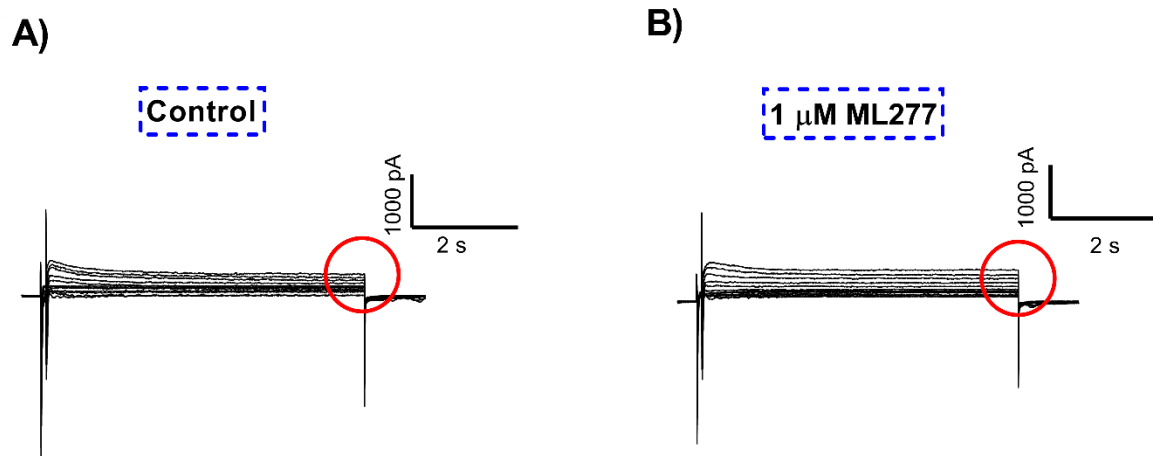


**Figure 4.5:** Comparison of the whole-cell patch clamp recordings in the absence and present of ML277, highlighted the treatment effect on  $I_{Ks}$ .

A, Representative traces of isolated rat ventricular cell at the control condition. B, Recording trace of single ventricular myocyte after being perfused with 1  $\mu$ M ML277, ML277 treatment selectively increases the slowly activating delayed rectifier potassium channel, as indicated by red circles.

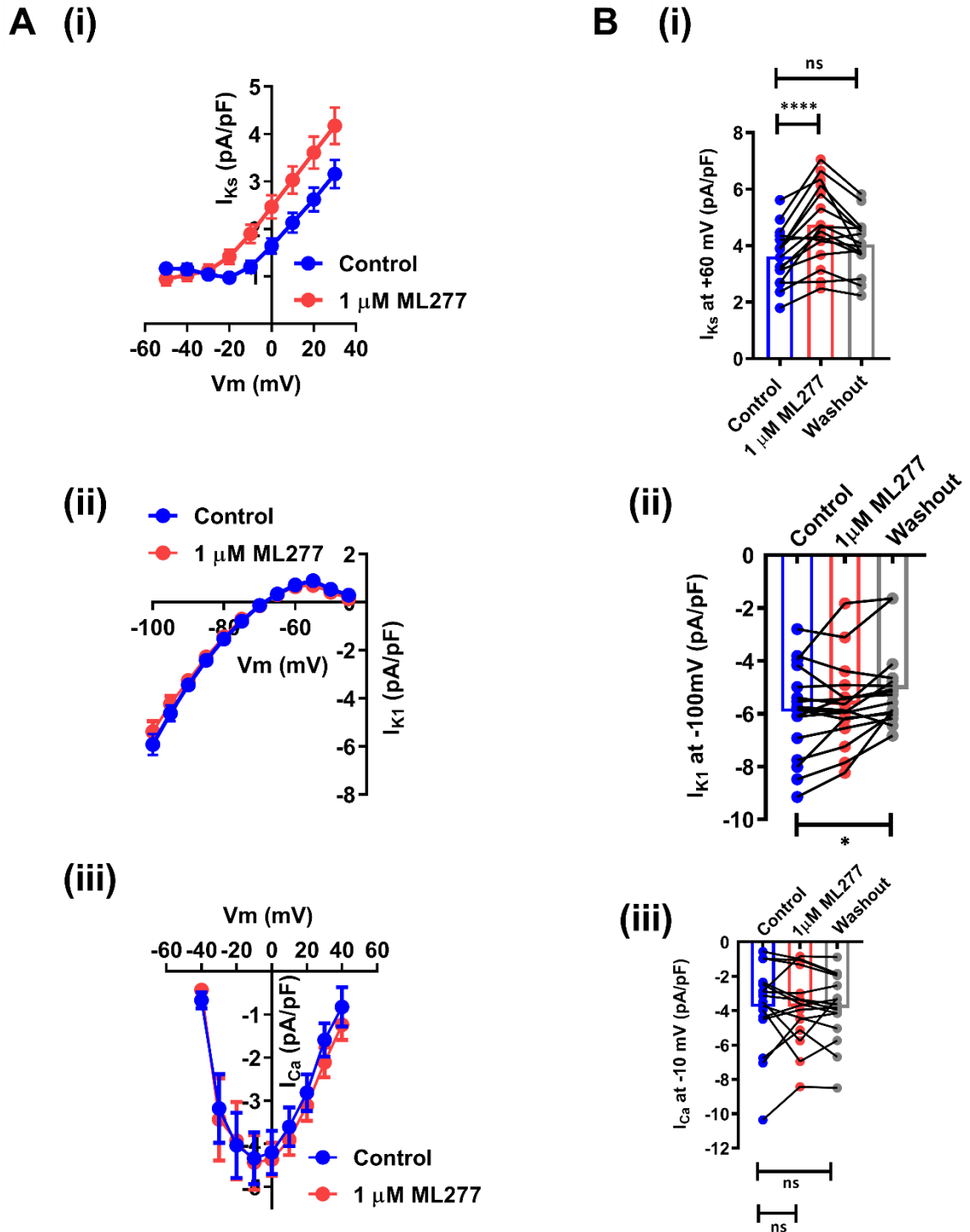


Figure 4.6: The limited effect of ML277 on the activation of  $I_{Ks}$ .

A, A voltage-current relationship of different cardiac ion currents ( $I_{Ks}$  (i),  $I_{K1}$  (ii), and  $I_{Ca}$  (iii)) of cardiomyocytes in control conditions (blue line) and during the application of ML277 (red line). B, Graphs showing the mean data in the control conditions,  $1 \mu\text{M}$  ML277 treatment, and following washout of ML277. B(i), ML277 caused a significant activation of  $I_{Ks}$  ( $n=16$ ,  $****p<0.0001$ ), that

*showed no difference to control following washout ( $n=16$ ,  $p=0.09$ ). B(ii) Bar chart showing that 1  $\mu$ M ML277 did not induce any change in  $I_{K1}$  at -100 mV ( $n=16$ ,  $p=0.22$ ), however there was a significant decrease in  $I_{K1}$  in washout recordings versus controls ( $n=16$ ,  $p=0.02$ ). B(iii)  $I_{Ca}$  (at -10 mV) currents were not significantly affected by the application of ML277 and did not change following washout of ML277 ( $n=16$ ,  $p=0.99$  and  $p=0.98$ , respectively). (one-way ANOVA with Holm-Sidak post-test).*

#### 4.2.4 JNJ303 blocks $I_{Ks}$ cardiac currents

The converse of our hypothesis (that a shortening of the APD by  $I_{Ks}$  potentiation is cardioprotective) is that blocking of  $I_{Ks}$  could be cardiotoxic. JNJ303 is an  $I_{Ks}$ -specific blocker that is thought to bind to a unique pocket that is exposed when the KCNQ1 and KCNE1 subunits are co-assembled (Towart et al., 2009). To confirm that the compound was selective for the  $I_{Ks}$ , whole-cell recording was carried out using the protocol for ML277 described in Section 4.2.3. Cardiomyocytes were perfused with NT solution, and the protocol was run twice under these control conditions. Further experiments were then run following the perfusion of NT containing 1  $\mu$ M JNJ303. Application of JNJ303 to ventricular cells led to a notably reduced  $I_{Ks}$  (Figure 4.7). The application of JNJ303 may have a detrimental impact on cardiac muscles by delaying the repolarisation phase of the cardiac action potential.

A current voltage (I-V) curve was plotted following normalisation of the currents to their cell capacitance and compared with JNJ303 (Figure 4.8). Figure 4.8A(i) shows that the I-V relationship of  $I_{Ks}$  had decreased current amplitude in the presence of 1  $\mu$ M JNJ303 when compared to control conditions. At a membrane potential of +60 mV, the mean  $I_{Ks}$  ( $n=6$ ) decreased from  $3.2\pm0.2$  pA/pF at baseline to  $2.6\pm0.2$  pA/pF under 1  $\mu$ M JNJ303 treatment ( $n=6$ ,  $p=0.01$ , Figure 4.8B(i)). After the washout of JNJ303 treatment, the mean  $I_{Ks}$  increased, and was no longer significantly changed compared to control conditions ( $3.0\pm0.2$  pA/pF,  $n=6$ ,  $p=0.29$ ) (Figure 4.8B(i)).

I-V relationships for  $I_{K1}$  and  $I_{Ca}$  during JNJ303 perfusion were compared to control conditions (Figure 4.8A(ii) and (iii), respectively,  $n=6$ ). 1  $\mu$ M JNJ303 did not affect the  $I_{K1}$  at -100 mV (- $6.2\pm1.3$  pA/pF to  $-5.2\pm0.9$  pA/pF (Control vs JNJ303,  $n=6$ ,  $p=0.35$ , Figure 4.8B(ii)). In addition to that, the mean  $I_{K1}$  ( $n=6$ ) was not altered from the controls to  $-4.9\pm0.7$  pA/pF with washout, ( $n=6$ ,  $p=0.24$ , Figure 4.8B(ii)). Calcium currents were measured at -10 mV voltage steps and

showed no inhibition by 1  $\mu$ M JNJ303 (-9.9 $\pm$ 1.8 to -8.5 $\pm$ 1.3 pA/pF (control vs. JNJ303, n=6, p=0.13, Figure 4.8B(iii)). The mean  $I_{Ca}$  at -10 mV was not further affected following the washout of the pharmacological treatment (-9.9 $\pm$ 1.8 pA/pF to -7.9 $\pm$ 0.9 pA/pF (Control vs washout, n=6, p=0.21,Figure 4.8B(iii))).

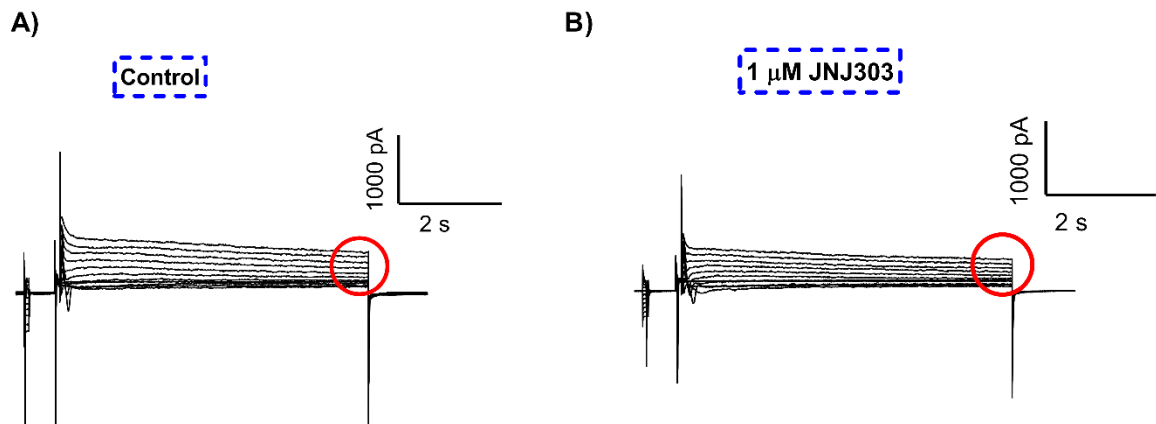


**Figure 4.7:** Comparison between single cardiomyocytes under control condition with NT solution and after the administration of JNJ303, using whole-cell patch clamp recordings with a voltage clamp mode.

*A, Recording trace of cardiomyocyte under control condition. B, Recording of the same single cardiomyocyte after perfusion with 1  $\mu$ M JNJ303, JNJ303 reduced the delayed rectifier potassium channel ( $I_{Ks}$ ), as indicated by the red circles.*

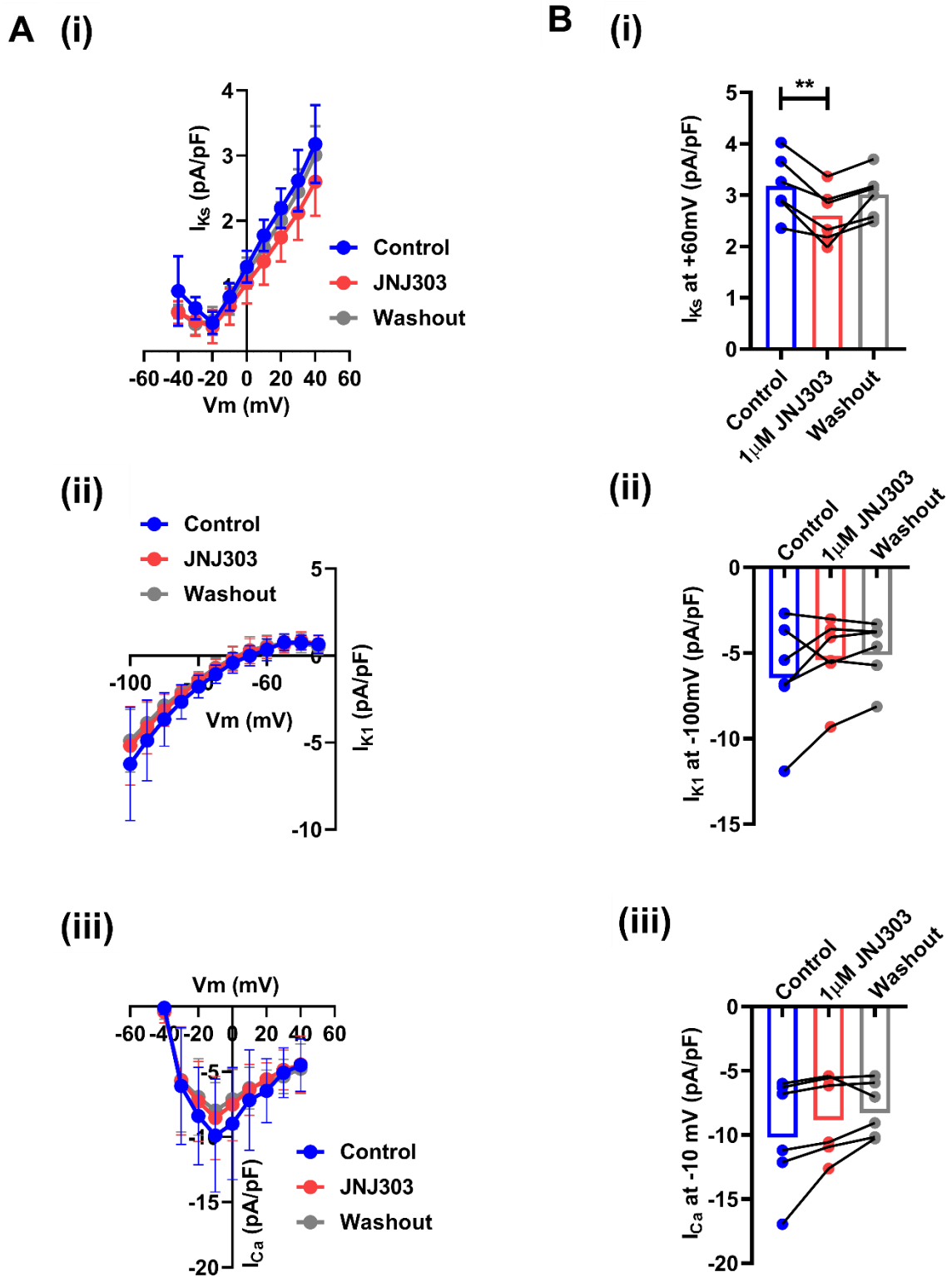
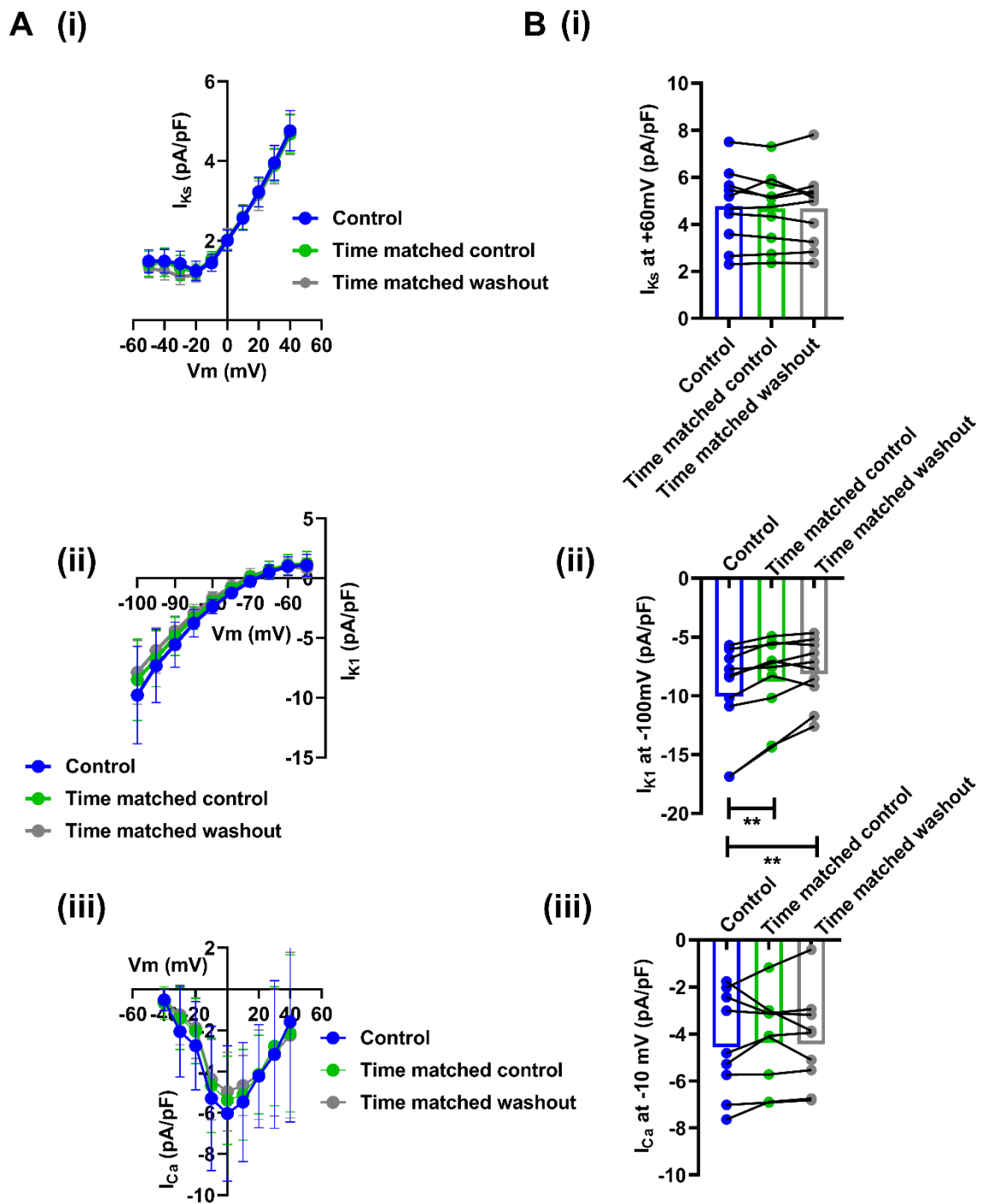


Figure 4.8: The effect of JNJ303 on the blocking of  $I_{Ks}$ .

A, A current-voltage relationship of different ionic currents ( $I_{Ks}$  (i),  $I_{K1}$  (ii) and  $I_{Ca}$  (iii)) in cardiomyocytes under control conditions (blue line), during the application of  $1 \mu M$  JNJ303 (red line) and following the washout of the treatment (gray line). B, Graphs showing the mean data in the control conditions,  $1 \mu M$  JNJ303 treatment, and following washout of JNJ303. B(i), JNJ303 caused a significant block of  $I_{Ks}$

( $n=6$ ,  $**p=0.01$ ), and showed no difference to control following washout ( $n=6$ ,  $p=0.29$ ). B(ii) Bar chart showing that 1  $\mu$ M JNJ303 did not induce any change in  $I_{K1}$  at -100 mV ( $n=6$ ,  $p=0.35$ ), and showed no difference to control following washout ( $n=6$ ,  $p=0.24$ ). B(iii)  $I_{Ca}$  (at -10 mV) currents were not significantly affected by the application of JNJ303 and did not change following washout of JNJ303 ( $n=6$ ,  $p=0.13$ ,  $p=0.21$ , respectively). (one-way ANOVA with Holm-Sidak post-test).

Time-matched recordings were carried out to determine whether decreases in  $I_{K1}$  and  $I_{Ca}$  could be attributed to rundown. Figure 4.9A shows the current-voltage (I-V) relationship for  $I_{Ks}$ ,  $I_{K1}$  and  $I_{Ca}$  in the presence of vehicle (DMSO) at time points equivalent to control, drug administration and washout. The mean  $I_{Ks}$  ( $n=10$ ) was not altered from  $4.8\pm0.2$  pA/pF at baseline to  $4.7\pm0.1$  pA/pF at the equivalent time of drug addition, and to  $4.7\pm0.1$  pA/pF at time matched washout ( $n=10$ ,  $p=0.71$ ,  $p=0.69$ , respectively) (Figure 4.9B(i)). At -100 mV, the mean  $I_{K1}$  ( $n=10$ ) significantly decreased from  $-9.8\pm1.2$  pA/pF in control conditions, to  $-8.5\pm0.3$  pA/pF at a time equivalent to drug and to  $-7.9\pm0.3$  pA/pF at a time matched washout ( $n=10$ ,  $p=0.002$ ,  $p=0.008$ , respectively, Figure 4.9B(ii)).  $I_{Ca}$  at -10 mV were also not significantly altered, recording from  $-4.4 \pm 0.2$  pA/pF to  $-4.2\pm0.3$  pA/pF and to  $-4.3\pm0.4$  pA/pF ( $n=10$ ,  $p=0.74$ ,  $p=0.92$ , respectively, Figure 4.9B(iii)). Consequently, the control experiments concluded that there is an absence of rundown in  $I_{Ks}$  and  $I_{Ca}$  at the time-matched recordings. These findings suggest that 1  $\mu$ M JNJ303 is a selective inhibitor of  $I_{Ks}$ .



**Figure 4.9:** The possibility of run-down in the currents at equivalent time of drug recordings in the absence of the drug with recordings in the presence of NT solution.

*A, A current-voltage relationship of different ion currents ( $I_{Ks}$  (i),  $I_{K1}$  (ii) and  $I_{Ca}$  (iii)) in cardiomyocytes under control conditions (blue line), following of the time-matched control (green line) and following of the time-matched washout (gray line). B, Graphs showing the mean data in a time-matched fashion so that the control currents are measured in the presence of vehicle at a time matched (relative to whole-cell access being obtained) to that of the corresponding measurements in the presence of ML277/or JNJ303.  $I_{Ks}$  (at +60 mV) currents were not significantly affected by the application of vehicle at a time matched fashion ( $n=10$ ,  $p=0.71$ ,  $p=0.69$ , respectively). B(ii) Bar chart showing that vehicle*

(DMSO) caused a significant decrease in  $I_{K1}$  at -100 mV at a time matched fashion ( $n=10$ ,  $**p=0.002$ ,  $**p=0.008$ , respectively). B(iii)  $I_{Ca}$  (at -10 mV) currents were not significantly affected by the application of vehicle at a time matched fashion ( $n=10$ ,  $p=0.74$ ,  $p=0.92$ , respectively). (one-way ANOVA with Holm-Sidak post-test).

#### 4.2.5 ML277 increases $I_{Ks}$ over the duration of a normal human cardiac action potential

In normal human cardiomyocytes, the action potential duration (APD) at resting conditions, of around 60 – 70 beats per minute, is around 300 ms in duration (Antzelevitch et al., 1999; Qu and Chung, 2012). The outward currents contribute to terminate the action potential duration, including the components of the delayed rectifier potassium current ( $I_{Kr}$  and  $I_{Ks}$ ) in human. However, in rat cardiomyocytes, there are two main components of the outward currents: the transient outward current ( $I_{to}$ ) and the delayed rectifier potassium current ( $I_K$ ), which contribute to terminate the cardiac action potential (Himmel et al., 1999).  $I_{to}$  is characterised by rapidly activating and inactivating outward current, whereas,  $I_{Ks}$  is characterised by slowly activating and inactivating current. A voltage protocol was used to investigate the effect of ML277 on the current over the normal duration of the human action potential, to see whether  $I_{Ks}$  activity would become more visible over this 300 ms timescale. The voltage protocol depolarised the cell to +20 mV, with a ramp to +10 mV over 300 ms, and then a ramp back down to the resting membrane potential of -70 mV, with a frequency of 1 Hz. The  $I_{Ks}$  was measured at the end of this protocol where the slowly activating current would most likely be distinguished. To examine this, whole-cell recording was used and currents were evoked by depolarising the membrane to +20 mV from a holding potential of -70 mV as shown in Figure 4.10. The cell membrane was then repolarised to +10 mV down a slow ramp over 300 ms (Figure 4.10). However, a main limitation of the experimental protocol is that other ion currents might contribute to the  $I_{Ks}$  that was measured in rat ventricular myocytes (Himmel et al., 1999). For instance, rat  $I_{ss}$  contributes to the total outward current.

Initially, the cells were perfused with NT solution for 2 min to reach a steady state before the application of pharmacological treatments. Once equilibrated, 1  $\mu$ M ML277 in NT solution was applied for 5 min. Figure 4.10A shows a representative recording of the protocol in control conditions and during the perfusion of ML277. ML277 led to a significant increase in

$I_{Ks}$ , from  $2.2 \pm 0.2$  pA/pF to  $2.5 \pm 0.2$  pA/pF (Control vs. 1  $\mu$ M ML277, n=11 for both conditions, p=0.009, Figure 4.10B). The mean data for the  $I_{Ks}$  in control conditions was compared to cells following the washout of the drug ( $2.4 \pm 0.1$  pA/pF), demonstrating a washout of the ML277 current potentiation (n=11, p=0.07, Figure 4.10B). However, the limitation of this study that there is possibility of other ion currents might involve to the current measured such as  $I_{to}$ ,  $I_{ss}$   $K_{ir6.1}$  containing  $K_{ATP}$  currents.

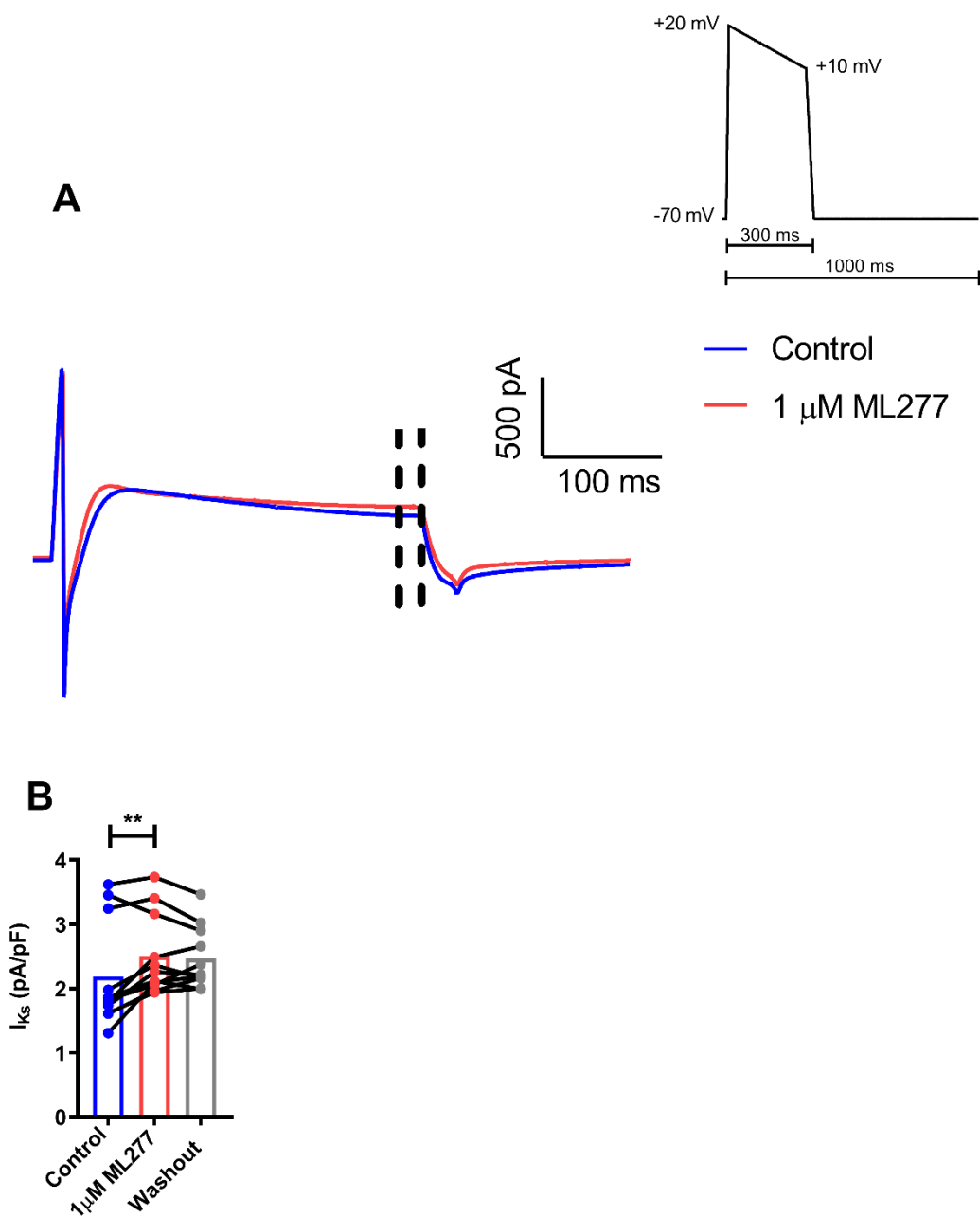


**Figure 4.10:** A whole-cell recording was used to examine the effect of ML277 on  $I_{Ks}$  over the normal human action potential.

*A, Representative current traces recording showing the voltage-clamp protocol outlined. The  $I_{Ks}$  was measured as mean of the end of 300 ms of each recording which annotated in the region between two black cursors. B, Graphs showing the mean data for cardiomyocytes in control conditions compared to 1  $\mu$ M ML277 treatment and following the washout of the drug. ML277 significantly increased  $I_{Ks}$  ( $n=11$ , \*\* $p=0.009$ ). This potentiation was reversed on washout of ML277 ( $n=11$ ,  $p=0.07$ ). (One-way ANOVA with Holm-Sidak post-test).*

#### 4.2.6 The activation curve of ML277 in rat cardiomyocytes

ML277-induced alterations in the voltage-dependent activation of KCNQ1/KCNE1 channels can be observed by eliciting tail current from a series of pre-pulse steps (-60 mV to +60 mV) for 6 s and then measured immediately following a fixed step to -30 mV, as shown in Figure 4.11A. Measurement of the tail current at -30 mV was selected because the driving force of currents is uniform at the second step that elicits the tail (Liin et al., 2015; Wu and Larsson, 2020). The tail current is decaying current which represents open voltage and time dependent conductance elicited by the first fixed step. Initially, the cells were perfused with NT solution for 3 min to measure the control conditions (Figure 4.11B(i)). After running the control recording protocol, cardiomyocytes were perfused with an NT solution containing 1  $\mu$ M ML277. Application of ML277 led to a notable increase in the tail current following pre-pulses of -40 to 0 mV, compared to the control (Figure 4.11B(ii)). This tail current was plotted as fraction of maximal activation over the pre-pulse voltage steps (Figure 4.11C). Normalised tail currents were then fitted to the Boltzmann curve.

To test whether ML277 had an effect on the activation kinetics of  $I_{Ks}$ , the tail current was measured after applying 1  $\mu$ M ML277 and this was compared to control conditions (Figure 4.11C). The activation curve of  $I_{Ks}$  shows that ML277 tended to induce a leftward shift compared to the control condition, which was represented as a shifting in the half-activation potential ( $V_{0.5}$ ) from -8.2 mV to -29.4 mV (Control vs 1  $\mu$ M ML277). This means that the potentiation of the  $I_{Ks}$  had a powerful effect on the repolarisation phase because the  $I_{Ks}$  at the plateau of the action potential was significantly larger by ~10 pA after exposure to ML277. This negative shift indicates that the  $I_{Ks}$  channel opened quickly at more negative membrane potentials and therefore affected cardiac APDs more rapidly.

This experimental protocol was used to record  $I_{Ks}$ , however, there is a possibility of the presence of other outward currents than  $I_{Ks}$  in rat ventricular myocytes. To add more confidence about the tail current being carried out by the  $I_{Ks}$ , the results should be applicable also to a selective blocker of  $I_{Ks}$  (such as JNJ303).

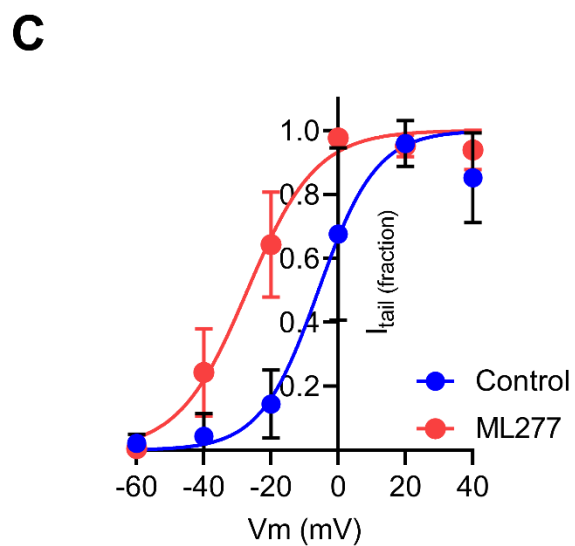
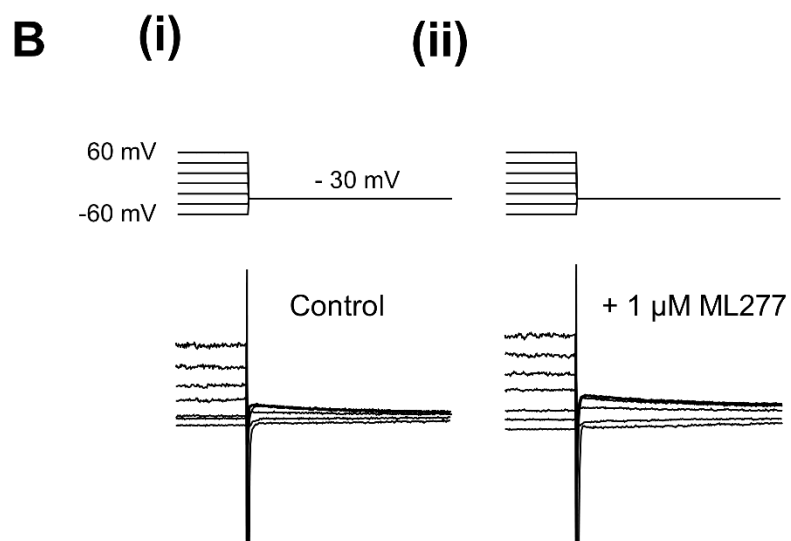
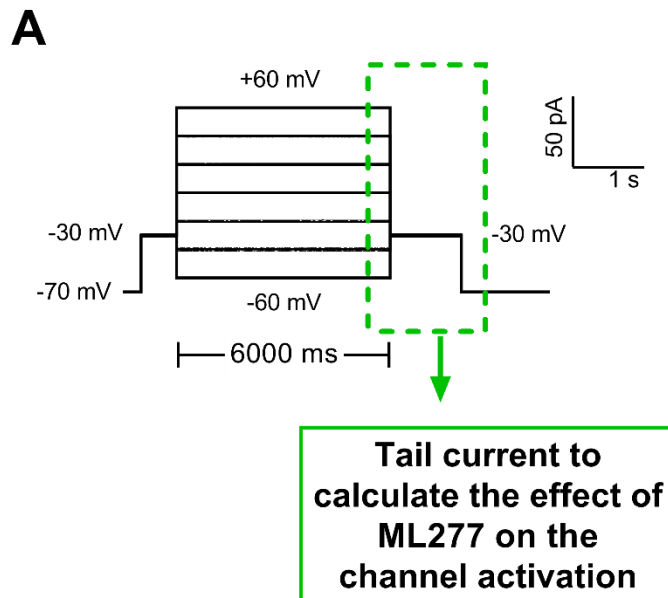


**Figure 4.11:** The activation curve of ML277 shows that the activation of the  $I_{Ks}$  occurred at resting potentials that were more negative.

*A, shows the protocol to measure ML277 activation of  $I_{Ks}$  in rat cardiomyocytes, using whole-cell patch clamp. B, Example traces of single ventricular myocyte showing the tail currents on repolarisation to -30 mV at the control condition (i) and after being perfused with 1  $\mu$ M ML277 (ii). ML277 treatment increases the tail currents on repolarisation. C, Voltage-dependent activation curves are shown in the absence and presence of 1  $\mu$ M ML277. Data recorded from an n of 6 cells and presented as mean  $\pm$  SEM.*

#### 4.2.7 $I_{Ks}$ activation reduced the peak amplitude and duration of the calcium transient

The hypothesis in this chapter links the shortening of the cardiac action potential with the selective potentiation of the  $I_{Ks}$  and, consequently, the reduction of calcium loading to reduce energy consumption during each contractile cycle. To investigate whether the calcium transients could be regulated by potentiation of the  $I_{Ks}$ , isolated cardiomyocytes were loaded with fura-2-AM, a  $\text{Ca}^{2+}$ -sensitive dye, for 20 min. Isolated myocytes were stimulated at 1 Hz to trigger cardiac action potentials. The cells were perfused with NT solution for 2 min followed by 1  $\mu$ M ML277 in NT solution for 3 min. The  $\text{Ca}^{2+}$  transients were recorded at the end of each stage for 30 seconds.

Figure 4.12A shows a representative recording of  $\text{Ca}^{2+}$  transients in control conditions and after the perfusion of ML277. For the analysis, the ratio of emission signals (340:380) was measured together with the area under the curve (AUC). The application of 1  $\mu$ M ML277 led to a notable reduction in  $\text{Ca}^{2+}$  transients compared to in control solution. A significant decline in  $\text{Ca}^{2+}$  transients was recorded from  $0.4 \pm 0.01$  (controls,  $n=8$ ) to  $0.3 \pm 0.1$  (1  $\mu$ M ML277,  $n=8$ ,  $p=0.006$ , Figure 4.12B(i)). Figure 4.12B(ii) demonstrates that 1  $\mu$ M ML277 caused a significant shortening in the AUC of the  $\text{Ca}^{2+}$  transients, from  $0.07 \pm 0.02$  (controls,  $n=8$ ) to  $0.06 \pm 0.02$  (ML277,  $n=8$ ,  $p=0.013$ ). A significant reduction in the duration of the  $\text{Ca}^{2+}$  transients after the application of 1  $\mu$ M ML277 ( $n=8$ ,  $p=0.003$ ), as shown in Figure 4.12B(iii). These data showed that selective potentiator of  $I_{Ks}$  reduced the accumulation of intracellular  $\text{Ca}^{2+}$ . Although both excitation signals of Fura-2 would decay at the same rate and therefore the ratio would

remain constant, future research including time-match controls will be required to exclude possible photobleaching and/or extrusion of Fura-2 from the cells.

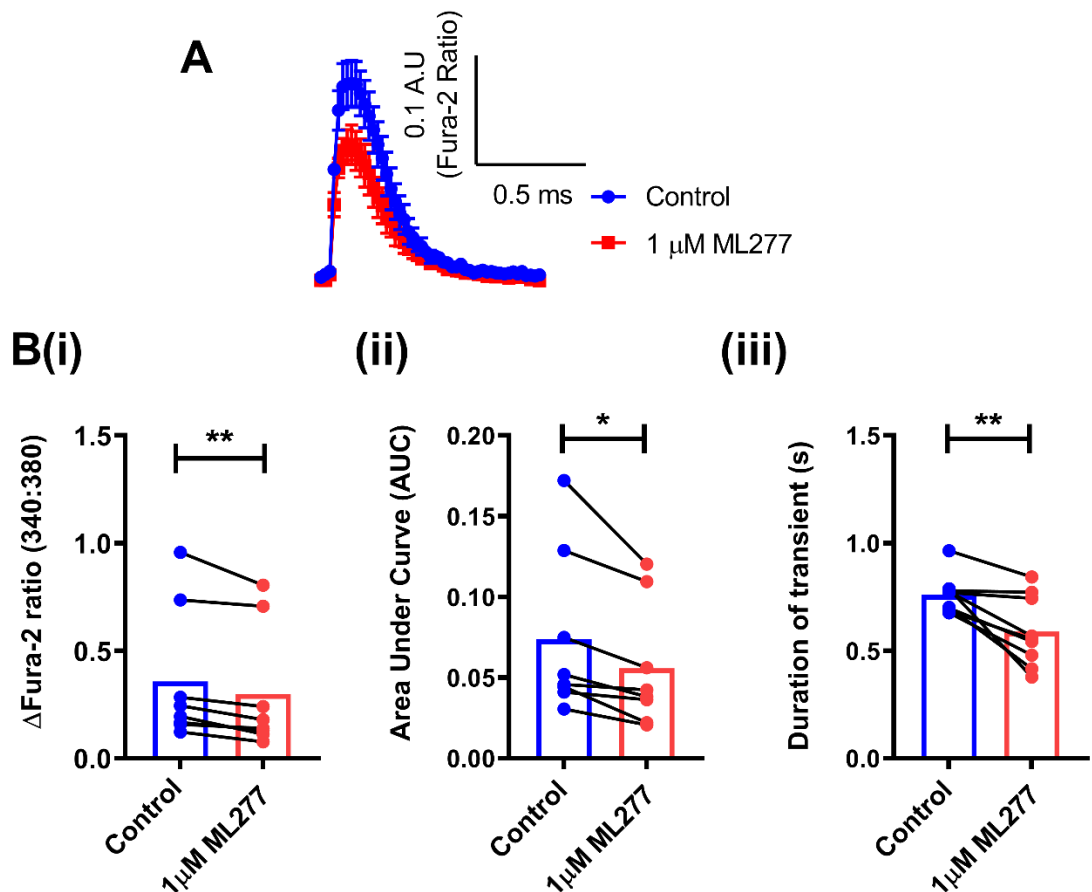


Figure 4.12: ML277 treatment reduced  $\text{Ca}^{2+}$  transients.

*A, Representative traces of  $\text{Ca}^{2+}$  transients during cardiac action potentials in rat cardiomyocytes using Fura-2-AM as a sensitive intracellular calcium indicator to examine the difference between controls and 1  $\mu\text{M}$  ML277. B(i), Graph showing that 1  $\mu\text{M}$  ML277 reduced the amplitude of  $\text{Ca}^{2+}$  transients ( $n = 8$ , \*\* $p = 0.006$ , paired t-test). B(ii), Graph showing that 1  $\mu\text{M}$  ML277 reduced the area under the curve of the  $\text{Ca}^{2+}$  transients ( $n=8$ , \* $p=0.013$ , paired t-test) compared to the control conditions. B(iii), Graph showing that 1  $\mu\text{M}$  ML277 reduced the mean transient duration ( $n=8$ , \*\* $p=0.003$ , paired t-test).*

#### 4.2.8 $I_{Ks}$ inhibition enhanced the peak amplitude and prolonged the calcium transient duration

The results above showed that the selective blockage of  $I_{Ks}$  caused a small but insignificant prolongation of the cardiac APD (Section 4.2.2). We therefore hypothesised that  $I_{Ks}$  inhibition affected the intracellular  $\text{Ca}^{2+}$  release as measured using a calcium-sensitive dye, fura-2-AM.

To examine this pharmacological effect,  $\text{Ca}^{2+}$  transients from isolated rat cardiomyocytes were measured after loading these cells for 20 min in fura-2-AM. As with the ML277 recordings, the  $\text{Ca}^{2+}$  transients were recorded for 30 seconds during two stages: after perfusion with NT solution for 2 min and after perfusion for 3 min with 1  $\mu\text{M}$  JNJ303 in NT solution.

Figure 4.13 shows the calcium transient recordings in the control condition and after the perfusion of JNJ303 treatment. There was a statistically insignificant increase in  $\text{Ca}^{2+}$  transients with JNJ303 from  $0.04 \pm 0.003$  to  $0.05 \pm 0.006$  (control vs. 1  $\mu\text{M}$  JNJ303,  $n=11$  for both groups,  $p=0.07$ , Figure 4.13B(i)). Furthermore, 1  $\mu\text{M}$  JNJ303 caused a significant increase in the AUC of the  $\text{Ca}^{2+}$  transients from  $0.009 \pm 0.0008$  to  $0.012 \pm 0.002$  (control vs. 1  $\mu\text{M}$  JNJ303,  $n=11$  for both groups,  $p=0.04$ , Figure 4.13B(ii)). Figure 4.13B(iii) demonstrates that 1  $\mu\text{M}$  JNJ303 did not increase the duration of  $\text{Ca}^{2+}$  transients ( $n = 11$ ,  $p=0.289$ ). In our future work we intended to measure  $\text{Ca}^{2+}$  transients at time-match control data or recovery of the  $\text{Ca}^{2+}$  transient amplitude following washout of 1  $\mu\text{M}$  JNJ303 to exclude photobleaching and/or extrusion of Fura-2 from the cells. However, as previously discussed that the photobleaching of Fura-2 would tend to occur in both wavelengths simultaneously and therefore this leaves the ratio unchanged.

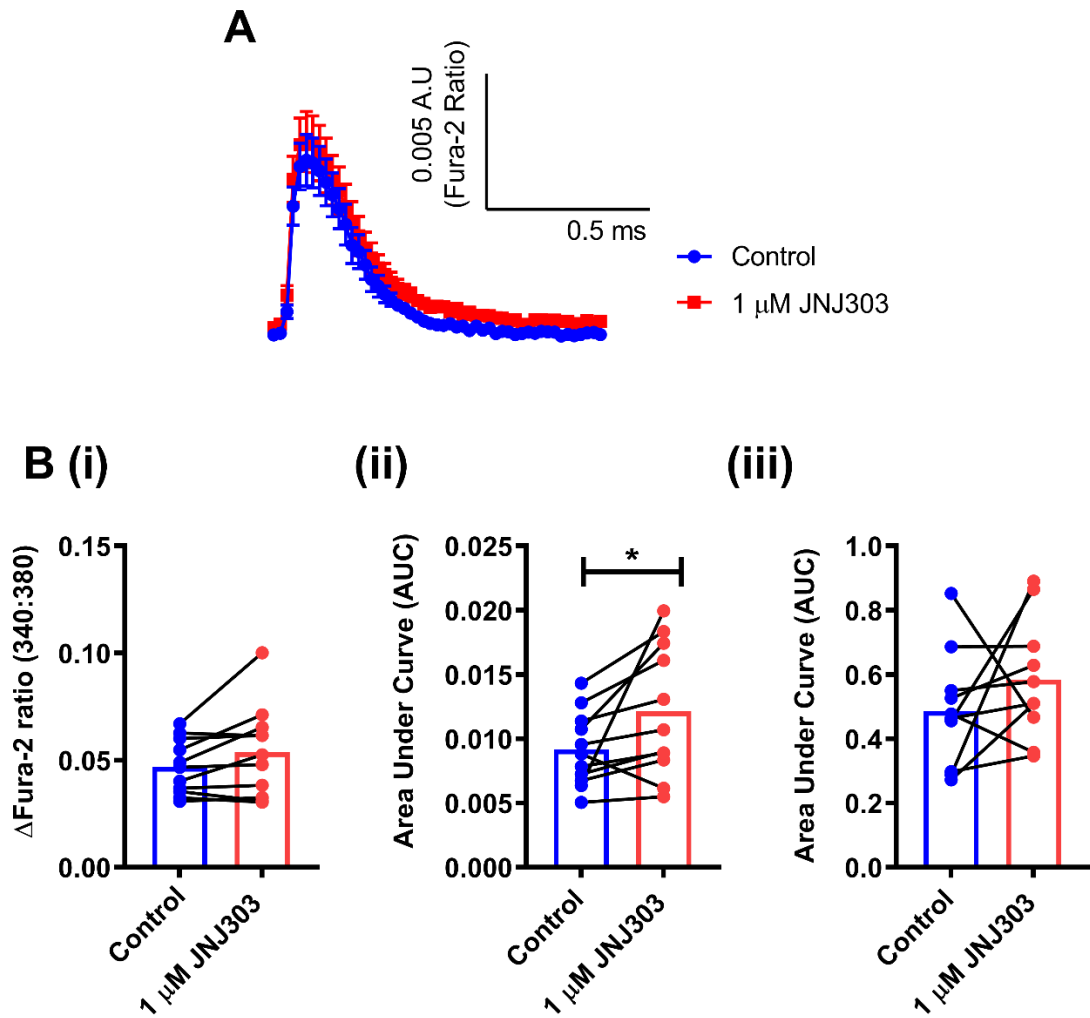


**Figure 4.13:** JNJ303 treatment tended to prolong the duration of the  $\text{Ca}^{2+}$  transients, which may have detrimental impacts on cardiac muscle.

*A, Representative traces of  $\text{Ca}^{2+}$  transients during cardiac action potentials in rat cardiomyocytes using Fura-2-AM as a sensitive intracellular calcium indicator to examine the difference between controls and 1  $\mu\text{M}$  JNJ303. B(i), Graph showing 1  $\mu\text{M}$  JNJ303 caused a small insignificant increase in the amplitude of  $\text{Ca}^{2+}$  transients ( $n=11$ ,  $p=0.07$  for the paired t-test). B(ii), Graph showing that 1  $\mu\text{M}$  JNJ303 increased the area under the curve of the  $\text{Ca}^{2+}$  transients ( $n=11$ ,  $*p=0.04$  for the paired t-test) when compared to the control conditions. B(iii), Graph showing that 1  $\mu\text{M}$  JNJ303 did not increase the transient duration ( $n = 11$ ,  $p=0.289$ , paired t-test).*

### 4.3 Discussion

In this chapter, the imparting of cardioprotection via pharmacological manipulation of cardiac action potentials was investigated. The results suggest that  $I_{\text{Ks}}$ , which is formed by co-expression of KCNQ1- with the KCNE1-subunits, play a role in regulating electrical activity by

inducing a shortening of action potential duration and ultimately cardiac contractility by reducing intracellular  $\text{Ca}^{2+}$ , presumably by causing L-type channels to close more quickly. Considering these electrophysiological properties, the  $I_{\text{Ks}}$  of isolated rat cardiomyocytes were examined using an electrophysiological approach and with selective pharmacological activator and blocker. This current was augmented using a potent activator of  $I_{\text{Ks}}$ , ML277; whilst blockage of  $I_{\text{Ks}}$ , using the  $I_{\text{Ks}}$  blocker, JNJ303. The effects of these two pharmacological modulators support a functional role for KCNQ1/KCNE1 channels in rat ventricular myocytes, as assessed by patch-clamp electrophysiology and fluorescence imaging. The  $I_{\text{Ks}}$  activator shortened the cardiac action potential of rat cardiomyocytes, and reduced the amplitude and the area under the curve of the  $\text{Ca}^{2+}$  transients. It is hypothesised that this shortening of the action potential reduced the time that the L-type-channels were open for and so altered  $\text{Ca}^{2+}$  entry via L-type calcium channels, potentially reducing  $\text{Ca}^{2+}$  loading which may have a protective role in the heart. Further investigations of the effects of action potential duration on the L-type channel directly would be required to understand this further. The  $I_{\text{Ks}}$  activator and blocker in this study were tested at concentrations used in previous studies (Yu et al., 2013a; Towart et al., 2009; Jost et al., 2007).

#### 4.3.1 The potentiation of the $I_{\text{Ks}}$ channel imparts cardioprotection via direct modulation of the cardiac action potential

Several studies in the literature have documented that a significant accumulation of  $I_{\text{Ks}}$  contributes to the shortening of repolarisation, which is usually seen as a shortening of the length of the cardiac cycle, resulting in a reduction of cardiac damage (Magyar et al., 2006; Seeböhm et al., 2003a). Despite these studies being well documented regarding the beneficial role of  $I_{\text{Ks}}$  against arrhythmia, this is the first study aimed at establishing the cardioprotective role of  $I_{\text{Ks}}$  potentiation against cardiac ischaemia. To investigate the properties of  $I_{\text{Ks}}$  in the heart, activation of this current via specific pharmacological treatments is essential to understand its channel-gating kinetic properties and therefore their ability to prevent life-threatening cardiac damage will be tested in the next result chapter. The selectivity of ML277 has been reported by comparing its effects on  $I_{\text{Ks}}$  (Yu et al., 2013b; Mattmann et al., 2012). The concentration-response curve of ML277 was generated by Yu et al. (2013), which showed an  $\text{EC}_{50}$  of 0.26  $\mu\text{M}$  with ML277 treatment and that the maximal response of current

accumulation was achieved at concentrations greater than 1  $\mu$ M (Mattmann et al., 2012). It was also documented that 1  $\mu$ M ML277 led to an increase in the  $I_{Ks}$  by 266% at 40 mV in a CHO cell line with different expressed ratios for the KCNQ1:KCNE1 complex. In guinea pigs and canine cardiomyocytes,  $I_{Ks}$  amplitudes have also been shown to increase by 22% and 228%, respectively (Xu et al., 2015). The data presented in Figure 4.6 are in line with previous studies, as 1  $\mu$ M ML277 caused a significant increase in  $I_{Ks}$  amplitudes at +60 mV in isolated rat cardiomyocytes.

However, a drawback of the current protocol that was used to record the  $I_{Ks}$  is that it does not isolate  $I_{Ks}$  from other potassium currents. Previous studies suggested that there are at least four different components that might contribute to outward current in rat cardiomyocytes, including the transient outward current ( $I_{to}$ ), the delayed-rectifier potassium current ( $I_K$ ), the inward rectifier current ( $I_{K1}$ ) and the non-inactivating steady-state current ( $I_{ss}$ ) (Himmel et al., 1999; Choisy et al., 2004). For rat  $I_{ss}$ , had properties inconsistent with the properties of  $I_{Ks}$  (Himmel et al., 1999). For component  $I_{to}$ , this current appears as a rapidly activating by 2.6 times faster than  $I_K$ , and rapidly inactivating by around 3.9 times faster than  $I_K$  (Himmel et al., 1999). Therefore, the end-pulse current under these recording conditions would likely include  $I_{ss}$  in addition to a possible contribution of  $I_{Ks}$ . While rat  $I_{ss}$  is inhibited by external application of the  $\alpha 1$ -adrenoceptor agonist phenylephrine (PE), further research will be needed to verify whether these  $K^+$  currents have been measured from  $I_{Ks}$  or other potassium currents might have contributed to the currents measured in this study.

Since the  $I_{Ks}$  channel activates slowly during the plateau phase of cardiac action potentials at a more positive membrane potential, a very minor  $I_{Ks}$  may strengthen the repolarisation and play a role in normal action potentials (Varró et al., 2000; Jost et al., 2005). However, the selective augmentation of the  $I_{Ks}$  using a direct pharmacological modulator plays an important role by limiting excessive lengthening of APDs, contributing to the shortening of repolarisation. By using human induced pluripotent stem cell (iPSC)-derived cardiomyocytes, 1  $\mu$ M ML277 induced a 35% shortening of APD (Yu et al., 2013a). This is in a good agreement with our observations in Figure 4.2, which showed that 1  $\mu$ M ML277 led to a significant shortening of the  $APD_{90}$  in ventricular myocytes. This suggests that the targeting of this cardiac ion channel is important in the phase 3 repolarisation of cardiac action potentials and

the large amount of  $K^+$  efflux, contributing to quick repolarisation and shortened cardiac APDs. Therefore, the activation of these outward  $K^+$  channels might cause a reduction in contractility by reducing intracellular calcium overload, thus may contribute to reduce the utilisation of intracellular ATP.

There are also suggestions that the  $I_{Ks}$  activator can alter the kinetic characteristics of this ion channel (Murray et al., 2016; Hou et al., 2017; Wang et al., 2020). Using a CHO cell line, Yu et al. demonstrated that ML277 induced a hyperpolarising shift of the  $I_{Ks}$  activation curve at different voltage steps by  $\sim 16$  mV, hyperpolarising the membrane potential from  $-16.8 \pm 0.7$  mV to  $-32.7 \pm 1.3$  mV (controls vs.  $1 \mu M$  ML277) (Yu et al., 2013a). This result is similar to Abitbol et al.'s study, which used another  $I_{Ks}$  activator in xenopus oocytes and caused a leftward shift in the voltage dependence of activation by  $\sim 17$  mV (Abitbol et al., 1999). More recently, this observation was supported by Xu et al., who reported that ML277 affected the  $I_{Ks}$  activation curve negatively by  $\sim 30$  mV in canine cardiomyocytes (Xu et al., 2015). The data presented in Figure 4.11 show that the activation voltage curve was shifted negatively by  $\sim 21$  mV from  $-8.2$  mV (Controls) to  $-29.4$  mV ( $1 \mu M$  ML277). This result suggests that the potentiation of  $I_{Ks}$  with ML277 may have a protective role in the heart, as the membrane potential does not have to change that much for the channel to open. Therefore, the early opening of the  $I_{Ks}$  channel at a more negative membrane potential could have a more potent effect on the cardiac APD. Although the pharmacological activator of  $I_{Ks}$  was believed to elicit more APD shortening and there has been an effort to consider selective  $I_{Ks}$  activators as a potential therapy against ischaemia to preserve ATP, the long-lasting activation of  $I_{Ks}$  may be detrimental when it is shifted too far as it may prevent evocation of cardiac action potentials and lead to arrhythmias.

#### 4.3.2 The inhibition of the $I_{Ks}$ channel may cause a cardiotoxic effect via direct modulation of the cardiac action potential

The potentiation of  $I_{Ks}$  could impart cardioprotection via repolarisation shortening; therefore, it was hypothesised that the pharmacological blockade of  $I_{Ks}$  would lengthen APDs and might potentially be cardiotoxic. A considerable amount of literature has been published on the effect of selective  $I_{Ks}$  blockers in heart regulation; however, there are controversial results

about their effects on ventricular repolarisation. Several researchers have reported that the selective inhibition of  $I_{Ks}$  causes significant lengthening of cardiac APDs, which consequently induces long QT syndrome (Sun et al., 2001; Emori and Antzelevitch, 2001; Burashnikov and Antzelevitch, 2002). This has been seen in the case of  $I_{Ks}$  mutations, which contribute to cardiac disorders such as Romano-Ward syndrome (KCNQ1 loss of function) and Jervell and Lange-Nielsen syndromes (KCNQ1/KCNE1 loss of function) (Zehlein et al., 2004; Schwartz et al., 2006). Another study by Casimiro et al. reached a similar conclusion, finding a critical role of the  $I_{Ks}$  channel in the regulation of mouse cardiomyocytes and noting that the deletion of KCNQ1 contributed functionally to life-threatening long QT syndrome (Casimiro et al., 2001). This observation occurs due to the inhibition of one of the outward potassium currents, which plays a role in the repolarisation of ventricular muscle, leading to a delay of repolarisation and, consequently, prolonged APD. On the other hand, there are other studies reporting different results. Several researchers have shown that the inhibition of  $I_{Ks}$  by selective blockers did not significantly prolong APDs (Varró et al., 2000; Lengyel et al., 2001; Jost et al., 2005). A possible reason for this is that the activity of  $I_{Ks}$  is characterised by a slow process during the plateau phase of the normal action potential. This means that once  $I_{Ks}$  activates, there is only a small amount of current that would not be expected to cause a significant change in the repolarisation phase of AP. Therefore, under normal physiological conditions, blockade of  $I_{Ks}$  contributes minimally to the cardiac repolarization, especially in mice and rat ventricular myocytes. However, lengthening of the APD beyond its normal duration (>300 ms) may provide  $I_{Ks}$  with more opportunities to influence the repolarisation process and therefore protect the heart from excessive APD prolongation. This observation suggested that the effect of  $I_{Ks}$  blocking agents is increased during prolonged APDs.

The experimental data are controversial, and there is no general agreement on APD prolongation after the inhibition of  $I_{Ks}$ ; therefore, further study would be essential. The data presented in this chapter examined the effect of JNJ303 as a selective  $I_{Ks}$  blocker on the heart regulation. In our experiments using isolated rat ventricular myocytes, JNJ303 induced a small but insignificant prolongation of the  $APD_{90}$ . A possible explanation for this result may be that the main repolarisation current within adult rat myocytes is the transient outward current ( $I_{to}$ ) (Wettwer et al., 1993; Oudit et al., 2001; Arrigoni and Crivori, 2007). It also seems possible that the failed effect of the JNJ303 blocker on the APD of rat ventricular cells is due to the

inhibitory action of JNJ303 becomes noticeable effect with higher expression of KCNE1 (Wrobel, 2013). Apkon and Nerbonne pointed to some instances of the complete absence of  $I_{Ks}$  function in rat ventricular muscle despite the obvious expression of KCNQ1/KCNE1 complex as noticed in previous studies (Apkon and Nerbonne, 1991).

A decreased of total  $I_{Ks}$  following administration of JNJ303 have been shown in Figure 4.8. JNJ303 was found to be selective with no significant effect on the other investigated cardiac ion channels ( $I_{Ca}$  and  $I_{K1}$ ).

#### 4.3.3 $I_{Ks}$ channel modulators alter calcium influx by limiting the opening time of the L-type calcium channel

This chapter set out with the aim of assessing the importance of  $I_{Ks}$  modulators in regulating intracellular calcium and therefore might limit the utilisation of intracellular ATP during ischaemic insult. It has been documented that modulation of the  $I_{Ks}$  channel has the ability to alter  $Ca^{2+}$  transients via modulation of the cardiac APD (Bartos et al., 2017). Prior studies have noted the importance of  $I_{Ks}$  in the regulation of intracellular calcium using the whole-cell patch technique. It was found that the increased force of contraction in isolated guinea pig ventricular myocytes increased outward potassium currents (Tohse, 1990). Therefore, there may be a strong link between the levels of intracellular calcium and the opening of  $I_{Ks}$  channels. In the current study, the levels of  $Ca^{2+}$  transients in control conditions and during infusion with a selective  $I_{Ks}$  activator and blocker were measured. The intracellular  $Ca^{2+}$  was measured using fura-2 as a fluorescent indicator. A significant shortening of  $Ca^{2+}$  transients after treatment with ML277, a selective  $I_{Ks}$  opener, was noted (Figure 4.12). In contrast, JNJ303, an  $I_{Ks}$  blocker, caused a significant prolongation of  $Ca^{2+}$  transients as shown in Figure 4.13. For instance, during sympathetic stimulation, the stimulation of  $\beta$ -adrenergic receptors contributes to increase the outward  $I_{Ks}$ , which consequently counterbalances the concomitant increase in the influx of calcium current. As a result, the prolongation of the cardiac APD is limited and therefore, that allows an efficient time for diastolic filling between heart beats. These findings match those observed in the alteration of cardiac action potential (in section 4.2.1 and section 4.2.2), which suggests that the  $I_{Ks}$  channel plays an important role in balancing of the  $Ca^{2+}$  entry through the voltage-gated calcium channels via enhancing the

delayed rectifier potassium currents to modulate the plateau phase of cardiac action potential. As a result, the potentiation of  $I_{Ks}$  could play an important role during instances of metabolic stress, such as myocardial ischaemia where it contributes to limit the time of calcium influx and repolarisation.

Returning to the hypothesis posed at the beginning of this study, it is now possible to state that a potentiation of the  $I_{Ks}$  in cardiomyocytes may be cardioprotective by shortening the cardiac action potential, reducing intracellular calcium loading and thus could preserve cellular ATP. Despite  $I_{Ks}$  blockage having a small effect on cardiac APDs, this pharmacological blocker caused a significant decreased in the outward current amplitude and consequently prolonged  $\text{Ca}^{2+}$  transients and thus may contribute to cardiotoxicity. This hypothesis will be further examined in the next result chapter.

# Chapter 5 The cardioprotective role of $I_{K_s}$ potentiation

## 5.1 Introduction

In the previous results chapter, it was demonstrated that the acceleration of ventricular repolarisation via pharmacologically targeting  $I_{K_s}$  channels imparted a shortened action potential duration. The shortening of APD by selectively activating  $I_{K_s}$  (ML277) reduces calcium overload and may limit intracellular ATP consumption. This result was demonstrated using patch clamp electrophysiological recordings and fluorescence imaging. In this chapter, the cardioprotective role of the  $I_{K_s}$  potentiation on the cellular level and the whole heart was investigated using a selective pharmacological activator and blocker.

The importance of the  $I_{K_s}$  to the normal physiological function of the heart is highlighted by the fact that it can cause several inherited pathological conditions. Loss-of-function mutations lead to the pro-arrhythmic prolongation of the cardiac action potential, while gain-of-function mutations cause pro-arrhythmic shortening of the cardiac action potential (Zehelein et al., 2004; Schwartz et al., 2006; Loussouarn et al., 2006). It is hypothesised that the modification of  $I_{K_s}$  plays a key role in cardioprotection against arrhythmic episodes. This indicates a need to understand how modification of this  $I_{K_s}$  channel affects myocardial function in the setting of acute coronary ischaemia. Briefly, it has been reported that cardiac ion channels, such as the  $K_{ATP}$  channel, limit ischaemic damage by shortening the action potential duration to regulate calcium entry and therefore reduce energy consumption (Fujita and Kurachi, 2000; Brennan et al., 2015). The outcome of this protection suggests correlation between the potentiation of other cardiac potassium currents, such as  $I_{K_s}$ , and limited ischaemic damage.

Whether the cardioprotection of  $I_{K_s}$  potentiation could be achieved after exposing isolated rat myocytes to metabolic inhibition and reperfusion protocol was tested. Furthermore, the cardiotoxic effect of  $I_{K_s}$  inhibition was examined throughout the simulated ischaemia and reperfusion protocol. This protocol with selective pharmacological tools was used to investigate contractile function, using the endpoints to assess cellular injury in isolated myocytes. In addition to that, *ex vivo* coronary ligation experiments in adult male rat hearts were used, cannulating on a Langendorff apparatus. This protocol was used to assess the

protection of pharmacological manipulation of the  $I_{Ks}$  on the whole heart by measuring the effect on infarct size.

The objective of this chapter was to study cardiac  $I_{Ks}$  as a potential target to limit ischaemia/reperfusion injury. ML277 was used to potentiate  $I_{Ks}$  to determine whether there was a direct effect of its activity on the cellular function of isolated single cardiomyocytes. Following on from this, it was further investigated in whole-hearts following perfusion with ML277. By recording the effect on JNJ303 treatment on the contractile function from isolated cardiomyocytes and on the infarct size from Langendorff perfused intact hearts, it was also hypothesised that there was a potential cardiotoxicity with  $I_{Ks}$  inhibition. In this chapter, the use of  $I_{Ks}$  as a pharmacological target for imparting cardioprotection was assessed.

## 5.2 Results

### 5.2.1 Potentiation of $I_{Ks}$ does not delay $K_{ir}6.2$ channel openings during metabolic inhibition

It is hypothesised that a delay in the time taken to activate of cardiac  $K_{ATP}$  ( $K_{ir}6.2/SUR2A$ ) current in a cardioprotected state is caused by a delay in ATP depletion during a major ischaemic insult. As the previous results chapter suggests, selective potentiation of the  $I_{Ks}$  alters of a number of cellular functions, including shortening cardiac action potential. It was hypothesised that this would reduce intracellular calcium and, therefore, preserve cellular ATP. Therefore, the first set experimental analyses in this chapter examined the effect of  $I_{Ks}$  potentiation on the time to activation of the cardiac  $K_{ir}6.2/SUR2A$  current. To investigate this, cell-attached patch recording was used to record cardiac  $K_{ir}6.2/SUR2A$  activity in isolated cardiomyocytes. In cell-attached patch recording, the membrane potential of the cell-attached patch on a cardiomyocyte was held at around -110 mV to investigate the openings of ventricular  $K^+$  channel, which was achieved by holding the pipette potential at +40 mV and assuming a resting membrane potential of ~-70 mV. At this negative membrane potential, inward rectifier potassium channels, such as  $K_{ir}2$  and  $K_{ir}6$ , will be the primary open channels. These channels are readily differentiated by their single channel current amplitude and kinetics.  $K_{ir}2$  channels have a conductance of around 30 pS and so have a single channel current of around 3.5 pA in these conditions. The kinetics of the  $K_{ir}2$  channels show long

openings that do not display a bursting pattern. The  $K_{ir}6.1$  channels show a bursting activity with a single channel current amplitude of 5.5 – 6 pA. When analysing these cell-attached records, the threshold for channel detection can be set to treat the opening of  $K_{ir}2$  as a shift in baseline.  $K_{ir}6.2$  channels only open in metabolic inhibition when there is significant ATP depletion, triggering the activation of a larger (~70 pS) channel with a single channel current amplitude of 10 – 11 pA. The bursting behaviour of this channel gives a characteristic open and closed level with no obvious sub-condutance states, differentiating it from the opening of multiple  $K_{ir}6.1$  channels. With increasing openings of  $K_{ir}6.2$  channels, the single channel current may increase as the resting membrane potential of the cell becomes more hyperpolarised. The channel that underlie  $I_{Na}$ ,  $I_{Ca}$ ,  $I_{Ks}$  and  $I_{Kr}$  normally pass currents at positive membrane potentials and so these channels will be in a closed state at -110 mV. It is unlikely that these voltage-gated channels will make any contribution to the single channel activity in these cell-attached recordings.

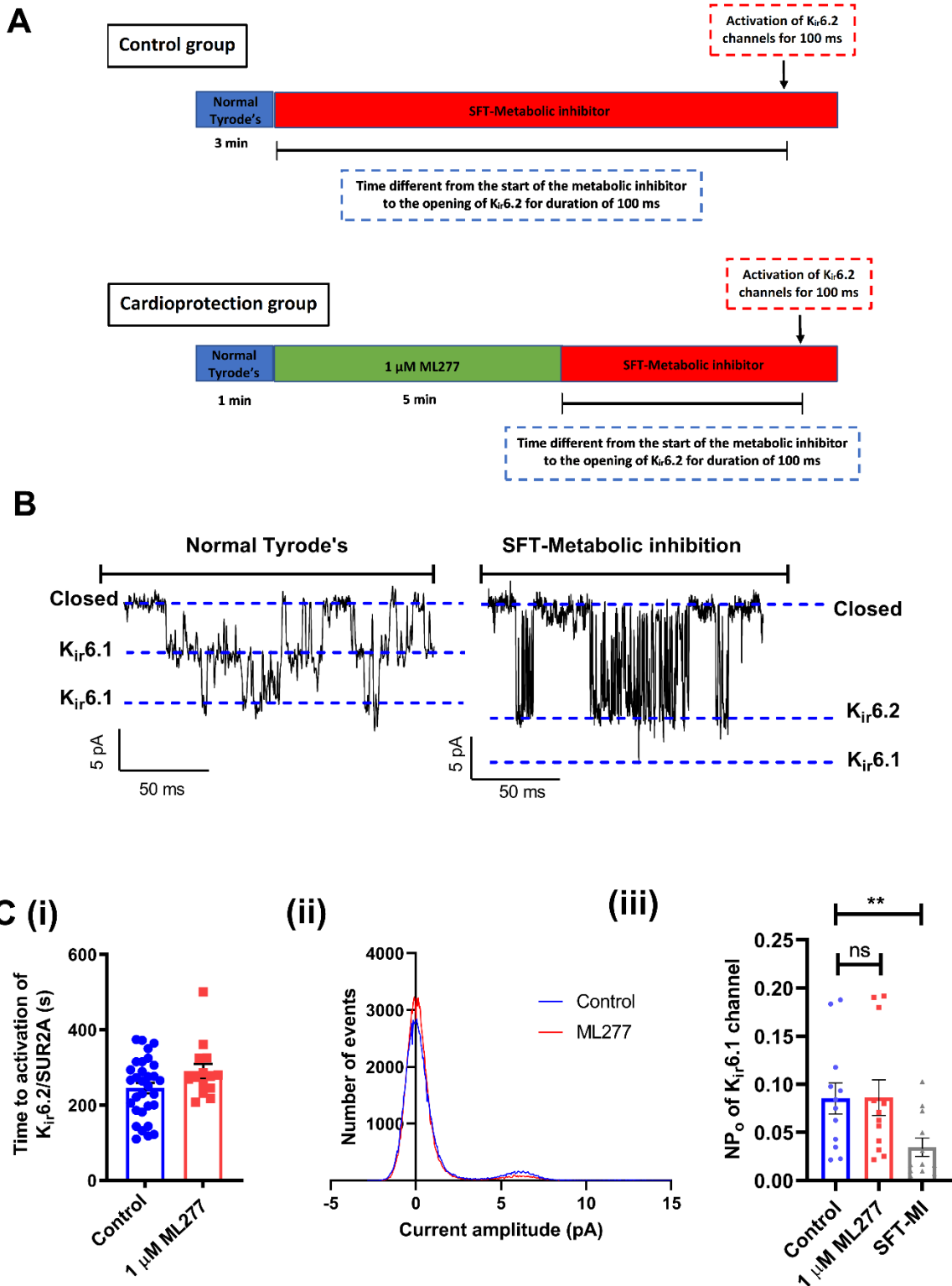
In order to differentiate between cardioprotected cells and non-cardioprotected cells, cardiomyocytes underwent a separate protocol, as shown in Figure 5.1A. In the control group, unprotected cells were perfused with NT for 3 min, and then metabolic inhibition was used to activate the cardiac  $K_{ATP}$  current by exposing the cells to substrate-free metabolic inhibition Tyrode's solution (SFT-MI) containing cyanide and iodoacetic acid to inhibit glycolysis and the electron transport chain respectively. Cardioprotected cells were treated with 1  $\mu$ M ML277 for 5 min prior the application of the metabolic inhibition. The  $K_{ir}6.2/SUR2A$  channel complex is activated by metabolic inhibition and so can be used as a surrogate marker of ATP depletion. The opening of the  $K_{ATP}$  complex was defined as a burst of single channel activity, with an amplitude of ~10 pA, that lasts for longer than 100 ms. The time to the first burst of activity was measured as the time difference from the beginning of the metabolic inhibitor to the first burst of activity greater than 100 ms.

Figure 5.1B shows a representative trace of cardiac  $K_{ATP}$  current activity on the cell membrane of rat cardiomyocytes, showing two levels of the cardiac  $K_{ATP}$  current amplitude: ~5 pA in control conditions with multiple openings of the same channel type, attributed to the relatively ATP-insensitive  $K_{ir}6.1$  channel, and ~10 pA following introduction of the metabolic inhibitor activating the  $K_{ir}6.2$  containing ATP-sensitive pore. The most widely studied cardiac

$K_{ATP}$  ( $K_{ir}6.2/SUR2A$ ) current opens after a fall in ATP level during metabolic inhibition (Voitychuk et al., 2011). Treatment with 1  $\mu M$  ML277 led to a small, but not significant, delay in the  $K_{ir}6.2/SUR2A$  opening during metabolic inhibition, from  $245.2 \pm 14.1$ s (control, n=31) to  $289.8 \pm 19.8$ s (1  $\mu M$  ML277, n=14, p=0.08), as shown in Figure 5.1C(i).

In chapter 3, data was presented giving evidence for the presence of  $K_{ir}6.1$ , with a smaller single channel current amplitude than  $K_{ir}6.2/SUR2A$ , in the myocardium. This channel opens in resting conditions was hypothesised to play an important role in the regulation of APD and in improving the calcium handling. For these reasons, potentiation of the opening of  $K_{ir}6.1$  channel is considered as a potential cardioprotective mechanism. The effect of ML277 on  $K_{ir}6.1$  channel open probability ( $NP_o$ ) was tested as a potential mechanism by which ML277 may impart additional protection. Representative amplitude histograms of  $K_{ir}6.1$  in control and in 1  $\mu M$  ML277 are shown in Figure 5.1C(ii). From Figure 5.1C(ii) it can be seen that the administration of ML277 caused no change in the peak open or closed level of  $K_{ir}6.1$  channel compared to control.

Figure 5.1C(iii) shows the mean open probability ( $NP_o$ ), suggesting that ML277 did not cause any significant change in the  $NP_o$  of  $K_{ir}6.1$  channel, from  $0.085 \pm 0.02$  (control, n=12) to  $0.086 \pm 0.02$  (1  $\mu M$  ML277, n=12, p=0.95). However,  $NP_o$  of the  $K_{ir}6.1$  channel was significant decreased following metabolic inhibition compared to controls ( $0.085 \pm 0.02$  vs  $0.034 \pm 0.01$ , n=12, p=0.01). These findings indicate that a 1  $\mu M$  ML277 did not increase open probability of the  $K_{ir}6.1$  channel.



**Figure 5.1:** Potentiation of the  $I_Ks$  does not delay cardiac  $K_{ir}6.2/SUR2A$  channel opening following metabolic inhibition.

**A, Cell-attached patch configuration with metabolic inhibition protocols to trigger the cardiac  $K_{ir}6.2/SUR2A$  channel opening. Under control condition protocol, isolated cardiomyocytes were initially perfused for 3 min with NT, followed by substrate-free metabolic inhibition Tyrode's solution (SFT-MI).**

*The cardioprotection protocol was differed by introducing ML277 prior to the application of the metabolic inhibitor. To investigate the difference between these two groups, the time difference from the start of the metabolic inhibitor to the time when the cardiac  $K_{ir}6.2/SUR2A$  activated for a duration of 100 ms was calculated. B, Representative traces recorded from cell-attached patch at  $\sim -110$  mV. Under normal conditions, there were at least two  $K_{ir}6.1$  channels opening with a single channel current amplitude of  $\sim 5$  pA each. However, there was a large current amplitude channel ( $\sim 10$  pA) that indicated the activation of the cardiac  $K_{ir}6.2/SUR2A$  channel in response to ATP depletion. C(i), Bar chart showing the mean of total cells for the time to activation of cardiac  $K_{ATP}$  ( $K_{ir}6.2/SUR2A$ ) current, was not delayed (control,  $n=31$  vs.  $1 \mu\text{M}$  ML277,  $n=14$ ,  $p=0.08$ ) (unpaired t-test). C(ii), Representative amplitude histograms (1 min interval) assessed in control and in  $1 \mu\text{M}$  ML277, showing no change in the peak of opening level of  $K_{ir}6.1$  at  $\sim 5.5$  pA in the presence of ML277 compared to control value. C(iii), Bar chart showing the mean  $NP_o$  of  $K_{ir}6.1$  channels in control cells, in cells treated with  $1 \mu\text{M}$  ML277 and following the perfusion of SFT-metabolic inhibition. There was no significant change in  $NP_o$  following perfusion with ML277, however, there was a significant decrease in  $NP_o$  following the perfusion of SFT-metabolic inhibition, compared to controls ( $n=12$ ,  $p=0.95$ ,  $p=0.01$ , respectively) (One-way ANOVA with Holm-Sidak post-test).*

Although the selective activation of the  $I_{Ks}$  did not significantly delay the time to  $K_{ir}6.2/SUR2A$  activation, there was a small delay. To further investigate this, it was hypothesised that  $I_{Ks}$  potentiation may induce hyperpolarisation of the membrane potential. To investigate this, current clamp recordings were made to measure the membrane potential in response to perfusion with ML277 and metabolic inhibition. Figure 5.2A shows that the membrane potential hyperpolarised from  $-60.8 \pm 6.3$  mV to  $-63.1 \pm 2.9$  mV (control vs.  $1 \mu\text{M}$  ML277,  $n=5$ ,  $p=0.63$ ), however this was not a significant effect. The effect of metabolic inhibitors such as DNP (2,4-Dinitrophenol) on the membrane potential of rat cardiomyocytes was recorded and showed a significant depolarisation of the cell membrane, from  $-70.7 \pm 0.7$  mV at controls ( $n=9$ ) to  $-62.2 \pm 2.8$  mV (DNP,  $n=9$ ,  $**p=0.01$ , Figure 5.2B). Further to this, the combination of  $I_{Ks}$  potentiation and metabolic inhibition caused a significant depolarisation of the membrane potential, going from  $-71.7 \pm 0.5$  mV to  $-67.0 \pm 0.8$  mV (control vs.  $1 \mu\text{M}$  ML277,  $n=6$ ,  $**p=0.01$ , Figure 5.2C). Following perfusion with a solution containing both  $1 \mu\text{M}$  ML277 and DNP, the membrane potential showed a trend towards hyperpolarisation, although this was not significant,  $-67.0 \pm 0.8$  mV in  $1 \mu\text{M}$  ML277+DNP ( $n=6$ ),  $-63.1 \pm 3.0$  mV in  $1 \mu\text{M}$  ML277 ( $n=5$ ,  $p=0.42$ ), and  $-62.2 \pm 2.8$  mV in DNP ( $n=9$ ,  $p=0.27$ ). There was also a no significant difference between  $1 \mu\text{M}$  ML277 treatment and the application of DNP alone ( $p=0.73$ ). These findings suggest that  $I_{Ks}$  potentiation had no effect on membrane potential as would be expected for a voltage-gated channel.

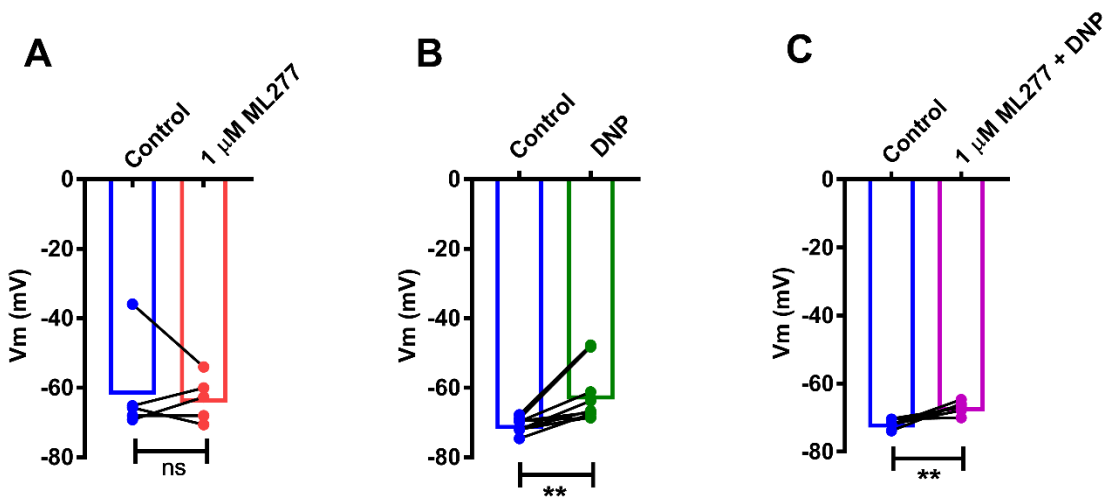


**Figure 5.2:** ML277 did not cause hyperpolarisation of the membrane potential.

A, Graph showing that ML277 treatment caused no change in membrane potential ( $p=0.63$ , paired t-test). B, Graph showing that metabolic inhibition, such as with DNP (2,4-Dinitrophenol), led to a significant depolarisation of cell membrane of rat cardiomyocytes ( $**p=0.01$ , paired t-test). C, Graph showing that membrane potential was significantly depolarised after exposing the isolated cardiomyocytes to the combination of  $I_{Ks}$  potentiation and metabolic inhibition ( $**p=0.01$ , paired t-test). Together these results showed that the presence of ML277 with metabolic inhibition caused no change in membrane potential, compared to application separately with 1  $\mu$ M ML277 treatment and DNP alone ( $p=0.42$ ,  $p=0.27$ , respectively, one-way ANOVA Holm-Sidak post-test).

### 5.2.2 ML277 imparts cardioprotection from metabolic inhibition and washout protocol in a concentration-dependent manner

As mentioned in the previous chapter,  $I_{Ks}$  potentiation caused a shortening of cardiac action potential, and we hypothesised that the pharmacological modulation of this channel could impart cardioprotection via limiting the calcium influx by shortening the duration that calcium channels remain open. The reduction in calcium accumulation reduces the energy needed to remove the calcium from the cell via the calcium ATPase. In order to investigate ML277-induced cardioprotection, isolated cardiomyocytes underwent two protocols, as shown in Figure 5.3A, subjected to metabolic inhibition to induce reperfusion injury. Cardiomyocytes were perfused with NT for 3 min, then 7 min with substrate-free metabolic inhibition Tyrode's solution (SFT-MI), followed by 10 min reperfusion with NT. Cardioprotected cells were pre-

treated for 5 min with different concentrations of ML277 and compared to unprotected cells in the control protocol. Cardiomyocytes were stimulated to contract at 1 Hz via electric field stimulation (EFS) throughout this protocol in order to assess the contractile function. Several parameters were measured to reflect the contractile function, including the time for contractile failure (as a measure of the time to ATP depletion), the percentage of cell recovering their contractile function and the percentage of cell survival as measured using Trypan Blue exclusion.

Using the times to contractile failure and contractile recovery, a time course was constructed, as shown in Figure 5.3B(i). This figure illustrates the effect of metabolic inhibition on cells and a reversible inhibition of ATP generation as on myocardial reperfusion. It was found that preconditioning myocytes with ML277 resulted in increased recovery of contractile function compared to untreated cardiomyocytes.

To assess the protective effect of  $I_{Ks}$  potentiation, the time from the onset of metabolic inhibition to the time when the cells failed to contract was measured in both the control and pre-treated groups, as shown in Figure 5.3B(ii). The time to contractile failure was significantly prolonged, from  $144.0 \pm 2.4$  s (control, n=21) to  $147.8 \pm 2.6$  s (100 nM ML277, n=12, p=0.42),  $166.9 \pm 2.7$  s (300 nM ML277, n=14, \*\*\*\*p<0.0001),  $192.3 \pm 4.0$  s (1000 nM ML277, n=18, \*\*\*\*p<0.0001) and  $201.1 \pm 4.3$  s (3000 nM ML277, n=12, \*\*\*\*p<0.0001). The results shown in Figure 5.3B(ii), indicate that pre-treatment with ML277 led to a significant delay in the time of contractile failure, and this was ML277 concentration dependent.

Further investigation assessed the cardioprotective effect of ML277 at the end of the reperfusion period, which was achieved by counting the percentage of cells regaining contractile function. In the control experiment,  $31.4 \pm 1.5\%$  of cardiomyocytes recovered their contractile function following 10 min of wash out (n=21) (Figure 5.3B(iii)); therefore, any cell preparation with a contractile recovery greater than ~30% was considered a cardioprotected condition. Figure 5.3B(iii) shows that the application of ML277 significantly increased contractile recovery in a concentration-dependent manner, going from  $34.8 \pm 1.7\%$  (100 nM ML277, n=12, p=0.18),  $49.9 \pm 1.5\%$  (300 nM ML277, n=14, \*\*\*\*p<0.0001),  $71.5 \pm 2.2\%$  (1000 nM ML277, n=18, \*\*\*\*p<0.0001) and  $70.2 \pm 1.6\%$  (3000 nM ML277, n=12, \*\*\*\*p<0.0001).

Additionally, dead cells were stained with Trypan blue at the end of the reperfusion period to examine the effect of this pharmacological treatment on cell survival. The mean percentage of cell survival at the end of reperfusion increased from  $66.4\pm1.2\%$  (control, n=21) to  $67.8\pm1.1\%$  (100 nM ML277, n=12, p=0.39),  $78.2\pm1.1\%$  (300 nM ML277, n=14, \*\*\*p<0.0001),  $88.8\pm1.0\%$  (1000 nM ML277, n=18, \*\*\*p<0.0001) and  $90.5\pm0.9\%$  (3000 nM ML277, n=12, \*\*\*p<0.0001) (Figure 5.3B(iv)).

These results suggest that pre-treatment with ML277 led to maintaining the contractile function for longer after the application of SFT-MI. Furthermore, increasing the concentration of ML277 provides improved cardioprotection by increasing contractile recovery and increasing cell survival. This provides important insight into the use of pharmacological  $I_{Ks}$  potentiation to impart cardioprotection.

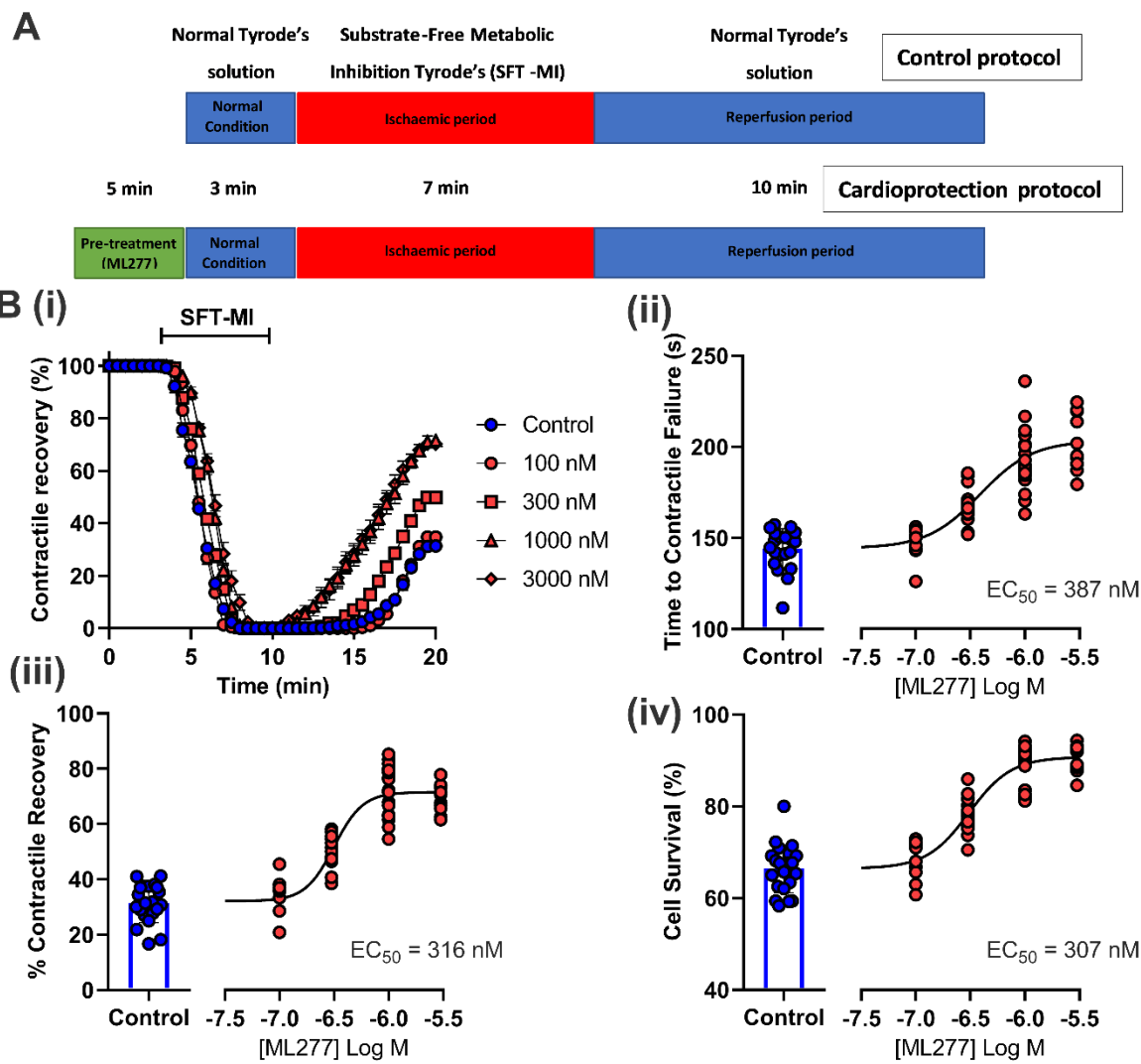


**Figure 5.3:** Pre-treatment with ML277 imparts cardioprotection in isolated cardiomyocytes.

**A, Metabolic inhibition and reperfusion protocols.** For the control condition protocol, cardiomyocytes were initially perfused for 3 min with NT, 7 min with substrate-free metabolic inhibition Tyrode's solution (SFT-MI) and then washed out for 10 min with NT. The cardioprotective protocol was varied by applying ML277 prior to the start of the control condition protocol. **B(i),** Time course showing the percentage of rod-shaped cardiomyocytes contracting in response to the stimulator during perfusion with SFT-MI and reperfusion with NT. **B(ii),** Time to contractile failure from the onset of metabolic inhibition, which shows a was significantly prolonged after perfusion with 300 nM ML277, 1000 nM ML277, and 3000 nM ML277 ( $n=14$ ,  $n=18$ ,  $n=12$ , respectively); however, 100 nM ML277 led to insignificant change ( $n=12$ ). **B(iii),** The percentage of cardiomyocytes regaining contractile function in response to the stimulator by the end of reperfusion shows the application of ML277 significantly increased contractile recovery in a concentration-dependent manner except 100 nM ML277. **B(iv),** Bar chart showing the mean percentage of cell survival at the end of reperfusion, increases in response to ML277 treatments with concentration dependent. (One-way ANOVA Holm-Sidak post- test).

### 5.2.3 JNJ303 is cardiotoxic to cells during metabolic inhibition and washout protocol

The previous chapter highlights that a selective blocker of the  $I_{Ks}$  channel caused a small but insignificant prolongation of the cardiac action potential and a significant increase in the AUC of the  $Ca^{2+}$  transients. It was hypothesised that  $I_{Ks}$  inhibition would have a cardiotoxic effect on ventricular myocytes. To investigate the cardiotoxic mechanisms of  $I_{Ks}$  inhibition, isolated ventricular myocytes were exposed to JNJ303 during metabolic inhibition and on reperfusion. As with the ML277 recordings from the metabolic inhibition and wash out protocol, similar parameters were used to examine the effect of JNJ303 on contractile function. For instance, the time to contractile failure, the percentage of contractile recovery and the percentage of cell survival were measured from both control and pharmacological recordings. This recording was carried out using a protocol similar to ML277 as described in Figure 5.4A.

Figure 5.4B(i) shows the percentage of contractile isolated myocytes in response to metabolic inhibition and their recovery on the reperfusion, which were recorded every 30 sec throughout the protocol.

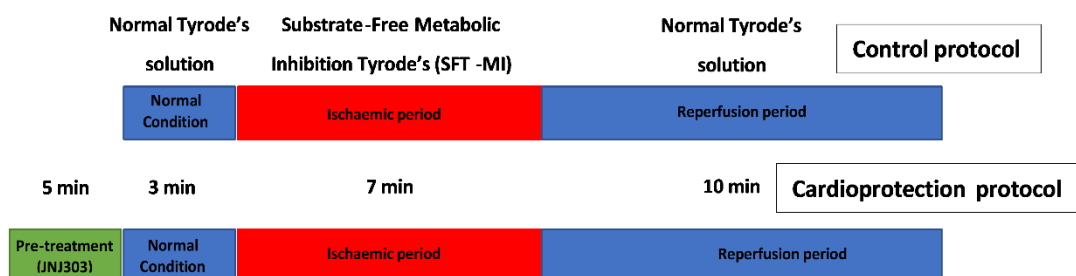
In order to investigate the cardiotoxicity of JNJ303, time to contractile failure was measured from the onset of metabolic inhibition to time of loss of contractility of cardiomyocytes. Figure 5.4B(ii) shows that the application of this pharmacological treatment caused a significant shortening of time to contractile failure, going from  $143.0 \pm 2.9$  s at control ( $n=21$ ) to  $125.4 \pm 4.0$  s following perfusion with  $1 \mu M$  JNJ303 ( $n=6$ ,  $**p=0.003$ ). This result indicates the cardiotoxicity of  $I_{Ks}$  inhibition, showing an acceleration of the time to contractile failure, specifically during severe metabolic stress.

To further examine the effects of the selective blocker of  $I_{Ks}$  on contractile function, the percentage of contractile recovery on the reperfusion period was used as a cardiotoxic indicator. The percentage contractile recovery was significantly decreased following JNJ303 treatment, going from  $32.0 \pm 1.7\%$  to  $17.7 \pm 1.2\%$  (control,  $n=9$  vs  $1 \mu M$  JNJ303,  $n=6$ ,  $****p<0.0001$ ) (Figure 5.4B(iii)). Figure 5.4B(iv) shows that pre-treatment with JNJ303 led to

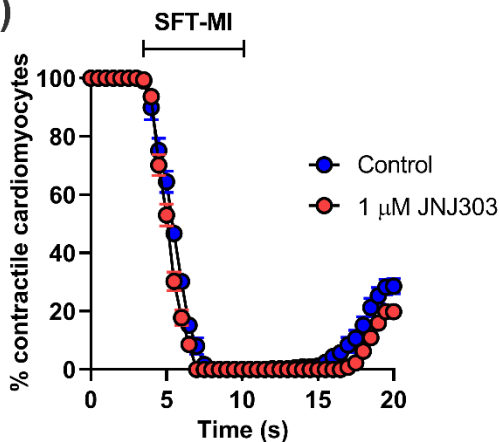
cause a significant decline in cell survival, from  $67.7 \pm 1.3\%$  at the control ( $n=9$ ) to  $55.4 \pm 2.9\%$  at  $1 \mu\text{M}$  JNJ303 ( $n=6$ , \*\*\* $p=0.0008$ ).

It is apparent from Figure 5.4 that  $I_{\text{Ks}}$  inhibition is cardiotoxic to ventricular myocytes during severe metabolic inhibition, such as myocardial ischaemia. This outcome was revealed in several ways, including shortened the time to contractile failure and decreased contractile recovery and cell survival.

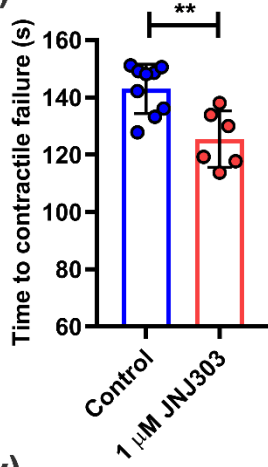
**A**



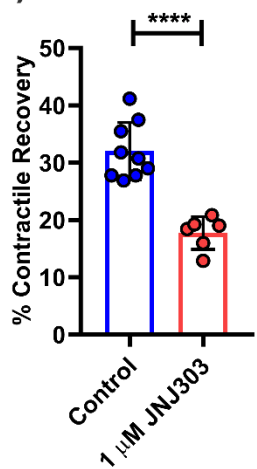
**B (i)**



**(ii)**



**(iii)**



**(iv)**

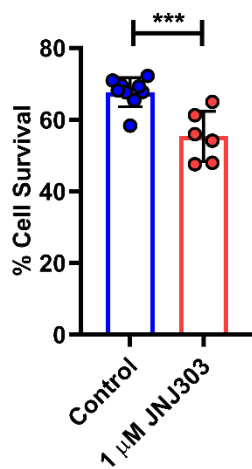


**Figure 5.4:** Pre-treatment with JNJ303 causes cardiotoxicity in isolated rat ventricular cells.

*A, Metabolic inhibition and reperfusion protocols. At the control experimental protocol, cardiomyocytes were initially perfused with NT for 3 min, then 7 min with substrate-free metabolic inhibition Tyrode's solution (SFT-MI) to simulate ischaemia and then for 10 min with NT to simulate reperfusion. Cardioprotection was achieved by administering JNJ303 prior to the start of the control condition protocol. B(i), Time course showing the percentage of rod-shaped cardiomyocytes contracting in response to the stimulator throughout the experimentation. B(ii), Time to contractile failure from the application of the metabolic inhibitor (SFT-MI), which shows a significant reduction (\*\*p=0.003). B(iii), The percentage of ventricular myocytes recovering contractile function in response to the stimulator by the end of reperfusion shows a significant decrease (\*\*\*\*p<0.0001). B(iv); Graphs showing a significant reduction in the mean percentage of cell survival at the end of reperfusion (\*\*p=0.0008). (Unpaired t- test).*

#### 5.2.4 ML277 protects the whole heart from damage during a whole-heart *ex vivo* coronary ligation protocol

The results in Section 5.2.2 show that  $I_{Ks}$  potentiation minimised damage after metabolic inhibition by improving contractile recovery and cell survival. To investigate whether there was an effect in the whole heart, a Langendorff experimental model of *ex vivo* coronary ligation was used to measure the effect of  $I_{Ks}$  potentiation on the infarct size. The protocol was shown in Figure 5.5A to expose the isolated heart muscle into ischaemia and reperfusion. The heart was stabilised for 1 hr, the LAD was ligated for 40 min to cause a regional ischaemia and then ligation was released to allow for 3 hr of reperfusion. Heart slices were stained using different pigmentations to produce three different colours: blue pigment indicated non-affected regions (Evans Blue dye), red pigment indicated areas at risk and white pigment indicated dead tissue (stained with TTC), as described in Section 2.6C. To determine the cardioprotective effect of ML277 on infarct size, the drug was perfused throughout the experiment, and the effect on the infarct size was measured.

Figure 5.5B shows representative scanned images from adult rat hearts, comparing the cardioprotected heart with 1  $\mu$ M ML277 to the control heart. The application of ML277 reduced the infarct size (a small white area) compared to the control.

The percentage of infarct size was significantly reduced in the pharmacological treatment group, and this was ML277 concentration dependent, going from 35.6 $\pm$ 1.8% (control, n=16)

to  $33.4 \pm 1.8\%$  (100 nM ML277,  $n=5$ ,  $p=0.45$ ),  $20.8 \pm 2.6\%$  (300 nM ML277,  $n=4$ ,  $****p<0.0001$ ) and  $12.6 \pm 1.2\%$  (1 $\mu$ M ML277,  $n=5$ ,  $****p<0.0001$ ) (Figure 5.5C). The current finding adds substantially to our hypothesis of the cardioprotective role of  $I_{Ks}$  potentiation against the damage from myocardial ischaemia.

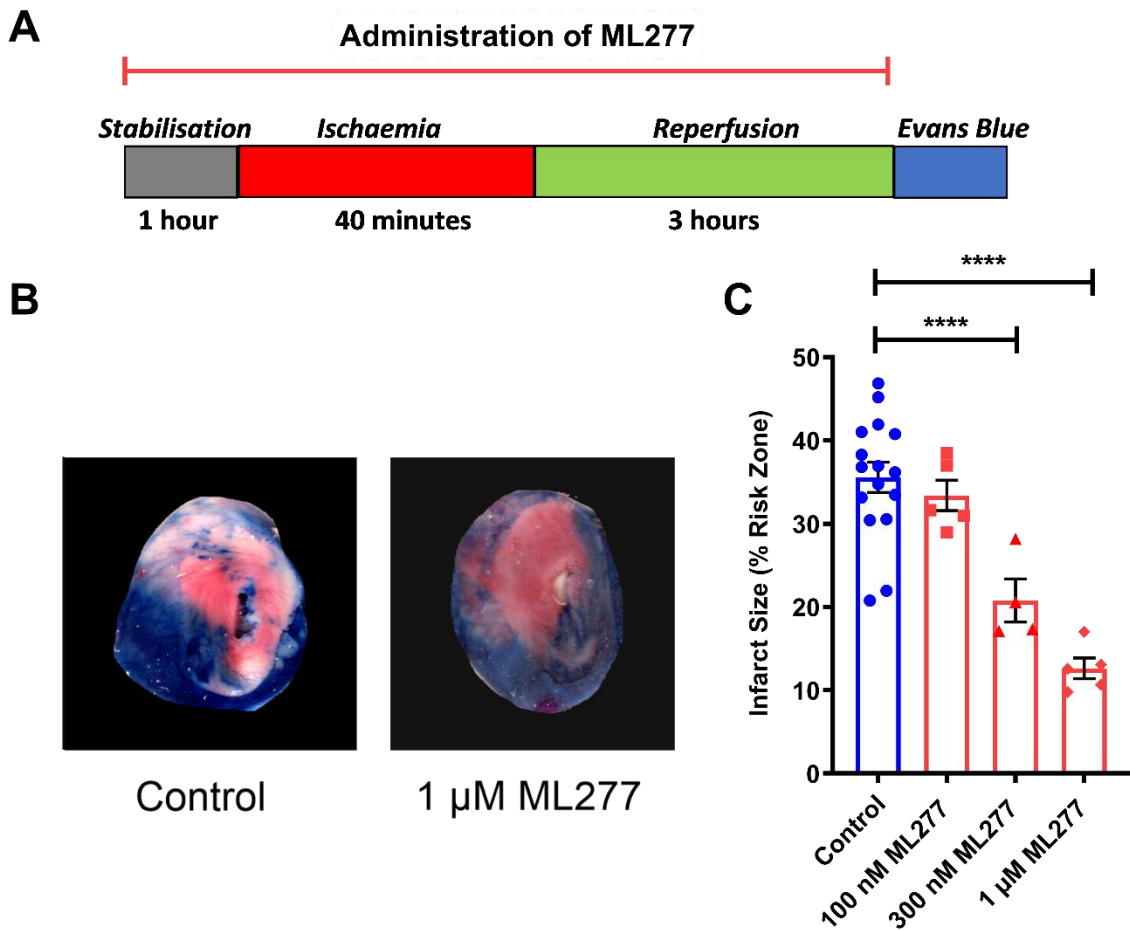


**Figure 5.5:** ML277 imparts cardioprotection by reducing the infarct size in the whole heart after coronary ligation using the Langendorff technique.

*A, Protocol designed to examine the effect of  $I_{Ks}$  potentiation on the damage from myocardial ischaemia and reperfusion injury: rat hearts were stabilised for 1 hr with NT perfusion, the coronary artery was ligated for 40 min to induce regional ischaemia, and myocardial reperfusion with NT was simulated by un-ligation the coronary artery for 3 hr. Then, TTC staining perfusion was used to investigate the infarct size. ML277 was perfused throughout this experimental protocol. B, Representative scanned images of stained hearts during control and 1  $\mu$ M ML277, which showed a reduction of infarct size (white tissue) after the pharmacological treatment. C, Graph showing the mean of infarct size with a reduction in concentration dependent infarct size (Control,  $n=16$  vs  $p=0.45$  (100 nM ML277,  $n=5$ ),  $****p<0.0001$  (300 nM ML277,  $n=4$ ), and  $****p<0.0001$  (1  $\mu$ M ML277,  $n=5$ )). (One-way ANOVA Holm-Sidak post- test).*

### 5.2.5 JNJ303 increases infarct size in a whole-heart *ex vivo* coronary ligation model

Data from the contractile function protocol, as shown in Section 5.2.30, indicated the cardiotoxicity of JNJ303 on the contractility of isolated cardiomyocytes after metabolic inhibition and reperfusion. To investigate the cardiotoxicity effect of this pharmacological treatment on the infarct size of the whole heart, *ex vivo* coronary ligation with the Langendorff method was used (Figure 5.6A). Solution containing JNJ303 was perfused throughout this protocol to measure the detrimental impact on the size of the infarct area. Representative sliced images from adult rat hearts in the control condition and during the perfusion of 1  $\mu$ M JNJ303 are shown in Figure 5.6B. The infarct size was increased with JNJ303, which was obvious from an extension of white tissue on a slice of the pharmacological version.

Figure 5.6C shows that inhibition of  $I_{Ks}$  led to a significant increase in infarct size, going from  $35.6 \pm 1.8\%$  to  $50.0 \pm 1.5\%$  (control, n=16 vs 1  $\mu$ M JNJ303, n=5, \*\*\*p=0.0005). This result suggests that the pharmacological blockade of  $I_{Ks}$  has the potential to be cardiotoxic by enlarging the infarct size.

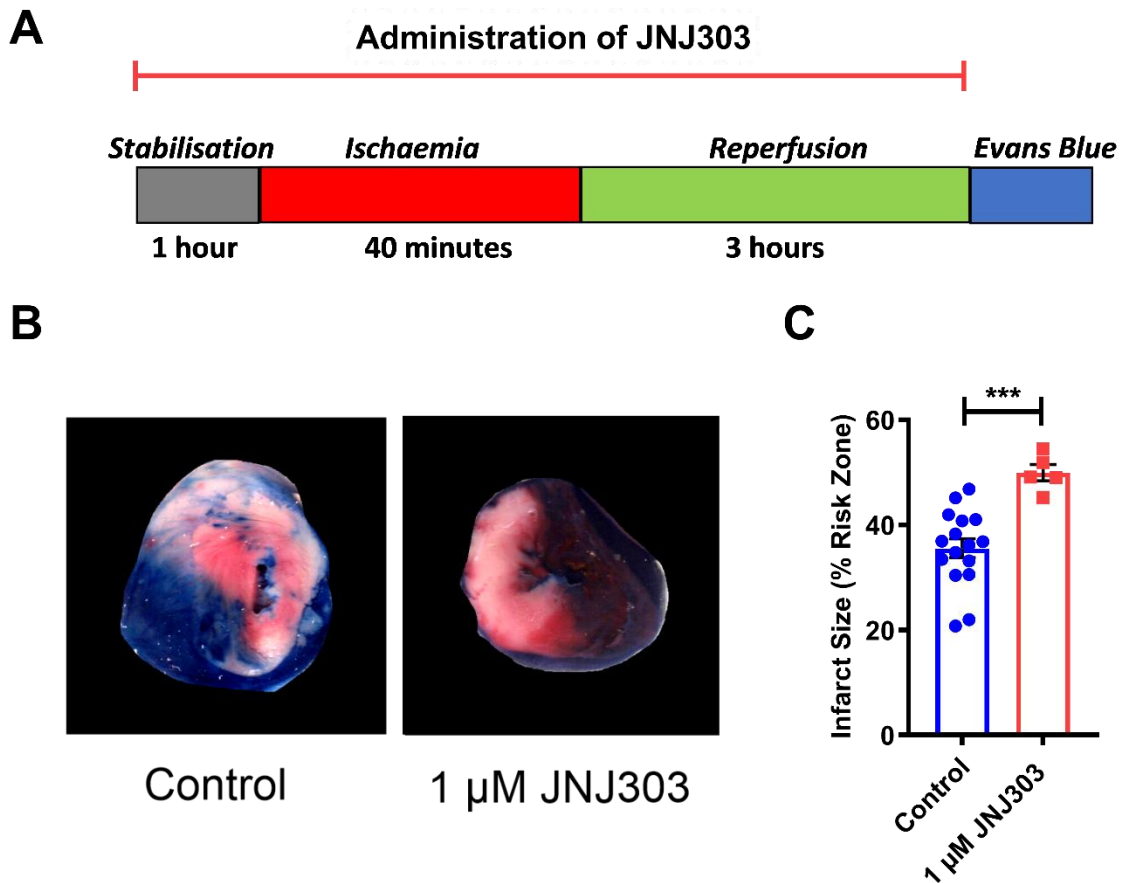


**Figure 5.6:** JNJ303 causes cardiotoxicity by increasing the infarct size in the whole heart after blocking the coronary artery using the Langendorff approach.

*A, A designed protocol used to examine the effect of a selective blocker of  $I_{\text{Ks}}$  on the size of damage after myocardial ischaemia/reperfusion injury: intact hearts were stabilised with NT solution for 1 hr, myocardial ischaemia via ligation was induced in the coronary artery for 40 min and then the coronary artery was un-ligated to simulate myocardial reperfusion with NT for 3 hr. To investigate the infarct size, TTC staining was used. JNJ303 was perfused throughout the protocol. B, Representative scanned images of stained rat hearts were used to compare the control and  $1 \mu\text{M}$  JNJ303. These example images show a larger infarct size after the pharmacological treatment. C, Mean data showing an increase in the percentage of infarct size (control,  $n=16$  vs JNJ303,  $n=5$ ,  $***p=0.0005$ ) (Unpaired t-test).*

### 5.2.6 ML277 imparts cardioprotection when introduced during the coronary artery block or reperfusion

Strong evidence of the cardioprotective effect of ML277 on the reduction of infarct size was found once the activation of  $I_{\text{Ks}}$  commenced prior to the coronary ligation, as shown in Section 5.2.4. Despite the potentially important finding that  $I_{\text{Ks}}$  potentiation could protect against

myocardial ischaemia-reperfusion injury, translating this finding into a clinically relevant scenario is difficult in the *ex vivo* model. This is because myocardial ischaemia is unpredictable in human beings and it would be unlikely that you would be able to give a drug, such as ML277 pre-emptively in acute coronary syndromes due to their unpredictability. In order to investigate this novel target of cardioprotection and investigate the potential clinically feasibility, two strategies have been tried using a whole-rat-heart *ex vivo* coronary ligation protocol. The first protective method was achieved by applying ML277 after 20 min of coronary artery block, which represents the scenario of a patients undergoing acute myocardial infarction and given ML277 once ischaemia was established. The second protocol was to add this pharmacological agent during the reperfusion stage, which the drug could be clinically applied with stenting or thrombolysis, which may provide evidence to attenuate reperfusion injury in clinical settings. As ML277 protects the whole heart during the entire *ex vivo* coronary ligation protocol (Section 5.2.4), a similar protocol was used during a selective targeting time, which involved 1 hr for heart stabilisation, 40 min for coronary ligation and 3 hr for reperfusion (Figure 5.7A).

Figure 5.7B shows that the protective effects of ML277 on infarct size were maintained, although there was variety in the introduction times of pharmacological treatment. After 20 min of coronary artery block, a reduction in the infarct size was significant with 1  $\mu$ M ML277, decreasing from  $35.6 \pm 1.8\%$  to  $11.7 \pm 1.8\%$  (control, n=16 vs 1 $\mu$ M ML277, n=4, \*\*\*\*p<0.0001) (Figure 5.7). Additionally, ML277 significantly reduced infarct size when was applied at only reperfusion period,  $35.6 \pm 1.8\%$  for control (n=16) vs  $16.8 \pm 1.2\%$  for the pharmacological group (n=4, \*\*\*\*p<0.0001) (Figure 5.7). These results emphasise the efficacy of the cardioprotection afforded by  $I_{Ks}$  potentiation, which has been investigated over different times of whole-heart coronary ligation protocol and therefore are probably applicable in clinical settings to prevent life-threatening cardiac damage.

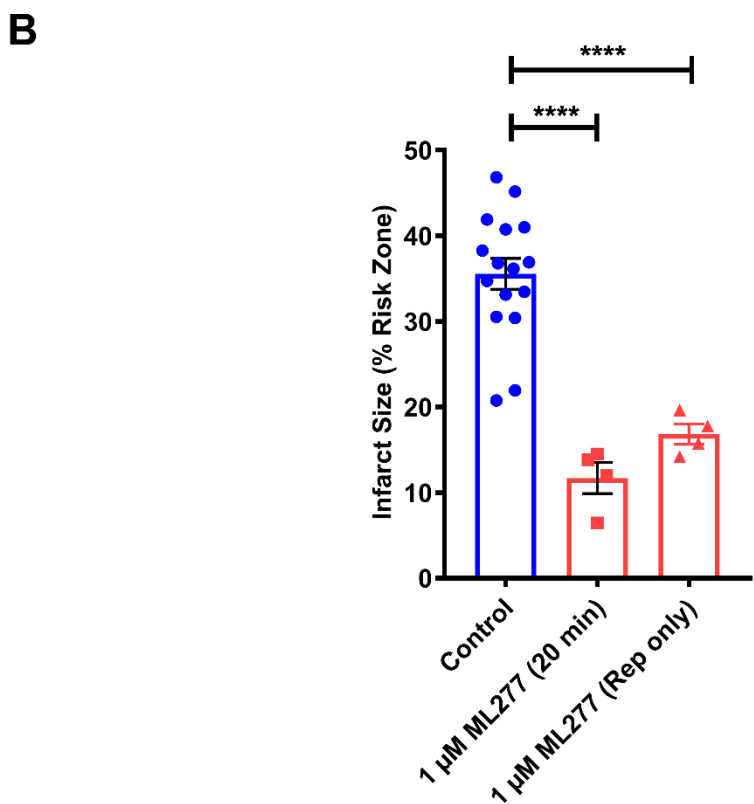
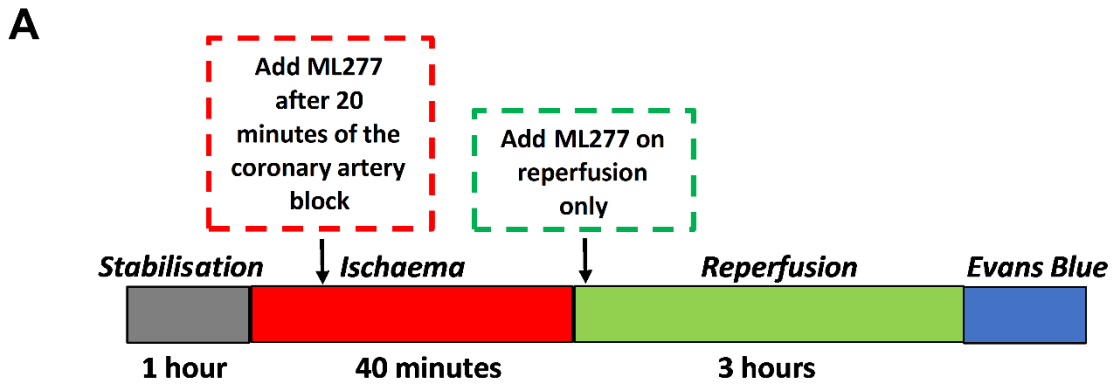


**Figure 5.7:** ML277 imparts cardioprotection by reducing infarct size in the whole heart when applied during coronary artery ligation or only during reperfusion.

*A, Protocol designed to examine the effect of  $I_{Ks}$  potentiation on the damage from myocardial ischaemia and reperfusion injury with the application time of the pharmacological treatment. ML277 was perfused at two certain points: after 20 min of blocking LAD or at the reperfusion period. B, Graph showing the mean infarct size with a reduction in infarct at both times, during myocardial ischaemia and at reperfusion (control, (n=16) vs 1 $\mu$ M ML277 after 20 min of coronary ligation (n=4), and 1 $\mu$ M ML277 at reperfusion only (n=4), \*\*\*\*p<0.0001 for both times of drug application) (One-way ANOVA Holm-Sidak post- test).*

## 5.3 Discussion

It is interesting to note that in all the experimental studies presented in this chapter, potentiation of the cardiac  $I_{Ks}$  plays an important role in cardioprotection. The protective effect gained from targeting this channel for myocardial function against damage in the setting of acute coronary ischaemia was a major aim in this chapter. As mentioned in the literature review, in most cardioprotected cells there was an improved cell survival following an ischaemic insult, which has led to limiting the myocardial damage by shortening the cardiac potential duration to reduce calcium load and so reduce the utilisation of ATP. This led to the hypothesis that pharmacological modulation of  $I_{Ks}$  has a protective potential against ischaemic damage. In the first result chapter, findings were presented showing that the pharmacological modulation of cardiac action potential via targeting the  $I_{Ks}$  reduces calcium overload and consequently preserves intracellular ATP. With the importance of the  $I_{Ks}$  channel in cardiac repolarisation, the ability of  $I_{Ks}$  modulation to protect the heart against damage from myocardial ischaemia is an increasingly important area in the cardioprotection field. The experiments described in this chapter were designed to investigate the effects of a selective pharmacological activator and blocker after metabolic inhibition. The first finding from a patch-clamp recording is that  $I_{Ks}$  potentiation caused a delay in the time for opening  $K_{ir}6.2/SUR2A$ , albeit insignificant, which is considered a major phenotype in cardioprotected cells. It was also found that a direct modulation of this  $I_{Ks}$  can affect the contractile function of isolated cardiomyocytes using a metabolic inhibition and reperfusion protocol. Additionally, a whole-heart *ex vivo* coronary ligation protocol was used as the cardioprotective effect of  $I_{Ks}$  on infarct size after an ischaemic insult.

### 5.3.1 Perfusion with the pharmacological $I_{Ks}$ potentiation imparts cardioprotection to cardiomyocytes and isolated hearts

It is well documented in the literature that the opening of the cardiac  $K_{ATP}$  ( $K_{ir}6.2/SUR2A$ ) current plays an essential role in metabolic stress to limit ATP consumption (Kitakaze, 2010; Brennan et al., 2015; Wojtovich et al., 2010). Therefore, a delayed activation of this Sarco $K_{ATP}$  is suggested as one of the hallmarks of ischaemic preconditioning. This result was based upon data collected over 10 years, and it was hypothesised that in cardioprotected cells, the activity of the cardiac  $K_{ATP}$  channel only occurs from substantial and severe ATP depletion to impart

protection via shortened APD and a negative-shifted membrane potential. To investigate the cardioprotective mechanism of  $I_{Ks}$ , cell-attached patch recording was used to measure the effect of  $I_{Ks}$  potentiation on the time to activate the cardiac  $K_{ir}6.2/SUR2A$  current in cardioprotected myocytes compared to control cells. Pre-treating isolated cardiomyocytes with 1  $\mu$ M ML277 led to a non-significant delay of the activity of cardiac  $K_{ATP}$ , as shown in Figure 5.1. This finding suggests that ML277 did not effect on the cardiac membrane potential which fits with the previous result chapter in Figure 4.2A (ii). This is consistent with the data in Figure 5.2, which showed that the cardiac membrane potential did not have a negative-shift following  $I_{Ks}$  potentiation treatment of isolated cardiomyocytes. It was also hypothesised in the literature that  $I_{Ks}$  activates in phase 3 repolarisation and has no role on resting membrane potential (Nicolas et al., 2008). The possible explanation for a small delay in cardiac  $K_{ir}6.2/SUR2A$  complex opening in the presence of  $I_{Ks}$  potentiation: ML277 induced a hyperpolarising shift of the  $I_{Ks}$  activation curve. This could be a plausible opening of the  $I_{Ks}$  channel when the cell membrane was held at more negative potential for cell-attached patch recording. This finding was encouraging because the resting membrane potential was not affected by the pharmacological activation of the  $I_{Ks}$  and thus provides a degree of safety as it would not prevent the membrane potential reaching the threshold to trigger cardiac action potential. Furthermore, in these experiments, the cardiomyocyte was quiescent, not stimulated to fire action potentials, and therefore would not necessarily have an opportunity for ML277 to fully affect the membrane potential.

Previous studies suggest that during ischaemia, the function of cardiac contractility increases in response to the insufficiency of oxygen supply and ultimately leads to energy depletion (Rosano et al., 2008). Regulating contractile function plays an important role during hypoxia to impart cardioprotection via limited ischaemia-induced myocardial death and increased infarct size. The results presented in this chapter support the hypothesis that contractile function was improved in cardioprotected myocytes compared to non-protected cells by using the metabolic inhibition and reperfusion protocol. Upon treatment with 1  $\mu$ M ML277 to potentiate the  $I_{Ks}$ , the time to contractile failure and the percentage of contractile recovery and cell survival were significantly increased, as shown in Figure 5.3. A similar trend was shown in sympathetic stimulation, causing an increase in the activity of  $I_{Ks}$  to provide a protective mechanisms against excessive prolongation of cardiac action potential in order to

decrease cardiac contractility (Nicolas et al., 2008; Kurokawa et al., 2003). However, in normal physiological conditions, the reduction in force of contraction by  $I_{Ks}$  potentiation had no significant effect because  $I_{Ks}$  is not the main repolarisation current within the rat ventricles, and it ultimately had limited efficacy on cardiac APD (Arrigoni and Crivori, 2007).

Given the considerable cellular protection of  $I_{Ks}$  potentiation on contractile recovery and cell survival, the whole-heart *ex vivo* coronary ligation was used to investigate the protection in models with myocardial ischaemia and reperfusion injury (Bell et al., 2011). This experimental technique detected the effect of pharmacological  $I_{Ks}$  potentiation on infarct size. The current study found that infarct size was significantly reduced in the pharmacological treatment group when ML277 was perfused throughout the experiment (Figure 5.5). In support of this hypothesis, the down-regulation of  $I_{Ks}$  was documented in infarcted canine hearts (Jiang et al., 2000; Dun and Boyden, 2005). This result explained why the outward potassium currents responsible for repolarisation are exposed to change during myocardial ischaemia (Guo et al., 2012). The  $I_{Ks}$  is also reported to be reduced after 2 days following *in vivo* coronary ligation of rabbit hearts (Guo et al., 2012). Although the cardioprotective effect of  $I_{Ks}$  potentiation against the damage of myocardial ischaemia has been documented, these results cannot be translated into the clinical setting. The reason for this is the unpredictable incidence of myocardial ischaemia in human beings. To investigate this pharmacological treatment under similar conditions to patients who are suffering from acute myocardial ischaemia, this treatment was applied after 20 min of coronary artery block or at the reperfusion period. The data presented in Figure 5.7 suggest that the percentage of infarct size was significantly reduced with 1  $\mu$ M ML277 at different time points during myocardial ischaemia. These data fit with the earlier results chapter; it was shown that the pharmacological potentiation of this channel has a cardioprotective effect via shortened APD, limited time of VGCC and preservation of intracellular ATP to maintain a functional heart. Together, the result of isolated cardiomyocytes and isolated whole hearts provide important insights into the protective mechanisms of  $I_{Ks}$  potentiation against damage after myocardial ischaemia.

Previous studies have reported that adenosine plays an important role in triggering a cardioprotective phenotype in hypoxic myocytes (Liu et al., 1991; Cohen et al., 2000). This ligand activates PKC via binding it to G-protein-coupled receptors (GPCR) or tyrosine kinase-

linked receptors on the cell membrane. Therefore, this provides evidence for the role of PKC as a central line in cardioprotection, and so, further work is required to establish the link between  $I_{Ks}$  activation and PKC. Despite numerous studies of successful outcomes on adenosine-induced ischaemic preconditioning, a major problem is that during stress conditions, there is a high probability of interrupting these pathways during cardioprotective intervention. As mentioned in the literature review, the co-assembly of KCNQ1 and KCNE1 to form a functional  $I_{Ks}$  channel is mainly expressed in two cell types: cardiac myocytes and inner ear cells (Wrobel et al., 2012). Due to a direct targeting of this cardiac ion channel, the use of a pharmacological modulator of the  $I_{Ks}$  complex imparts cardioprotection with limited off-target effects. Based on these data, it has been suggested that a direct electrical modulation of the  $I_{Ks}$  channel may be clinically useful as a novel pharmacological cardioprotection.

### 5.3.2 Perfusion with the pharmacological $I_{Ks}$ inhibition causes a cardiotoxic effect to cardiomyocytes and isolated hearts

The results of this chapter show that pre-treated myocytes with a specific  $I_{Ks}$  blocker such as JNJ303 result in cardiotoxic effect during myocardial ischaemia, decreasing the time to contractile failure and the percentage of contractile recovery and cell survival (Figure 5.4). This finding is consistent with Van der Linde et al. (Van der Linde et al., 2010) and suggests that the administration of JNJ303 in anaesthetised dogs causes a mismatch between electrical activity and the mechanical response. Therefore, the abnormality in the cardiac contractility was reflected in these groups, known as Torsade de pointes arrhythmias. These results agree with the findings of the first results chapter, in which the blockade of  $I_{Ks}$  caused a small increase in action potential duration and cardiac contractility through the accumulation of intracellular  $\text{Ca}^{2+}$  as voltage-gated  $\text{Ca}^{2+}$  channels remains open (Section 4.2.2 and Section 4.2.8). Considering the slow activation of  $I_{Ks}$ , this current has only affected cardiac repolarisation to a minimal extent during normal physiological conditions (Varró et al., 2000; Jost et al., 2005). It can therefore be assumed that at normal repolarisation, the pharmacological blockade of  $I_{Ks}$  can decrease a repolarisation reserve current; however, the harmful impact of blocking this current could be extended in the presence of pathological conditions such as during myocardial ischaemia or elevated sympathetic activity. Hence, it could conceivably be hypothesised that  $I_{Ks}$  block by pharmaceuticals is a lesser concern

compared to block of  $I_{Kr}$ , given  $I_{Kr}$  is the major outward repolarising current in the myocardium (Sato et al., 2000a; Abbott et al., 1999). However, more research on the cardiotoxic effect of this selective blocker of  $I_{Ks}$  needs to be undertaken because, as mentioned by Wrobel, the level of cardiotoxicity after JNJ303 treatment increases with higher expression of the KCNE1 encoded  $\beta$ -subunit of the  $I_{Ks}$  complex (Wrobel, 2013).

With successive increases in cardiomyocyte damage after metabolic inhibition with JNJ303 treatment, perfused, isolated hearts provided further evidence to the effect of this pharmacological blockage on damage after an ischaemic event. The current results in Figure 5.6 found that the infarct size was increased after perfusing the isolated hearts with a solution containing JNJ303 throughout the Langendorff preparation protocol. This finding supports the idea of an  $I_{Ks}$  blockade-induced prolongation of action potential in a diseased heart. This lengthening of cardiac APD allows the accumulation of intracellular calcium and, therefore, enhances the use of intracellular ATP for a short time following myocardial ischaemia (Bányász et al., 2004). In the earlier results chapter, it was shown that the pharmacological inhibition of the  $I_{Ks}$  channel caused a non-significant prolongation of APD under normal physiological conditions, as shown in Figure 4.3. These data support the hypothesis that  $I_{Ks}$  blockers may be potent cardiotoxic agents with dangerous prolongation of APD in pathological conditions, however, this is ineffective in control conditions. These results indicate that ATP depletion was faster among the pre-treated group with  $I_{Ks}$  blockers particularly, among acute myocardial ischaemia.

Based on the data presented in this chapter, it is hypothesised that increased KCNQ1/KCNE1 currents in cardiac myocytes could provide cardioprotection against damage from myocardial ischaemia and reperfusion injury. These findings suggest that the modification of  $I_{Ks}$  acts as a novel cardioprotection intervention via several aspects. It could maintain cell survival for a long time by delaying the activation of the cardiac  $K_{ATP}$  channel to preserve intracellular ATP. The observed increase in the time to contractile failure, the percentage of contractile recovery and the percentage of cell survival could be attributed to improved contractile function after myocardial ischaemia. Furthermore, reduction of infarct size could be achieved by targeting this cardiac channel. In contrast, blockage of the KCNQ1/KCNE1 currents is

cardiotoxic. Further research should investigate the effect of this pharmacological manipulation in diseased human hearts to provide novel insights for clinical use.

# Chapter 6 General Discussion

## 6.1 An overview of the findings

According to the World Health Organisation (WHO), acute coronary syndromes are one of the greatest causes of mortality and morbidity worldwide (O'gara et al., 2013; WHO, 2021). An accumulation of plaque inside the coronary artery lumen is a key concern in acute coronary syndrome patients, as it contributes to coronary artery diseases due to the blocking of blood flow into the cardiac muscle (Naghavi et al., 2003). Although there is evidence supporting the reduction of the mortality rate after an invasive therapeutic technique, such as percutaneous coronary intervention, this group of patients remain at a high risk of death (Ibáñez et al., 2015). The issue of ongoing intermittent ischaemia and reperfusion (I/R) injury has received considerable intense attention over the past century; however, there are still no approved therapeutic treatments to protect the cardiac muscle from damage after myocardial ischaemia and reperfusion injury. It has long been suggested that intrinsic cardioprotective pathways are able to reduce infarct size by activating intracellular signalling that imparts protection by shortening the episode of ischaemia. This has been documented in pre-clinical animal models of cardioprotected cells, which are characterised by the shortening of the cardiac action potential duration that reduces electrical excitability, resulting in the reduction of  $\text{Ca}^{2+}$  entry into the cell via limiting the opening time of L-type calcium channels (Murry et al., 1986; Kitakaze, 2010). Despite the significant evidence of pre-clinical success of cardioprotective interventions, it has failed to translate into the clinical setting. It is unclear whether the mechanisms underlying cardioprotection in man are different or whether there are other confounders that we have not currently identified. This disparity between pre-clinical and lack of clinical translation means that the whole area of intrinsic cardioprotection in man is controversial.

This current study focused on the shortening of the action potential duration observed in cardioprotected cells, which limits the accumulation of cytoplasmic calcium through a reduced opening duration of L-type channels, so reducing the influx of calcium. A shorter action potential duration was achieved by directly modulating two cardiac ion channels, which might have contributed to reducing the damage caused by myocardial ischaemia and reperfusion injury.  $\text{K}^+$  channels play an essential role in regulating the normal electrical activity

of cardiac muscle by controlling the repolarisation following a cardiac action potential, and they control the resting membrane potential. This led to the hypothesis that  $I_{Ks}$  and  $K_{ir}6.1$ -containing  $K_{ATP}$  potentiators could provide an effective protective mechanism against damage from myocardial ischaemia. To assess whether the modulating of these potassium channels could impart cardioprotection, this study set out to determine the cardioprotective role of these channels in ventricular myocytes. Briefly, the study demonstrated that  $I_{Ks}$  and  $K_{ir}6.1$ -containing  $K_{ATP}$  activators impart cardioprotection, which results in a reduction in infarct size. Moreover, modulating of these channels was found to improve the contractile function against the damage from metabolic inhibition and reperfusion injury by delaying contractile failure. The rate of contractile recovery also increased with an increase in cell survival.

Chapters 3 and 4 describe experiments relating to investigating whether pharmacological activator and blockade of  $I_{Ks}$  have a cardioprotective role against ischaemia-reperfusion injury. This study provides the first evidence for the cardioprotective role of KCNQ1/KCNE1 channels in rat cardiomyocytes. We showed that selective activation of this outward  $K^+$  current ( $1 \mu M$  ML277) led to a significant shortening of the  $APD_{90}$  in ventricular myocytes. As the potentiation of  $I_{Ks}$  plays a significant role in the regulation of the action potential duration in speeding up repolarisation, we hypothesised that the  $I_{Ks}$  plays an important role in the regulation of intracellular calcium, probably by reducing the utilisation of intracellular ATP. The data presented in this study showed a significant shortening of  $Ca^{2+}$  transients after treatment with this potent  $I_{Ks}$  activator. By contrast, the observed small but insignificant prolongation of the  $APD_{90}$  and a significant prolongation of  $Ca^{2+}$  transients following the selective blockade of  $I_{Ks}$  (JNJ303) could be attributed to cardiotoxicity. These findings raise the hypothesis that the potentiation of KCNQ1/KCNE1 channels is a cardioprotective factor in reducing ATP consumption. Cardioprotected myocytes with a selective  $I_{Ks}$  activator showed a delay in the activity of cardiac  $K_{ATP}$ ,  $K_{ir}6.2/SUR2A$  channels, which has been suggested as a hallmark of ischaemic preconditioning (Kitakaze, 2010; Wojtovich et al., 2010; Brennan et al., 2015). This indicates that activating  $I_{Ks}$  leads to maintaining intracellular ATP for a long time following an ischaemic insult. Furthermore, following the metabolic inhibition and reperfusion protocol, the present findings seem to support the idea of the cardioprotective role of  $I_{Ks}$  potentiation and that  $I_{Ks}$  play an important role in the regulation of contractile function to adapt to the insufficiency of oxygen supply during myocardial ischaemia. This was

documented by demonstrating a significant increase in the time to contractile failure, the percentage of contractile recovery, and cell survival in the pre-treated cells with  $I_{Ks}$  potentiation. The cardioprotective effect was abrogated following the administration of a selective  $I_{Ks}$  blocker. Following the promising results in isolated cardiomyocytes treated with  $I_{Ks}$  potentiation, it was interesting to consider how  $I_{Ks}$  modulation affects the infarct size of the whole-heart *ex vivo* coronary ligation model. The results of this study showed that the activation of  $I_{Ks}$  exerted a protective effect by reducing infarct size, whereas blocking of  $I_{Ks}$  led to a larger area of infarction. These new findings confirm an important link between a shortening of action potential duration seen after the administration of a selective  $I_{Ks}$  activator, and the mediation of cardioprotection against damage from myocardial ischaemia and reperfusion injury.

Chapter 5 describes an investigation into the functional presence of pore-forming subunits of  $K_{ATP}$  channels other than the canonical  $Kir6.2/SUR2A$  channel in ventricular muscle. The functional role of this newly-identified  $K_{ATP}$  channel was examined in normal physiological conditions and in conditions of metabolic-stress. As part of an ongoing study in our research group, the new pore-forming subunit of  $K_{ATP}$  channels was characterised using cell-attached patch recording, which passed a single current amplitude of ~5 pA, giving rise to a conductance of ~39 pS, in normal physiological conditions. It seems possible that this newly identified  $K_{ATP}$  channel comprises a  $Kir6.1$  pore-forming subunit because of the conductance, its sensitivity to glibenclamide and PNU37883A and that this channel was relatively insensitive to ATP, demonstrated by a constitutive activity. This finding supports the hypothesis that the canonical cardiac  $Kir6.2/SUR2A$  channel acts as a metabolic sensor rather than a cardioprotective effector. We hypothesise that this second channel is activated following cardioprotective stimuli, which protects the cell by shortening the action potential to impart early-stage protection (Brennan et al., 2015). The data presented in this study demonstrated that selective modulation of  $Kir6.1$ -containing  $K_{ATP}$  channels impart protection via direct modulation of the action potential duration. The action potential duration was shortened with a  $K_{ATP}$  channels activator at a low concentration (150  $\mu$ M) of pinacidil, that did not significantly potentiate  $Kir6.2$ -containing  $K_{ATP}$  channels (Satoh et al., 1998; Nakayama et al., 1990). A prolongation of the action potential duration was observed after the selective blocking of  $Kir6.1$  pore-forming subunit  $K_{ATP}$  channels using PNU37883A. As the modulation of

$K_{ir}6.1$ -containing channels in the ventricular myocyte led to an effect on ventricular repolarisation by the manipulation of action potential duration, we hypothesised that  $K_{ir}6.1$  forming subunit  $K_{ATP}$  channels plays a role in the regulation of the accumulation of cytoplasmic calcium, therefore limiting ATP consumption. Data presented in this study show that the activation of different pore-forming subunits of  $K_{ATP}$  channels in the cardiac membrane surface resulted in differential shortening of the calcium transient as follows: 1) a severe shortening or abrogation of  $Ca^{2+}$  transients was recorded after activation of cardiac  $K_{ATP}$  ( $K_{ir}6.2/SUR2A$ ) channels with a high pinacidil concentration (200  $\mu M$ ), and 2) a lower level of  $Ca^{2+}$  transients shortening was documented after potentiation of  $K_{ir}6.1$ -containing channels with a low pinacidil concentration (50  $\mu M$ ). However, the inhibition of the cardiac  $K_{ir}6.1$ -containing  $K_{ATP}$  channels (3  $\mu M$  PNU) caused a significant prolongation of  $Ca^{2+}$  transients. The findings showed that the time to  $K_{ir}6.2/SUR2A$  channels activation following metabolic inhibition was significantly delayed in pre-treated cardiomyocytes with potentiation of  $K_{ir}6.1$ -containing  $K_{ATP}$  channels (100  $\mu M$  pinacidil), thereby delaying ATP depletion as part of the cardioprotective mechanism. It was further documented that the potentiation of  $K_{ir}6.1$ -containing  $K_{ATP}$  channels contributed to a cardioprotective phenotype by improving the contractile function after ischaemic-reperfusion injury; for instance, it led to an increase in the time to contractile failure and the percentage of contractile recovery and cell survival in cardioprotected myocytes. A high concentration (200  $\mu M$ ) of pinacidil caused a reduction in cardiac contractility before the application of the metabolic inhibitor, suggesting that activation of cardiac  $K_{ATP}$  ( $K_{ir}6.2/SUR2A$ ) channels is responsible to prevent the membrane potential to reach the threshold for activating an action potential, therefore limit the ability of the contractile function of cells at the start of the experiment, to limiting further ATP consumption. This cardioprotective factor was eliminated following the blockade of cardiac  $K_{ir}6.1$  containing  $K_{ATP}$  channels with 3  $\mu M$  PNU treatment. We further investigated whether the potentiation of  $K_{ir}6.1$ -containing  $K_{ATP}$  channels can affect the infarct size of the whole-heart *ex vivo* coronary ligation model. We previously observed that the activation of  $K_{ir}6.1$ -containing  $K_{ATP}$  channels (10  $\mu M$  pinacidil) led to a significant reduction in infarct size, whereas inhibition of this channel (3  $\mu M$  PNU) caused a significant increase in infarct size. The results from the study in this chapter provide evidence of two types of  $K_{ATP}$  channel on the surface of ventricular cardiomyocytes, including  $K_{ir}6.2/SUR2A$  channels and Sarco $K_{ir}6.1/SUR2B$  channels. These channels could impart cardioprotection at different times.

The newly identified cardiac Kir6.1 containing K<sub>ATP</sub> channel plays a key role in normal physiological conditions and imparts early-stage protection against damage from myocardial ischaemia-reperfusion injury. However, Kir6.2/SUR2A channel is activated in response to severe ATP depletion to impart late-stage protection. Importantly, the data presented here document a link between manipulation of action potential duration via direct modulation of K<sub>ATP</sub> channels and imparting the cardioprotective effect against damage from myocardial ischaemia-reperfusion injury.

Given the protective effects of potentiating both I<sub>Ks</sub> and I<sub>KATP</sub>, it might be worth combining drugs targeting both currents for added benefit. Experiments using both ML277, as an I<sub>Ks</sub> activator, and pinacidil, as a K<sub>ATP</sub> channel activator, can show whether combining the drugs would have an effect that is more significant than either of each. It will also show how this can affect the APD. Precise regulation of the cardiac APD is essential as the APD determines the refractory period of the heart. If the APD becomes too short, premature re-excitation can occur, leading to unwanted arrhythmias.

This study highlights that a shortening of the cardiac action potential could be a novel cardioprotective mechanism. The increase in repolarising current by direct pharmacological potentiation of potassium currents could mark a novel mechanism by which cardioprotection could be imparted where intricate cellular signalling may fail in the clinic.

## 6.2 Clinical implications and translational aspects

The I<sub>Ks</sub> activator, ML277, was developed as an anti-arrhythmic drug and has been shown to potentiate the repolarisation reserve current in pre-clinical models (Mattmann et al., 2012; Yu et al., 2013a; van Bavel et al., 2021; Hou et al., 2019). The ability of ML277 to confer acute cardioprotection seems to be due to the activation of the I<sub>Ks</sub>. An ideal follow on investigation would be to measure the cardioprotective effect following the administration of ML277 in patients suffering from acute myocardial ischaemia, as the drug could reduce the damage from ischaemia and arrhythmia. Despite the beneficial effect of ML277 treatment against an increase in repolarisation time, there has been no clinical use of this pharmacological agent, partly due to the efficacy of the drug and its chemical properties making it a poor

pharmaceutical agent. The formation of the  $I_{Ks}$  requires the co-assembly of the KCNQ1  $\alpha$ -subunit and KCNE1  $\beta$ -subunit, and they are only expressed in cardiac myocytes and inner ear cells (Wrobel et al., 2012). Thus,  $I_{Ks}$  in ventricular cells are a good starting point for selectively targeting  $K^+$  channel activation in the heart and could be a potential treatment in future studies. Furthermore,  $I_{Ks}$  activation would potentially have milder side effects. One further drawback of this pharmacological agent is that the compounds is a Kv7.1 (KCNQ1) selective activator, rather than  $I_{Ks}$ . The activation by ML277 is less with progressive increases in the expression ratio of the KCNQ1:KCNE1 complex (Yu et al., 2013b), therefore it would be advantageous to develop a compound that is a selective  $I_{Ks}$  potentiator. This may be possible given that JNJ303 is thought to be  $I_{Ks}$  selective by binding in a pocket that is only exposed when KCNQ1 and KCNE1 exist in a complex.

The  $K_{ATP}$  channel activator, pinacidil, was approved as an antihypertensive drug that produced vascular dilation (Selvam et al., 2010; Koliopoulos et al., 1984). This drug is generally well tolerated in humans with relatively mild side effects, such as headache (Rastogi and Pragya, 2012). Previous studies suggest that vasodilation with pinacidil requires  $\sim 0.2 \mu M$  to cause pinacidil-induced  $K_{ir}6.1$  containing channels opening, and  $\sim 40 \mu M$  would cause pinacidil-induced  $K_{ir}6.2$  containing channels opening (Suzuki et al., 2001; Lodwick et al., 2014). The ultimate aim of this pharmacological treatment at a low concentration ( $\sim 10 \mu M$ ) would be to improve myocardial function and reduce the final infarct size following administration to patients suffering from ST-elevation myocardial infarction. One drawback of this drug is that  $K_{ir}6.1$  pore-forming channels are weakly rectifying, and, therefore, the activation of this channel will affect the resting membrane potential and increase the possibility of not reaching the threshold of activation to trigger an action potential. It should be noted that in experiments carried out in this study, it took a concentration of  $200 \mu M$  pinacidil to cause complete action potential and contractile failure in cells.

This pharmacological treatment could possibly be used to modify the heart's response against the damage from chronic ischaemia-reperfusion injury, perhaps by improving the contractile function and reducing the infarct size. This new therapeutic strategy could be administered when patients are diagnosed with acute coronary syndrome and could also be part of the clinical reperfusion intervention.

### 6.3 Future work

The experiments using rat ventricular myocytes and isolated rat hearts have proven successful in demonstrating that targeting of the  $I_{Ks}$  and cardiac  $Kir6.1$ -containing channels can protect against ischaemia-reperfusion injury. However, the study of the cardioprotective effects of these potassium channels against the damage following myocardial ischaemia leaves open some questions that require further investigation.

- 1- A common issue in research in the cardioprotection field has been the translation step from pre-clinical studies into clinical trials. In future investigations, it might be possible to assess pharmacological treatments on cardiomyocytes isolated from tissue samples of patients undergoing cardiac surgery procedures. The drugs could also be tested against ischaemia in patients diagnosed with acute myocardial ischaemia.
- 2- Myocardial arrhythmias are a major cause of death, with ~2 million people in the UK expected to suffer from the conditions during their lifetime. Broadly, the dysregulation of  $Ca^{2+}$  signalling underlies certain arrhythmias, where the ion triggers after-depolarisations to restimulate muscle contraction. The management of after-depolarisations, or aberrant intracellular calcium release events, is an important clinical tool for preventing arrhythmias. Cardioprotection against ischaemia and arrhythmias, therefore, has a common underlying mechanism of reducing cellular excitability. Thus, the effect of these cardiac ion channels on the anti-arrhythmic outcomes could be assessed.
- 3- Assessing the effect of  $I_{Ks}$  or  $IK_{ATP}$  potentiation could also be performed *in vivo* in coronary ligation surgery models, which would allow deeper investigations and optimization of the potentiation to reduce infarct size in animals exposed to these pharmacological treatments.

- 4- A thorough assessment of  $I_{Ks}$  activity,  $K_{ir}6.1$  activity, and an early cardioprotected phenotype in cardiomyocytes isolated from tissue specific with knockout models and transgenic animals is needed to fully elucidate the role of these ion channels following myocardial injury.

## 6.4 Overall conclusion

A common uniting theme in all these investigations in this thesis is the ability of cardiac ion channel activity to induce cardioprotection in the ventricular myocardium through the manipulation of cardiac action potential duration, which limits the time for calcium influx and reduces ATP consumption. The question arises, would it be simpler to use  $Ca^{2+}$  channel inhibitors to protect the heart against myocardial ischaemia-reperfusion injury? Previous studies have demonstrated that calcium channel blockers, particularly L-type  $Ca^{2+}$  channel blockers, are associated with an increase in the occurrence of myocardial infarction (Ivanov et al., 2004; Psaty et al., 1995; Eisenberg et al., 2004). This inhibitory mechanism causes bradycardia via slowing the depolarisation, because this channel plays an important role in phase 2 ventricular action potential. This may result in reducing the blood flow via the coronary artery and reducing the cardiac output. As there are a controversy regarding the risk of cardiovascular events following calcium channel inhibition, therefore the data from this work suggest that a reduction of calcium overload could indirectly be achieved by potassium channel activation to provide a protective effect. The mechanism of the protection is hypothesised to be by accelerating the repolarisation of the cell membrane, which consequently leads to the shortening of the action potential, the limiting of calcium influx time, and reduction of ATP consumption. Therefore, limiting cellular calcium overload is thought to be protective in the heart against damage from myocardial ischaemia. The cell membrane of ventricular myocytes has a large diversity of  $K^+$  channels; however, this study was focused on targeting two types of  $K^+$  channels: the slowly activating delayed rectifier potassium ( $I_{Ks}$ ) and newly-identified cardiac  $K_{ir}6.1$ -containing  $K_{ATP}$  channels. Our results demonstrated that selective activators of these potassium channels act as a novel cardioprotection intervention via an increase in the time to contractile failure, the percentage of contractile recovery, and the percentage of cell survival. These pharmacological treatment outcomes could also be attributed to the reduced infarct size. However, inhibition of cardiac

ion channels is cardiotoxic. Taken together, this work contributes to the existing knowledge of cardioprotection by providing novel insights into these pharmacological manipulations for clinical use against damage from myocardial ischaemia and reperfusion injury. However, some important limitations of this study indicate avenues for further research, and thus must be considered. First, these experiments were not subjected to stress-responses; hence, the effect of stress conditions on the protective pathway should be investigated in an *in vivo* model. Second, the rat model brings with it limitations regarding differences in action potential compared to human cardiomyocytes, which may be expected to have variations in calcium handling and repolarising currents. Future studies should be performed in large animal species to examine the cardioprotective effect of these potassium channels against damage from ischaemia-reperfusion injury.

## References

- Abbott, G. W. 2016. KCNE4 and KCNE5: K<sup>+</sup> channel regulation and cardiac arrhythmogenesis. *Gene*, 593(2), pp 249-260.
- Abbott, G. W. & Goldstein, S. A. 1998. A superfamily of small potassium channel subunits: form and function of the MinK-related peptides (MiRPs). *Quarterly reviews of biophysics*, 31(4), pp 357-398.
- Abbott, G. W., Sesti, F., Splawski, I., Buck, M. E., Lehmann, M. H., Timothy, K. W., Keating, M. T. & Goldstein, S. A. 1999. MiRP1 forms IKr potassium channels with HERG and is associated with cardiac arrhythmia. *Cell*, 97(2), pp 175-187.
- Abitbol, I., Peretz, A., Lerche, C., Busch, A. E. & Attali, B. 1999. Stilbenes and fenamates rescue the loss of I<sub>Ks</sub> channel function induced by an LQT5 mutation and other I<sub>sK</sub> mutants. *The EMBO journal*, 18(15), pp 4137-4148.
- Adelman, J. P., Clapham, D. E., Hibino, H., Inanobe, A., Jan, L. Y., Karschin, A., Kubo, Y., Kurachi, Y., Lazdunski, M. & Miki, T. 2019. Inwardly rectifying potassium channels (version 2019.4) in the IUPHAR/BPS Guide to Pharmacology Database. *IUPHAR/BPS Guide to Pharmacology CITE*, 2019(4), pp.
- Adkins, G. B. & Curtis, M. J. 2015. Potential role of cardiac chloride channels and transporters as novel therapeutic targets. *Pharmacology & therapeutics*, 145(67-75).
- Aggarwal, N. T., Shi, N. Q. & Makielinski, J. C. 2013. ATP-sensitive potassium currents from channels formed by Kir6 and a modified cardiac mitochondrial SUR2 variant. *Channels (Austin)*, 7(6), pp 493-502.
- Aguilar-Bryan, L. & Bryan, J. 1999. Molecular biology of adenosine triphosphate-sensitive potassium channels. *Endocr Rev*, 20(2), pp 101-35.
- Ahern, C. A. & Kobertz, W. R. 2009. Chemical tools for K<sup>+</sup> channel biology. *Biochemistry*, 48(3), pp 517-526.
- Ahmed, T., Sorgdrager, B. J., Cannegieter, S. C., van der Laarse, A., Schalij, M. J. & Jukema, W. 2012. Pre-infarction angina predicts thrombus burden in patients admitted for ST-segment elevation myocardial infarction. *EuroIntervention*, 7(12), pp 1396-405.
- Aidley, D. J. & Stanfield, P. R. 1996. *Ion channels: molecules in action*: Cambridge University Press.

Albrecht, J. 2017. *The Effect of the KV7/KCNE 1 Inhibitor JNJ 303 on Heart Slices and the L-type Calcium Channel of Cardiac Cells*. Deutsche Zentralbibliothek für Medizin.

Alejandro, A., S. Eliza, H., Colin G, N. & Monica, S. R. 2009. Molecular biology of K<sub>ATP</sub> channels and implications for health and disease. *IUBMB life*, 61(10), pp 971-978.

Alhayek, S. & Preuss, C. V. 2020. Beta 1 receptors. *StatPearls [Internet]*.

Alvarez, B. V., Kieller, D. M., Quon, A. L., Markovich, D. & Casey, J. R. 2004. Slc26a6: a cardiac chloride-hydroxyl exchanger and predominant chloride-bicarbonate exchanger of the mouse heart. *The Journal of Physiology*, 561(3), pp 721-734.

Anderson, M. E. 2004. Calmodulin kinase and L-type calcium channels: A recipe for arrhythmias? *Trends in cardiovascular medicine*, 14(4), pp 152-161.

Anderson, R. H., Yanni, J., Boyett, M. R., Chandler, N. J. & Dobrzynski, H. 2009. The anatomy of the cardiac conduction system. *Clinical Anatomy: The Official Journal of the American Association of Clinical Anatomists and the British Association of Clinical Anatomists*, 22(1), pp 99-113.

Angelo, K., Jespersen, T., Grunnet, M., Nielsen, M. S., Klaerke, D. A. & Olesen, S.-P. 2002. KCNE5 induces time-and voltage-dependent modulation of the KCNQ1 current. *Biophysical journal*, 83(4), pp 1997-2006.

Antcliff, J. F., Haider, S., Proks, P., Sansom, M. S. & Ashcroft, F. M. 2005. Functional analysis of a structural model of the ATP-binding site of the K<sub>ATP</sub> channel Kir6. 2 subunit. *The EMBO journal*, 24(2), pp 229-239.

Antzelevitch, C., Shimizu, W., YAN, G. X., Sicouri, S., Weissenburger, J., Nesterenko, V. V., Burashnikov, A., DI DIEGO, J., SAFFITZ, J. & Thomas, G. P. 1999. The M cell: its contribution to the ECG and to normal and abnormal electrical function of the heart. *Journal of cardiovascular electrophysiology*, 10(8), pp 1124-1152.

Apkon, M. & Nerbonne, J. M. 1991. Characterization of two distinct depolarization-activated K<sup>+</sup> currents in isolated adult rat ventricular myocytes. *The Journal of general physiology*, 97(5), pp 973-1011.

Argaud, L., Gateau-Roesch, O., Muntean, D., Chalabreysse, L., Loufouat, J., Robert, D. & Ovize, M. 2005. Specific inhibition of the mitochondrial permeability transition prevents lethal reperfusion injury. *Journal of molecular and cellular cardiology*, 38(2), pp 367-374.

- Armstrong, C. M. 2003. Voltage-gated K channels. *Science's STKE*, 2003(188), pp re10-re10.
- Arrigoni, C. & Crivori, P. 2007. Assessment of QT liabilities in drug development. *Cell biology and toxicology*, 23(1), pp 1-13.
- Ashcroft, F. M. 2005. ATP-sensitive potassium channelopathies: focus on insulin secretion. *The Journal of clinical investigation*, 115(8), pp 2047-2058.
- Ashcroft, F. M. & Gribble, F. M. 1998. Correlating structure and function in ATP-sensitive K<sup>+</sup> channels. *Trends in neurosciences*, 21(7), pp 288-294.
- Ashcroft, F. M. & Gribble, F. M. 2000. New windows on the mechanism of action of K<sub>ATP</sub> channel openers. *Trends in pharmacological sciences*, 21(11), pp 439-445.
- Ashcroft, F. M. & Kakei, M. 1989. ATP-sensitive K<sup>+</sup> channels in rat pancreatic beta-cells: modulation by ATP and Mg<sup>2+</sup> ions. *The Journal of physiology*, 416(1), pp 349-367.
- Ashcroft, F. M. & Rorsman, P. 1989. Electrophysiology of the pancreatic β-cell. *Progress in biophysics and molecular biology*, 54(2), pp 87-143.
- Ashcroft, S. J. & Ashcroft, F. M. 1990. Properties and functions of ATP-sensitive K-channels. *Cellular signalling*, 2(3), pp 197-214.
- Ashfield, R., Gribble, F. M., Ashcroft, S. & Ashcroft, F. M. 1999. Identification of the high-affinity tolbutamide site on the SUR1 subunit of the K (ATP) channel. *Diabetes*, 48(6), pp 1341-1347.
- Aziz, Q., Finlay, M., Montaigne, D., Ojake, L., Li, Y., Anderson, N., Ludwig, A. & Tinker, A. 2018. ATP-sensitive potassium channels in the sinoatrial node contribute to heart rate control and adaptation to hypoxia. *Journal of Biological Chemistry*, 293(23), pp 8912-8921.
- Aziz, Q., Li, Y., Anderson, N., Ojake, L., Tsisanova, E. & Tinker, A. 2017. Molecular and functional characterization of the endothelial ATP-sensitive potassium channel. *Journal of Biological Chemistry*, 292(43), pp 17587-17597.
- Aziz, Q., Thomas, A. M., Gomes, J., Ang, R., Sones, W. R., Li, Y., Ng, K.-E., Gee, L. & Tinker, A. 2014. The ATP-sensitive potassium channel subunit, Kir6. 1, in vascular smooth muscle plays a major role in blood pressure control. *Hypertension*, 64(3), pp 523-529.

- Aziz, Q., Thomas, A. M., Khambra, T. & Tinker, A. 2012. Regulation of the ATP-sensitive potassium channel subunit, Kir6. 2, by a  $\text{Ca}^{2+}$ -dependent protein kinase C. *Journal of Biological Chemistry*, 287(9), pp 6196-6207.
- Babenko, A., Aguilar-Bryan, L. & Bryan, J. 1998. A view of sur/KIR6. X,  $\text{K}_{\text{ATP}}$  channels. *Annual review of physiology*, 60(1), pp 667-687.
- Babenko, A. P., Gonzalez, G. & Bryan, J. 1999. Two regions of sulfonylurea receptor specify the spontaneous bursting and ATP inhibition of  $\text{K}_{\text{ATP}}$  channel isoforms. *Journal of Biological Chemistry*, 274(17), pp 11587-11592.
- Babenko, A. P., Gonzalez, G. C. & Bryan, J. 2000. Hetero-concatemeric KIR6. X4/SUR14 channels display distinct conductivities but uniform ATP inhibition. *Journal of Biological Chemistry*, 275(41), pp 31563-31566.
- Bajgar, R., Seetharaman, S., Kowaltowski, A. J., Garlid, K. D. & Paucek, P. 2001. Identification and properties of a novel intracellular (mitochondrial) ATP-sensitive potassium channel in brain. *Journal of Biological Chemistry*, 276(36), pp 33369-33374.
- Bányász, T., Koncz, R., Fulop, L., Szentandrassy, N., Magyar, J. & Nánási, P. P. 2004. Profile of  $I_{\text{Ks}}$  During the Action Potential Questions the Therapeutic Value of  $I_{\text{Ks}}$  Blockade. *Current medicinal chemistry*, 11(1), pp 45-60.
- Bao, L., Kefaloyianni, E., Lader, J., Hong, M., Morley, G., Fishman, G. I., Sobie, E. A. & Coetze, W. A. 2011. Unique properties of the ATP-sensitive  $\text{K}^+$  channel in the mouse ventricular cardiac conduction system. *Circulation: Arrhythmia and Electrophysiology*, 4(6), pp 926-935.
- Barcenas-Ruiz, L., Beuckelmann, D. & Wier, W. 1987. Sodium-calcium exchange in heart: membrane currents and changes in  $[\text{Ca}^{2+}]$ . *i. Science*, 238(4834), pp 1720-1722.
- Barhanin, J., Lesage, F., Guillemare, E., Fink, M., Lazdunski, M. & Romey, G. 1996a. K V LQT1 and IsK (minK) proteins associate to form the  $I_{\text{Ks}}$  cardiac potassium current. *Nature*, 384(6604), pp 78.
- Barhanin, J., Lesage, F., Guillemare, E., Fink, M., Lazdunski, M. & Romey, G. 1996b. K(V)LQT1 and IsK (minK) proteins associate to form the  $I_{(\text{Ks})}$  cardiac potassium current. *Nature*, 384(6604), pp 78-80.
- Baron, A., van Bever, L., Monnier, D., Roatti, A. & Baertschi, A. J. 1999. A novel  $\text{K}_{\text{ATP}}$  current in cultured neonatal rat atrial appendage cardiomyocytes. *Circulation research*, 85(8), pp 707-715.

Barrese, V., Stott, J. B. & Greenwood, I. A. 2018. KCNQ-encoded potassium channels as therapeutic targets. *Annual review of pharmacology and toxicology*, 58(625-648).

Bartlett, K. & Eaton, S. 2004. Mitochondrial  $\beta$ -oxidation. *European Journal of Biochemistry*, 271(3), pp 462-469.

Bartos, D. C., Morotti, S., Ginsburg, K. S., Grandi, E. & Bers, D. M. 2017. Quantitative analysis of the  $\text{Ca}^{2+}$ -dependent regulation of delayed rectifier  $\text{K}^+$  current  $I_{\text{Ks}}$  in rabbit ventricular myocytes. *The Journal of physiology*, 595(7), pp 2253-2268.

Batey, A. J. & Coker, S. J. 2002. Proarrhythmic potential of halofantrine, terfenadine and clofilium in a modified *in vivo* model of torsade de pointes. *British journal of pharmacology*, 135(4), pp 1003-1012.

Bednarczyk, P., Dołowy, K. & Szewczyk, A. 2005. Matrix  $\text{Mg}^{2+}$  regulates mitochondrial ATP-dependent potassium channel from heart. *FEBS letters*, 579(7), pp 1625-1632.

Bednarczyk, P., Dołowy, K. & Szewczyk, A. 2008. New properties of mitochondrial ATP-regulated potassium channels. *Journal of bioenergetics and biomembranes*, 40(4), pp 325.

Beech, D., Zhang, H., Nakao, K. & Bolton, T. 1993. K channel activation by nucleotide diphosphates and its inhibition by glibenclamide in vascular smooth muscle cells. *British journal of pharmacology*, 110(2), pp 573-582.

Behzadi, M., Joukar, S. & Beik, A. 2018. Opioids and cardiac arrhythmia: a literature review. *Medical principles and practice*, 27(5), pp 401-414.

Bell, R. M., Mocanu, M. M. & Yellon, D. M. 2011. Retrograde heart perfusion: the Langendorff technique of isolated heart perfusion. *Journal of molecular and cellular cardiology*, 50(6), pp 940-950.

Bendahhou, S., Marionneau, C., Haurogne, K., Larroque, M.-M., Derand, R., Szuts, V., Escande, D., Demolombe, S. & Barhanin, J. 2005. In vitro molecular interactions and distribution of KCNE family with KCNQ1 in the human heart. *Cardiovascular research*, 67(3), pp 529-538.

Bernardi, H., Fosset, M. & Lazdunski, M. 1992. ATP/ADP binding sites are present in the sulfonylurea binding protein associated with brain ATP-sensitive potassium channels. *Biochemistry*, 31(27), pp 6328-6332.

Bers, D. M. 2002. Cardiac excitation–contraction coupling. *Nature*, 415(6868), pp 198-205.

Bett, G. C., Morales, M. J., Beahm, D. L., Duffey, M. E. & Rasmusson, R. L. 2006. Ancillary subunits and stimulation frequency determine the potency of chromanol 293B block of the KCNQ1 potassium channel. *The Journal of physiology*, 576(3), pp 755-767.

BHF, B. H. F. 2021. *Heart Statistics* [Online]. Available: <https://www.bhf.org.uk/what-we-do/our-research/heart-statistics> [Accessed June 29, 2021].

Bienengraeber, M., Alekseev, A. E., Abraham, M. R., Carrasco, A. J., Moreau, C., Vivaudou, M., Dzeja, P. P. & Terzic, A. 2000. ATPase activity of the sulfonylurea receptor: a catalytic function for the K<sub>ATP</sub> channel complex. *The FASEB Journal*, 14(13), pp 1943-1952.

Bienengraeber, M., Olson, T. M., Selivanov, V. A., Kathmann, E. C., O'Cochlain, F., Gao, F., Karger, A. B., Ballew, J. D., Hodgson, D. M. & Zingman, L. V. 2004. ABCC9 mutations identified in human dilated cardiomyopathy disrupt catalytic K ATP channel gating. *Nature genetics*, 36(4), pp 382-387.

Bierbower, S. M., Choveau, F. S., Lechleiter, J. D. & Shapiro, M. S. 2015. Augmentation of M-type (KCNQ) potassium channels as a novel strategy to reduce stroke-induced brain injury. *Journal of Neuroscience*, 35(5), pp 2101-2111.

Blaustein, M. P. & Lederer, W. J. 1999. Sodium/calcium exchange: its physiological implications. *Physiological reviews*, 79(3), pp 763-854.

Block, F., Pergande, G. & Schwarz, M. 1997. Flupirtine reduces functional deficits and neuronal damage after global ischemia in rats. *Brain research*, 754(1-2), pp 279-284.

Boengler, K., Hilfiker-Kleiner, D., Heusch, G. & Schulz, R. 2010. Inhibition of permeability transition pore opening by mitochondrial STAT3 and its role in myocardial ischemia/reperfusion. *Basic research in cardiology*, 105(6), pp 771-785.

Boengler, K., Ungefug, E., Heusch, G. & Schulz, R. 2013. The STAT3 inhibitor statin impairs cardiomyocyte mitochondrial function through increased reactive oxygen species formation. *Current pharmaceutical design*, 19(39), pp 6890-6895.

Boim, M., Ho, K., Shuck, M., Bienkowski, M., Block, J., Slightom, J., Yang, Y., Brenner, B. & Hebert, S. 1995. ROMK inwardly rectifying ATP-sensitive K<sup>+</sup> channel. II. Cloning and distribution of alternative forms. *American Journal of Physiology-Renal Physiology*, 268(6), pp F1132-F1140.

Bozler, E. 1943. The initiation of impulses in cardiac muscle. *American Journal of Physiology-Legacy Content*, 138(2), pp 273-282.

Bray, K. M., Newgreen, D., Small, R., Southerton, J., Taylor, S., Weir, S. W. & Weston, A. 1987. Evidence that the mechanism of the inhibitory action of pinacidil in rat and guinea-pig smooth muscle differs from that of glyceryl trinitrate. *British journal of pharmacology*, 91(2), pp 421.

Brennan, S., Jackson, R., Patel, M., Sims, M. W., Hudman, D., Norman, R. I., Lodwick, D. & Rainbow, R. D. 2015. Early opening of sarcolemmal ATP-sensitive potassium channels is not a key step in PKC-mediated cardioprotection. *Journal of molecular and cellular cardiology*, 79(42-53).

Bromage, D. I., Pickard, J. M., Rossello, X., Ziff, O. J., Burke, N., Yellon, D. M. & Davidson, S. M. 2017. Remote ischaemic conditioning reduces infarct size in animal in vivo models of ischaemia-reperfusion injury: a systematic review and meta-analysis. *Cardiovascular research*, 113(3), pp 288-297.

Brueggemann, L. I., Mackie, A. R., Cribbs, L. L., Freda, J., Tripathi, A., Majetschak, M. & Byron, K. L. 2014. Differential protein kinase C-dependent modulation of Kv7. 4 and Kv7. 5 subunits of vascular Kv7 channels. *Journal of Biological Chemistry*, 289(4), pp 2099-2111.

Bryan, J., Muñoz, A., Zhang, X., Düfer, M., Drews, G., Krippeit-Drews, P. & Aguilar-Bryan, L. 2007. ABCC8 and ABCC9: ABC transporters that regulate K<sup>+</sup> channels. *Pflügers Archiv-European Journal of Physiology*, 453(5), pp 703-718.

Budas, G. R., Churchill, E. N. & Mochly-Rosen, D. 2007. Cardioprotective mechanisms of PKC isozyme-selective activators and inhibitors in the treatment of ischemia-reperfusion injury. *Pharmacological research*, 55(6), pp 523-536.

Burashnikov, A. & Antzelevitch, C. 2002. Prominent I<sub>Ks</sub> in epicardium and endocardium contributes to development of transmural dispersion of repolarization but protects against development of early afterdepolarizations. *Journal of cardiovascular electrophysiology*, 13(2), pp 172-177.

Burke, M. A., Mutharasan, R. K. & Ardehali, H. 2008. The sulfonylurea receptor, an atypical ATP-binding cassette protein, and its regulation of the K<sub>ATP</sub> channel. *Circulation research*, 102(2), pp 164-176.

Burley, D. S., Ferdinand, P. & Baxter, G. F. 2007. Cyclic GMP and protein kinase-G in myocardial ischaemia-reperfusion: opportunities and obstacles for survival signaling. *British journal of pharmacology*, 152(6), pp 855-869.

Burton, R. A., Lee, P., Casero, R., Garny, A., Siedlecka, U., Schneider, J. E., Kohl, P. & Grau, V. 2014. Three-dimensional histology: tools and application to quantitative assessment of cell-type distribution in rabbit heart. *Europace*, 16(suppl\_4), pp iv86-iv95.

Busch, A., Herzer, T., Wagner, C., Schmidt, F., Raber, G., Waldegger, S. & Lang, F. 1994. Positive regulation by chloride channel blockers of IsK channels expressed in Xenopus oocytes. *Molecular pharmacology*, 46(4), pp 750-753.

Busch, A., Suessbrich, H., Waldegger, S., Sailer, E., Greger, R., Lang, H.-J., Lang, F., Gibson, K. & Maylie, J. 1996. Inhibition of IsK in guinea pig cardiac myocytes and guinea pig IsK channels by the chromanol 293B. *Pflügers Archiv-European Journal of Physiology*, 432(6), pp 1094-1096.

Campbell, C. M., Campbell, J. D., Thompson, C. H., Galimberti, E. S., Darbar, D., Vanoye, C. G. & George Jr, A. L. 2013. Selective targeting of gain-of-function KCNQ1 mutations predisposing to atrial fibrillation. *Circulation: Arrhythmia and Electrophysiology*, 6(5), pp 960-966.

Campo, G., Pavasini, R., Morciano, G., Lincoff, M. A., Gibson, M. C., Kitakaze, M., Lonborg, J., Ahluwalia, A., Ishii, H. & Frenneaux, M. 2017. Data on administration of cyclosporine, nicorandil, metoprolol on reperfusion related outcomes in ST-segment elevation myocardial infarction treated with percutaneous coronary intervention. *Data in brief*, 14(197-205).

Casimiro, M. C., Knollmann, B. C., Ebert, S. N., Vary, J. C., Greene, A. E., Franz, M. R., Grinberg, A., Huang, S. P. & Pfeifer, K. 2001. Targeted disruption of the Kcnq1 gene produces a mouse model of Jervell and Lange-Nielsen Syndrome. *Proceedings of the National Academy of Sciences*, 98(5), pp 2526-2531.

Catterall, W., Perez-Reyes, E., Snitch, T. & Striessnig, J. 2005. International Union of Pharmacology. XLVIII. Nomenclature and structure-function relationships of voltage-gated calcium channels. *Pharmacol Rev*, 57(411-425).

Catterall, W. A. 2000a. From ionic currents to molecular mechanisms: the structure and function of voltage-gated sodium channels. *Neuron*, 26(1), pp 13-25.

Catterall, W. A. 2000b. Structure and regulation of voltage-gated Ca<sup>2+</sup> channels. *Annual review of cell and developmental biology*, 16(1), pp 521-555.

Catterall, W. A. 2014. Structure and function of voltage-gated sodium channels at atomic resolution. *Experimental physiology*, 99(1), pp 35-51.

Chadha, P. S., Jepps, T. A., Carr, G., Stott, J. B., Zhu, H.-L., Cole, W. C. & Greenwood, I. A. 2014. Contribution of Kv7. 4/Kv7. 5 heteromers to intrinsic and calcitonin gene-related peptide-induced cerebral reactivity. *Arteriosclerosis, thrombosis, and vascular biology*, 34(4), pp 887-893.

Chang, A., Abderemane-Ali, F., Hura, G. L., Rossen, N. D., Gate, R. E. & Minor Jr, D. L. 2018. A calmodulin C-lobe  $\text{Ca}^{2+}$ -dependent switch governs Kv7 channel function. *Neuron*, 97(4), pp 836-852. e6.

Chang, N., Liang, T., Lin, X., Kang, Y., Xie, H., Feng, Z.-P. & Gaisano, H. Y. 2011. Syntaxin-1A interacts with distinct domains within nucleotide-binding folds of sulfonylurea receptor 1 to inhibit  $\beta$ -cell ATP-sensitive potassium channels. *Journal of Biological Chemistry*, 286(26), pp 23308-23318.

Chen, J., Zheng, R., Melman, Y. F. & McDonald, T. V. 2009. Functional interactions between KCNE1 C-terminus and the KCNQ1 channel. *PLoS One*, 4(4), pp e5143.

Chen, L., Kurokawa, J. & Kass, R. S. 2005. Phosphorylation of the A-kinase-anchoring protein Yotiao contributes to protein kinase A regulation of a heart potassium channel. *Journal of Biological Chemistry*, 280(36), pp 31347-31352.

Chen, Y.-H., Xu, S.-J., Bendahhou, S., Wang, X.-L., Wang, Y., Xu, W.-Y., Jin, H.-W., Sun, H., Su, X.-Y. & Zhuang, Q.-N. 2003. KCNQ1 gain-of-function mutation in familial atrial fibrillation. *Science*, 299(5604), pp 251-254.

Cheng, H. & Lederer, W. 2008. Calcium sparks. *Physiological reviews*, 88(4), pp 1491-1545.

Choisy, S. C., Hancox, J. C., Arberry, L. A., Reynolds, A. M., Shattock, M. J. & James, A. F. 2004. Evidence for a novel  $\text{K}^+$  channel modulated by  $\alpha 1\text{A}$ -adrenoceptors in cardiac myocytes. *Molecular pharmacology*, 66(3), pp 735-748.

Chorvat, R. J., Zaczek, R. & Brown, B. S. 1998. Ion channel modulators that enhance acetylcholine release: potential therapies for Alzheimer's disease. *Expert opinion on investigational drugs*, 7(4), pp 499-518.

Choveau, F. S., Abderemane-Ali, F., Coyan, F. C., Es-Salah-Lamoureux, Z., Baro, I. & Loussouarn, G. 2012. Opposite effects of the S4–S5 linker and PIP2 on voltage-gated

channel function: KCNQ1/KCNE1 and other channels. *Frontiers in pharmacology*, 3(125).

Clusin, W. T. 2008. Mechanisms of calcium transient and action potential alternans in cardiac cells and tissues. *American Journal of Physiology-Heart and Circulatory Physiology*, 294(1), pp H1-H10.

Coetzee, W. A., Amarillo, Y., Chiu, J., Chow, A., Lau, D., McCormack, T., Morena, H., Nadal, M. S., Ozaita, A. & Pountney, D. 1999. Molecular diversity of K<sup>+</sup> channels. *Annals of the New York Academy of Sciences*, 868(1), pp 233-255.

Cohen, M. V., Baines, C. P. & Downey, J. M. 2000. Ischemic preconditioning: from adenosine receptor to K<sub>ATP</sub> channel. *Annual review of physiology*, 62(1), pp 79-109.

Cole, W. C., McPherson, C. D. & Sontag, D. 1991. ATP-regulated K<sup>+</sup> channels protect the myocardium against ischemia/reperfusion damage. *Circulation Research*, 69(3), pp 571-581.

Cook, D. L., Satin, L. S., Ashford, M. L. & Hales, C. N. 1988. ATP-sensitive K<sup>+</sup> channels in pancreatic β-cells: spare-channel hypothesis. *Diabetes*, 37(5), pp 495-498.

Cooper, G. M., Hausman, R. E. & Hausman, R. E. 2007. *The cell: a molecular approach*: ASM press Washington, DC.

Cosconati, S., Marinelli, L., Lavecchia, A. & Novellino, E. 2007. Characterizing the 1, 4-dihydropyridines binding interactions in the L-type Ca<sup>2+</sup> channel: model construction and docking calculations. *Journal of medicinal chemistry*, 50(7), pp 1504-1513.

Cui, Y., Giblin, J. P., Clapp, L. H. & Tinker, A. 2001. A mechanism for ATP-sensitive potassium channel diversity: Functional coassembly of two pore-forming subunits. *Proceedings of the National Academy of Sciences*, 98(2), pp 729-734.

Cui, Y., Tinker, A. & Clapp, L. H. 2003. Different molecular sites of action for the K<sub>ATP</sub> channel inhibitors, PNU-99963 and PNU-37883A. *British journal of pharmacology*, 139(1), pp 122-128.

Cukras, C. A., Jeliazkova, I. & Nichols, C. G. 2002. The role of NH2-terminal positive charges in the activity of inward rectifier K<sub>ATP</sub> channels. *The Journal of general physiology*, 120(3), pp 437-446.

- Cung, T.-T., Morel, O., Cayla, G., Rioufol, G., Garcia-Dorado, D., Angoulvant, D., Bonnefoy-Cudraz, E., Guérin, P., Elbaz, M. & Delarche, N. 2015. Cyclosporine before PCI in patients with acute myocardial infarction. *New England Journal of Medicine*, 373(11), pp 1021-1031.
- Curtis, B. M. & Catterall, W. A. 1984. Purification of the calcium antagonist receptor of the voltage-sensitive calcium channel from skeletal muscle transverse tubules. *Biochemistry*, 23(10), pp 2113-2118.
- Cutler, M. J., Rosenbaum, D. S. & Dunlap, M. E. 2007. Structural and electrical remodeling as therapeutic targets in heart failure. *Journal of electrocardiology*, 40(6), pp S1-S7.
- D'Alonzo, A. J., Darbenzio, R. B., Parham, C. S. & Grover, G. J. 1992. Effects of intracoronary cromakalim on postischaemic contractile function and action potential duration. *Cardiovascular research*, 26(11), pp 1046-1053.
- D'hahan, N., Moreau, C., Prost, A.-L., Jacquet, H., Alekseev, A. E., Terzic, A. & Vivaudou, M. 1999. Pharmacological plasticity of cardiac ATP-sensitive potassium channels toward diazoxide revealed by ADP. *Proceedings of the National Academy of Sciences*, 96(21), pp 12162-12167.
- Dabrowski, M., Trapp, S. & Ashcroft, F. M. 2003. Pyridine nucleotide regulation of the  $K_{ATP}$  channel Kir6.2/SUR1 expressed in Xenopus oocytes. *The Journal of physiology*, 550(2), pp 357-363.
- Dahlem, Y. A., Horn, T. F., Buntinas, L., Gonoi, T., Wolf, G. & Siemen, D. 2004. The human mitochondrial  $K_{ATP}$  channel is modulated by calcium and nitric oxide: a patch-clamp approach. *Biochimica et Biophysica Acta (BBA)-Bioenergetics*, 1656(1), pp 46-56.
- Dart, C. 2014. Verdict in the Smooth Muscle  $K_{ATP}$  Channel Case: Guilty of Blood Pressure Control But Innocent of Sudden Death Phenotype. Am Heart Assoc.
- Davies, L. M., Purves, G. I., Barrett-Jolley, R. & Dart, C. 2010. Interaction with caveolin-1 modulates vascular ATP-sensitive potassium ( $K_{ATP}$ ) channel activity. *The Journal of physiology*, 588(17), pp 3255-3266.
- Davis, L. M., Rodefeld, M. E., Green, K., Beyer, E. C. & Saffitz, J. E. 1995. Gap junction protein phenotypes of the human heart and conduction system. *Journal of cardiovascular electrophysiology*, 6(10), pp 813-822.
- de los Angeles Tejada, M., Stolpe, K., Meinild, A.-K. & Klaerke, D. A. 2012. Clofilium inhibits Slick and Slack potassium channels. *Biologics: targets & therapy*, 6(465).

De Wet, H., Fotinou, C., Amad, N., Dreger, M. & Ashcroft, F. M. 2010. The ATPase activities of sulfonylurea receptor 2A and sulfonylurea receptor 2B are influenced by the C-terminal 42 amino acids. *The FEBS journal*, 277(12), pp 2654-2662.

Debska, G., Kicinska, A., Skalska, J., Szewczyk, A., May, R., Elger, C. E. & Kunz, W. S. 2002. Opening of potassium channels modulates mitochondrial function in rat skeletal muscle. *Biochimica et Biophysica Acta (BBA)-Bioenergetics*, 1556(2-3), pp 97-105.

Dębska, G., May, R., Kicińska, A., Szewczyk, A., Elger, C. E. & Kunz, W. S. 2001. Potassium channel openers depolarize hippocampal mitochondria. *Brain research*, 892(1), pp 42-50.

Del Valle, H. B., Yaktine, A. L., Taylor, C. L. & Ross, A. C. 2011. Dietary reference intakes for calcium and vitamin D.

Delaney, J. T., Muhammad, R., Blair, M. A., Kor, K., Fish, F. A., Roden, D. M. & Darbar, D. 2012. A KCNJ8 mutation associated with early repolarization and atrial fibrillation. *Europace*, 14(10), pp 1428-1432.

Desmet, W., Bogaert, J., Dubois, C., Sinnaeve, P., Adriaenssens, T., Pappas, C., Ganame, J., Dymarkowski, S., Janssens, S. & Belmans, A. 2011. High-dose intracoronary adenosine for myocardial salvage in patients with acute ST-segment elevation myocardial infarction. *European heart journal*, 32(7), pp 867-877.

Deuchars, S. A. & K. Lall, V. 2011. Sympathetic preganglionic neurons: properties and inputs. *Comprehensive Physiology*, 5(2), pp 829-869.

Dhein, S., Van Koppen, C. J. & Brodde, O.-E. 2001. Muscarinic receptors in the mammalian heart. *Pharmacological research*, 44(3), pp 161-182.

DiFrancesco, D. 2010. The role of the funny current in pacemaker activity. *Circulation research*, 106(3), pp 434-446.

Dobrowolski, R. & Willecke, K. 2009. Connexin-caused genetic diseases and corresponding mouse models. *Antioxidants & redox signaling*, 11(2), pp 283-296.

Dobrzynski, H., Anderson, R. H., Atkinson, A., Borbas, Z., D'Souza, A., Fraser, J. F., Inada, S., Logantha, S. J., Monfredi, O. & Morris, G. M. 2013. Structure, function and clinical relevance of the cardiac conduction system, including the atrioventricular ring and outflow tract tissues. *Pharmacology & therapeutics*, 139(2), pp 260-288.

Dobrzynski, H., Boyett, M. R. & Anderson, R. H. 2007. New insights into pacemaker activity: promoting understanding of sick sinus syndrome. *Circulation*, 115(14), pp 1921-1932.

Doerr, T., Denger, R., Doerr, A. & Trautwein, W. 1990. Ionic currents contributing to the action potential in single ventricular myocytes of the guinea pig studied with action potential clamp. *Pflügers Archiv*, 416(3), pp 230-237.

Dörge, H., Schulz, R., Belosjorow, S., Post, H., Van De Sand, A., Konietzka, I., Frede, S., Hartung, T., Vinent-Johansen, J. & Youker, K. A. 2002. Coronary microembolization: the role of TNF- $\alpha$  in contractile dysfunction. *Journal of Molecular and Cellular Cardiology*, 34(1), pp 51-62.

Drain, P., Li, L. & Wang, J. 1998.  $K_{ATP}$  channel inhibition by ATP requires distinct functional domains of the cytoplasmic C terminus of the pore-forming subunit. *Proceedings of the National Academy of Sciences*, 95(23), pp 13953-13958.

Du, R.-H., Dai, T., Cao, W.-J., Lu, M., Ding, J.-h. & Hu, G. 2014. Kir6.2-containing ATP-sensitive  $K^+$  channel is required for cardioprotection of resveratrol in mice. *Cardiovascular diabetology*, 13(1), pp 1-9.

Dun, W. & Boyden, P. A. 2005. Diverse phenotypes of outward currents in cells that have survived in the 5-day-infarcted heart. *American Journal of Physiology-Heart and Circulatory Physiology*, 289(2), pp H667-H673.

Dutta, S., Mincholé, A., Quinn, T. A. & Rodriguez, B. 2017. Electrophysiological properties of computational human ventricular cell action potential models under acute ischemic conditions. *Progress in biophysics and molecular biology*, 129(40-52).

Ebashi, S., EBASHI, F. & KODAMA, A. 1967. Troponin as the  $Ca^{++}$ -receptive protein in the contractile system. *The Journal of Biochemistry*, 62(1), pp 137-138.

Eckert, R., Randall, R. & Augustine, G. 1988. *Animal physiology: mechanisms and adaptations*: WH Freeman & Co.

Edwards, A. G. & Louch, W. E. 2017. Species-dependent mechanisms of cardiac arrhythmia: a cellular focus. *Clinical Medicine Insights: Cardiology*, 11(1179546816686061.

Eisen, A., Fisman, E. Z., Rubenfire, M., Freimark, D., McKechnie, R., Tenenbaum, A., Motro, M. & Adler, Y. 2004. Ischemic preconditioning: nearly two decades of research. A comprehensive review. *Atherosclerosis*, 172(2), pp 201-210.

Eisenberg, M. J., Brox, A. & Bestawros, A. N. 2004. Calcium channel blockers: an update. *The American journal of medicine*, 116(1), pp 35-43.

Eisner, D. A., Caldwell, J. L., Trafford, A. W. & Hutchings, D. C. 2020. The control of diastolic calcium in the heart: basic mechanisms and functional implications. *Circulation research*, 126(3), pp 395-412.

Elliott, E. B., Kelly, A., Smith, G. L. & Loughrey, C. M. 2012. Isolated rabbit working heart function during progressive inhibition of myocardial SERCA activity. *Circulation research*, 110(12), pp 1618-1627.

Ellison, G., Torella, D., Karakikes, I., Goldpink, D. F. & Nadal-Ginard, B. 2006. Myocardial damage induces a growth factor para/autocrine loop in the spared myocytes which fosters cardiac stem cell activation and ensuing myocyte regeneration. Am Heart Assoc.

Emori, T. & Antzelevitch, C. 2001. Cellular basis for complex T waves and arrhythmic activity following combined IKr and IKs block. *Journal of cardiovascular electrophysiology*, 12(12), pp 1369-1378.

Enyedi, P. & Czirják, G. 2010. Molecular background of leak K<sup>+</sup> currents: two-pore domain potassium channels. *Physiological reviews*, 90(2), pp 559-605.

Escande, D., Thuringer, D., Le Guern, S., Courteix, J., Laville, M. & Cavero, I. 1989. Potassium channel openers act through an activation of ATP-sensitive K<sup>+</sup> channels in guinea-pig cardiac myocytes. *Pflügers Archiv*, 414(6), pp 669-675.

Fabiato, A. 1985. Simulated calcium current can both cause calcium loading in and trigger calcium release from the sarcoplasmic reticulum of a skinned canine cardiac Purkinje cell. *The Journal of general physiology*, 85(2), pp 291-320.

Fabiato, A. & Fabiato, F. 1975. Contractions induced by a calcium-triggered release of calcium from the sarcoplasmic reticulum of single skinned cardiac cells. *The Journal of physiology*, 249(3), pp 469-495.

Fabiato, A. & Fabiato, F. 1978. Calcium-induced release of calcium from the sarcoplasmic reticulum of skinned cells from adult human, dog, cat, rabbit, rat, and frog hearts and from fetal and new-born rat ventricles. *Annals of the New York Academy of Sciences*, 307(491-522).

- Faivre, J.-F. & Findlay, I. 1990. Action potential duration and activation of ATP-sensitive potassium current in isolated guinea-pig ventricular myocytes. *Biochimica et Biophysica Acta (BBA)-Biomembranes*, 1029(1), pp 167-172.
- Farraj, A. K., Hazari, M. S. & Cascio, W. E. 2011. The utility of the small rodent electrocardiogram in toxicology. *Toxicological sciences*, 121(1), pp 11-30.
- Fedele, F., Mancone, M., Chilian, W. M., Severino, P., Canali, E., Logan, S., De Marchis, M. L., Volterrani, M., Palmirota, R. & Guadagni, F. 2013. Role of genetic polymorphisms of ion channels in the pathophysiology of coronary microvascular dysfunction and ischemic heart disease. *Basic research in cardiology*, 108(6), pp 1-12.
- Fedorov, V. V., Glukhov, A. V., Ambrosi, C. M., Kostecki, G., Chang, R., Janks, D., Schuessler, R. B., Moazami, N., Nichols, C. G. & Efimov, I. R. 2011. Effects of  $K_{ATP}$  channel openers diazoxide and pinacidil in coronary-perfused atria and ventricles from failing and non-failing human hearts. *Journal of molecular and cellular cardiology*, 51(2), pp 215-225.
- Fermini, B. & Priest, B. 2008. *Ion channels*: Springer Science & Business Media.
- Findlay, I. 1992. Inhibition of ATP-sensitive  $K^+$  channels in cardiac muscle by the sulphonylurea drug glibenclamide. *Journal of Pharmacology and Experimental Therapeutics*, 261(2), pp 540-545.
- Findlay, I. & Dunne, M. J. 1986. ATP maintains ATP-inhibited  $K^+$  channels in an operational state. *Pflügers Archiv*, 407(2), pp 238-240.
- Fishman, G. I., Eddy, R. L., Shows, T. B., Rosenthal, L. & Leinwand, L. A. 1991. The human connexin gene family of gap junction proteins: distinct chromosomal locations but similar structures. *Genomics*, 10(1), pp 250-256.
- Flagg, T. P., Kurata, H. T., Masia, R., Caputa, G., Magnuson, M. A., Lefer, D. J., Coetzee, W. A. & Nichols, C. G. 2008. Differential structure of atrial and ventricular  $K_{ATP}$ : atrial  $K_{ATP}$  channels require SUR1. *Circulation research*, 103(12), pp 1458-1465.
- Flanagan, S. E., Clauin, S., Bellanné-Chantelot, C., de Lonlay, P., Harries, L. W., Gloyn, A. L. & Ellard, S. 2009. Update of mutations in the genes encoding the pancreatic beta-cell  $K_{ATP}$  channel subunits Kir6. 2 (KCNJ11) and sulfonylurea receptor 1 (ABCC8) in diabetes mellitus and hyperinsulinism. *Human mutation*, 30(2), pp 170-180.
- Foster, D. B., Ho, A. S., Rucker, J., Garlid, A. O., Chen, L., Sidor, A., Garlid, K. D. & O'Rourke, B. 2012. Mitochondrial ROMK channel is a molecular component of mito $K_{ATP}$ . *Circulation research*, 111(4), pp 446-454.

Foster, M. N. & Coetze, W. A. 2016.  $K_{ATP}$  channels in the cardiovascular system. *Physiological reviews*, 96(1), pp 177-252.

Fretwell, L. & Woolard, J. 2013. Cardiovascular responses to retigabine in conscious rats—under normotensive and hypertensive conditions. *British journal of pharmacology*, 169(6), pp 1279-1289.

Friedman, A. K., Juarez, B., Ku, S. M., Zhang, H., Calizo, R. C., Walsh, J. J., Chaudhury, D., Zhang, S., Hawkins, A. & Dietz, D. M. 2016. KCNQ channel openers reverse depressive symptoms via an active resilience mechanism. *Nature communications*, 7(1), pp 1-7.

Fröhlich, H., Boini, K. M., Seeböhm, G., Strutz-Seeböhm, N., Ureche, O. N., Föller, M., Eichenmüller, M., Shumilina, E., Pathare, G. & Singh, A. K. 2011. Hypothyroidism of gene-targeted mice lacking *Kcnq1*. *Pflügers Archiv-European Journal of Physiology*, 461(1), pp 45-52.

Fujita, A. & Kurachi, Y. 2000. Molecular aspects of ATP-sensitive  $K^+$  channels in the cardiovascular system and  $K^+$  channel openers. *Pharmacology & therapeutics*, 85(1), pp 39-53.

Fujita, H., Ogura, T., Tamagawa, M., Uemura, H., Sato, T., Ishida, A., Imamaki, M., Kimura, F., Miyazaki, M. & Nakaya, H. 2006. A key role for the subunit SUR2B in the preferential activation of vascular  $K_{ATP}$  channels by isoflurane. *British journal of pharmacology*, 149(5), pp 573-580.

Gambardella, J., Trimarco, B., Iaccarino, G. & Santulli, G. 2017. New insights in cardiac calcium handling and excitation-contraction coupling. *Heart Failure: From Research to Clinical Practice*, 373-385.

Garlid, K. 1988. Mitochondrial volume control. Integration of Mitochondrial Function. *Lemasters JJ, Hackenbrock CR, Thurman RG, Westerhoff HV*.

Garlid, K. D. 1996. Cation transport in mitochondria—the potassium cycle. *Biochimica et Biophysica Acta (BBA)-Bioenergetics*, 1275(1-2), pp 123-126.

Garlid, K. D., Pucek, P., Yarov-Yarovoy, V., Murray, H. N., Darbenzio, R. B., D'Alonzo, A. J., Lodge, N. J., Smith, M. A. & Grover, G. J. 1997. Cardioprotective effect of diazoxide and its interaction with mitochondrial ATP-sensitive  $K^+$  channels: possible mechanism of cardioprotection. *Circulation research*, 81(6), pp 1072-1082.

Gerlach, U., Brendel, J., Lang, H.-J., Paulus, E. F., Weidmann, K., Brüggemann, A., Busch, A. E., Suessbrich, H., Bleich, M. & Greger, R. 2001. Synthesis and activity of novel and selective  $I_{KS}$ -channel blockers. *Journal of medicinal chemistry*, 44(23), pp 3831-3837.

Ghosh, S., Nunziato, D. A. & Pitt, G. S. 2006. KCNQ1 assembly and function is blocked by long-QT syndrome mutations that disrupt interaction with calmodulin. *Circulation research*, 98(8), pp 1048-1054.

Giorgi, E. & Stein, W. 1981. The transport of steroids into animal cells in culture. *Endocrinology*, 108(2), pp 688-697.

Gläser, S., Steinbach, M., Opitz, C., Wruck, U. & Kleber, F. X. 2001. Torsades de pointes caused by Mibepradil. *European journal of heart failure*, 3(5), pp 627-630.

Glukhov, A. V., Flagg, T. P., Fedorov, V. V., Efimov, I. R. & Nichols, C. G. 2010. Differential  $K_{ATP}$  channel pharmacology in intact mouse heart. *Journal of molecular and cellular cardiology*, 48(1), pp 152-160.

Goldin, A. L. 2002. Evolution of voltage-gated  $Na^+$  channels. *Journal of Experimental Biology*, 205(5), pp 575-584.

Goldin, A. L., Barchi, R. L., Caldwell, J. H., Hofmann, F., Howe, J. R., Hunter, J. C., Kallen, R. G., Mandel, G., Meisler, M. H. & Netter, Y. B. 2000. Nomenclature of voltage-gated sodium channels. *Neuron*, 28(2), pp 365-368.

Goldstein, S. A., Bayliss, D. A., Kim, D., Lesage, F., Plant, L. D. & Rajan, S. 2005. International Union of Pharmacology. LV. Nomenclature and molecular relationships of two-P potassium channels. *Pharmacological reviews*, 57(4), pp 527-540.

Gómez, A. M., Cheng, H., Lederer, W. J. & Bers, D. M. 1996.  $Ca^{2+}$  diffusion and sarcoplasmic reticulum transport both contribute to  $[Ca^{2+}]_i$  decline during  $Ca^{2+}$  sparks in rat ventricular myocytes. *The Journal of Physiology*, 496(2), pp 575-581.

Gorboulev, V., Schürmann, A., Vallon, V., Kipp, H., Jaschke, A., Klessen, D., Friedrich, A., Scherneck, S., Rieg, T. & Cunard, R. 2012.  $Na^+$ -D-glucose cotransporter SGLT1 is pivotal for intestinal glucose absorption and glucose-dependent incretin secretion. *Diabetes*, 61(1), pp 187-196.

Gourdie, R. G. & Lo, C. W. 1999. Cx43 ( $\alpha 1$ ) gap junctions in cardiac development and disease. *Current Topics in Membranes*. Elsevier.

Grahammer, F., Warth, R., Barhanin, J., Bleich, M. & Hug, M. J. 2001a. The Small Conductance K<sup>+</sup> Channel, KCNQ1 EXPRESSION, FUNCTION, AND SUBUNIT COMPOSITION IN MURINE TRACHEA. *Journal of Biological Chemistry*, 276(45), pp 42268-42275.

Grahammer, F., Wittekindt, O. H., Nitschke, R., Herling, A. W., Lang, H. J., Bleich, M., Schmitt-Gräff, A., Barhanin, J. & Warth, R. 2001b. The cardiac K<sup>+</sup> channel KCNQ1 is essential for gastric acid secretion. *Gastroenterology*, 120(6), pp 1363-1371.

Gralinski, M. R. 2003. The dog's role in the preclinical assessment of QT interval prolongation. *Toxicologic pathology*, 31(1\_suppl), pp 11-16.

Grant, A. O. 2009. Cardiac ion channels. *Circulation: Arrhythmia and Electrophysiology*, 2(2), pp 185-194.

Greener, I., Monfredi, O., Inada, S., Chandler, N., Tellez, J., Atkinson, A., Taube, M.-A., Billeter, R., Anderson, R. & Efimov, I. 2011. Molecular architecture of the human specialised atrioventricular conduction axis. *Journal of molecular and cellular cardiology*, 50(4), pp 642-651.

Gribble, F. M., Tucker, S. J. & Ashcroft, F. M. 1997. The essential role of the Walker A motifs of SUR1 in K-ATP channel activation by Mg-ADP and diazoxide. *The EMBO Journal*, 16(6), pp 1145-1152.

Grossman, A. N., Opie, L. H., Beshansky, J. R., Ingwall, J. S., Rackley, C. E. & Selker, H. P. 2013. Glucose-insulin-potassium revived: current status in acute coronary syndromes and the energy-depleted heart. *Circulation*, 127(9), pp 1040-1048.

Grover, G. J., Dzwonczyk, S., Parham, C. S. & Sraph, P. G. 1990. The protective effects of cromakalim and pinacidil on reperfusion function and infarct size in isolated perfused rat hearts and anesthetized dogs. *Cardiovascular drugs and therapy*, 4(2), pp 465-474.

Grover, G. J. & Garlid, K. D. 2000. ATP-sensitive potassium channels: a review of their cardioprotective pharmacology. *Journal of molecular and cellular cardiology*, 32(4), pp 677-695.

Grunnet, M., Jespersen, T., Rasmussen, H. B., Ljungstrøm, T., Jorgensen, N. K., Olesen, S. P. & Klaerke, D. A. 2002. KCNE4 is an inhibitory subunit to the KCNQ1 channel. *The Journal of physiology*, 542(1), pp 119-130.

Guo, R., Gu, J., Zong, S., Wu, M. & Yang, M. 2018. Structure and mechanism of mitochondrial electron transport chain. *Biomedical journal*, 41(1), pp 9-20.

Guo, X., Gao, X., Wang, Y., Peng, L., Zhu, Y. & Wang, S. 2012.  $I_{KS}$  protects from ventricular arrhythmia during cardiac ischemia and reperfusion in rabbits by preserving the repolarization reserve. *PLoS One*, 7(2), pp e31545.

Gutknecht, J., Bisson, M. & Tosteson, F. 1977. Diffusion of carbon dioxide through lipid bilayer membranes. Effects of carbonic anhydrase, bicarbonate, and unstirred layers. *The Journal of general physiology*, 69(6), pp 779.

Guzzini, F., Baroffio, R., Coppetti, D. & Gasparini, P. 1990. Severe ventricular arrhythmia secondary to indapamide-induced hypopotassemia. *La Clinica Terapeutica*, 135(4), pp 283-287.

Haitin, Y. & Attali, B. 2008. The C-terminus of Kv7 channels: a multifunctional module. *The Journal of physiology*, 586(7), pp 1803-1810.

Halestrap, A. P., Clarke, S. J. & Javadov, S. A. 2004. Mitochondrial permeability transition pore opening during myocardial reperfusion—a target for cardioprotection. *Cardiovascular research*, 61(3), pp 372-385.

Hambrock, A., Löffler-Walz, C., Kloot, D., Delabar, U., Horio, Y., Kurachi, Y. & Quast, U. 1999. ATP-sensitive  $K^+$  channel modulator binding to sulfonylurea receptors SUR2A and SUR2B: opposite effects of MgADP. *Molecular Pharmacology*, 55(5), pp 832-840.

Hamill, O. P., Marty, A., Neher, E., Sakmann, B. & Sigworth, F. J. 1981. Improved patch-clamp techniques for high-resolution current recording from cells and cell-free membrane patches. *Pflügers Archiv*, 391(2), pp 85-100.

Hanley, P. J., Dröse, S., Brandt, U., Lareau, R. A., Banerjee, A. L., Srivastava, D., Banaszak, L. J., Barycki, J. J., Van Veldhoven, P. P. & Daut, J. 2005. 5-Hydroxydecanoate is metabolised in mitochondria and creates a rate-limiting bottleneck for  $\beta$ -oxidation of fatty acids. *The Journal of physiology*, 562(2), pp 307-318.

Hanley, P. J., Mickel, M., Löffler, M., Brandt, U. & Daut, J. 2002.  $K_{ATP}$  channel-independent targets of diazoxide and 5-hydroxydecanoate in the heart. Wiley Online Library.

Hanson, R. 1989. The role of ATP in metabolism. *Biochemical Education*, 17(2), pp 86-92.

Hauserloy, D. J., Barabas, J. A., Bøtker, H. E., Davidson, S. M., Di Lisa, F., Downey, J., Engstrom, T., Ferdinand, P., Carbrera-Fuentes, H. A. & Heusch, G. 2016a. Ischaemic conditioning and targeting reperfusion injury: a 30 year voyage of discovery. *Basic research in cardiology*, 111(6), pp 1-24.

- Hausenloy, D. J., Candilio, L., Evans, R., Ariti, C., Jenkins, D. P., Kolvekar, S., Knight, R., Kunst, G., Laing, C. & Nicholas, J. M. 2016b. Effect of Remote Ischaemic preconditioning on Clinical outcomes in patients undergoing Coronary Artery bypass graft surgery (ERICCA study): a multicentre double-blind randomised controlled clinical trial. *Efficacy and Mechanism Evaluation*, 3(4), pp 1-58.
- Hausenloy, D. J., Duchen, M. R. & Yellon, D. M. 2003. Inhibiting mitochondrial permeability transition pore opening at reperfusion protects against ischaemia-reperfusion injury. *Cardiovascular research*, 60(3), pp 617-625.
- Hausenloy, D. J., Lecour, S. & Yellon, D. M. 2011. Reperfusion injury salvage kinase and survivor activating factor enhancement prosurvival signaling pathways in ischemic postconditioning: two sides of the same coin. *Antioxidants & redox signaling*, 14(5), pp 893-907.
- Hausenloy, D. J., Ong, S.-B. & Yellon, D. M. 2009. The mitochondrial permeability transition pore as a target for preconditioning and postconditioning. *Basic research in cardiology*, 104(2), pp 189-202.
- Hausenloy, D. J. & Yellon, D. M. 2004. New directions for protecting the heart against ischaemia-reperfusion injury: targeting the Reperfusion Injury Salvage Kinase (RISK)-pathway. *Cardiovascular research*, 61(3), pp 448-460.
- Hausenloy, D. J. & Yellon, D. M. 2008. Remote ischaemic preconditioning: underlying mechanisms and clinical application. *Cardiovascular research*, 79(3), pp 377-386.
- Hausenloy, D. J. & Yellon, D. M. 2013. Myocardial ischemia-reperfusion injury: a neglected therapeutic target. *The Journal of clinical investigation*, 123(1), pp 92-100.
- Hayashi, H., Iwata, M., Tsuchimori, N. & Matsumoto, T. 2014. Activation of peripheral KCNQ channels attenuates inflammatory pain. *Molecular pain*, 10(1744-8069-10-15).
- Hayashi, T., Martone, M. E., Yu, Z., Thor, A., Doi, M., Holst, M. J., Ellisman, M. H. & Hoshijima, M. 2009. Three-dimensional electron microscopy reveals new details of membrane systems for  $\text{Ca}^{2+}$  signaling in the heart. *Journal of cell science*, 122(7), pp 1005-1013.
- He, J.-Q., Conklin, M. W., Foell, J. D., Wolff, M. R., Haworth, R. A., Coronado, R. & Kamp, T. J. 2001. Reduction in density of transverse tubules and L-type  $\text{Ca}^{2+}$  channels in canine tachycardia-induced heart failure. *Cardiovascular research*, 49(2), pp 298-307.

Heijman, J., Spätjens, R. L., Seyen, S. R., Lentink, V., Kuijpers, H. J., Boulet, I. R., de Windt, L. J., David, M. & Volders, P. G. 2012. Dominant-negative control of cAMP-dependent  $I_{KS}$  upregulation in human long-QT syndrome type 1. *Circulation research*, 110(2), pp 211-219.

Heinemann, S. H., Terlau, H., Stühmer, W., Imoto, K. & Numa, S. 1992. Calcium channel characteristics conferred on the sodium channel by single mutations. *Nature*, 356(6368), pp 441-443.

Herring, N. & Paterson, D. J. 2018. *Levick's introduction to cardiovascular physiology*: CRC Press.

Hibino, H., Inanobe, A., Furutani, K., Murakami, S., Findlay, I. & Kurachi, Y. 2010. Inwardly rectifying potassium channels: their structure, function, and physiological roles. *Physiological reviews*, 90(1), pp 291-366.

Hii, J. T., Duff, H. J. & Burgess, E. D. 1991. Clinical pharmacokinetics of propafenone. *Clinical pharmacokinetics*, 21(1), pp 1-10.

Hille, B. 1978. Ionic channels in excitable membranes. Current problems and biophysical approaches. *Biophysical Journal*, 22(2), pp 283-294.

Himmel, H. M., Wettwer, E., Li, Q. & Ravens, U. 1999. Four different components contribute to outward current in rat ventricular myocytes. *American Journal of Physiology-Heart and Circulatory Physiology*, 277(1), pp H107-H118.

Hirano, Y., Fozzard, H. A. & January, C. T. 1989. Characteristics of L-and T-type  $\text{Ca}^{2+}$  currents in canine cardiac Purkinje cells. *American Journal of Physiology-Heart and Circulatory Physiology*, 256(5), pp H1478-H1492.

Hiraoka, M., Kawano, S., Hirano, Y. & Furukawa, T. 1998. Role of cardiac chloride currents in changes in action potential characteristics and arrhythmias. *Cardiovascular research*, 40(1), pp 23-33.

Ho, K., Nichols, C. G., Lederer, W. J., Lytton, J., Vassilev, P. M., Kanazirska, M. V. & Hebert, S. C. 1993. Cloning and expression of an inwardly rectifying ATP-regulated potassium channel. *Nature*, 362(6415), pp 31-38.

Hodgkin, A. & Huxley, A. 1990. A quantitative description of membrane current and its application to conduction and excitation in nerve. *Bulletin of mathematical biology*, 52(1-2), pp 25-71.

Hodgkin, A. L. & Huxley, A. F. 1952. A quantitative description of membrane current and its application to conduction and excitation in nerve. *The Journal of physiology*, 117(4), pp 500.

Hodgkin, A. L. & Katz, B. 1949. The effect of sodium ions on the electrical activity of the giant axon of the squid. *The Journal of physiology*, 108(1), pp 37.

Hofmann, F., Ammendola, A. & Schlossmann, J. 2000. Rising behind NO: cGMP-dependent protein kinases. *Journal of cell science*, 113(10), pp 1671-1676.

Hofmann, F., Flockerzi, V., Kahl, S. & Wegener, J. W. 2014. L-type CaV1. 2 calcium channels: from in vitro findings to in vivo function. *Physiological reviews*, 94(1), pp 303-326.

Hou, P., Eldstrom, J., Shi, J., Zhong, L., McFarland, K., Gao, Y., Fedida, D. & Cui, J. 2017. Inactivation of KCNQ1 potassium channels reveals dynamic coupling between voltage sensing and pore opening. *Nature communications*, 8(1), pp 1-11.

Hou, P., Shi, J., White, K. M., Gao, Y. & Cui, J. 2019. ML277 specifically enhances the fully activated open state of KCNQ1 by modulating VSD-pore coupling. *Elife*, 8(e48576).

Huang, H., Pugsley, M. K., Fermini, B., Curtis, M. J., Koerner, J., Accardi, M. & Authier, S. 2017. Cardiac voltage-gated ion channels in safety pharmacology: Review of the landscape leading to the CiPA initiative. *Journal of pharmacological and toxicological methods*, 87(11-23).

Huang, P., Li, C., Fu, T., Zhao, D., Yi, Z., Lu, Q., Guo, L. & Xu, X. 2015. Flupirtine attenuates chronic restraint stress-induced cognitive deficits and hippocampal apoptosis in male mice. *Behavioural brain research*, 288(1-10).

Huang, Y., McClenaghan, C., Harter, T. M., Hinman, K., Halabi, C. M., Matkovich, S. J., Zhang, H., Brown, G. S., Mecham, R. P. & England, S. K. 2018. Cardiovascular consequences of K<sub>ATP</sub> overactivity in Cantu syndrome. *JCI insight*, 3(15), pp.

Humphrey, S., Smith, M., Cimini, M., Buchanan, L., Gibson, J., Khan, S. & Meisheri, K. 1996. Cardiovascular effects of the K-ATP channel blocker U-37883A and structurally related morpholinoguanidines. *Methods and findings in experimental and clinical pharmacology*, 18(4), pp 247-260.

Iannotti, F. A., Panza, E., Barrese, V., Viggiano, D., Soldovieri, M. V. & Taglialatela, M. 2010. Expression, localization, and pharmacological role of Kv7 potassium channels in

skeletal muscle proliferation, differentiation, and survival after myotoxic insults. *Journal of Pharmacology and Experimental Therapeutics*, 332(3), pp 811-820.

Ibáñez, B., Heusch, G., Ovize, M. & Van de Werf, F. 2015. Evolving therapies for myocardial ischemia/reperfusion injury. *Journal of the American College of Cardiology*, 65(14), pp 1454-1471.

Ibanez, B., Macaya, C., Sánchez-Brunete, V., Pizarro, G., Fernández-Friera, L., Mateos, A., Fernández-Ortiz, A., García-Ruiz, J. M., García-Álvarez, A. & Iñiguez, A. 2013. Effect of early metoprolol on infarct size in ST-segment-elevation myocardial infarction patients undergoing primary percutaneous coronary intervention: the effect of metoprolol in cardioprotection during an acute myocardial infarction (METOCARD-CNIC) trial. *Circulation*, 128(14), pp 1495-1503.

Ibanez, B., Prat-González, S., Speidl, W. S., Vilahur, G., Pinero, A., Cimmino, G., García, M. J., Fuster, V., Sanz, J. & Badimon, J. J. 2007. Early metoprolol administration before coronary reperfusion results in increased myocardial salvage: analysis of ischemic myocardium at risk using cardiac magnetic resonance. *Circulation*, 115(23), pp 2909-2916.

Imagawa, J.-i., Baxter, G. F. & Yellon, D. M. 1998. Myocardial protection afforded by nicorandil and ischaemic preconditioning in a rabbit infarct model in vivo. *Journal of cardiovascular pharmacology*, 31(1), pp 74-79.

Inagaki, K., Begley, R., Ikeno, F. & Mochly-Rosen, D. 2005. Cardioprotection by  $\epsilon$ -protein kinase C activation from ischemia: continuous delivery and antiarrhythmic effect of an  $\epsilon$ -protein kinase C-activating peptide. *Circulation*, 111(1), pp 44-50.

Inagaki, N., Gonoi, T., Clement, J. P., Namba, N., Inazawa, J., Gonzalez, G., Aguilar-Bryan, L., Seino, S. & Bryan, J. 1995a. Reconstitution of  $I_{KATP}$ : an inward rectifier subunit plus the sulfonylurea receptor. *Science*, 270(5239), pp 1166-1170.

Inagaki, N., Gonoi, T., Iv, J. P. C., Wang, C.-Z., Aguilar-Bryan, L., Bryan, J. & Seino, S. 1996. A family of sulfonylurea receptors determines the pharmacological properties of ATP-sensitive  $K^+$  channels. *Neuron*, 16(5), pp 1011-1017.

Inagaki, N., Gonoi, T. & Seino, S. 1997. Subunit stoichiometry of the pancreatic  $\beta$ -cell ATP-sensitive  $K^+$  channel. *FEBS letters*, 409(2), pp 232-236.

Inagaki, N., Tsuura, Y., Namba, N., Masuda, K., Gonoi, T., Horie, M., Seino, Y., Mizuta, M. & Seino, S. 1995b. Cloning and Functional Characterization of a Novel ATP-sensitive Potassium Channel Ubiquitously Expressed in Rat Tissues, including Pancreatic Islets,

Pituitary, Skeletal Muscle, and Heart (\*). *Journal of Biological Chemistry*, 270(11), pp 5691-5694.

Inoue, I., Nagase, H., Kishi, K. & Higuti, T. 1991. ATP-sensitive K<sup>+</sup> channel in the mitochondrial inner membrane. *Nature*, 352(6332), pp 244-247.

Iost, N., Virag, L., Opincariu, M., Szecsi, J., Varro, A. & Papp, J. G. 1998. Delayed rectifier potassium current in undiseased human ventricular myocytes. *Cardiovascular research*, 40(3), pp 508-515.

Isomoto, S., Kondo, C., Yamada, M., Matsumoto, S., Higashiguchi, O., Horio, Y., Matsuzawa, Y. & Kurachi, Y. 1996. A novel sulfonylurea receptor forms with BIR (Kir6.2) a smooth muscle type ATP-sensitive K<sup>+</sup> channel. *Journal of Biological Chemistry*, 271(40), pp 24321-24324.

Ivanov, S. V., Ward, J. M., Tessarollo, L., McAreavey, D., Sachdev, V., Fananapazir, L., Banks, M. K., Morris, N., Djurickovic, D. & Devor-Henneman, D. E. 2004. Cerebellar ataxia, seizures, premature death, and cardiac abnormalities in mice with targeted disruption of the Cacna2d2 gene. *The American journal of pathology*, 165(3), pp 1007-1018.

Jabůrek, M., Yarov-Yarovoy, V., Paucek, P. & Garlid, K. D. 1998. State-dependent inhibition of the mitochondrial K<sub>ATP</sub> channel by glyburide and 5-hydroxydecanoate. *Journal of Biological Chemistry*, 273(22), pp 13578-13582.

James, A. F., Choisy, S. C. & Hancox, J. C. 2007. Recent advances in understanding sex differences in cardiac repolarization. *Progress in biophysics and molecular biology*, 94(3), pp 265-319.

Janczewski, A. M., Spurgeon, H. A. & Lakatta, E. G. 2002. Action potential prolongation in cardiac myocytes of old rats is an adaptation to sustain youthful intracellular Ca<sup>2+</sup> regulation. *Journal of molecular and cellular cardiology*, 34(6), pp 641-648.

Jensen, M. O., Jogini, V., Borhani, D. W., Leffler, A. E., Dror, R. O. & Shaw, D. E. 2012. Mechanism of voltage gating in potassium channels. *Science*, 336(6078), pp 229-33.

Jepps, T. A., Greenwood, I. A., Moffatt, J. D., Sanders, K. M. & Ohya, S. 2009. Molecular and functional characterization of Kv7 K<sup>+</sup> channel in murine gastrointestinal smooth muscles. *American Journal of Physiology-Gastrointestinal and Liver Physiology*, 297(1), pp G107-G115.

Jiang, M., Cabo, C., Yao, J.-A., Boyden, P. A. & Tseng, G.-N. 2000. Delayed rectifier K currents have reduced amplitudes and altered kinetics in myocytes from infarcted canine ventricle. *Cardiovascular research*, 48(1), pp 34-43.

Jiang, M., Wang, Y. & Tseng, G.-N. 2017. Adult ventricular myocytes segregate KCNQ1 and KCNE1 to keep the  $I_{Ks}$  amplitude in check until when larger  $I_{Ks}$  is needed. *Circulation: Arrhythmia and Electrophysiology*, 10(6), pp e005084.

Jost, N., Papp, J. G. & Varró, A. 2007. Slow delayed rectifier potassium current ( $I_{Ks}$ ) and the repolarization reserve. *Annals of Noninvasive Electrocardiology*, 12(1), pp 64-78.

Jost, N., Virág, L., Bitay, M., Takács, J., Lengyel, C., Biliczki, P., Nagy, Z., Bogáts, G., Lathrop, D. A. & Papp, J. G. 2005. Restricting excessive cardiac action potential and QT prolongation: a vital role for  $I_{Ks}$  in human ventricular muscle. *Circulation*, 112(10), pp 1392-1399.

Joukar, S. 2021. A comparative review on heart ion channels, action potentials and electrocardiogram in rodents and human: extrapolation of experimental insights to clinic. *Laboratory Animal Research*, 37(1), pp 1-15.

Jovanović, S., Ballantyne, T., Du, Q., Blagojević, M. & Jovanović, A. 2016. Phenylephrine preconditioning in embryonic heart H9c2 cells is mediated by up-regulation of SUR2B/Kir6. 2: a first evidence for functional role of SUR2B in sarcolemmal  $K_{ATP}$  channels and cardioprotection. *The international journal of biochemistry & cell biology*, 70(23-28).

Kamb, A., Iverson, L. E. & Tanouye, M. A. 1987. Molecular characterization of Shaker, a *Drosophila* gene that encodes a potassium channel. *Cell*, 50(3), pp 405-413.

Kamp, T. J. & Hell, J. W. 2000. Regulation of cardiac L-type calcium channels by protein kinase A and protein kinase C. *Circulation research*, 87(12), pp 1095-1102.

Kang, G., Leech, C. A., Chepurny, O. G., Coetzee, W. A. & Holz, G. G. 2008. Role of the cAMP sensor Epac as a determinant of  $K_{ATP}$  channel ATP sensitivity in human pancreatic  $\beta$ -cells and rat INS-1 cells. *The Journal of physiology*, 586(5), pp 1307-1319.

Karemaker, J. M. 2017. An introduction into autonomic nervous function. *Physiological measurement*, 38(5), pp R89.

Kattar, N. & Flowers, T. 2020. Anatomy, Head and Neck, Sympathetic Chain. *StatPearls [Internet]*.

Kavak, S., Emre, M., Tetiker, T., Kavak, T., Kolcu, Z. & Günay, İ. 2008. Effects of rosiglitazone on altered electrical left ventricular papillary muscle activities of diabetic rat. *Naunyn-Schmiedeberg's archives of pharmacology*, 376(6), pp 415-421.

Kawashima, T. 2005. The autonomic nervous system of the human heart with special reference to its origin, course, and peripheral distribution. *Anatomy and embryology*, 209(6), pp 425-438.

Keith, A. & Flack, M. 1907. The form and nature of the muscular connections between the primary divisions of the vertebrate heart. *Journal of anatomy and physiology*, 41(Pt 3), pp 172.

Khan, S. A., Higdon, N. R., Hester, J. B. & Meisher, K. D. 1997. Pharmacological characterization of novel cyanoguanidines as vascular  $K_{ATP}$  channel blockers. *Journal of Pharmacology and Experimental Therapeutics*, 283(3), pp 1207-1213.

Kharkovets, T., Hardelin, J.-P., Safieddine, S., Schweizer, M., El-Amraoui, A., Petit, C. & Jentsch, T. J. 2000. KCNQ4, a  $K^+$  channel mutated in a form of dominant deafness, is expressed in the inner ear and the central auditory pathway. *Proceedings of the National Academy of Sciences*, 97(8), pp 4333-4338.

Kistamas, K., Veress, R., Horvath, B., Banyasz, T., Nanasi, P. P. & Eisner, D. A. 2020. Calcium handling defects and cardiac arrhythmia syndromes. *Frontiers in pharmacology*, 11(72).

Kitakaze, M. 2010. How to mediate cardioprotection in ischemic hearts—accumulated evidence of basic research should translate to clinical medicine. *Cardiovascular drugs and therapy*, 24(3), pp 217-223.

Kitakaze, M., Asakura, M., Kim, J., Shintani, Y., Asanuma, H., Hamasaki, T., Seguchi, O., Myoishi, M., Minamino, T. & Ohara, T. 2007. Human atrial natriuretic peptide and nicorandil as adjuncts to reperfusion treatment for acute myocardial infarction (J-WIND): two randomised trials. *The Lancet*, 370(9597), pp 1483-1493.

Klabunde, R. E. 2017. Cardiac electrophysiology: normal and ischemic ionic currents and the ECG. *Advances in physiology education*, 41(1), pp 29-37.

Kleber, A. G. 1983. Resting membrane potential, extracellular potassium activity, and intracellular sodium activity during acute global ischemia in isolated perfused guinea pig hearts. *Circulation Research*, 52(4), pp 442-450.

Kobertz, W. R. 2014. Stoichiometry of the cardiac  $I_{KS}$  complex. *Proceedings of the National Academy of Sciences*, 111(14), pp 5065-5066.

Koh, S., Bradley, K., Rae, M., Keef, K., Horowitz, B. & Sanders, K. 1998. Basal activation of ATP-sensitive potassium channels in murine colonic smooth muscle cell. *Biophysical journal*, 75(4), pp 1793-1800.

Koliopoulos, K., Papadoyannis, D. & Karatzas, N. 1984. Pinacidil, a new vasodilator, in the treatment of patients with moderate to severe hypertension. *European journal of clinical pharmacology*, 27(3), pp 287-289.

Kondo, C., Isomoto, S., Matsumoto, S., Yamada, M., Horio, Y., Yamashita, S., Takemura-Kameda, K., Matsuzawa, Y. & Kurachi, Y. 1996. Cloning and functional expression of a novel isoform of ROMK inwardly rectifying ATP-dependent  $K^+$  channel, ROMK6 (Kir1.1 f). *FEBS letters*, 399(1-2), pp 122-126.

Kono, Y., Horie, M., Takano, M., Otani, H., Xie, L.-H., Akao, M., Tsuji, K. & Sasayama, S. 2000. The properties of the Kir6.1-6.2 tandem channel co-expressed with SUR2A. *Pflügers Archiv*, 440(5), pp 692-698.

Korchev, Y. E., Negulyaev, Y. A., Edwards, C. R., Vodyanoy, I. & Lab, M. J. 2000. Functional localization of single active ion channels on the surface of a living cell. *Nature cell biology*, 2(9), pp 616-619.

Korsgaard, M. P., Hartz, B. P., Brown, W. D., Ahring, P. K., Strøbaek, D. & Mirza, N. R. 2005. Anxiolytic effects of Maxipost (BMS-204352) and retigabine via activation of neuronal Kv7 channels. *Journal of Pharmacology and Experimental Therapeutics*, 314(1), pp 282-292.

Koster, J., Marshall, B., Ensor, N. e. a., Corbett, J. & Nichols, C. 2000. Targeted overactivity of  $\beta$  cell  $K_{ATP}$  channels induces profound neonatal diabetes. *Cell*, 100(6), pp 645-654.

Kovalev, H., Quayle, J., Kamishima, T. & Lodwick, D. 2004. Molecular analysis of the subtype-selective inhibition of cloned  $K_{ATP}$  channels by PNU-37883A. *British journal of pharmacology*, 141(5), pp 867-873.

Kowaltowski, A. J., Seetharaman, S., Pucek, P. & Garlid, K. D. 2001. Bioenergetic consequences of opening the ATP-sensitive  $K^+$  channel of heart mitochondria. *American Journal of Physiology-Heart and Circulatory Physiology*, 280(2), pp H649-H657.

- Krieg, T., Qin, Q., McIntosh, E. C., Cohen, M. V. & Downey, J. M. 2002. ACh and adenosine activate PI3-kinase in rabbit hearts through transactivation of receptor tyrosine kinases. *American Journal of Physiology-Heart and Circulatory Physiology*, 283(6), pp H2322-H2330.
- Kubisch, C., Schroeder, B. C., Friedrich, T., Lütjohann, B., El-Amraoui, A., Marlin, S., Petit, C. & Jentsch, T. J. 1999. KCNQ4, a novel potassium channel expressed in sensory outer hair cells, is mutated in dominant deafness. *Cell*, 96(3), pp 437-446.
- Kubo, Y., Baldwin, T. J., Nung Jan, Y. & Jan, L. Y. 1993. Primary structure and functional expression of a mouse inward rectifier potassium channel. *Nature*, 362(6416), pp 127-133.
- Kumar, A. & Cannon, C. P. Acute coronary syndromes: diagnosis and management, part I. Mayo Clinic Proceedings, 2009. Elsevier, 917-938.
- Kurata, H. T., Diraviyam, K., Marton, L. J. & Nichols, C. G. 2008. Blocker protection by short spermine analogs: refined mapping of the spermine binding site in a Kir channel. *Biophysical journal*, 95(8), pp 3827-3839.
- Kurata, H. T. & Fedida, D. 2006. A structural interpretation of voltage-gated potassium channel inactivation. *Progress in biophysics and molecular biology*, 92(2), pp 185-208.
- Kurokawa, J., Chen, L. & Kass, R. S. 2003. Requirement of subunit expression for cAMP-mediated regulation of a heart potassium channel. *Proceedings of the National Academy of Sciences*, 100(4), pp 2122-2127.
- Lacerda, L., Somers, S., Opie, L. H. & Lecour, S. 2009. Ischaemic postconditioning protects against reperfusion injury via the SAFE pathway. *Cardiovascular research*, 84(2), pp 201-208.
- Le Good, J. A., Ziegler, W. H., Parekh, D. B., Alessi, D. R., Cohen, P. & Parker, P. J. 1998. Protein kinase C isotypes controlled by phosphoinositide 3-kinase through the protein kinase PDK1. *Science*, 281(5385), pp 2042-2045.
- Lecour, S. 2009. Activation of the protective Survivor Activating Factor Enhancement (SAFE) pathway against reperfusion injury: does it go beyond the RISK pathway? *Journal of molecular and cellular cardiology*, 47(1), pp 32-40.
- Lecour, S., Suleman, N., Deuchar, G. A., Somers, S., Lacerda, L., Huisamen, B. & Opie, L. H. 2005. Pharmacological preconditioning with tumor necrosis factor- $\alpha$  activates signal transducer and activator of transcription-3 at reperfusion without involving classic

prosurvival kinases (Akt and extracellular signal-regulated kinase). *Circulation*, 112(25), pp 3911-3918.

Lederer, W. & Nichols, C. 1989. Nucleotide modulation of the activity of rat heart ATP-sensitive K<sup>+</sup> channels in isolated membrane patches. *The Journal of Physiology*, 419(1), pp 193-211.

Lengyel, C., Iost, N., Virág, L., Varró, A., Lathrop, D. A. & Papp, J. G. 2001. Pharmacological block of the slow component of the outward delayed rectifier current (I<sub>Ks</sub>) fails to lengthen rabbit ventricular muscle QTc and action potential duration. *British journal of pharmacology*, 132(1), pp 101-110.

Lenz, M., Kaun, C., Krychtiuk, K. A., Haider, P., Brekalo, M., Maier, N., Goederle, L., Binder, C. J., Huber, K. & Hengstenberg, C. 2021. Effects of nicorandil on inflammation, apoptosis and atherosclerotic plaque progression. *Biomedicines*, 9(2), pp 120.

Lerche, C., Bruhova, I., Lerche, H., Steinmeyer, K., Wei, A. D., Strutz-Seebohm, N., Lang, F., Busch, A. E., Zhorov, B. S. & Seebohm, G. 2007. Chromanol 293B binding in KCNQ1 (Kv7. 1) channels involves electrostatic interactions with a potassium ion in the selectivity filter. *Molecular pharmacology*, 71(6), pp 1503-1511.

Levick, J. R. 2013. *An introduction to cardiovascular physiology*: Butterworth-Heinemann.

Levin, M. D., Singh, G. K., Zhang, H. X., Uchida, K., Kozel, B. A., Stein, P. K., Kovacs, A., Westenbroek, R. E., Catterall, W. A., Grange, D. K. and Nichols, C.G. 2016. K<sub>ATP</sub> channel gain-of-function leads to increased myocardial L-type Ca<sup>2+</sup> current and contractility in Cantu syndrome. *Proceedings of the National Academy of Sciences*, 113(24), pp 6773-6778.

Li, A., Knutsen, R. H., Zhang, H., Osei-Owusu, P., Moreno-Dominguez, A., Harter, T. M., Uchida, K., Remedi, M. S., Dietrich, H. H. & Bernal-Mizrachi, C. 2013. Hypotension due to Kir6. 1 gain-of-function in vascular smooth muscle. *Journal of the American Heart Association*, 2(4), pp e000365.

Li, N., Wu, J.-X., Ding, D., Cheng, J., Gao, N. & Chen, L. 2017. Structure of a pancreatic ATP-sensitive potassium channel. *Cell*, 168(1-2), pp 101-110. e10.

Li, P., Rubaiy, H. N., Chen, G., Hallett, T., Zaibi, N., Zeng, B., Saurabh, R. & Xu, S. 2020. T-type Ca<sup>2+</sup> channel blocker mibepradil inhibits ORAI store-operated channels. *Journal of Molecular and Cellular Cardiology*, 140(26-27).

- Li, Y., Zayzman, M. A., Wu, D., Shi, J., Guan, M., Virgin-Downey, B. & Cui, J. 2011. KCNE1 enhances phosphatidylinositol 4, 5-bisphosphate (PIP2) sensitivity of  $I_{KS}$  to modulate channel activity. *Proceedings of the National Academy of Sciences*, 108(22), pp 9095-9100.
- Light, P., Comtois, A. & Renaud, J. 1994. The effect of glibenclamide on frog skeletal muscle: evidence for  $K^+$  ATP channel activation during fatigue. *The Journal of physiology*, 475(3), pp 495-507.
- Liin, S. I., Silverå Ejneby, M., Barro-Soria, R., Skarsfeldt, M. A., Larsson, J. E., Starck Härlin, F., Parkkari, T., Bentzen, B. H., Schmitt, N. & Larsson, H. P. 2015. Polyunsaturated fatty acid analogs act antiarrhythmically on the cardiac  $I_{KS}$  channel. *Proceedings of the National Academy of Sciences*, 112(18), pp 5714-5719.
- Liin, S. I., Yazdi, S., Ramentol, R., Barro-Soria, R. & Larsson, H. P. 2018. Mechanisms underlying the dual effect of polyunsaturated fatty acid analogs on Kv7. 1. *Cell reports*, 24(11), pp 2908-2918.
- Lim, K. H., Javadov, S. A., Das, M., Clarke, S. J., Suleiman, M. S. & Halestrap, A. P. 2002. The effects of ischaemic preconditioning, diazoxide and 5-hydroxydecanoate on rat heart mitochondrial volume and respiration. *The Journal of physiology*, 545(3), pp 961-974.
- Lim, W., Messow, C. & Berry, C. 2012. Cyclosporin variably and inconsistently reduces infarct size in experimental models of reperfused myocardial infarction: a systematic review and meta-analysis. *British journal of pharmacology*, 165(7), pp 2034-2043.
- Lin, D., Sterling, H., Lerea, K. M., Giebisch, G. & Wang, W.-H. 2002. Protein kinase C (PKC)-induced phosphorylation of ROMK1 is essential for the surface expression of ROMK1 channels. *Journal of Biological Chemistry*, 277(46), pp 44278-44284.
- Linton, K. J. & Higgins, C. F. 2007. Structure and function of ABC transporters: the ATP switch provides flexible control. *Pflügers Archiv-European Journal of Physiology*, 453(5), pp 555-567.
- Liss, B., Bruns, R. & Roeper, J. 1999. Alternative sulfonylurea receptor expression defines metabolic sensitivity of K-ATP channels in dopaminergic midbrain neurons. *The EMBO Journal*, 18(4), pp 833-846.
- Liu, D.-W., Gintant, G. A. & Antzelevitch, C. 1993. Ionic bases for electrophysiological distinctions among epicardial, midmyocardial, and endocardial myocytes from the free wall of the canine left ventricle. *Circulation research*, 72(3), pp 671-687.

- Liu, G., Thornton, J., Van Winkle, D., Stanley, A., Olsson, R. & Downey, J. 1991. Protection against infarction afforded by preconditioning is mediated by A1 adenosine receptors in rabbit heart. *Circulation*, 84(1), pp 350-356.
- Liu, H., Cala, P. M. & Anderson, S. E. 1998. Ischemic preconditioning: effects on pH, Na and Ca in newborn rabbit hearts during ischemia/reperfusion. *Journal of molecular and cellular cardiology*, 30(3), pp 685-697.
- Liu, L., Wang, F., Lu, H., Ren, X. & Zou, J. 2014. Chromanol 293B, an inhibitor of KCNQ1 channels, enhances glucose-stimulated insulin secretion and increases glucagon-like peptide-1 level in mice. *Islets*, 6(4), pp e962386.
- Liu, M. B., de Lange, E., Garfinkel, A., Weiss, J. N. & Qu, Z. 2015. Delayed afterdepolarizations generate both triggers and a vulnerable substrate promoting reentry in cardiac tissue. *Heart rhythm*, 12(10), pp 2115-2124.
- Liu, Q., Chen, D., Wang, Y., Zhao, X. & Zheng, Y. 2012. Cardiac autonomic nerve distribution and arrhythmia. *Neural regeneration research*, 7(35), pp 2834.
- Liu, S. Q. 2007. *Bioregenerative engineering: principles and applications*: John Wiley & Sons.
- Liu, Y., Ren, G., O'Rourke, B., Marbán, E. & Seharaseyon, J. 2001. Pharmacological comparison of native mitochondrial K<sub>ATP</sub> channels with molecularly defined surface K<sub>ATP</sub> channels. *Molecular pharmacology*, 59(2), pp 225-230.
- Lodwick, D., Rainbow, R. D., Rubaiy, H. N., Al Johi, M., Vuister, G. W. & Norman, R. I. 2014. Sulfonylurea receptors regulate the channel pore in ATP-sensitive potassium channels via an intersubunit salt bridge. *Biochemical Journal*, 464(3), pp 343-354.
- Lønborg, J., Kelbæk, H., Vejlstrup, N., Bøtker, H. E., Kim, W. Y., Holmvang, L., Jørgensen, E., Helqvist, S., Saunamäki, K. & Terkelsen, C. J. 2012a. Exenatide reduces final infarct size in patients with ST-segment–elevation myocardial infarction and short-duration of ischemia. *Circulation: Cardiovascular Interventions*, 5(2), pp 288-295.
- Lønborg, J., Kelbæk, H., Vejlstrup, N., Bøtker, H. E., Kim, W. Y., Holmvang, L., Jørgensen, E., Helqvist, S., Saunamäki, K. & Thuesen, L. 2012b. Influence of pre-infarction angina, collateral flow, and pre-procedural TIMI flow on myocardial salvage index by cardiac magnetic resonance in patients with ST-segment elevation myocardial infarction. *European Heart Journal–Cardiovascular Imaging*, 13(5), pp 433-443.
- Lønborg, J., Vejlstrup, N., Kelbæk, H., Bøtker, H. E., Kim, W. Y., Mathiasen, A. B., Jørgensen, E., Helqvist, S., Saunamäki, K. & Clemmensen, P. 2012c. Exenatide reduces reperfusion

injury in patients with ST-segment elevation myocardial infarction. *European heart journal*, 33(12), pp 1491-1499.

Lopatin, A. N., Makhina, E. N. & Nichols, C. G. 1994. Potassium channel block by cytoplasmic polyamines as the mechanism of intrinsic rectification. *Nature*, 372(6504), pp 366-369.

Louch, W. E., Bito, V., Heinzel, F. R., Macianskiene, R., Vanhaecke, J., Flameng, W., Mubagwa, K. & Sipido, K. R. 2004. Reduced synchrony of  $\text{Ca}^{2+}$  release with loss of T-tubules—a comparison to  $\text{Ca}^{2+}$  release in human failing cardiomyocytes. *Cardiovascular research*, 62(1), pp 63-73.

Louch, W. E., Mørk, H. K., Sexton, J., Strømme, T. A., Laake, P., Sjaastad, I. & Sejersted, O. M. 2006. T-tubule disorganization and reduced synchrony of  $\text{Ca}^{2+}$  release in murine cardiomyocytes following myocardial infarction. *The Journal of physiology*, 574(2), pp 519-533.

Loussouarn, G., Baró, I. & Escande, D. 2006. KCNQ1  $\text{K}^+$  Channel—Mediated Cardiac Channelopathies. *Ion Channels*. Springer.

Lucas, K. A., Pitari, G. M., Kazerounian, S., Ruiz-Stewart, I., Park, J., Schulz, S., Chepenik, K. P. & Waldman, S. A. 2000. Guanylyl cyclases and signaling by cyclic GMP. *Pharmacological reviews*, 52(3), pp 375-414.

Lundby, A., Tseng, G.-N. & Schmitt, N. 2010. Structural basis for KV7. 1-KCNEx interactions in the  $I_{\text{KS}}$  channel complex. *Heart Rhythm*, 7(5), pp 708-713.

Mackie, A. R. & Byron, K. L. 2008. Cardiovascular KCNQ (Kv7) potassium channels: physiological regulators and new targets for therapeutic intervention. *Molecular pharmacology*, 74(5), pp 1171-1179.

Maeda, M. 2022. Membranes and transport. *Medical Biochemistry-E-Book*, 37.

Magyar, J., Horváth, B., Bányaśz, T., Szentandrásy, N., Birinyi, P., Varró, A., Szakónyi, Z., Fülöp, F. & Nánási, P. P. 2006. L-364,373 fails to activate the slow delayed rectifier  $\text{K}^+$  current in canine ventricular cardiomyocytes. *Naunyn-Schmiedeberg's archives of pharmacology*, 373(1), pp 85-90.

Mahaffey, K. W., Puma, J. A., Barbagelata, N. A., DiCarli, M. F., Leesar, M. A., Browne, K. F., Eisenberg, P. R., Bolli, R., Casas, A. C. & Molina-Viamonte, V. 1999. Adenosine as an adjunct to thrombolytic therapy for acute myocardial infarction: results of a multicenter, randomized, placebo-controlled trial: the Acute Myocardial Infarction

STudy of ADenosine (AMISTAD) trial. *Journal of the American College of Cardiology*, 34(6), pp 1711-1720.

Main, M. J., Cryan, J. E., Dupere, J. R., Cox, B., Clare, J. J. & Burbidge, S. A. 2000. Modulation of KCNQ2/3 potassium channels by the novel anticonvulsant retigabine. *Molecular Pharmacology*, 58(2), pp 253-262.

Makino, A., Firth, A. L. & Yuan, J. X. J. 2011. Endothelial and smooth muscle cell ion channels in pulmonary vasoconstriction and vascular remodeling. *Comprehensive Physiology*, 1(3), pp 1555-1602.

Mangoni, M. E., Traboulsi, A., Leoni, A.-L., Couette, B., Marger, L., Le Quang, K., Kupfer, E., Cohen-Solal, A., Vilar, J. & Shin, H.-S. 2006. Bradycardia and slowing of the atrioventricular conduction in mice lacking CaV3. 1/α1G T-type calcium channels. *Circulation research*, 98(11), pp 1422-1430.

Mani, B. K., Robakowski, C., Brueggemann, L. I., Cribbs, L. L., Tripathi, A., Majetschak, M. & Byron, K. L. 2016. Kv7. 5 potassium channel subunits are the primary targets for PKA-dependent enhancement of vascular smooth muscle Kv7 currents. *Molecular pharmacology*, 89(3), pp 323-334.

Manning Fox, J. E., Kanji, H. D., French, R. J. & Light, P. E. 2002. Cardioselectivity of the sulphonylurea HMR 1098: studies on native and recombinant cardiac and pancreatic K<sub>ATP</sub> channels. *British journal of pharmacology*, 135(2), pp 480-488.

Martin, G. M., Kandasamy, B., DiMaio, F., Yoshioka, C. & Shyng, S.-L. 2017. Anti-diabetic drug binding site in a mammalian K<sub>ATP</sub> channel revealed by Cryo-EM. *Elife*, 6(e31054).

Matsushita, K., Kinoshita, K., Matsuoka, T., Fujita, A., Fujikado, T., Tano, Y., Nakamura, H. & Kurachi, Y. 2002. Intramolecular interaction of SUR2 subtypes for intracellular ADP-induced differential control of K<sub>ATP</sub> channels. *Circulation research*, 90(5), pp 554-561.

Mattmann, M. E., Yu, H., Lin, Z., Xu, K., Huang, X., Long, S., Wu, M., McManus, O. B., Engers, D. W. & Le, U. M. 2012. Identification of (R)-N-(4-(4-methoxyphenyl) thiazol-2-yl)-1-tosylpiperidine-2-carboxamide, ML277, as a novel, potent and selective Kv7. 1 (KCNQ1) potassium channel activator. *Bioorganic & medicinal chemistry letters*, 22(18), pp 5936-5941.

McCrossan, Z. A., Lewis, A., Panaghie, G., Jordan, P. N., Christini, D. J., Lerner, D. J. & Abbott, G. W. 2003. MinK-related peptide 2 modulates Kv2. 1 and Kv3. 1 potassium channels in mammalian brain. *Journal of Neuroscience*, 23(22), pp 8077-8091.

McCrossan, Z. A., Roepke, T. K., Lewis, A., Panaghie, G. & Abbott, G. W. 2009. Regulation of the Kv2. 1 potassium channel by MinK and MiRP1. *Journal of Membrane Biology*, 228(1), pp 1-14.

McNicholas, C. M., MacGregor, G. G., Islas, L. D., Yang, Y., Hebert, S. C. & Giebisch, G. 1998. pH-dependent modulation of the cloned renal K<sup>+</sup> channel, ROMK. *American Journal of Physiology-Renal Physiology*, 275(6), pp F972-F981.

McNICHOLAS, C. M., Yang, Y., Giebisch, G. & Hebert, S. C. 1996. Molecular site for nucleotide binding on an ATP-sensitive renal K<sup>+</sup> channel (ROMK2). *American Journal of Physiology-Renal Physiology*, 271(2), pp F275-F285.

Mechmann, S. & Pott, L. 1986. Identification of Na-Ca exchange current in single cardiac myocytes. *Nature*, 319(6054), pp 597-599.

Mehta, S. R., Yusuf, S., Díaz, R., Zhu, J., Pais, P., Xavier, D., Paolasso, E., Ahmed, R., Xie, C. & Kazmi, K. 2005. Effect of glucose-insulin-potassium infusion on mortality in patients with acute ST-segment elevation myocardial infarction: the CREATE-ECLA randomized controlled trial. *Jama*, 293(4), pp 437-446.

Meier, J. A., Hyun, M., Cantwell, M., Raza, A., Mertens, C., Raje, V., Sisler, J., Tracy, E., Torres-Odio, S. & Gispert, S. 2017. Stress-induced dynamic regulation of mitochondrial STAT3 and its association with cyclophilin D reduce mitochondrial ROS production. *Science signaling*, 10(472), pp.

Meisheri, K. D., Humphrey, S. J., Khan, S. A., Cipkus-Dubray, L. A., Smith, M. P. & Jones, A. W. 1993. 4-morpholinecarboximidine-N-1-adamantyl-N'-cyclohexylhydrochloride (U-37883A): pharmacological characterization of a novel antagonist of vascular ATP-sensitive K<sup>+</sup> channel openers. *Journal of Pharmacology and Experimental Therapeutics*, 266(2), pp 655-665.

Melman, Y. F., Krumerman, A. & McDonald, T. V. 2002. A single transmembrane site in the KCNE-encoded proteins controls the specificity of KvLQT1 channel gating. *Journal of Biological Chemistry*, 277(28), pp 25187-25194.

Melman, Y. F., Um, S. Y., Krumerman, A., Kagan, A. & McDonald, T. V. 2004. KCNE1 binds to the KCNQ1 pore to regulate potassium channel activity. *Neuron*, 42(6), pp 927-937.

Miki, T., Liss, B., Minami, K., Shiuchi, T., Saraya, A., Kashima, Y., Horiuchi, M., Ashcroft, F., Minokoshi, Y. & Roeper, J. 2001. ATP-sensitive K<sup>+</sup> channels in the hypothalamus are essential for the maintenance of glucose homeostasis. *Nature neuroscience*, 4(5), pp 507-512.

Miki, T. & Seino, S. 2005. Roles of  $K_{ATP}$  channels as metabolic sensors in acute metabolic changes. *Journal of molecular and cellular cardiology*, 38(6), pp 917-925.

Miki, T., Suzuki, M., Shibasaki, T., Uemura, H., Sato, T., Yamaguchi, K., Koseki, H., Iwanaga, T., Nakaya, H. & Seino, S. 2002. Mouse model of Prinzmetal angina by disruption of the inward rectifier Kir6.1. *Nature medicine*, 8(5), pp 466-472.

Miki, T., Tashiro, F., Iwanaga, T., Nagashima, K., Yoshitomi, H., Aihara, H., Nitta, Y., Gonoi, T., Inagaki, N. & Miyazaki, J.-i. 1997. Abnormalities of pancreatic islets by targeted expression of a dominant-negative  $K_{ATP}$  channel. *Proceedings of the National Academy of Sciences*, 94(22), pp 11969-11973.

Mizumura, T., Nithipatikom, K. & Gross, G. J. 1996. Infarct size-reducing effect of nicorandil is mediated by the  $K_{ATP}$  channel but not by its nitrate-like properties in dogs. *Cardiovascular research*, 32(2), pp 274-285.

Monfredi, O., Dobrzynski, H., Mondal, T., Boyett, M. R. & Morris, G. M. 2010. The anatomy and physiology of the sinoatrial node—a contemporary review. *Pacing and clinical electrophysiology*, 33(11), pp 1392-1406.

Mooney, J. & Rawls, S. M. 2017. KCNQ2/3 channel agonist flupirtine reduces cocaine place preference in rats. *Behavioural pharmacology*, 28(5), pp 405.

Morecroft, I., Murray, A., Nilsen, M., Gurney, A. & MacLean, M. 2009. Treatment with the Kv7 potassium channel activator flupirtine is beneficial in two independent mouse models of pulmonary hypertension. *British journal of pharmacology*, 157(7), pp 1241-1249.

Morrissey, A., Parachuru, L., Leung, M., Lopez, G., Nakamura, T. Y., Tong, X., Yoshida, H., Srivastava, S., Chowdhury, P. D. & Artman, M. 2005a. Expression of ATP-sensitive  $K^+$  channel subunits during perinatal maturation in the mouse heart. *Pediatric research*, 58(2), pp 185-192.

Morrissey, A., Rosner, E., Lanning, J., Parachuru, L., Chowdhury, P. D., Han, S., Lopez, G., Tong, X., Yoshida, H. & Nakamura, T. Y. 2005b. Immunolocalization of  $K_{ATP}$  channel subunits in mouse and rat cardiac myocytes and the coronary vasculature. *BMC physiology*, 5(1), pp 1.

Murray, C. I., Westhoff, M., Eldstrom, J., Thompson, E., Emes, R. & Fedida, D. 2016. Unnatural amino acid photo-crosslinking of the  $I_KS$  channel complex demonstrates a KCNE1:KCNQ1 stoichiometry of up to 4:4. *Elife*, 5(e11815).

Murry, C., Jennings, R. & Reimer, K. 1986. Preconditioning with ischemia: A delay of lethal cell injury in ischemic myocardium Circulation. 1986; 74: 1124–36 doi: 10.1161/01. CIR, 74(1124).

Naghavi, M., Libby, P., Falk, E., Casscells, S. W., Litovsky, S., Rumberger, J., Badimon, J. J., Stefanadis, C., Moreno, P. & Pasterkamp, G. 2003. From vulnerable plaque to vulnerable patient: a call for new definitions and risk assessment strategies: Part I. *Circulation*, 108(14), pp 1664-1672.

Nakai, Y., Horimoto, H., Mieno, S. & Sasaki, S. 2001. Mitochondrial ATP-sensitive potassium channel plays a dominant role in ischemic preconditioning of rabbit heart. *European surgical research*, 33(2), pp 57-63.

Nakajo, K., Ulbrich, M. H., Kubo, Y. & Isacoff, E. Y. 2010. Stoichiometry of the KCNQ1-KCNE1 ion channel complex. *Proceedings of the National Academy of Sciences*, 107(44), pp 18862-18867.

Nakayama, K., Fan, Z., Marumo, F. & Hiraoka, M. 1990. Interrelation between pinacidil and intracellular ATP concentrations on activation of the ATP-sensitive K<sup>+</sup> current in guinea pig ventricular myocytes. *Circulation research*, 67(5), pp 1124-1133.

Nerbonne, J. M. & Kass, R. S. 2005. Molecular physiology of cardiac repolarization. *Physiological reviews*, 85(4), pp 1205-1253.

Neyroud, N., Tesson, F., Denjoy, I., Leibovici, M., Donger, C., Barhanin, J., Fauré, S., Gary, F., Coumel, P. & Petit, C. 1997. A novel mutation in the potassium channel gene KVLQT1 causes the Jervell and Lange-Nielsen cardioauditory syndrome. *Nature genetics*, 15(2), pp 186.

Ng, G. A., Brack, K. E. & Coote, J. H. 2001. Effects of direct sympathetic and vagus nerve stimulation on the physiology of the whole heart—a novel model of isolated Langendorff perfused rabbit heart with intact dual autonomic innervation. *Experimental physiology*, 86(3), pp 319-329.

Ng, K.-E., Schwarzer, S., Duchen, M. R. & Tinker, A. 2010. The intracellular localization and function of the ATP-sensitive K<sup>+</sup> channel subunit Kir6. 1. *Journal of Membrane Biology*, 234(2), pp 137-147.

Nichols, C. & Lopatin, A. 1997. Inward rectifier potassium channels. *Annual review of physiology*, 59(1), pp 171-191.

Nichols, C. G. 2006. K ATP channels as molecular sensors of cellular metabolism. *Nature*, 440(7083), pp 470-476.

Nichols, C. G., Koster, J. & Remedi, M. 2007.  $\beta$ -cell hyperexcitability: From hyperinsulinism to Diabetes. *Diabetes, Obesity and Metabolism*, 9(81-88).

Nichols, C. G., Singh, G. K. & Grange, D. K. 2013.  $K_{ATP}$  channels and cardiovascular disease: suddenly a syndrome. *Circulation research*, 112(7), pp 1059-1072.

Nicolas, C. S., Park, K.-H., El Harchi, A., Camonis, J., Kass, R. S., Escande, D., Mérot, J., Loussouarn, G., Le Bouffant, F. & Baró, I. 2008.  $I_KS$  response to protein kinase A-dependent KCNQ1 phosphorylation requires direct interaction with microtubules. *Cardiovascular research*, 79(3), pp 427-435.

Nilius, B., Hess, P., Lansman, J. & Tsien, R. 1985. A novel type of cardiac calcium channel in ventricular cells. *Nature*, 316(6027), pp 443-446.

Noble, D. & Tsien, R. 1969. Outward membrane currents activated in the plateau range of potentials in cardiac Purkinje fibres. *The Journal of physiology*, 200(1), pp 205-231.

Noda, M., Shimizu, S., Tanabe, T., Takai, T., Kayano, T., Ikeda, T., Takahashi, H., Nakayama, H., Kanaoka, Y. & Minamino, N. 1984. Primary structure of Electrophorus electricus sodium channel deduced from cDNA sequence. *Nature*, 312(5990), pp 121-127.

Noma, A. 1983. ATP-regulated  $K^+$  channels in cardiac muscle. *Nature*, 305(5930), pp 147-148.

Noma, A. 1993. Gating properties of ATP-sensitive  $K^+$  channels in the heart. *Cardiovascular drugs and therapy*, 7(3), pp 515-520.

Notsu, T., Tanaka, I., Takano, M. & Noma, A. 1992. Blockade of the ATP-sensitive  $K^+$  channel by 5-hydroxydecanoate in guinea pig ventricular myocytes. *Journal of Pharmacology and Experimental Therapeutics*, 260(2), pp 702-708.

O'Connell, T. D., Jensen, B. C., Baker, A. J. & Simpson, P. C. 2014. Cardiac alpha1-adrenergic receptors: novel aspects of expression, signaling mechanisms, physiologic function, and clinical importance. *Pharmacological reviews*, 66(1), pp 308-333.

O'gara, P. T., Kushner, F. G., Ascheim, D. D., Casey Jr, D. E., Chung, M. K., De Lemos, J. A., Ettinger, S. M., Fang, J. C., Fesmire, F. M. & Franklin, B. A. 2013. 2013 ACCF/AHA guideline for the management of ST-elevation myocardial infarction: executive

summary: a report of the American College of Cardiology Foundation/American Heart Association Task Force on Practice Guidelines. *Circulation*, 127(4), pp 529-555.

Olgar, Y., Durak, A., Bitirim, C. V., Tuncay, E. & Turan, B. 2022. Insulin acts as an atypical KCNQ1/KCNE1-current activator and reverses long QT in insulin-resistant aged rats by accelerating the ventricular action potential repolarization through affecting the  $\beta_3$ -adrenergic receptor signaling pathway. *Journal of Cellular Physiology*, 237(2), pp 1353-1371.

Ortiz, D., Gossack, L., Quast, U. & Bryan, J. 2013. Reinterpreting the action of ATP analogs on  $K_{ATP}$  channels. *Journal of Biological Chemistry*, 288(26), pp 18894-18902.

Osteen, J. D., Gonzalez, C., Sampson, K. J., Iyer, V., Rebollo, S., Larsson, H. P. & Kass, R. S. 2010. KCNE1 alters the voltage sensor movements necessary to open the KCNQ1 channel gate. *Proceedings of the National Academy of Sciences*, 107(52), pp 22710-22715.

Oudit, G. Y., Kassiri, Z., Sah, R., Ramirez, R. J., Zobel, C. & Backx, P. H. 2001. The molecular physiology of the cardiac transient outward potassium current ( $I_{to}$ ) in normal and diseased myocardium. *Journal of molecular and cellular cardiology*, 33(5), pp 851-872.

Panaghie, G. & Abbott, G. W. 2007. The role of S4 charges in voltage-dependent and voltage-independent KCNQ1 potassium channel complexes. *J Gen Physiol*, 129(2), pp 121-33.

Paucek, P., Mironova, G., Mahdi, F., Beavis, A., Woldegiorgis, G. & Garlid, K. 1992. Reconstitution and partial purification of the glibenclamide-sensitive, ATP-dependent  $K^+$  channel from rat liver and beef heart mitochondria. *Journal of Biological Chemistry*, 267(36), pp 26062-26069.

Payandeh, J., Scheuer, T., Zheng, N. & Catterall, W. A. 2011. The crystal structure of a voltage-gated sodium channel. *Nature*, 475(7356), pp 353-358.

Pelletier, M. R., Pahapill, P. A., Pennefather, P. S. & Carlen, P. L. 2000. Analysis of single  $K_{ATP}$  channels in mammalian dentate gyrus granule cells. *Journal of Neurophysiology*, 84(5), pp 2291-2301.

Pelzmann, B., Hallström, S., Schaffer, P., Lang, P., Nadlinger, K., Birkmayer, G. D., Vrecko, K., Reibnegger, G. & Koidl, B. 2003. NADH supplementation decreases pinacidil-primed IK (ATP) in ventricular cardiomyocytes by increasing intracellular ATP. *British journal of pharmacology*, 139(4), pp 749-754.

Piccini, M., Vitelli, F., Seri, M., Galietta, L. J., Moran, O., Bulfone, A., Banfi, S., Pober, B. & Renieri, A. 1999. KCNE1-like gene is deleted in AMME contiguous gene syndrome: identification and characterization of the human and mouse homologs. *Genomics*, 60(3), pp 251-257.

Pieske, B., Maier, L. S. & Schmidt-Schweda, S. 2002. Sarcoplasmic reticulum  $\text{Ca}^{2+}$  load in human heart failure. *Basic research in cardiology*, 97(1), pp 163-171.

Pinalli, C., Bennett, H., Davenport, J. B., Trafford, A. W. & Kitmitto, A. 2013. Three-dimensional reconstruction of cardiac sarcoplasmic reticulum reveals a continuous network linking transverse-tubules: this organization is perturbed in heart failure. *Circulation research*, 113(11), pp 1219-1230.

Piot, C., Croisille, P., Staat, P., Thibault, H., Rioufol, G., Mewton, N., Elbelghiti, R., Cung, T. T., Bonnefoy, E. & Angoulvant, D. 2008. Effect of cyclosporine on reperfusion injury in acute myocardial infarction. *New England Journal of Medicine*, 359(5), pp 473-481.

Pizarro, G., Fernández-Friera, L., Fuster, V., Fernández-Jiménez, R., García-Ruiz, J. M., García-Álvarez, A., Mateos, A., Barreiro, M. V., Escalera, N. & Rodriguez, M. D. 2014. Long-term benefit of early pre-reperfusion metoprolol administration in patients with acute myocardial infarction: results from the METOCARD-CNIC trial (Effect of Metoprolol in Cardioprotection During an Acute Myocardial Infarction). *Journal of the American College of Cardiology*, 63(22), pp 2356-2362.

Plant, L. D. 2012. A role for K<sub>2P</sub> channels in the operation of somatosensory nociceptors. *Frontiers in molecular neuroscience*, 5(21).

Plant, L. D., Xiong, D., Dai, H. & Goldstein, S. A. 2014. Individual I<sub>Ks</sub> channels at the surface of mammalian cells contain two KCNE1 accessory subunits. *Proceedings of the National Academy of Sciences*, 111(14), pp E1438-E1446.

Ploug, K. B., Boni, L. J., Baun, M., Hay-Schmidt, A., Olesen, J. & Jansen-Olesen, I. 2008. K<sub>ATP</sub> channel expression and pharmacological in vivo and in vitro studies of the K<sub>ATP</sub> channel blocker PNU-37883A in rat middle meningeal arteries. *British journal of pharmacology*, 154(1), pp 72-81.

Pongs, O., Kecskemethy, N., Müller, R., Krah-Jentgens, I., Baumann, A., Kiltz, H., Canal, I., Llamazares, S. & Ferrus, A. 1988. Shaker encodes a family of putative potassium channel proteins in the nervous system of *Drosophila*. *The EMBO Journal*, 7(4), pp 1087-1096.

- Proks, P., Gribble, F. M., Adhikari, R., Tucker, S. J. & Ashcroft, F. M. 1999. Involvement of the N-terminus of Kir6. 2 in the inhibition of the  $K_{ATP}$  channel by ATP. *The Journal of physiology*, 514(1), pp 19-25.
- Prole, D. L. & Marrion, N. V. 2004. Ionic permeation and conduction properties of neuronal KCNQ2/KCNQ3 potassium channels. *Biophysical journal*, 86(3), pp 1454-1469.
- Psaty, B. M., Heckbert, S. R., Koepsell, T. D., Siscovick, D. S., Raghunathan, T. E., Weiss, N. S., Rosendaal, F. R., Lemaitre, R. N., Smith, N. L. & Wahl, P. W. 1995. The risk of myocardial infarction associated with antihypertensive drug therapies. *Jama*, 274(8), pp 620-625.
- Pu, J.-L., Ye, B., Kroboth, S. L., McNally, E. M., Makielinski, J. C. & Shi, N.-Q. 2008. Cardiac sulfonylurea receptor short form-based channels confer a glibenclamide-insensitive  $K_{ATP}$  activity. *Journal of molecular and cellular cardiology*, 44(1), pp 188-200.
- Purtell, K., Paroder-Belenitsky, M., Reyna-Neyra, A., Nicola, J. P., Koba, W., Fine, E., Carrasco, N. & Abbott, G. W. 2012. The KCNQ1-KCNE2  $K^+$  channel is required for adequate thyroid I<sup>-</sup> uptake. *The FASEB Journal*, 26(8), pp 3252-3259.
- Pusch, M., Magrassi, R., Wollnik, B. & Conti, F. 1998. Activation and inactivation of homomeric KvLQT1 potassium channels. *Biophysical Journal*, 75(2), pp 785-792.
- Qu, Z. & Chung, D. 2012. Mechanisms and determinants of ultralong action potential duration and slow rate-dependence in cardiac myocytes.
- Quayle, J. M., Bonev, A. D., Brayden, J. E. & Nelson, M. T. 1994. Calcitonin gene-related peptide activated ATP-sensitive  $K^+$  currents in rabbit arterial smooth muscle via protein kinase A. *The Journal of physiology*, 475(1), pp 9-13.
- Quayle, J. M., Bonev, A. D., Brayden, J. E. & Nelson, M. T. 1995. Pharmacology of ATP-sensitive  $K^+$  currents in smooth muscle cells from rabbit mesenteric artery. *American Journal of Physiology-Cell Physiology*, 269(5), pp C1112-C1118.
- Ragsdale, D. S., McPhee, J. C., Scheuer, T. & Catterall, W. A. 1994. Molecular determinants of state-dependent block of Na<sup>+</sup> channels by local anesthetics. *Science*, 265(5179), pp 1724-1728.
- Rainbow, R., Norman, R., Hudman, D., Davies, N. & Standen, N. 2005. Reduced effectiveness of HMR 1098 in blocking cardiac sarcolemmal  $K_{ATP}$  channels during metabolic stress. *Journal of molecular and cellular cardiology*, 39(4), pp 637-646.

- Rainbow, R. D., Lodwick, D., Hudman, D., Davies, N. W., Norman, R. I. & Standen, N. 2004. SUR2A C-terminal fragments reduce  $K_{ATP}$  currents and ischaemic tolerance of rat cardiac myocytes. *The Journal of physiology*, 557(3), pp 785-794.
- Rastogi, V. & Pragya, P. U. 2012. A brief view on antihypertensive drugs delivery through transdermal patches. *International Journal Of Pharmaceutical Sciences And Research*, 3(7), pp 1955.
- Redrobe, J. P. & Nielsen, A. N. 2009. Effects of neuronal Kv7 potassium channel activators on hyperactivity in a rodent model of mania. *Behavioural brain research*, 198(2), pp 481-485.
- Rennie, K. J., Weng, T. & Correia, M. J. 2001. Effects of KCNQ channel blockers on  $K^+$  currents in vestibular hair cells. *American Journal of Physiology-Cell Physiology*, 280(3), pp C473-C480.
- Repuente, V. P., Nakamura, H., Fujita, A., Horio, Y., Findlay, I., Pott, L. & Kurachi, Y. 1999. Extracellular links in Kir subunits control the unitary conductance of SUR/Kir6. 0 ion channels. *The EMBO Journal*, 18(12), pp 3317-3324.
- Reuter, H. 1979. Properties of two inward membrane currents in the heart. *Annual review of physiology*, 41(1), pp 413-424.
- Ribalet, B., John, S. A. & Weiss, J. N. 2003. Molecular basis for Kir6. 2 channel inhibition by adenine nucleotides. *Biophysical journal*, 84(1), pp 266-276.
- Robbins, J. 2001. KCNQ potassium channels: physiology, pathophysiology, and pharmacology. *Pharmacol Ther*, 90(1), pp 1-19.
- Robertson, B. E., Bonev, A. D. & Nelson, M. T. 1996. Inward rectifier  $K^+$  currents in smooth muscle cells from rat coronary arteries: block by  $Mg^{2+}$ ,  $Ca^{2+}$ , and  $Ba^{2+}$ . *American Journal of Physiology-Heart and Circulatory Physiology*, 271(2), pp H696-H705.
- Rocchetti, M., Freli, V., Perego, V., Altomare, C., Mostacciulo, G. & Zaza, A. 2006. Rate dependency of  $\beta$ -adrenergic modulation of repolarizing currents in the guinea-pig ventricle. *The Journal of physiology*, 574(1), pp 183-193.
- Roden, D. M. 1998. Taking the “idio” out of “idiosyncratic”: predicting torsades de pointes. *Pacing and Clinical Electrophysiology*, 21(5), pp 1029-1034.

Rodriguez, B., Trayanova, N. & Noble, D. 2006. Modeling cardiac ischemia. *Annals of the New York academy of sciences*, 1080(1), pp 395-414.

Roeper, B. L., Jochen 2001. Molecular physiology of neuronal K-ATP channels. *Molecular membrane biology*, 18(2), pp 117-127.

Rohr, S. 2004. Role of gap junctions in the propagation of the cardiac action potential. *Cardiovascular research*, 62(2), pp 309-322.

Roolvink, V., Ibáñez, B., Ottervanger, J. P., Pizarro, G., Van Royen, N., Mateos, A., Dambrink, J.-H. E., Escalera, N., Lipsic, E. & Albarran, A. 2016. Early intravenous beta-blockers in patients with ST-segment elevation myocardial infarction before primary percutaneous coronary intervention. *Journal of the American College of Cardiology*, 67(23), pp 2705-2715.

Roos, S. T., Timmers, L., Biesbroek, P. S., Nijveldt, R., Kamp, O., van Rossum, A. C., van Hout, G. P., Stella, P. R., Doevedans, P. A. & Knaapen, P. 2016. No benefit of additional treatment with exenatide in patients with an acute myocardial infarction. *International journal of cardiology*, 220(809-814).

Rosano, G., Fini, M., Caminiti, G. & Barbaro, G. 2008. Cardiac metabolism in myocardial ischemia. *Current pharmaceutical design*, 14(25), pp 2551-2562.

Rosati, B., Dun, W., Hirose, M., Boyden, P. A. & McKinnon, D. 2007. Molecular basis of the T- and L-type  $\text{Ca}^{2+}$  currents in canine Purkinje fibres. *The Journal of Physiology*, 579(2), pp 465-471.

Ross, A. M., Gibbons, R. J., Stone, G. W., Kloner, R. A., Alexander, R. W. & Investigators, A.-I. 2005. A randomized, double-blinded, placebo-controlled multicenter trial of adenosine as an adjunct to reperfusion in the treatment of acute myocardial infarction (AMISTAD-II). *Journal of the American College of Cardiology*, 45(11), pp 1775-1780.

Rossello, X. & Yellon, D. M. 2016. A critical review on the translational journey of cardioprotective therapies! *International journal of cardiology*, 220(176-184).

Rossello, X. & Yellon, D. M. 2018. The RISK pathway and beyond. *Basic research in cardiology*, 113(1), pp 2.

Roura-Ferrer, M., Etxebarria, A., Solé, L., Oliveras, A., Comes, N., Villarroel, Á. & Felipe, A. 2009. Functional implications of KCNE subunit expression for the Kv7. 5 (KCNQ5) channel. *Cellular Physiology and Biochemistry*, 24(5-6), pp 325-334.

Ruth, P., Rohrkasten, A., Biel, M., Bosse, E., Regulla, S., Meyer, H. E., Flockerzi, V. & Hofmann, F. 1989. Primary structure of the beta subunit of the DHP-sensitive calcium channel from skeletal muscle. *Science*, 245(4922), pp 1115-1118.

Sakura, H., Ämmälä, C., Smith, P., Gribble, F. & Ashcroft, F. 1995. Cloning and functional expression of the cDNA encoding a novel ATP-sensitive potassium channel subunit expressed in pancreatic  $\beta$ -cells, brain, heart and skeletal muscle. *FEBS letters*, 377(3), pp 338-344.

Salata, J. J., Jurkiewicz, N. K., Wang, J., Evans, B. E., Orme, H. T. & Sanguinetti, M. C. 1998. A novel benzodiazepine that activates cardiac slow delayed rectifier  $K^+$  currents. *Molecular pharmacology*, 54(1), pp 220-230.

Salata, J. J. & Zipes, D. P. 2020. Autonomic nervous system control of heart rate and atrioventricular nodal conduction. *Reflex control of the circulation*, 67-101.

Samson, R., Baydoun, H., Jaiswal, A. & Le Jemtel, T. H. 2015. Cardiac adrenergic nervous system and left ventricular remodeling. *The American journal of the medical sciences*, 350(4), pp 321-326.

Sanguinetti, M. C., Curran, M. E., Zou, A., Shen, J., Spector, P. S., Atkinson, D. L. & Keating, M. T. 1996. Coassembly of K(V)LQT1 and minK (IsK) proteins to form cardiac I( $K_S$ ) potassium channel. *Nature*, 384(6604), pp 80-3.

Sankaranarayanan, R., Kistamás, K., Greensmith, D. J., Venetucci, L. A. & Eisner, D. A. 2017. Systolic  $[Ca^{2+}]_i$  regulates diastolic levels in rat ventricular myocytes. *The Journal of physiology*, 595(16), pp 5545-5555.

Santana, L. F., Cheng, E. P. & Lederer, W. J. 2010. How does the shape of the cardiac action potential control calcium signaling and contraction in the heart? *Journal of molecular and cellular cardiology*, 49(6), pp 901-903.

Santulli, G., Nakashima, R., Yuan, Q. & Marks, A. R. 2017. Intracellular calcium release channels: an update. *The Journal of physiology*, 595(10), pp 3041-3051.

Sato, N., Tanaka, H., Habuchi, Y. & Giles, W. R. 2000a. Electrophysiological effects of ibutilide on the delayed rectifier  $K^+$  current in rabbit sinoatrial and atrioventricular node cells. *European journal of pharmacology*, 404(3), pp 281-288.

- Sato, T., Sasaki, N., Seharaseyon, J., O'Rourke, B. & Marbán, E. 2000b. Selective pharmacological agents implicate mitochondrial but not sarcolemmal K<sub>ATP</sub> channels in ischemic cardioprotection. *Circulation*, 101(20), pp 2418-2423.
- Satoh, E., Yamada, M., Kondo, C., Repunte, V. P., Horio, Y., Iijima, T. & Kurachi, Y. 1998. Intracellular nucleotide-mediated gating of SUR/Kir6.0 complex potassium channels expressed in a mammalian cell line and its modification by pinacidil. *The Journal of physiology*, 511(3), pp 663-674.
- Schmidt, C., Wiedmann, F., Beyersdorf, C., Zhao, Z., El-Battrawy, I., Lan, H., Szabo, G., Li, X., Lang, S. & Korkmaz-Icöz, S. 2019. Genetic Ablation of TASK-1 (Tandem of P Domains in a Weak Inward Rectifying K<sup>+</sup> Channel–Related Acid-Sensitive K<sup>+</sup> Channel-1)(K2P3.1) K<sup>+</sup> Channels Suppresses Atrial Fibrillation and Prevents Electrical Remodeling. *Circulation: Arrhythmia and Electrophysiology*, 12(9), pp e007465.
- Schroeder, B. C., Hechenberger, M., Weinreich, F., Kubisch, C. & Jentsch, T. J. 2000a. KCNQ5, a novel potassium channel broadly expressed in brain, mediates M-type currents. *J Biol Chem*, 275(31), pp 24089-95.
- Schroeder, B. C., Waldegger, S., Fehr, S., Bleich, M., Warth, R., Greger, R. & Jentsch, T. J. 2000b. A constitutively open potassium channel formed by KCNQ1 and KCNE3. *Nature*, 403(6766), pp 196-9.
- Schulman, D., Latchman, D. S. & Yellon, D. M. 2002. Urocortin protects the heart from reperfusion injury via upregulation of p42/p44 MAPK signaling pathway. *American Journal of Physiology-Heart and Circulatory Physiology*, 283(4), pp H1481-H1488.
- Schwake, M., Pusch, M., Kharkovets, T. & Jentsch, T. J. 2000. Surface expression and single channel properties of KCNQ2/KCNQ3, M-type K<sup>+</sup> channels involved in epilepsy. *J Biol Chem*, 275(18), pp 13343-8.
- Schwartz, P. J., Spazzolini, C., Crotti, L., Batten, J., Amlie, J. P., Timothy, K., Shkolnikova, M., Berul, C. I., Bitner-Glindzicz, M. & Toivonen, L. 2006. The Jervell and Lange-Nielsen syndrome: natural history, molecular basis, and clinical outcome. *Circulation*, 113(6), pp 783-790.
- Sedivy, V., Joshi, S., Ghaly, Y., Mizera, R., Zaloudikova, M., Brennan, S., Novotna, J., Herget, J. & Gurney, A. M. 2015. Role of Kv7 channels in responses of the pulmonary circulation to hypoxia. *American Journal of Physiology-Lung Cellular and Molecular Physiology*, 308(1), pp L48-L57.

Seebohm, G., Pusch, M., Chen, J. & Sanguinetti, M. C. 2003a. Pharmacological activation of normal and arrhythmia-associated mutant KCNQ1 potassium channels. *Circulation research*, 93(10), pp 941-947.

Seebohm, G., Sanguinetti, M. C. & Pusch, M. 2003b. Tight coupling of rubidium conductance and inactivation in human KCNQ1 potassium channels. *The Journal of physiology*, 552(2), pp 369-378.

Seharaseyong, J., Ohler, A., Sasaki, N., Fraser, H., Sato, T., Johns, D. C., Brian, O. & Marbán, E. 2000. Molecular composition of mitochondrial ATP-sensitive potassium channels probed by viral Kir gene transfer. *Journal of molecular and cellular cardiology*, 32(11), pp 1923-1930.

Seino, S. 1999. ATP-sensitive potassium channels: a model of heteromultimeric potassium channel/receptor assemblies. *Annual review of physiology*, 61(1), pp 337-362.

Selker, H. P., Beshansky, J. R., Sheehan, P. R., Massaro, J. M., Griffith, J. L., D'Agostino, R. B., Ruthazer, R., Atkins, J. M., Sayah, A. J. & Levy, M. K. 2012. Out-of-hospital administration of intravenous glucose-insulin-potassium in patients with suspected acute coronary syndromes: the IMMEDIATE randomized controlled trial. *Jama*, 307(18), pp 1925-1933.

Selvam, R. P., Singh, A. K. & Sivakumar, T. 2010. Transdermal drug delivery systems for antihypertensive drugs-A review. *Int J Pharm Biomed Res*, 1(1), pp 1-8.

Selyanko, A., Hadley, J., Wood, I., Abogadie, F., Jentsch, T. & Brown, D. 2000. Inhibition of KCNQ1-4 potassium channels expressed in mammalian cells via M1 muscarinic acetylcholine receptors. *The Journal of Physiology*, 522(3), pp 349-355.

Sepúlveda, F. V., Pablo Cid, L., Teulon, J. & Niemeyer, M. I. 2015. Molecular aspects of structure, gating, and physiology of pH-sensitive background K<sub>2</sub>P and Kir K<sup>+</sup>-transport channels. *Physiological reviews*, 95(1), pp 179-217.

Sesti, F. & Goldstein, S. A. 1998. Single-channel characteristics of wild-type I<sub>Ks</sub> channels and channels formed with two minK mutants that cause long QT syndrome. *The Journal of general physiology*, 112(6), pp 651-663.

Shamgar, L., Haitin, Y., Yisharel, I., Malka, E., Schottelndreier, H., Peretz, A., Paas, Y. & Attali, B. 2008. KCNE1 constrains the voltage sensor of Kv7.1 K<sup>+</sup> channels. *PLoS One*, 3(4), pp e1943.

- Shamgar, L., Ma, L., Schmitt, N., Haitin, Y., Peretz, A., Wiener, R., Hirsch, J., Pongs, O. & Attali, B. 2006. Calmodulin is essential for cardiac  $I_{KS}$  channel gating and assembly: impaired function in long-QT mutations. *Circulation research*, 98(8), pp 1055-1063.
- Shapiro, M. S., Roche, J. P., Kaftan, E. J., Cruzblanca, H., Mackie, K. & Hille, B. 2000. Reconstitution of muscarinic modulation of the KCNQ2/KCNQ3  $K^+$  channels that underlie the neuronal M current. *Journal of Neuroscience*, 20(5), pp 1710-1721.
- Shimoda, L. A. & Polak, J. 2011. Hypoxia. 4. Hypoxia and ion channel function. *American Journal of Physiology-Cell Physiology*, 300(5), pp C951-C967.
- Shuck, M. E., Bock, J. H., Benjamin, C. W., Tsai, T.-D., Lee, K. S., Slightom, J. L. & Bienkowski, M. J. 1994. Cloning and characterization of multiple forms of the human kidney ROM-K potassium channel. *Journal of Biological Chemistry*, 269(39), pp 24261-24270.
- Shyng, S.-L., Ferrigni, T. & Nichols, C. 1997. Regulation of  $K_{ATP}$  channel activity by diazoxide and MgADP: distinct functions of the two nucleotide binding folds of the sulfonylurea receptor. *The Journal of general physiology*, 110(6), pp 643-654.
- Shyng, S.-L. & Nichols, C. 1997. Octameric stoichiometry of the  $K_{ATP}$  channel complex. *The Journal of general physiology*, 110(6), pp 655-664.
- Silva, J. & Rudy, Y. 2005. Subunit interaction determines  $I_{KS}$  participation in cardiac repolarization and repolarization reserve. *Circulation*, 112(10), pp 1384-1391.
- Silverman, M. E., Grove, D. & Upshaw Jr, C. B. 2006. Why does the heart beat? The discovery of the electrical system of the heart. *Circulation*, 113(23), pp 2775-2781.
- Singh, H., Hudman, D., Lawrence, C., Rainbow, R. D., Lodwick, D. & Norman, R. I. 2003. Distribution of Kir6.0 and SUR2 ATP-sensitive potassium channel subunits in isolated ventricular myocytes. *Journal of molecular and cellular cardiology*, 35(5), pp 445-459.
- Söhl, G. & Willecke, K. 2003. An update on connexin genes and their nomenclature in mouse and man. *Cell communication & adhesion*, 10(4-6), pp 173-180.
- Soldovieri, M. V., Miceli, F. & Taglialatela, M. 2011. Driving with no brakes: molecular pathophysiology of Kv7 potassium channels. *Physiology*, 26(5), pp 365-376.
- Song, L.-S., Sobie, E. A., McCulle, S., Lederer, W., Balke, C. W. & Cheng, H. 2006. Orphaned ryanodine receptors in the failing heart. *Proceedings of the National Academy of Sciences*, 103(11), pp 4305-4310.

- Song, M.-K., Cui, Y.-Y., Zhang, W.-W., Zhu, L., Lu, Y. & Chen, H.-Z. 2009. The facilitating effect of systemic administration of Kv7/M channel blocker XE991 on LTP induction in the hippocampal CA1 area independent of muscarinic activation. *Neuroscience letters*, 461(1), pp 25-29.
- Sonne, D. P., Engstrøm, T. & Treiman, M. 2008. Protective effects of GLP-1 analogues exendin-4 and GLP-1 (9–36) amide against ischemia–reperfusion injury in rat heart. *Regulatory peptides*, 146(1-3), pp 243-249.
- Spruce, A., Standen, N. & Stanfield, P. 1985. Voltage-dependent ATP-sensitive potassium channels of skeletal muscle membrane. *Nature*, 316(6030), pp 736-738.
- Stephan, D., Winkler, M., Kühner, P., Russ, U. & Quast, U. 2006. Selectivity of repaglinide and glibenclamide for the pancreatic over the cardiovascular K<sub>ATP</sub> channels. *Diabetologia*, 49(9), pp 2039-2048.
- Stott, J. B., Jepps, T. A. & Greenwood, I. A. 2014. KV7 potassium channels: a new therapeutic target in smooth muscle disorders. *Drug discovery today*, 19(4), pp 413-424.
- Strutz-Seeböhm, N., Henrion, U., Steinke, K., Tapken, D., Lang, F. & Seeböhm, G. 2009. Serum- and glucocorticoid-inducible kinases (SGK) regulate KCNQ1/KCNE potassium channels. *Channels*, 3(2), pp 88-90.
- Strutz-Seeböhm, N., Seebohm, G., Fedorenko, O., Baltaev, R., Engel, J., Knirsch, M. & Lang, F. 2006. Functional coassembly of KCNQ4 with KCNE-β-subunits in Xenopus oocytes. *Cellular Physiology and Biochemistry*, 18(1-3), pp 57-66.
- Subczynski, W. K., Hyde, J. S. & Kusumi, A. 1989. Oxygen permeability of phosphatidylcholine-cholesterol membranes. *Proceedings of the National Academy of Sciences*, 86(12), pp 4474-4478.
- Sun, H.-s. & Feng, Z.-p. 2013. Neuroprotective role of ATP-sensitive potassium channels in cerebral ischemia. *Acta Pharmacologica Sinica*, 34(1), pp 24-32.
- Sun, J., Morgan, M., Shen, R.-F., Steenbergen, C. & Murphy, E. 2007. Preconditioning results in S-nitrosylation of proteins involved in regulation of mitochondrial energetics and calcium transport. *Circulation research*, 101(11), pp 1155-1163.
- Sun, X., Zayzman, M. A. & Cui, J. 2012. Regulation of voltage-activated K<sup>+</sup> channel gating by transmembrane β subunits. *Frontiers in pharmacology*, 3(63).

Sun, Z. Q., THOMAS, G. P. & ANTZELEVITCH, C. 2001. Chromanol 293B inhibits slowly activating delayed rectifier and transient outward currents in canine left ventricular myocytes. *Journal of cardiovascular electrophysiology*, 12(4), pp 472-478.

Surah-Narwal, S., Xu, S., McHugh, D., McDonald, R., Hough, E., Cheong, A., Partridge, C., Sivaprasadarao, A. & Beech, D. 1999. Block of human aorta Kir6. 1 by the vascular K<sub>ATP</sub> channel inhibitor U37883A. *British journal of pharmacology*, 128(3), pp 667-672.

Suriti, T. S. & Jan, L. Y. 2005. A potassium channel, the M-channel, as a therapeutic target. *Current opinion in investigational drugs (London, England: 2000)*, 6(7), pp 704-711.

Suzuki, M., Fujikura, K., Kotake, K., Inagaki, N., Seino, S. & Takata, K. 1999. Immuno-localization of sulphonylurea receptor 1 in rat pancreas. *Diabetologia*, 42(10), pp 1204-1211.

Suzuki, M., Kotake, K., Fujikura, K., Inagaki, N., Suzuki, T., Gonoi, T., Seino, S. & Takata, K. 1997. Kir6. 1: a possible subunit of ATP-sensitive K<sup>+</sup> channels in mitochondria. *Biochemical and biophysical research communications*, 241(3), pp 693-697.

Suzuki, M., Li, R. A., Miki, T., Uemura, H., Sakamoto, N., Ohmoto-Sekine, Y., Tamagawa, M., Ogura, T., Seino, S. & Marbán, E. 2001. Functional roles of cardiac and vascular ATP-sensitive potassium channels clarified by Kir6. 2-knockout mice. *Circulation research*, 88(6), pp 570-577.

Suzuki, M., Sasaki, N., Miki, T., Sakamoto, N., Ohmoto-Sekine, Y., Tamagawa, M., Seino, S., Marbán, E. & Nakaya, H. 2002. Role of sarcolemmal KATP channels in cardioprotection against ischemia/reperfusion injury in mice. *The Journal of clinical investigation*, 109(4), pp 509-516.

Takahashi, M., Seagar, M. J., Jones, J. F., Reber, B. & Catterall, W. A. 1987. Subunit structure of dihydropyridine-sensitive calcium channels from skeletal muscle. *Proceedings of the National Academy of Sciences*, 84(15), pp 5478-5482.

Takano, M., Qin, D. & Noma, A. 1990. ATP-dependent decay and recovery of K<sup>+</sup> channels in guinea pig cardiac myocytes. *American Journal of Physiology-Heart and Circulatory Physiology*, 258(1), pp H45-H50.

Takano, M., Xie, L. H., Otani, H. & Horie, M. 1998. Cytoplasmic terminus domains of Kir6. x confer different nucleotide-dependent gating on the ATP-sensitive K<sup>+</sup> channel. *The Journal of physiology*, 512(2), pp 395-406.

- Tamargo, J., Caballero, R., Gómez, R., Valenzuela, C. & Delpón, E. 2004. Pharmacology of cardiac potassium channels. *Cardiovascular research*, 62(1), pp 9-33.
- Tanemoto, M., Vanoye, C. G., Dong, K., Welch, R., Abe, T., Hebert, S. C. & Xu, J. Z. 2000. Rat homolog of sulfonylurea receptor 2B determines glibenclamide sensitivity of ROMK2 in *Xenopus laevis* oocyte. *American Journal of Physiology-Renal Physiology*, 278(4), pp F659-F666.
- Tapper, A. R. & George Jr, A. L. 2000. MinK subdomains that mediate modulation of and association with KvLQT1. *The Journal of general physiology*, 116(3), pp 379-390.
- Tarasov, A., Dusonchet, J. & Ashcroft, F. 2004. Metabolic regulation of the pancreatic beta-cell ATP-sensitive K<sup>+</sup> channel: a pas de deux. *Diabetes*, 53(suppl 3), pp S113-S122.
- Tempel, B. L., Papazian, D. M., Schwarz, T. L., Jan, Y. N. & Jan, L. Y. 1987. Sequence of a probable potassium channel component encoded at Shaker locus of *Drosophila*. *Science*, 237(4816), pp 770-775.
- Teramoto, N. 2006. Physiological roles of ATP-sensitive K<sup>+</sup> channels in smooth muscle. *The Journal of physiology*, 572(3), pp 617-624.
- Terracciano, C. & MacLeod, K. T. 1997. Measurements of Ca<sup>2+</sup> entry and sarcoplasmic reticulum Ca<sup>2+</sup> content during the cardiac cycle in guinea pig and rat ventricular myocytes. *Biophysical journal*, 72(3), pp 1319-1326.
- Terrenoire, C., Houslay, M. D., Baillie, G. S. & Kass, R. S. 2009. The cardiac I<sub>Ks</sub> potassium channel macromolecular complex includes the phosphodiesterase PDE4D3. *Journal of Biological Chemistry*, 284(14), pp 9140-9146.
- Terzic, A., Findlay, I., Hosoya, Y. & Kurachi, Y. 1994. Dualistic behavior of ATP-sensitive K<sup>+</sup> channels toward intracellular nucleoside diphosphates. *Neuron*, 12(5), pp 1049-1058.
- Terzic, A., Jahangir, A. & Kurachi, Y. 1995. Cardiac ATP-sensitive K<sup>+</sup> channels: regulation by intracellular nucleotides and K<sup>+</sup> channel-opening drugs. *American Journal of Physiology-Cell Physiology*, 269(3), pp C525-C545.
- Testai, L., Barrese, V., Soldovieri, M. V., Ambrosino, P., Martelli, A., Vinciguerra, I., Miceli, F., Greenwood, I. A., Curtis, M. J. & Breschi, M. C. 2015. Expression and function of Kv7.4 channels in rat cardiac mitochondria: possible targets for cardioprotection. *Cardiovascular research*, 110(1), pp 40-50.

- Tester, D. J., Tan, B.-H., Medeiros-Domingo, A., Song, C., Makielski, J. C. & Ackerman, M. J. 2011. Loss-of-function mutations in the KCNJ8-encoded Kir6. 1 K<sub>ATP</sub> channel and sudden infant death syndrome. *Circulation: Cardiovascular Genetics*, 4(5), pp 510-515.
- Thomas, A. M., Harmer, S. C., Khambra, T. & Tinker, A. 2011. Characterization of a binding site for anionic phospholipids on KCNQ1. *J Biol Chem*, 286(3), pp 2088-100.
- Thomas, J. A. & Marks, B. H. 1978. Plasma norepinephrine in congestive heart failure. *The American journal of cardiology*, 41(2), pp 233-243.
- Timmers, L., Henriques, J. P., de Kleijn, D. P., DeVries, J. H., Kemperman, H., Steendijk, P., Verlaan, C. W., Kerver, M., Piek, J. J. & Doevedans, P. A. 2009. Exenatide reduces infarct size and improves cardiac function in a porcine model of ischemia and reperfusion injury. *Journal of the American College of Cardiology*, 53(6), pp 501-510.
- Tinel, N., Diochot, S., Borsotto, M., Lazdunski, M. & Barhanin, J. 2000a. KCNE2 confers background current characteristics to the cardiac KCNQ1 potassium channel. *The EMBO journal*, 19(23), pp 6326-6330.
- Tinel, N., Diochot, S., Lauritzen, I., Barhanin, J., Lazdunski, M. & Borsotto, M. 2000b. M-type KCNQ2-KCNQ3 potassium channels are modulated by the KCNE2 subunit. *FEBS letters*, 480(2-3), pp 137-141.
- Tinker, A., Aziz, Q. & Thomas, A. 2014. The role of ATP-sensitive potassium channels in cellular function and protection in the cardiovascular system. *British journal of pharmacology*, 171(1), pp 12-23.
- Tohse, N. 1990. Calcium-sensitive delayed rectifier potassium current in guinea pig ventricular cells. *American Journal of Physiology-Heart and Circulatory Physiology*, 258(4), pp H1200-H1207.
- Torella, D., Ellison, G. M., Karakikes, I. & Nadal-Ginard, B. 2007. Growth-factor-mediated cardiac stem cell activation in myocardial regeneration. *Nature Clinical Practice Cardiovascular Medicine*, 4(1), pp S46-S51.
- Touboul, C., Angoulvant, D., Mewton, N., Ivanes, F., Muntean, D., Prunier, F., Ovize, M. & Bejan-Angoulvant, T. 2015. Ischaemic postconditioning reduces infarct size: systematic review and meta-analysis of randomized controlled trials. *Archives of cardiovascular diseases*, 108(1), pp 39-49.
- Towart, R., Linders, J. T., Hermans, A. N., Rohrbacher, J., Van der Linde, H. J., Ercken, M., Cik, M., Roevens, P., Teisman, A. & Gallacher, D. J. 2009. Blockade of the I<sub>Ks</sub> potassium

channel: An overlooked cardiovascular liability in drug safety screening? *Journal of pharmacological and toxicological methods*, 60(1), pp 1-10.

Tran, D. B., Weber, C. & Lopez, R. A. 2021. Anatomy, thorax, heart muscles. *StatPearls [Internet]*. StatPearls Publishing.

Trezise, D., Dale, T. & Main, M. 2009. Ion Channels. Principles, Terminology and Methodology. Oxford University Press: Oxford.

Trialists, F. T. 1994. Indications for fibrinolytic therapy in suspected acute myocardial infarction: collaborative overview of early mortality and major morbidity results from all randomised trials of more than 1000 patients. *The lancet*, 343(8893), pp 311-322.

Tricarico, D., Selvaggi, M., Passantino, G., De Palo, P., Dario, C., Centoducati, P., Tateo, A., Curci, A., Maqoud, F. & Mele, A. 2016. ATP sensitive potassium channels in the skeletal muscle function: involvement of the KCNJ11 (Kir6. 2) gene in the determination of mechanical warner bratzer shear force. *Frontiers in physiology*, 7(167).

Tristani-Firouzi, M. & Sanguinetti, M. C. 1998. Voltage-dependent inactivation of the human K<sup>+</sup> channel KvLQT1 is eliminated by association with minimal K<sup>+</sup> channel (minK) subunits. *The Journal of Physiology*, 510(1), pp 37-45.

Tsevi, I., Vicente, R., Grande, M., López-Iglesias, C., Figueras, A., Capellà, G., Condom, E. & Felipe, A. 2005. KCNQ1/KCNE1 channels during germ-cell differentiation in the rat: Expression associated with testis pathologies. *Journal of cellular physiology*, 202(2), pp 400-410.

Tsien, R. 1983. Calcium channels in excitable cell membranes. *Annual review of physiology*, 45(1), pp 341-358.

Tucker, S. J., Gribble, F. M., Proks, P., Trapp, S., Ryder, T. J., Haug, T., Reimann, F. & Ashcroft, F. M. 1998. Molecular determinants of K<sub>ATP</sub> channel inhibition by ATP. *The EMBO journal*, 17(12), pp 3290-3296.

Tucker, S. J., Gribble, F. M., Zhao, C., Trapp, S. & Ashcroft, F. M. 1997. Truncation of Kir6. 2 produces ATP-sensitive K<sup>+</sup> channels in the absence of the sulphonylurea receptor. *Nature*, 387(6629), pp 179-183.

Tzingounis, A. V., Heidenreich, M., Kharkovets, T., Spitzmaul, G., Jensen, H. S., Nicoll, R. A. & Jentsch, T. J. 2010. The KCNQ5 potassium channel mediates a component of the afterhyperpolarization current in mouse hippocampus. *Proceedings of the National Academy of Sciences*, 107(22), pp 10232-10237.

van Bavel, J., Beekman, J. D. & Vos, M. A. 2021. B-PO04-117  $I_{KS}$  CHANNEL ACTIVATION BY ML277 DELAYS AND REDUCES THE ARRHYTHMIC OUTCOME IN THE CHRONIC AV BLOCK DOG. *Heart Rhythm*, 18(8), pp S326-S327.

van Bever, L., Poitry, S., Faure, C., Norman, R. I., Roatti, A. & Baertschi, A. J. 2004. Pore loop-mutated rat KIR6. 1 and KIR6. 2 suppress  $K_{ATP}$  current in rat cardiomyocytes. *American Journal of Physiology-Heart and Circulatory Physiology*, 287(2), pp H850-H859.

Van der Linde, H., Van Deuren, B., Somers, Y., Loenders, B., Towart, R. & Gallacher, D. 2010. The electro-mechanical window: A risk marker for Torsade de Pointes in a canine model of drug induced arrhythmias. *British Journal of Pharmacology*, 161(7), pp 1444-1454.

Van Horn, W. D., Vanoye, C. G. & Sanders, C. R. 2011. Working model for the structural basis for KCNE1 modulation of the KCNQ1 potassium channel. *Current Opinion in Structural Biology*, 21(2), pp 283-291.

Varnum, M. D., Busch, A. E., Bond, C. T., Maylie, J. & Adelman, J. P. 1993. The min K channel underlies the cardiac potassium current  $I_{KS}$  and mediates species-specific responses to protein kinase C. *Proceedings of the National Academy of Sciences*, 90(24), pp 11528-11532.

Varró, A., Baláti, B., Iost, N., Takács, J., Virág, L., Lathrop, D. A., Csaba, L., Tálosi, L. & Papp, J. G. 2000. The role of the delayed rectifier component  $I_{KS}$  in dog ventricular muscle and Purkinje fibre repolarization. *The Journal of physiology*, 523(1), pp 67-81.

Varró, A., Lathrop, D., Hester, S., Nanasi, P. & Papp, J. 1993. Ionic currents and action potentials in rabbit, rat, and guinea pig ventricular myocytes. *Basic research in cardiology*, 88(2), pp 93-102.

Verheule, S. & Kaese, S. 2013. Connexin diversity in the heart: insights from transgenic mouse models. *Frontiers in pharmacology*, 4(81).

Vinten-Johansen, J., Zhao, Z.-Q., Jiang, R., Zatta, A. J. & Dobson, G. P. 2007. Preconditioning and postconditioning: innate cardioprotection from ischemia-reperfusion injury. *Journal of applied physiology*, 103(4), pp 1441-1448.

Voitychuk, O. I., Strutynskyi, R. B., Yagupolskii, L. M., Tinker, A., Moibenko, O. O. & Shuba, Y. M. 2011. Sarcolemmal cardiac  $K_{ATP}$  channels as a target for the cardioprotective effects of the fluorine-containing pinacidil analogue, flocalin. *British journal of pharmacology*, 162(3), pp 701-711.

- Walweel, K., Li, J., Molenaar, P., Imtiaz, M. S., Quail, A., dos Remedios, C. G., Beard, N. A., Dulhunty, A. F., van Helden, D. F. & Laver, D. R. 2014. Differences in the regulation of RyR2 from human, sheep, and rat by  $\text{Ca}^{2+}$  and  $\text{Mg}^{2+}$  in the cytoplasm and in the lumen of the sarcoplasmic reticulum. *Journal of General Physiology*, 144(3), pp 263-271.
- Wang, H.-S., Brown, B. S., McKinnon, D. & Cohen, I. S. 2000. Molecular basis for differential sensitivity of KCNQ and  $I_{\text{KS}}$  channels to the cognitive enhancer XE991. *Molecular Pharmacology*, 57(6), pp 1218-1223.
- Wang, H.-S., Pan, Z., Shi, W., Brown, B. S., Wymore, R. S., Cohen, I. S., Dixon, J. E. & McKinnon, D. 1998. KCNQ2 and KCNQ3 potassium channel subunits: molecular correlates of the M-channel. *Science*, 282(5395), pp 1890-1893.
- Wang, Q., Curran, M. E., Splawski, I., Burn, T., Millholland, J., VanRaay, T., Shen, J., Timothy, K., Vincent, G. & De Jager, T. 1996a. Positional cloning of a novel potassium channel gene: KVLQT1 mutations cause cardiac arrhythmias. *Nature genetics*, 12(1), pp 17-23.
- Wang, Q., Curran, M. E., Splawski, I., Burn, T. C., Millholland, J. M., VanRaay, T. J., Shen, J., Timothy, K. W., Vincent, G. M., de Jager, T., Schwartz, P. J., Toubin, J. A., Moss, A. J., Atkinson, D. L., Landes, G. M., Connors, T. D. & Keating, M. T. 1996b. Positional cloning of a novel potassium channel gene: KVLQT1 mutations cause cardiac arrhythmias. *Nat Genet*, 12(1), pp 17-23.
- Wang, S.-Q., Song, L.-S., Lakatta, E. G. & Cheng, H. 2001.  $\text{Ca}^{2+}$  signalling between single L-type  $\text{Ca}^{2+}$  channels and ryanodine receptors in heart cells. *Nature*, 410(6828), pp 592-596.
- Wang, X. & Fitts, R. H. 2020. Cardiomyocyte slowly activating delayed rectifier potassium channel: regulation by exercise and  $\beta$ -adrenergic signaling. *Journal of Applied Physiology*, 128(5), pp 1177-1185.
- Wang, X., Wu, J., Li, L., Chen, F., Wang, R. & Jiang, C. 2003. Hypercapnic acidosis activates  $K_{\text{ATP}}$  channels in vascular smooth muscles. *Circulation research*, 92(11), pp 1225-1232.
- Wang, Y., Eldstrom, J. & Fedida, D. 2020. Gating and regulation of KCNQ1 and KCNQ1+ KCNE1 channel complexes. *Frontiers in Physiology*, 11(504).
- Weernink, P. A. O., Han, L., Jakobs, K. H. & Schmidt, M. 2007. Dynamic phospholipid signaling by G protein-coupled receptors. *Biochimica et Biophysica Acta (BBA)-Biomembranes*, 1768(4), pp 888-900.

Wei, A., Jegla, T. & Salkoff, L. 1996. Eight potassium channel families revealed by the *C. elegans* genome project. *Neuropharmacology*, 35(7), pp 805-29.

Weinbrenner, C., Nelles, M., Herzog, N., Sárváry, L. & Strasser, R. H. 2002. Remote preconditioning by infrarenal occlusion of the aorta protects the heart from infarction: a newly identified non-neuronal but PKC-dependent pathway. *Cardiovascular research*, 55(3), pp 590-601.

Wellman, G., Barrett-Jolley, R., Köppel, H., Everitt, D. & Quayle, J. 1999. Inhibition of vascular  $K_{ATP}$  channels by U-37883A: a comparison with cardiac and skeletal muscle. *British journal of pharmacology*, 128(4), pp 909-916.

Werry, D., Eldstrom, J., Wang, Z. & Fedida, D. 2013. Single-channel basis for the slow activation of the repolarizing cardiac potassium current,  $I_{Ks}$ . *Proceedings of the National Academy of Sciences*, 110(11), pp E996-E1005.

Wettwer, E., Amos, G., Gath, J., Zerkowski, H.-R., Reidemeister, J.-C. & Ravens, U. 1993. Transient outward current in human and rat ventricular myocytes. *Cardiovascular research*, 27(9), pp 1662-1669.

WHO, W. H. O. 2021. *Cardiovascular diseases (CVDs)* [Online]. Available: [https://www.who.int/news-room/fact-sheets/detail/cardiovascular-diseases-\(cvds\)](https://www.who.int/news-room/fact-sheets/detail/cardiovascular-diseases-(cvds)) [Accessed June 29, 2021].

Wiener, R., Haitin, Y., Shamgar, L., Fernández-Alonso, M. C., Martos, A., Chomsky-Hecht, O., Rivas, G., Attali, B. & Hirsch, J. A. 2008. The KCNQ1 (Kv7. 1) COOH terminus, a multitiered scaffold for subunit assembly and protein interaction. *Journal of Biological Chemistry*, 283(9), pp 5815-5830.

Wink, M. 2010. Mode of action and toxicology of plant toxins and poisonous plants. *Julius-Kühn-Archiv*, 421), pp 93.

Wojtovich, A. P., Williams, D. M., Karcz, M. K., Lopes, C. M., Gray, D. A., Nehrke, K. W. & Brookes, P. S. 2010. A novel mitochondrial  $K_{ATP}$  channel assay. *Circulation research*, 106(7), pp 1190-1196.

Wrobel, E. 2013. Untersuchung des Mechanismus und der molekularen Bindestelle des Kv7. 1/KCNE1-Inhibitors JNJ303.

Wrobel, E., Tapken, D. & Seeböhm, G. 2012. The KCNE tango—how KCNE1 interacts with Kv7. 1. *Frontiers in pharmacology*, 3(142).

- Wu, D.-M., Jiang, M., Zhang, M., Liu, X.-S., Korolkova, Y. V. & Tseng, G.-N. 2006. KCNE2 is colocalized with KCNQ1 and KCNE1 in cardiac myocytes and may function as a negative modulator of  $I_{KS}$  current amplitude in the heart. *Heart Rhythm*, 3(12), pp 1469-1480.
- Wu, M., Huang, Z., Xie, H. & Zhou, Z. 2013. Nicorandil in patients with acute myocardial infarction undergoing primary percutaneous coronary intervention: a systematic review and meta-analysis. *PLoS one*, 8(10), pp e78231.
- Wu, X. & Larsson, H. P. 2020. Insights into cardiac  $I_{KS}$  (KCNQ1/KCNE1) channels regulation. *International journal of molecular sciences*, 21(24), pp 9440.
- Xiao, X.-H. & Allen, D. G. 1999. Role of  $Na^+$ / $H^+$  exchanger during ischemia and preconditioning in the isolated rat heart. *Circulation research*, 85(8), pp 723-730.
- Xie, L.-H., John, S. A., Ribalet, B. & Weiss, J. N. 2007. Activation of inwardly rectifying potassium (Kir) channels by phosphatidylinositol-4, 5-bisphosphate (PIP2): interaction with other regulatory ligands. *Progress in biophysics and molecular biology*, 94(3), pp 320-335.
- Xiong, Q., Sun, H. & Li, M. 2007. Zinc pyrithione-mediated activation of voltage-gated KCNQ potassium channels rescues epileptogenic mutants. *Nature chemical biology*, 3(5), pp 287-296.
- Xu, Y., Wang, Y., Zhang, M., Jiang, M., Rosenhouse-Dantsker, A., Wassenaar, T. & Tseng, G.-N. 2015. Probing binding sites and mechanisms of action of an  $I_{KS}$  activator by computations and experiments. *Biophysical journal*, 108(1), pp 62-75.
- Yamada, M., Isomoto, S., Matsumoto, S., Kondo, C., Shindo, T., Horio, Y. & Kurachi, Y. 1997. Sulphonylurea receptor 2B and Kir6. 1 form a sulphonylurea-sensitive but ATP-insensitive  $K^+$  channel. *The Journal of physiology*, 499(3), pp 715-720.
- Yang, W.-P., Levesque, P. C., Little, W. A., Conder, M. L., Shalaby, F. Y. & Blanar, M. A. 1997. KvLQT1, a voltage-gated potassium channel responsible for human cardiac arrhythmias. *Proceedings of the National Academy of Sciences*, 94(8), pp 4017-4021.
- Yang, Y. & Sigworth, F. J. 1998. Single-channel properties of  $I_{KS}$  potassium channels. *The Journal of general physiology*, 112(6), pp 665-678.
- Yarov-Yarovoy, V., DeCaen, P. G., Westenbroek, R. E., Pan, C.-Y., Scheuer, T., Baker, D. & Catterall, W. A. 2012. Structural basis for gating charge movement in the voltage

sensor of a sodium channel. *Proceedings of the National Academy of Sciences*, 109(2), pp E93-E102.

Yarov-Yarovoy, V., Pucek, P., Jabůrek, M. & Garlid, K. D. 1997. The nucleotide regulatory sites on the mitochondrial  $K_{ATP}$  channel face the cytosol. *Biochimica et Biophysica Acta (BBA)-Bioenergetics*, 1321(2), pp 128-136.

Ye, F., Winchester, D., Jansen, M., Lee, A., Silverstein, B., Stalvey, C., Khuddus, M., Mazza, J. & Yale, S. 2019. Assessing prognosis of acute coronary syndrome in recent clinical trials: a systematic review. *Clinical medicine & research*, 17(1-2), pp 11-19.

Ye, P., Zhu, Y. R., Gu, Y., Zhang, D. M. & Chen, S. L. 2018. Functional protection against cardiac diseases depends on ATP-sensitive potassium channels. *Journal of cellular and molecular medicine*, 22(12), pp 5801-5806.

Yellon, D. M. & Hausenloy, D. J. 2007. Myocardial reperfusion injury. *New England Journal of Medicine*, 357(11), pp 1121-1135.

Ytrehus, K., Liu, Y. & Downey, J. M. 1994. Preconditioning protects ischemic rabbit heart by protein kinase C activation. *American Journal of Physiology-Heart and Circulatory Physiology*, 266(3), pp H1145-H1152.

Yu, H., Lin, Z., Mattmann, M. E., Zou, B., Terrenoire, C., Zhang, H., Wu, M., McManus, O. B., Kass, R. S. & Lindsley, C. W. 2013a. Dynamic subunit stoichiometry confers a progressive continuum of pharmacological sensitivity by KCNQ potassium channels. *Proceedings of the National Academy of Sciences*, 110(21), pp 8732-8737.

Yu, H., Lin, Z., Xu, K., Huang, X., Long, S., Wu, M., McManus, O. B., Le Engers, J., Mattmann, M. E. & Engers, D. W. 2013b. Identification of a novel, small molecule activator of KCNQ1 channels. *Probe Reports from the NIH Molecular Libraries Program [Internet]*.

Yu, L., Jin, X., Cui, N., Wu, Y., Shi, Z., Zhu, D. & Jiang, C. 2012. Rosiglitazone selectively inhibits  $K_{ATP}$  channels by acting on the KIR6 subunit. *British journal of pharmacology*, 167(1), pp 26-36.

Yuan, W., Ginsburg, K. S. & Bers, D. M. 1996. Comparison of sarcolemmal calcium channel current in rabbit and rat ventricular myocytes. *The Journal of physiology*, 493(3), pp 733-746.

Yus-Najera, E., Santana-Castro, I. & Villarroel, A. 2002. The identification and characterization of a noncontinuous calmodulin-binding site in noninactivating voltage-dependent KCNQ potassium channels. *J Biol Chem*, 277(32), pp 28545-53.

- Zaczek, R., Chorvat, R., Saye, J., Pierdomenico, M., Maciag, C., Logue, A., Fisher, B., Rominger, D. & Earl, R. 1998. Two new potent neurotransmitter release enhancers, 10, 10-bis (4-pyridinylmethyl)-9 (10H)-anthracenone and 10, 10-bis (2-fluoro-4-pyridinylmethyl)-9 (10H)-anthracenone: comparison to linopirdine. *Journal of Pharmacology and Experimental Therapeutics*, 285(2), pp 724-730.
- Zamponi, G. W., Striessnig, J., Koschak, A. & Dolphin, A. C. 2015. The physiology, pathology, and pharmacology of voltage-gated calcium channels and their future therapeutic potential. *Pharmacological reviews*, 67(4), pp 821-870.
- Zehlein, J., Thomas, D., Khalil, M., Wimmer, A.-B., Koenen, M., Licka, M., Wu, K., Kiehn, J., Brockmeier, K. & Kreye, V. 2004. Identification and characterisation of a novel KCNQ1 mutation in a family with Romano–Ward syndrome. *Biochimica et Biophysica Acta (BBA)-Molecular Basis of Disease*, 1690(3), pp 185-192.
- Zerangue, N., Schwappach, B., Jan, Y. N. & Jan, L. Y. 1999. A new ER trafficking signal regulates the subunit stoichiometry of plasma membrane K<sub>ATP</sub> channels. *Neuron*, 22(3), pp 537-548.
- Zhang, C., Miki, T., Shibasaki, T., Yokokura, M., Saraya, A. & Seino, S. 2006. Identification and characterization of a novel member of the ATP-sensitive K<sup>+</sup> channel subunit family, Kir6. 3, in zebrafish. *Physiological genomics*, 24(3), pp 290-297.
- Zhang, H. & Bolton, T. 1995. Activation by intracellular GDP, metabolic inhibition and pinacidil of a glibenclamide-sensitive K-channel in smooth muscle cells of rat mesenteric artery. *British journal of pharmacology*, 114(3), pp 662-672.
- Zhang, M., Jiang, M. & Tseng, G.-N. 2001. minK-related peptide 1 associates with Kv4. 2 and modulates its gating function: potential role as β subunit of cardiac transient outward channel? *Circulation research*, 88(10), pp 1012-1019.
- Zhang, X., Ai, X., Nakayama, H., Chen, B., Harris, D. M., Tang, M., Xie, Y., Szeto, C., Li, Y. & Li, Y. 2016. Persistent increases in Ca<sup>2+</sup> influx through Cav1. 2 shortens action potential and causes Ca<sup>2+</sup> overload-induced afterdepolarizations and arrhythmias. *Basic research in cardiology*, 111(1), pp 1-16.
- Zhao, Z.-Q., Corvera, J. S., Halkos, M. E., Kerendi, F., Wang, N.-P., Guyton, R. A. & Vinten-Johansen, J. 2003. Inhibition of myocardial injury by ischemic postconditioning during reperfusion: comparison with ischemic preconditioning. *American Journal of Physiology-Heart and Circulatory Physiology*, 285(2), pp H579-H588.

Zhou, H., Tate, S. S. & Palmer, L. G. 1994. Primary structure and functional properties of an epithelial K channel. *American Journal of Physiology-Cell Physiology*, 266(3), pp C809-C824.

Zimmermann, H. 1988. Cholinergic synaptic vesicles. *The cholinergic synapse*. Springer.